ABSTRACT

Title of Document: MULTI-SCALE PEDOLOGIC INVESTIGATION OF MANGANIFEROUS SOILS IN THE MARYLAND PIEDMONT

Rebecca R. Bourgault, Master of Science, 2008

Directed By: Professor Martin C. Rabenhorst, Department of Environmental Science and Technology

Manganese oxides are usually found in trace quantities in soils, but they are important due to their effects on soil chemistry and morphology. There are rare soils in the Maryland Piedmont that have extremely high amounts of manganese oxides that have not been previously studied. These manganiferous soils were examined at multiple scales in order to determine their spatial extent, to characterize their fundamental morphology, mineralogy, and chemical and physical properties, and to better understand their pedogenesis. The soils occupy areas of 1-2 ha in size, within 200 km^2 in eastern Frederick County and western Carroll County. The soils can have as much as 140 g kg^{-1} Mn as oxides, which pigments the entire soil matrix black in subsoil horizons. It appears that the black, porous, Mn-rich material is derived directly from the dissolution of marble bedrock and accumulation of silicate residues plus Mn and Fe from within the rock.

MULTI-SCALE PEDOLOGIC INVESTIGATION OF MANGANIFEROUS SOILS IN THE MARYLAND PIEDMONT

By

Rebecca R. Bourgault

Thesis submitted to the Faculty of the Graduate School of the
University of Maryland, College Park in partial fulfillment
of the requirements for the degree of
Master of Science
2008

Advisory Committee:

Professor Martin Rabenhorst, Chair
Professor Bruce James
Professor Brian Needelman

For Mark and Elijah, my two favorite people

(And for the rest of my family, because you are my favorite people too)

ACKNOWLEDGEMENTS

I wish to acknowledge and sincerely thank the many people who, without their assistance, completing this study would not be possible.

I would first like to thank my advisor, Martin Rabenhorst, whose vast patience and kind encouragement have guided and inspired me to complete this project. Many thanks also to Bruce James, a mentor throughout my entire time at the University, and who so generously lent me a computer and an office space. Many more thanks to Brian Needelman for his teaching and support through the years.

Thanks to my fellow graduate students Philip Zurheide, Danielle Balduff, Rosalynd Orr, and Adam Gray for helping out in the field and lab a great deal. Thanks also to Nisha Maheswaran for the PSA work.

Thanks to James Doolittle, NRCS, for working with us on EMI surveys; Joseph Kraft, NRCS, for valuable information regarding the location of manganiferous soils; Sanjai Parikh, Univ. of Delaware, for assistance with FTIR analyses; Stan Schlosnagle, Univ. of Maryland, for carbon analysis and assistance with the ATV; and Mike Wilson, NRCS, for assistance with the U.S. soils characterization database.

I am greatly indebted to Paul Dotterer, Richard Grossnickle, and Richard Flickinger for allowing us to observe their extraordinary soils.

I must also acknowledge the personal support given to me by my family: my parents and step-parents, Mom and Jim, Dad and Beth; and my brothers, Aaron and Sammy. I can't thank you enough for being so supportive, and for helping out with baby Eli so I could finish my work.

And, last but not least, thanks to my husband, Mark, for everything.

TABLE OF CONTENTS

LIST OF TABLES

LIST OF FIGURES

CHAPTER 1

Introduction

In the Piedmont of Maryland, some unusual soils were discovered by the Natural Resources Conservation Service (NRCS) during the update of the Frederick County Soil Survey in 1997. They had subsoil horizons which were black in color (Munsell value/ chroma <2/1) and had very low bulk density, so they were morphologically similar to organic soils, but were found in well-drained upland conditions. Preliminary investigations showed that these soils had typically low concentrations of organic carbon, suggesting that the dark color was not related to soil organic matter (M. Rabenhorst, personal communication, 2005). Dithionite-citrate-bicarbonate (DCB) extractions revealed that the dark matrix color was actually derived from extraordinarily high concentrations of manganese, up to 150 g kg^{-1} DCB-extractable Mn (M. Rabenhorst, personal communication, 2005). Extremely high amounts of Fe, which is often associated with Mn, were also measured (up to 170 g kg^{-1} DCB-extractable Fe). By comparison, soils in the Mid-Atlantic region typically contain <50 g kg^{-1} Fe (Foss et al., 1969) and one-fiftieth that amount of Mn (Dixon and White, 2002), or <1 g kg^{-1} Mn. Although there is more Fe than Mn in these soils, they have been dubbed "manganiferous" as opposed to "ferromanganiferous" to emphasize the relative rarity of such abundant Mn.

In soils that are normally considered to have above-average Mn levels, Mn oxides can exist in ferromanganiferous nodules, concretions, soft masses, or coatings on surfaces called mangans. Manganese oxides do not normally exist in quantities sufficient

to pigment the entire soil matrix. The manganiferous soils to be investigated in this study are therefore defined by having amounts of disseminated Mn oxides sufficient to produce a distinctive, black soil matrix color in one or more horizons.

The manganiferous soils of Maryland occur in eastern Frederick County and western Carroll County. They lie in the Western Division of the Piedmont physiographic province, which is defined by weakly metamorphosed bedrock, undulating topography, and mainly Alfisols and Ultisols formed from residuum. The manganiferous soils were suspected by NRCS soil scientists to be the result of weathering of marble or other calcareous bedrock, based upon their apparent association with mapped geologic units and with calcareous rock-derived soils such as those of the Conestoga series. Soils derived from carbonate bedrock (limestone or marble), called *terra rossa* due to their reddish color, often have elevated amounts of Fe and Mn due to carbonate leaching and accumulation of non-carbonate residues from within the rock (Leinigen, 1929). However, these concentrations are typically much lower than those seen in the manganiferous soils of Maryland. For example, *terra rossa* soils studied in Croatia have an average of 51.9 g kg^{-1} Fe and 1.1 g kg^{-1} Mn (Durn et al., 2001). Hagerstown, a soil series found in Maryland which is formed from limestone residuum and would also be considered to be terra rossa, has up to 78 g kg^{-1} Fe in subsoil horizons (Soil Survey Staff, 2008).

The Frederick and Carroll County Soil Surveys do not explicitly mention or classify manganiferous soils. The Benevola series, mapped in Frederick Co., with marble residuum parent material, may have a black C horizon and ferromanganiferous nodules throughout the profile, and may be similar to some of the manganiferous soils with fine (clayey) particle-size. But, many of the manganiferous profiles have a coarser (loamy)

texture, and these have been included in the Conestoga and Letort mapping unit, mapped in Frederick and Carroll Counties (J. Kraft, personal communication, 2006). The Letort series was apparently chosen by the NRCS as a soil mapping "home" for the manganiferous soils because it is described as having a 10YR 3/2 C horizon and a fine-loamy particle size class. However, the official series description for Letort makes no mention of high Mn, and the dark colored C horizons of Letort are generally attributed to parent material (residuum from interbedded micaceous limestone, graphite phyllite and phyllite) and unrelated to Mn. Because the NRCS generally included the manganiferous soils (where they were found) in Conestoga and Letort mapping units, the soil survey can be used as a guide for locating the overall distribution of manganiferous soils.

Manganiferous soils are not known to be problem areas for agriculture or engineering. However, they are listed as "problem hydric" soils in the Mid-Atlantic Guide to Hydric Soils because they could possibly be mistaken for organic-rich soils by a field practitioner due to their dark color and low bulk density (Robinette et al., 2004). For those trained in studying soils in the field, this is perhaps not likely because they are of very limited extent and tend to be found in portions of the landscape associated with well-drained upland conditions. If there is any question in the field, an immediate, violent reaction of the soil material with 30% H_2O_2 confirms the presence of Mn oxides.

Manganese oxides, though usually found in trace quantities in soils, are important minerals in the soil environment due to their chemically reactive nature. They have a high specific surface and sorption potential, so they tend to retain nutrients and heavy metals such as cobalt and lead. Mn oxides can also participate in oxidation-reduction reactions, such as the oxidation of inert Cr(III) to toxic Cr(VI) (Bartlett and James, 1988). In

addition, Mn oxides can catalyze the polymerization of organic matter, and Mn is an essential plant and animal micronutrient. Manganese oxide minerals, although important chemical components of many soils, have not been extensively studied and characterized. This is due to their poorly crystalline nature, which makes identification by X-ray diffraction difficult, and their typically low concentrations, which makes some sort of pre-treatment usually necessary to concentrate them. The manganiferous soils observed in this study are a rare anomaly providing a unique opportunity to study Mn oxides in the soil environment.

The manganiferous soils of Maryland have not been previously studied in detail. Little is known about their spatial extent, fundamental properties, and origin. Therefore, the objectives of this research are 1) to determine the areal extent of manganiferous soils in the Piedmont of Maryland, and what governs their distribution across the landscape; 2) to determine the fundamental morphological, chemical, physical, and mineralogical characteristics of these soils; and 3) to better understand the pedogenesis of these soils.

CHAPTER 2

Literature Review

MANGANESE OXIDES IN SOILS

Distribution and Morphology

Manganese is ubiquitous in soils throughout the world, but it is usually present in trace amounts of less than 1 g kg^{-1} (Dixon and White, 2002) and not visible to the naked eye. Manganese oxides (Mn(III, IV) (hydr)oxides) and iron oxides (Fe(III) (hydr)oxides) are formed by similar processes and are intimately associated in soils. There is typically 50 times more Fe than Mn in soils (Dixon and White, 2002), or approximately 20-50 g Fe kg^{-1} in B horizons the Mid-Atlantic region (Foss et al., 1969). Mn oxides typically accumulate near the soil surface where conditions are most oxidizing, and plants tend to draw Mn upward (Uzochukwu and Dixon, 1986).

When concentrated as a result of alternating oxidizing-reducing conditions, Fe and Mn can occur together in brown-black ferromanganiferous concentrations or nodules. For example, the Official Series Description of the Jackland series (moderately well-drained to somewhat poorly drained, fine, smectitic, mesic Aquic Hapludalfs of the Piedmont), with up to 3 g kg^{-1} Mn (M. Rabenhorst, personal communication), documents >2% iron-manganese concretions throughout the profile, with black iron-manganese streaks in the B and C horizons. The strong pigmenting ability of brown-black Mn oxides allows them to color soil materials when present in small quantities, and they may mask reddish Fe oxides even when the ratio of Fe to Mn is 5.5:1 (Schwertmann and Fanning,

1976). Elless (1992) found that some black (N2) nodules in his study had an Fe to Mn ratio of approximately 4:1 (128 g kg^{-1} Fe and 35 g kg^{-1} Mn).

There are very few soils documented in the world with large amounts of Mn oxides (greater than 10 g kg^{-1} Mn). The only soils in the United States (in the NRCS characterization database) with greater than 10 g kg^{-1} Mn include a pedon within the Rio Arriba series in Puerto Rico, a Typic Paleudult formed in fine textured sediments of mixed origin on river terraces and alluvial fans, with 10-50 g kg^{-1} Mn in the Ap and upper Bt horizons; a pedon within the Thatuna series in Washington, a Boralfic Argixeroll formed in deep loess, with 17 g kg^{-1} Mn in the 2Bw horizon; a pedon within the Kasilof series in Alaska, a Typic Cryorthod with 23 g kg^{-1} Mn in the Cr; and a pedon within the Wahiawa series in Hawaii, a Kandiustalfic Eutrustox formed in residuum and alluvium weathered from basalt, with 18-33 g kg^{-1} Mn in the Ap horizon (Soil Survey Staff, 2008).

Outside of the U.S., the highest known soil Mn concentrations occur in the manganiferous oxisols of Graskop, Mpumalanga Province, South Africa. These soils have as much as 58.3 g kg^{-1} Mn and 89.0 g kg^{-1} Fe (DCB-extractable) and, as a result, have black matrix colors (5YR 2.5/1) in B horizons (Dowding and Fey, 2007). Also, there is as much as 287 g kg^{-1} Mn in the dolomite residuum (Hawker and Thompson, 1988). These soils have a characteristic sequence of horizons: a dark reddish brown A horizon with up to 30% ferromanganiferous nodules, gradually transitioning into a redder, finer-textured B horizon with up to 80% nodules, which grades into a structureless, very friable, black C horizon (Dowding and Fey, 2007). The manganiferous oxisols are generally deeper, redder, and more nodule-rich in lower-lying landscape positions. On slopes and higher landscape positions, the soils are shallower, have little or

no red B horizon, and have a thin black B horizon which has an abrupt contact with unweathered dolomite bedrock (Dowding and Fey, 2007).

Chemistry

The effects of Mn on the chemistry of soils are quite significant in spite of its normally low concentrations. Manganese has a large range in oxidation states (+2 to +7), and is very sensitive to changes in oxidation-reduction potential. In soils, Mn is usually present as Mn(III) and Mn(IV) in oxidizing conditions, in the form of solid, brown-black Mn (hydr)oxides. In reducing conditions, insoluble Mn(III, IV) is reduced to soluble Mn(II), which can be concentrated and precipitated again as Mn(III, IV) when oxidized. This cycling (oxidation/ reduction) of manganese is governed by both chemical and biological factors. At low pH, Mn(III, IV) may be reduced chemically. However, microorganisms, primarily bacteria, are responsible for catalyzing reduction of Mn(III, IV) at higher pH by using Mn as a terminal electron acceptor in the absence of O_2. Auto-oxidation of Mn(II) by atmospheric O_2 has not been demonstrated below pH 8 (Diem and Stumm, 1984). But, abiotic oxidation may occur in soils already containing Mn oxides. Mn(III, IV) oxides tend to auto-oxidize Mn(II), so new Mn oxides form on older oxide surfaces (Ross and Bartlett, 1981; Wada et al., 1978). Also, some chemoautotrophic bacteria and fungi are capable of oxidizing Mn(II) instead of carbon, accelerating the rate of Mn oxidation several orders of magnitude faster than abiotic processes (Tebo et al., 2005).

Manganese oxides are very reactive chemically due to their large specific surface and high sorption potential. This is true for Mn oxides when present in thin coatings, but also when they occur in coarse (sand- and silt-sized) particles, due to the small size of the crystallites and the porous nature of the nodules in which they are found (Uzochukwu and Dixon, 1986). Mn oxides have the ability to oxidize chemical species in the soil environment. Indeed, dissolved Mn(III) is the strongest oxidant in soils next to O_2 (Bartlett and James, 1993). A well-known example is the oxidation of Cr(III) to Cr(VI) mainly by Mn oxides in soils (Bartlett and James, 1988). Mn is an important catalyst in the polymerization of phenolic compounds, so it plays a role in the formation of humus (Bartlett, 1988; Shindo, 1990). Mn also appears to stabilize organic matter and prevent its oxidation to CO_2 (Bartlett and Ross, 2005). Another characteristic of Mn oxides is their ability to retain certain divalent metals. These so-called "manganophilic" elements, such as cobalt and lead, are adsorbed and oxidized at Mn oxide mineral surfaces. South African manganiferous soils have high enough levels of Co, Cu, Ni, Zn and Pb that they can be considered contaminated (Dowding and Fey, 2007). In addition, Uzochukwu and Dixon (1986) found a correlation between Mn content and amounts of Zn, Cu, Ba, and Li in soils of Texas and Alabama.

Manganese is an essential plant micronutrient. It is used in the enzyme that releases oxygen from H_2O in photosynthesis. However, excessive plant uptake of Mn(II) can cause toxicity. Plant toxicity has been a concern for agricultural operations in Hawaii, on the Wahiawa and other acid soil series derived from Mn-rich basalt (Hue et al., 1999). These soils have a total Mn concentration of 10 to 40 g kg^{-1} (Fujimoto and Sherman, 1948); but, toxicity is caused by conditions which favor bioavailable Mn^{2+}, namely low

pH and waterlogging (Hue et al., 1999).This problem is normally mitigated by liming the soil to approximately pH 6, which makes it more difficult for Mn oxides to be reduced without compromising the availability of other nutrients such as Fe and Zn (CTAHR, 1998).

Mineralogy

There are many different Mn oxide minerals found in soils. The specific Mn oxide mineral(s) present in a given soil depend largely on pH and degree of weathering. Some of the most common soil Mn oxides are birnessite, vernadite, cryptomelane, todorokite, and lithiophorite (Vodyanitskii, 2003). Birnessite ($(Na,Ca)Mn_7O_{14} \cdot 2.8H_2O$) has a lamellar structure, is typical for young calcareous soils throughout the world, and is the dominant Mn oxide found in ortsteins (Dixon and Skinner, 1992). Vernadite ($MnO_2 \cdot nH_2O$), a biogenic Mn oxide, has a pseudolamellar structure, has substitution of Fe for Mn, and is stable in a wide range of pH values, so is quite widespread (Vodyanitskii, 2003). Cryptomelane ($K(Mn^{4+}Mn^{3+})_8 \cdot (O,OH)_{16}$) has a tunnel structure, and is most stable in pH 7 or higher. It may form from birnessite upon saturation with K (Dixon and Skinner, 1992). Todorokite encompasses several minerals with varying ratios of Mn(III) to Mn(IV). The structure consists of chains joined by edges of octahedra. Todorokite was identified in calcareous concretions in the C horizon of Mollisols in central Texas (Dixon and Skinner, 1992). Lithiophorite ($LiAl_2(Mn_2^{4+}Mn^{3+})O_6(OH)_6$) has a mixed-layer gibbsite-like structure, has high thermodynamic stability, and is typical of highly weathered, acid soils, such as the Decatur soil formed from limestone residuum in

Alabama (Uzochukwu and Dixon, 1986), manganiferous oxisols in South Africa (Dowding and Fey, 2007), and Mn-rich oxisols in Hawaii (Golden et al., 1993). Lithiophorite is more crystalline, has a lower specific surface and is weathered more slowly than birnessite (Vodyanitskii, 2003).

Manganese oxide minerals, due to their typically low concentrations and poorly crystalline nature, are difficult to identify using standard techniques such as X-Ray Diffraction (XRD). Even when they occur in concentrations high enough to be detected with XRD, such as in ferromanganiferous nodules, Mn oxides often yield broad peaks that coincide with peaks of other common soil minerals such as kaolinite. This has sometimes been addressed by pre-treating the soil with NaOH in order to remove interfering phyllosilicates and concentrate the Mn oxides (Tokashiki et al., 1986). Successive selective dissolution (with hydroxylamine hydrochloride and dithionite-citrate-bicarbonate) may be used in conjunction with differential XRD in order to extract, identify, and quantify various operationally defined fractions of birnessite, lithiophorite, and goethite (Tokashiki et al., 2003; Neaman et al., 2004). Fourier Transform Infrared Spectroscopy (FTIR) is an alternative to XRD that is generally better at identifying poorly crystalline minerals. Potter and Rossman (1979) identified characteristic FTIR spectra for several common soil Mn oxide minerals.

SOILS FORMED FROM CARBONATE BEDROCK

Pedogenesis

Soils derived from limestone, dolostone or marble residuum parent material are often reddish in color, which is indicative of elevated Fe oxides. Elevated concentrations of associated Mn oxides are also common in these soils. For example, limestone-derived soils studied in Croatia have an average of 51.9 g kg^{-1} Fe and 1.1 g kg^{-1} Mn (Durn et al., 2001). The term terra rossa ("red earth") is a concept developed in the Mediterranean region to refer to these characteristic soils derived from carbonate rocks. Normally, elevated amounts of crystalline Fe oxides (hematite) are thought to be a product of intense mineral weathering in a tropical/ sub-tropical climate (such as in oxisols). However, terrae rossae are found in temperate climates, so it is likely that the hematite originates instead from limestone residue containing material from earlier-formed soils (Bronger et al., 1984). The long-standing "residual theory" holds that these soils are formed from carbonate dissolution and in situ accumulation of non-carbonate residue from within the rock (Leinigen, 1929). Under this theory, climate is not a very important factor in the pedogenesis of terra rossae (Bronger et al., 1984). Some authors have provided evidence to support the residual theory. For example, Bronger et al. (1984) compared limestone residues and their overlying soils from Slovakia. The authors concluded that little or no mineral weathering/ clay formation had occurred, but the soils were enriched in Fe compared to the limestone residues. Moresi and Mongelli (1988) also compared the mineralogy of non-carbonate residues from limestones and dolostones (collected via acid dissolution of the rocks) to the mineralogy of the overlying soils, and the chemical differences between the two are consistent with the residues being the

parent material of the soils. Manganiferous oxisols in South Africa are derived from a black, Mn-rich dolomite residuum. It is thought that the black material formed in situ as a result of congruent dissolution of the dolomite, leaving behind a porous, "sponge-like" accumulation of Fe and Mn oxides under oxidizing conditions (Hawker and Thompson, 1988). Limestones and dolostones tend to be relatively pure calcite ($CaCO_3$) or dolomite ($CaMg(CO_3)_2$), respectively. This implies that a large amount of rock would have to be dissolved in order for a soil to be developed from the non-carbonate residue. For nearly pure marbles of the Normanville Group in Australia, Foster and Chittleborough (2003) estimate that approximately 150 m of rock would need to be dissolved in order to leave behind 40 cm of soil.

Although the residual theory is widely accepted, some authors have shown that input of allochthonous materials may make an important contribution to terrae rossae in some areas of the world. For example, there is evidence that a significant portion of terra rossa soils the Mediterranean may be comprised of Saharan aeolian dust (Bronger and Bruhn-Lobin, 1997; Yaalon, 1997). Also, Olson et al. (1980) reject the residual theory for terrae rossae in a karst region of Indiana. The authors show that the soils in their study area do not appear to be related to the non-carbonate residue of the underlying limestone bedrock. The amount of limestone residue collected is insufficient to produce soils of the thickness observed. And, comparison of the residue's mineralogical composition and particle size to that of the overlying soils suggest that the soils are formed instead from sediment deposited onto the limestone surface. Foster et al. (2004) determined that the deeper horizons of the terrae rossae at their study site in Australia appeared to be largely derived from non-carbonate marble residue, but that the shallower horizons appeared to

have considerable input of colluvial material from upslope. Therefore, it is probable that either one or both processes (in situ accumulation of non-carbonate residue and input of allochthonous materials) could be forming soils over calcareous bedrock, depending on local conditions.

Distribution and Morphology of Carbonate Rock-Derived Soils in Maryland

There are some soils in Maryland formed from calcareous bedrock. Some examples are the Hagerstown, Frederick, and Baltimore series, which are red in color and may be considered terra rossa. Other examples include the Conestoga and Benevola series, which are usually not considered terra rossa due to the browner colors of their official series descriptions. These soil series are found in limited areas across the western half of the state, where most soils are formed from residuum or colluviated residuum (the eastern half of the state lies in the Coastal Plain Province, where soils are mainly formed from unconsolidated sediments). Soils in the Hagerstown and Frederick series are found in the Ridge and Valley Province, where the bedrock has been folded but not substantially metamorphosed. The Hagerstown series (fine, mixed, semiactive, mesic Typic Hapludalfs) is formed from limestone residuum. Hagerstown soils have reddish Bt horizons (hue of 5YR or 2.5YR, value of 4 or 5, and chroma of 4 to 8) and relatively fine textures (silty clay, clay, or silty clay loam). The Bt horizons also tend to have very dark gray (5YR 3/1) ferromanganiferous stains and concretions. Characterization data for the Hagerstown series show a maximum (DCB-extractable) Mn content of 2 to 6 g kg^{-1} and a maximum (DCB-extractable) Fe content of 78 g kg^{-1} in subsoil horizons (Soil Survey

Staff, 2008). The Frederick series (fine, mixed, semiactive, mesic Typic Paleudults) is formed in residuum derived mainly from dolomitic limestone with interbeds of sandstone, siltstone, and shale. The color and texture of the Bt horizon are similar to that of the Hagerstown. The Frederick series has a hue of 2.5YR or 5YR, value 4 through 6, and chroma 4 through 8. The texture of the upper part of the Bt horizon is clay loam, silty clay loam, silty clay, or clay; it is silty clay or clay in the lower part. The C horizon, where present, is yellowish red or reddish yellow with parent material-related mottles in shades of yellow, brown or red; the texture of the C horizon is silty clay or clay. The Frederick series has trace amounts of (DCB-extractable) Mn up to 1 g kg^{-1} (Soil Survey Staff, 2008).

Soils of the Baltimore series are found in the Eastern Division of the Piedmont physiographic province, which consists of relatively strongly metamorphosed igneous bedrock such as gneisses and phyllites, and some metamorphosed sedimentary bedrock such as marble. The Baltimore series (fine-loamy, mixed, semiactive, mesic Typic Hapludolls) is formed in residuum from mica phyllite over marble bedrock. Although it is not formed purely from marble, its red color gives it a terra rossa morphology. The Bt horizon of the Baltimore series (derived from mica phyllite residuum) has hue of 2.5YR or 5YR, value of 4 or 5 and chroma of 6 through 8. It is gravelly clay loam, gravelly silty clay loam, clay loam or silty clay loam in the fine earth fraction. The 2C horizon (presumably derived from marble residuum) has hue of 10YR through 5YR, value of 5 or 6 and chroma of 6 through 8, and its texture is loam or silt loam.

Soils in the Conestoga and Benevola series are found in the Western Division of the Piedmont, where the bedrock consists of weakly metamorphosed igneous and

sedimentary rocks, mainly phyllites and phyllites, also some metabasalt and limestone/ marble. The Conestoga series (fine-loamy, mixed, active, mesic Typic Hapludalfs) is formed in residuum mostly from micaeous limestone and calcareous phyllite. The Conestoga series is relatively bright in color throughout, but not as red as Hagerstown. The B horizon has hue of 7.5YR or 10YR, value of 4 or 6, and chroma of 4 through 8. The C horizon has hue of 7.5YR through 2.5Y, value of 4 through 7, and chroma of 4 through 8. The Benevola series (fine, mixed, semiactive, mesic Mollic Hapludalfs), is formed from marble residuum. These soils are of very limited extent, and are found in Frederick County. The Benevola series has dark reddish brown Bt horizons (hue of 2.5YR through 7.5YR, value 3 through 5, chroma 2 through 6) containing ferromanganiferous nodules, and it may sometimes have black (N2) C horizons; however, this black color is not a requirement for the series. It is assumed that the black color is due to an extremely high Mn content, though this is not explicitly stated in the official series description, and there are no NRCS characterization data available for this series. (However, Foss et al. (1969) measured 14.7 to 78.3 g kg^{-1} DCB-extractable Fe in a Benevola pedon.) The C horizon of the Benevola series may have a hue of N, or 2.5YR to 10YR, and a value of 2 through 6 and a chroma of 0 through 6; the texture is clay, silty clay, clay loam, or silty clay loam.

ELECTROMAGNETIC INDUCTION AND PEDOLOGY

Electromagnetic Induction (EMI) is a non-invasive soil mapping technique which has a variety of applications in pedology. An EMI meter measures the apparent electrical

conductivity (EC_a) of soils. Conductivity is the ability of a material to transmit an electrical current, and is an inherent property of the material. Because electrical conductivity of soils may vary based on many factors, EMI is only useful when an empirical relationship can be established between EC_a and the feature of interest. If a relationship is established based on field observations, then an informative EMI survey may be conducted quickly and efficiently.

The property which has the most widespread effect on soil electrical conductivity is grain size (Lund et al., 1999). Specifically, sands have low conductivity, silts have moderate conductivity, and clays have high conductivity, so EC_a and soil texture are strongly correlated (Williams and Hoey, 1987). Because of this, depth to a clay layer in a coarser-textured soil may be easily mapped (Doolittle et al., 1994; Cockx et al., 2007). Cation exchange capacity, which is a function of clay mineralogy, also affects EC_a (McBride et al., 1990). Soil salinity has a strong effect on EC_a as well (Rhoades and Corwin, 1981). In addition, fragic properties have been successfully mapped using EMI in Tennessee (Inman et al., 2002). The ability to map these properties at the field scale with EMI provides much information and has many implications for soil survey and precision agriculture. An EMI map may provide a more detailed assessment of the soil properties of a field of interest than a county soil survey, so it may supplement the information, and management decisions may be made on a finer scale (Lund et al., 1999).

CHAPTER 3

Spatial Investigations of Manganiferous Soils

INTRODUCTION

Some highly unusual manganiferous soils were discovered by scientists mapping soils for the Natural Resources Conservation Service (NRCS) in eastern Frederick County, Maryland, during the update of the Soil Survey in 1997. These soils, of limited extent, were found to contain extremely high amounts of Mn oxides (up to 150 g kg^{-1} DCB-extractable Mn) (Rabenhorst, personal communication), giving the whole soil matrix a very dark color (Munsell value and chroma <2/1) in some subsoil horizons due to the strong pigmenting ability of brown-black Mn oxides. NRCS soil scientists observed that the manganiferous soils were mainly found in areas where marble bedrock was mapped (J. Kraft, personal communication, 2006). Some of the manganiferous soils were classified within the established Benevola series, which, according to the Official Series Description, is formed in marble residuum, may have a black C horizon, and has a fine family particle-size class. It is presumed that the black color of the C horizon is derived from extremely high amounts of Mn, although this is not explicit in the Benevola Official Series Description. Many of the pedons described by NRCS soil scientists, however, did not fit within the Benevola series because they had loamy textures. Therefore, for mapping purposes, the NRCS considered them to be like the Letort series (and included them within the Conestoga and Letort mapping unit), which has a dark-colored C horizon (as dark as 10YR 3/2), and is formed in residuum from interbedded calcareous and non-calcareous metamorphic rocks. The Letort soil is generally considered to be formed from dark-colored graphitic phyllites or phyllites. The

Conestoga series is formed in residuum mostly from micaeous limestone and calcareous phyllite, has a fine-loamy particle size, and is relatively brighter and redder than Letort (with no evidence of extremely high amounts of Mn).

The manganiferous soils are found in the Western Division of the Piedmont physiographic province, which is characterized by its undulating (foothills) topography, weakly metamorphosed Precambrian bedrock, and soils formed mainly in residuum. The rocks of the area have much interbedding and folding, and are dominated by phyllites and metabasalts, but there are some small areas of limestone or marble. Thus, there are some areas of limited extent where soils (such as those classified as the Frederick, Benevola, or Conestoga series) are formed in residuum from calcareous rocks.

In South Africa, there is a limited area of similarly unusual manganiferous soils where Mn is found in extremely high concentrations (up to 58.3 g kg^{-1} Mn as Mn oxides) and the whole soil matrix is colored black (Dowding and Fey, 2007). These soils are thought to form as a result of congruent dissolution (i.e., simple dissolution of constituent ions) of dolomite and accumulation of Mn-rich non-carbonate residue (Hawker and Thompson, 1988). These manganiferous soils have a characteristic morphology and spatial variation with topography. In lower-lying landscape positions, the soils tend to be deeper, redder, and contain more ferromanganiferous nodules. On slopes and higher-lying landscape positions, the soils tend to be shallower, and sometimes have an abrupt contact with dolomite bedrock (Dowding and Fey, 2007).

Recently, Electromagnetic Induction (EMI) has been introduced as an efficient remote sensing method with a variety of practical applications in high-intensity soil

survey, which is defined as having a map scale larger than 1:12,000 (NRCS, 1999). EMI techniques measure apparent electrical conductivity (EC_a) of the soil, which can be affected by a variety of soil factors, including soil texture (Williams and Hoey, 1987), cation exchange capacity (McBride et al., 1990), and salinity (Rhoades and Corwin, 1981). Also, some pedologic features such as clay lenses may be mapped if an empirical relationship can be established between EC_a measurements and the feature of interest (Doolittle et al., 1994; Cockx et al., 2007). EMI surveys may supplement soil survey information by allowing one to obtain high-resolution spatial variations in EC_a that may be related to soil characteristics. This technique is most effective when the factor of interest is not confounded by other soil factors.

Aside from limited knowledge acquired by NRCS soil scientists, there is little known about the manganiferous soils of Maryland. We aim to make a more detailed assessment of the spatial distribution of these manganiferous soils and their relationship with geologic and soil surveys. Our objectives are, therefore, 1) to approximate the areal extent of manganiferous soils in the MD Piedmont, and 2) to better understand what governs their distribution across the landscape.

MATERIALS AND METHODS

Reconnaissance Assessment

Field reconnaissance was first required in order to identify where the manganiferous soils generally occur, and where areas of manganiferous soils might be accessible for further study. Using ArcGIS 9.0, digital soil survey and geology data for

Frederick and Carroll Counties were used to guide our field investigations. Since NRCS soil scientists had discovered some areas of manganiferous soils in eastern Frederick County, and had included them in the Conestoga and Letort mapping unit, we identified the study area as the full extent of the Conestoga and Letort mapping unit in Maryland, which included eastern Frederick County and far western Carroll County. Approximately one month (June 2006) was spent scouting the general vicinity where manganiferous soils were thought to occur (based on observations made by NRCS soil scientists), between Libertytown and Union Bridge, MD. Two approaches were used during the reconnaissance assessment. The first approach was "opportunistic" sampling, where we attempted to travel nearly every road in the study area, looking for road cuts and exposed agricultural fields that appeared especially dark in color. Any soil that was dark-colored and was easily accessible was examined. The second reconnaissance approach was guided by existing soil and geological information. Since manganiferous soils had been included in the Conestoga and Letort mapping unit, areas included in delineations of this map unit were visited. Because NRCS soil scientists thought that manganiferous soils tended to occur in relation to marble bedrock (J. Kraft, personal communication), areas mapped as marble in the geological survey were also examined.

At each location where soils were examined, GPS coordinates were logged using a handheld Garmin GPS unit, and a surface soil sample was collected to a depth of 5-10 cm. In some cases, a bucket auger was used to examine the soil up to 150 cm below the surface. Five drops of 10% hydrogen peroxide (H_2O_2) were applied to the soil material in the field to confirm the presence of Mn oxides. (Often, 30% H_2O_2 is used for this purpose, but for safety reasons it was preferred to use a lower concentration, and due to

the high concentrations of Mn oxides in the soils, 10% H_2O_2 proved adequate.) From tests on air-dried soil samples in the lab, it was noted that the strength of reaction of soil material with 10% H_2O_2 was related to the quantity of Mn oxides present. Therefore, a semi-quantitative scale was developed to rapidly estimate the amount of Mn oxides in a soil sample based on the strength of reaction with 10% H_2O_2 (Table 3-1). The strength of reaction was compared with the Mn content of selected samples, which was measured using a dithionite-citrate-bicarbonate extraction (a slightly modified version of the method of Mehra and Jackson (1960)). This permitted us to develop a semi-quantitative relationship between H_2O_2 reaction and the Mn content.

Table 3-1. Semi-quantitative test for Mn oxide content developed specifically for this study. Strength of reaction after application of 5 drops 10% H_2O_2 to soil indicates approximate Mn content.

Relative reaction strength	Observation	Approximate Mn content	
		Description	Value
			g kg^{-1}
0	No reaction evident	Typical (for non-manganiferous soils)	<1
1	Slight reaction	Typical (for non-manganiferous soils)	<1
2	Moderate reaction, little to no gas evolved	Moderately high	2-5
3	Moderately strong reaction, some gas evolved	High	5-10
4	Strong reaction, moderate amount of gas evolved	Very high	10-30
5	Very strong and fast reaction, much gas evolved	Extremely high	>30

Soil-Landscape Studies

After conducting the reconnaissance assessment, six sites with manganiferous soils were identified for more detailed transect work. The purposes of the transect work were 1) to estimate the size of manganiferous soil units; 2) to determine any possible relationship between the soils and landscape position; 3) to document the range in morphological properties of manganiferous soils; and 4) to identify possible sites for further intensive analysis.

At each transect site, a bucket auger was used to examine pedons along topographic gradients over landforms. Transects were generally located normal to the topographic gradient, and a series of observations was made along the transect. The locations of observations were chosen purposefully to capture the range of soil properties of the site. Typically, a pedon was initially examined where the soil was suspected to be manganiferous (using clues from the reconnaissance assessment such as a dark surface). Other pedons were then observed nearby. Five to twelve pedons were examined along each transect. Occasionally, rock fragments or shallow bedrock would prevent augering at a specific point along a transect, in which case observations were made as near as possible to the targeted location. Whenever possible, edges of the manganiferous soil units were identified, and soils were described as deeply as possible in order to fully document the soil properties. Standard field morphological descriptions at each point included horizon depth, moist Munsell color, texture by feel, color and abundance of features such as nodules (Schoeneberger et al., 2002), and the strength of reaction of the soil material with 10% H_2O_2 (in the field) using the scale developed specifically for this study (Table 3-1). GPS coordinates were recorded at each auger boring using a Garmin

handheld GPS unit. A rod and level were used to measure the relative elevation of the ground surface of the location of each pedon so that cross-sections of the sites could be constructed. Absolute elevation at each site was estimated using Maryland Geological Survey maps.

Electromagnetic Induction Survey

In November 2006, with the assistance of James Doolittle (USDA-NRCS), an initial pedestrian Electromagnetic Induction (EMI) survey was conducted at the Grossnickle site. An EMI meter (model EM38DD from Geonics Ltd.) was oriented to collect data in the vertical dipole orientation, measuring to a depth of 150 cm. The EMI meter was carried across the field, in transects of approximately 10 m apart, and measurements were taken approximately every 1 m. The EMI meter was also used to survey transects (in the area suspected to be highly manganiferous) approximately 5 m apart, with measurements taken approximately every 1 m. A GPS unit was configured to collect coordinates simultaneously with EC_a readings, using the NAV38DD program on an Allegro CX field computer. Later, three sites (the Dotterer, Grossnickle, and Flickinger sites) were each surveyed in March 2007 using the following methods. Two EMI meters (model EM38DD from Geonics Ltd.) were mounted on a plastic toboggan, which was towed behind a 4-wheel all-terrain vehicle. One of the meters was oriented in the horizontal position to measure to a depth of 75 cm, and the other meter was oriented in the vertical direction to measure to a depth of 150 cm. A GPS unit was configured to collect coordinates simultaneously with EC_a readings, using the NAV38DD program on

an Allegro CX field computer. The vehicle was driven over each field at 1 to 3 m s^{-1} in roughly parallel transects to collect data in a systematic manner. Transects were approximately 10-20 m apart, and readings were collected approximately every 2-4 m. At the time of this investigation, the soil temperature at a depth of 50 cm was 8°C. All EC_a data have been corrected to a standard temperature of 25°C by multiplying EC_a by a factor of 1.488 (J. Doolittle, personal communication). Maps were generated with ArcGIS 9.0 using ordinary kriging of data.

RESULTS AND DISCUSSION

Reconnaissance Assessment

Figure 3-1 shows the area where reconnaissance investigations of manganiferous soils in Maryland were focused, and also the general geology of the region. NRCS soil scientists found that manganiferous soils usually occurred in areas mapped as Sams Creek Marble and Wakefield Marble (J. Kraft, personal communication), which are both part of the Sams Creek Formation, which consists mainly of greenish metabasalt and phyllite, with few small lenses of marble and quartzite. Sams Creek Marble is a fine-grained, white to grey and reddish-purple calcitic and dolomitic marble up to 6 meters thick. The Wakefield Marble member, which occurs in the lower part of the Sams Creek Formation, is mainly white to grey, and contains interbedded green and purple phyllite. Some zones of the marble are primarily calcitic, while other zones are primarily dolomitic. The thickness of the Wakefield Marble member is estimated to range between 1 and 150 m.

General Location and Geology of Study Area

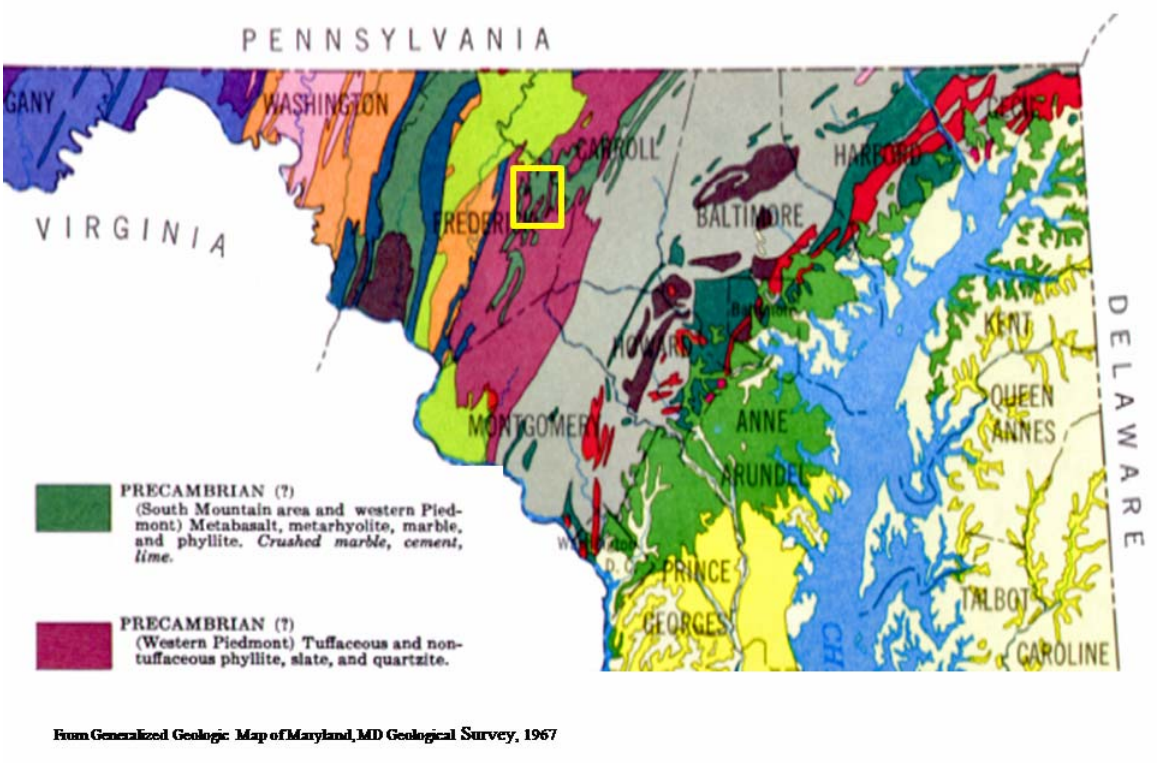

Fig. 3-1. The yellow rectangle shows the approximate location of manganiferous soils/ reconnaissance sampling in Frederick County, MD, in the Western Division of the Piedmont. The geology of the area is dominated by metabasalt and phyllite, with some areas of marble, metarhyolite, slate, and quartzite.

Our reconnaissance investigations demonstrated that soils in or near areas mapped as Sams Creek Marble or Wakefield Marble generally showed stronger reactions with hydrogen peroxide (2-3 on scale in Table 3-1) (indicating higher Mn concentrations) than soils overlying other geologic units. In addition, it seems that soils which occur within delineations of the Conestoga and Letort or Benevola map units (or close to those areas) tended to produce stronger reactions with hydrogen peroxide during the reconnaissance assessment (Fig. 3-2), indicating higher Mn contents. For comparison, soils formed in the New Oxford sedimentary bedrock to the northwest of the study area (northwest of Route

75 in Fig. 3-2), where marble and delineations of the Conestoga and Letort and Benevola map units are absent, produce weak reactions (0-1 on scale in Table 3-1) with hydrogen peroxide. These results generally support the observations reported by the NRCS.

Although the blackest horizons (most enriched in Mn) typically occur below the surface (see Figs. 3-5, 3-6, 3-8, 3-11, and 3-12), the manganiferous soils commonly have enough Mn oxides in the surface horizon to cause a relatively strong reaction (2-3 on scale in Table 3-1) with 10% H_2O_2. Therefore, our reconnaissance assessment of surface horizons proved useful in identifying general areas where manganiferous soils occur. There is no evidence that manganiferous soils occur beyond the general region of approximately 200 km^2 where the Conestoga and Letort and Benevola mapping units are described.

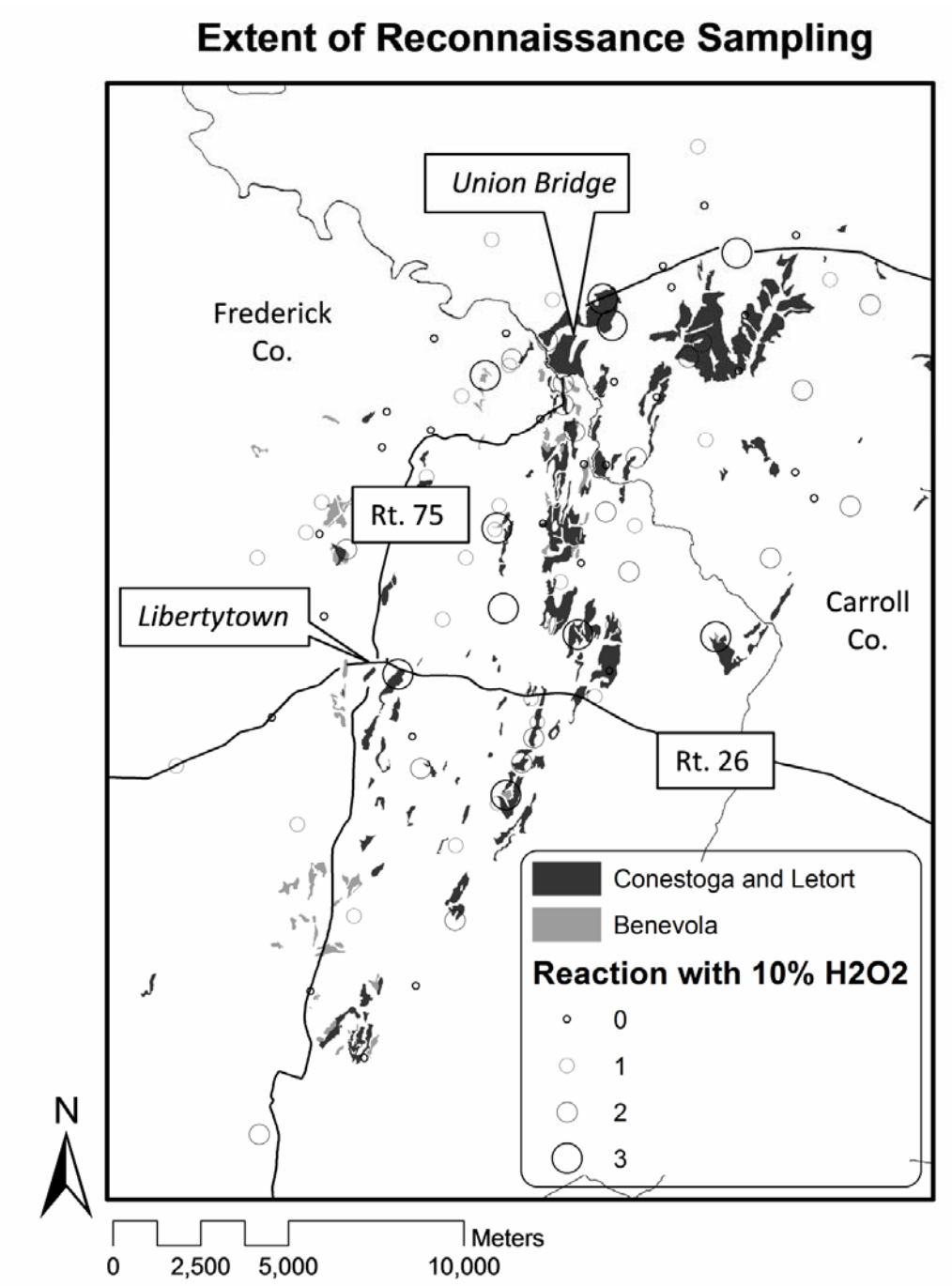

Fig. 3-2. Map showing eastern Frederick County and western Carroll County, where manganiferous soils had been reported. Map shows full extent of two mapping units associated with manganiferous soils: the Conestoga and Letort mapping unit, and the Benevola mapping unit (from the Frederick County Soil Survey, NRCS, 2002, and the Carroll County Soil Survey, 1969). Each circle represents a location where the surface soil horizon was examined during the reconnaissance assessment. Size of circle indicates semi-quantitative Mn content based on strength of reaction with 10% H_2O_2 (same scale as in Table 3-1): 0-1 is approx. <1 g kg^{-1} Mn (typical for most soils); 2 is approx. 2-5 g kg^{-1} Mn; and 3 is approx. 5-10 g kg^{-1} Mn.

Soil-Landscape Studies

Six sites containing manganiferous soils were identified where transects across landscapes could be studied. The Dotterer and Grossnickle sites (identified by their respective landowners) and the Pearre Road site were previously known to the NRCS. The Flickinger site (also identified by landowner), Clemsonville Road and Emerson Burrier Road sites were identified during the reconnaissance survey.

Dotterer Site

The Dotterer (DOT) site is located approximately 5 km north of Libertytown, MD (Fig. 3-3). This area is mapped as the Ijamsville Formation (Maryland Geological Survey, 1986), which consists mainly of purple phyllite, and the soils surrounding the manganiferous soils at this site contain considerable amounts of phyllite fragments, which may be seen on and below the soil surface. A phyllite outcrop could be observed in the field as well (visible as a small wooded patch east of Pedon 221 in Fig. 3-4). In the area sampled at the DOT site, soils occur within a delineation of the Conestoga and Letort mapping unit, and in addition to the dark soils, there are various other light-colored soils surrounding the area, which would be considered more typical for those formed in phyllite residuum (Fig. 3-4). Since the Conestoga and Letort mapping unit (and manganiferous soils) are associated with marble bedrock, and since marble exists in this region as small lenses, it is likely that the DOT site is underlain by a marble lens that was overlooked during the geologic mapping.

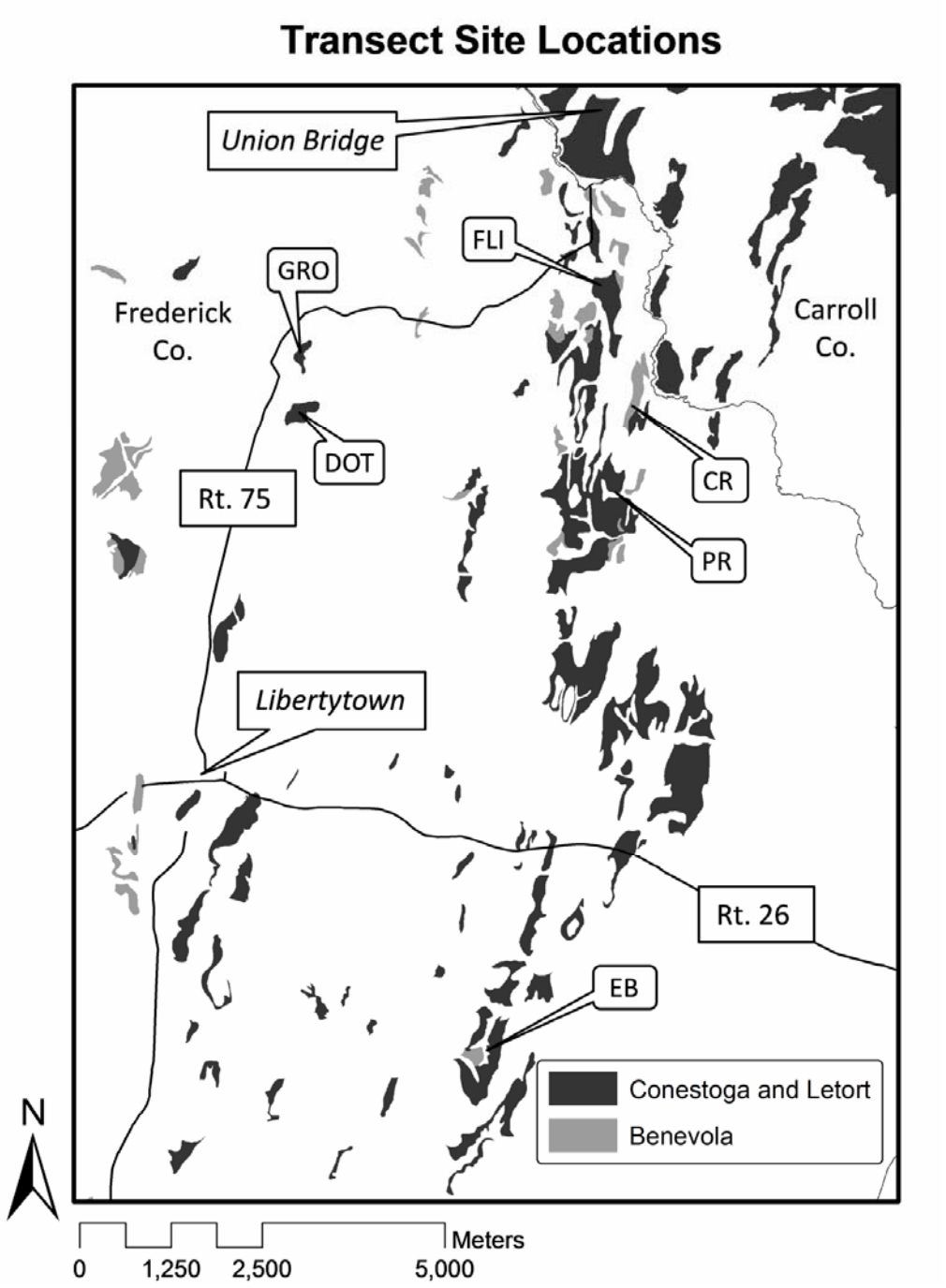

Fig. 3-3. Map showing locations of transect sites, all within the vicinity of Libertytown and Union Bridge, Maryland. CR=Clemsonville Rd.; DOT=Dotterer; EB=Emerson Burrier Rd.; FLI=Flickinger; GRO=Grossnickle; PR=Pearre Rd. Extent of mapping units (Conestoga and Letort and Benevola) associated with manganiferous soils are shown (from the Frederick County Soil Survey, NRCS, 2002, and the Carroll County Soil Survey, NRCS, 1969).

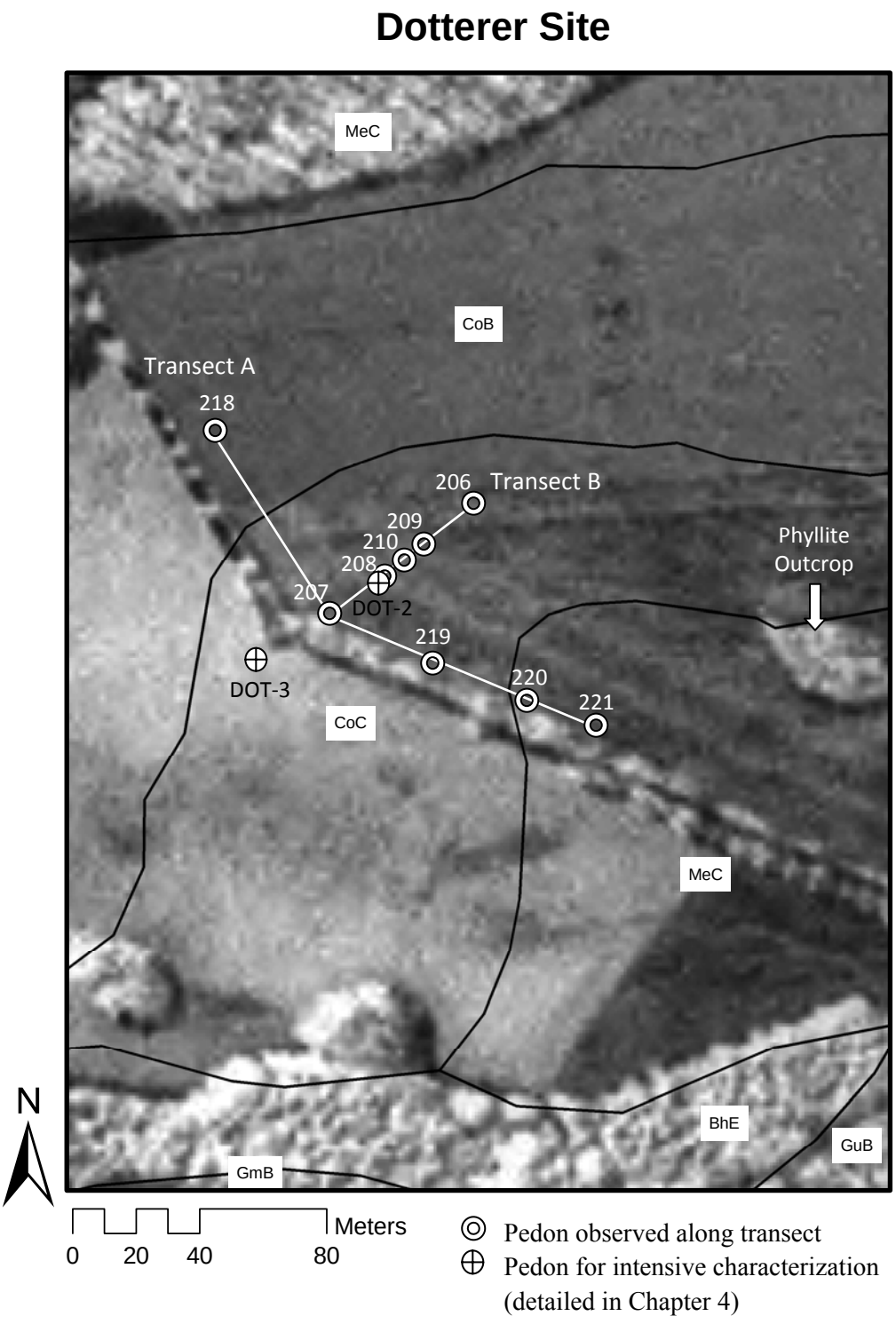

Fig. 3-4. Soil survey map (from the Frederick County Soil Survey, NRCS, 2002) of the Dotterer site showing locations of Transects A and B. BhE=Blocktown gravelly loam, 25 to 45% slopes; CoB=Conestoga and Letort silt loams, 3 to 8% slopes; CoC= Conestoga and Letort silt loams, 8 to 15% slopes; GuB=Glenville-Baile silt loams, 3 to 8% slopes; MeC=Mt. Airy channery loam, 8 to 15% slopes.

Dotterer Transect A (Fig. 3-5) shows a very deep (up to 7 m) but localized accumulation of black (5YR 1/1) soil material with low bulk density and a loam or silt loam texture at pedons 207 and 219. This black material reacts violently with 10% H_2O_2 (5 on scale in Table 1), so it contains extremely high amounts of Mn oxides. Pedons 207, 219, and 220 all show very dark colors in subsoil horizons, and react strongly with hydrogen peroxide. These highly manganiferous pedons are located at shoulder and backslope landscape positions. At pedons 221 and 218, the soil is much lighter in color, and the presence of purple-blue phyllite channers, saprolite, or bedrock prevented augering beyond shallow depths.

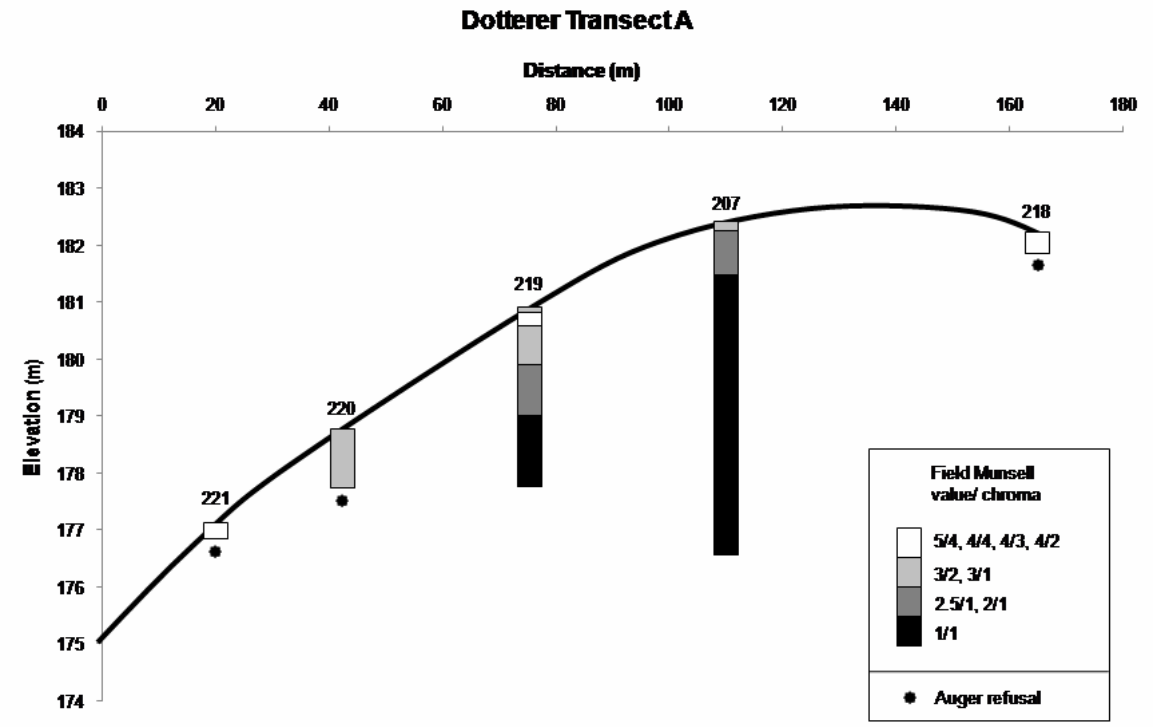

Fig. 3-5. Vertical cross-section of Dotterer Transect A, summarizing the matrix colors of the pedons. (Accompanying morphological descriptions may be found in Appendix A.)

Dotterer Transect B (Fig. 3-6) runs perpendicular to Dotterer Transect A, and intersects it at pedon 207 (Fig. 3-4). Dotterer Transect B shows a thick accumulation of Mn-enriched soil at pedons 207 and 208, with gradation in color from a Munsell value of 1 at pedon 207 to Munsell values of 2 and 3 at pedons 208 and 210. Beyond pedon 210, the soils are much shallower and lighter in color.

The manganiferous pedons at the DOT site (207, 208, 210, 219, and 220) would probably be included within the mapping concept of Letort-type soils by the NRCS due to their very dark C horizons and loamy texture throughout. However, the manganiferous soils truly do not fit the Letort official series description. The dark color of manganiferous soils is derived from extremely high amounts of Mn, rather than graphitic carbon in the phyllite and phyllite residuum parent material of true Letort soils (which are mapped in eastern Pennsylvania). In addition, manganiferous soils (especially pedon 207) have horizons darker than Munsell value/ chroma of 3/2, which is the requirement for the Letort series, so these soils cannot be properly classified as Letort, or likely any established series. The lighter-colored pedons rich in phyllite which surround the manganiferous soils occur within a delineation of the Mt. Airy channery loam mapping unit (Fig. 3-4). However, these non-manganiferous soils are more similar to the Linganore series (Loamy-skeletal, mixed, active, mesic Ultic Hapludalfs formed in residuum from hard micaceous phyllites and phyllites) because they have argillic horizons (see Appendix A for morphological descriptions).

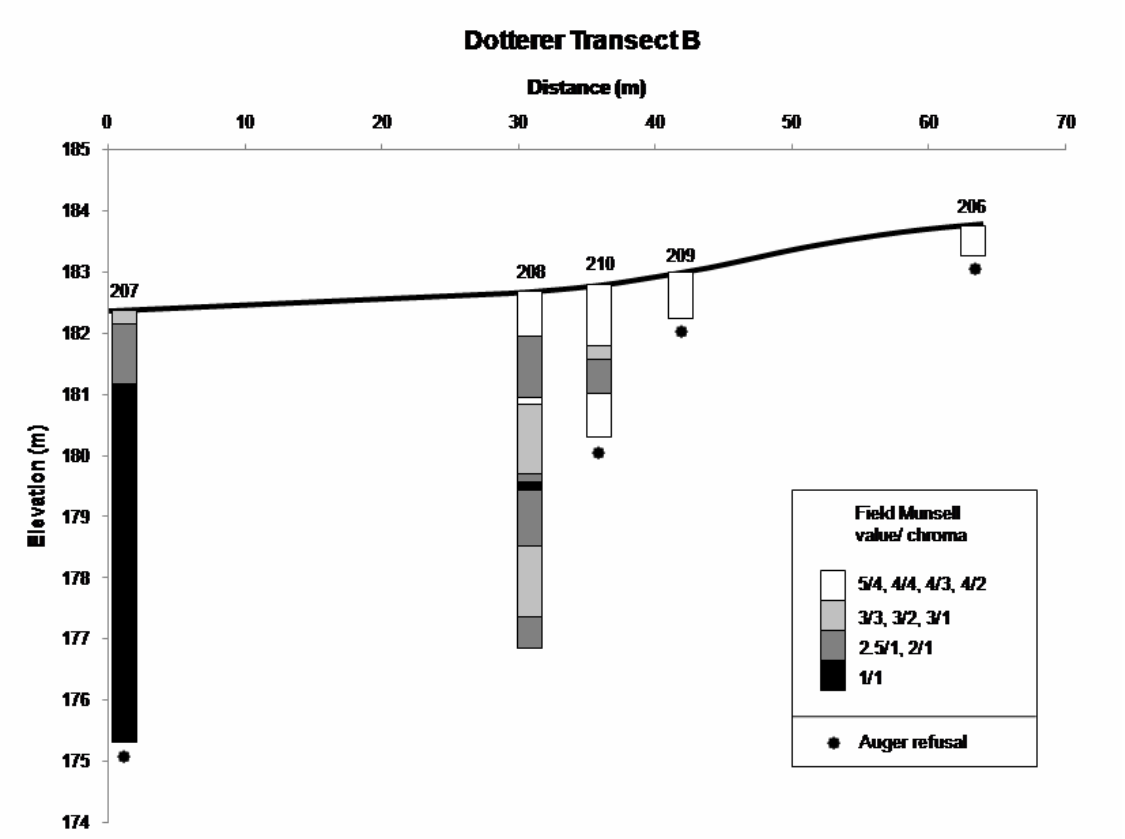

Fig. 3-6. Vertical cross-section of Dotterer Transect B, summarizing the matrix colors of the pedons. (Accompanying morphological descriptions may be found in Appendix A.)

Based upon observations of the vertical cross-sections of DOT Transects A and B (Figs. 3-5 and 3-6), it seems that the area of manganiferous soil at this site is approximately 1 ha or less.

Grossnickle Site

The Grossnickle (GRO) site is located approximately 0.5 km north of the Dotterer site, or 5.5 km north of Libertytown, MD (Fig. 3-3). Like the Dotterer site, the geological mapping of this area shows it is in the Ijamsville Formation, but is likely underlain by a marble lens for the same reasons. The area sampled at the GRO site is included within a delineation of the Conestoga and Letort mapping unit, with other mapping units typical of non-manganiferous soils (such as Glenelg or Mt. Airy) surrounding the area (Fig. 3-7).

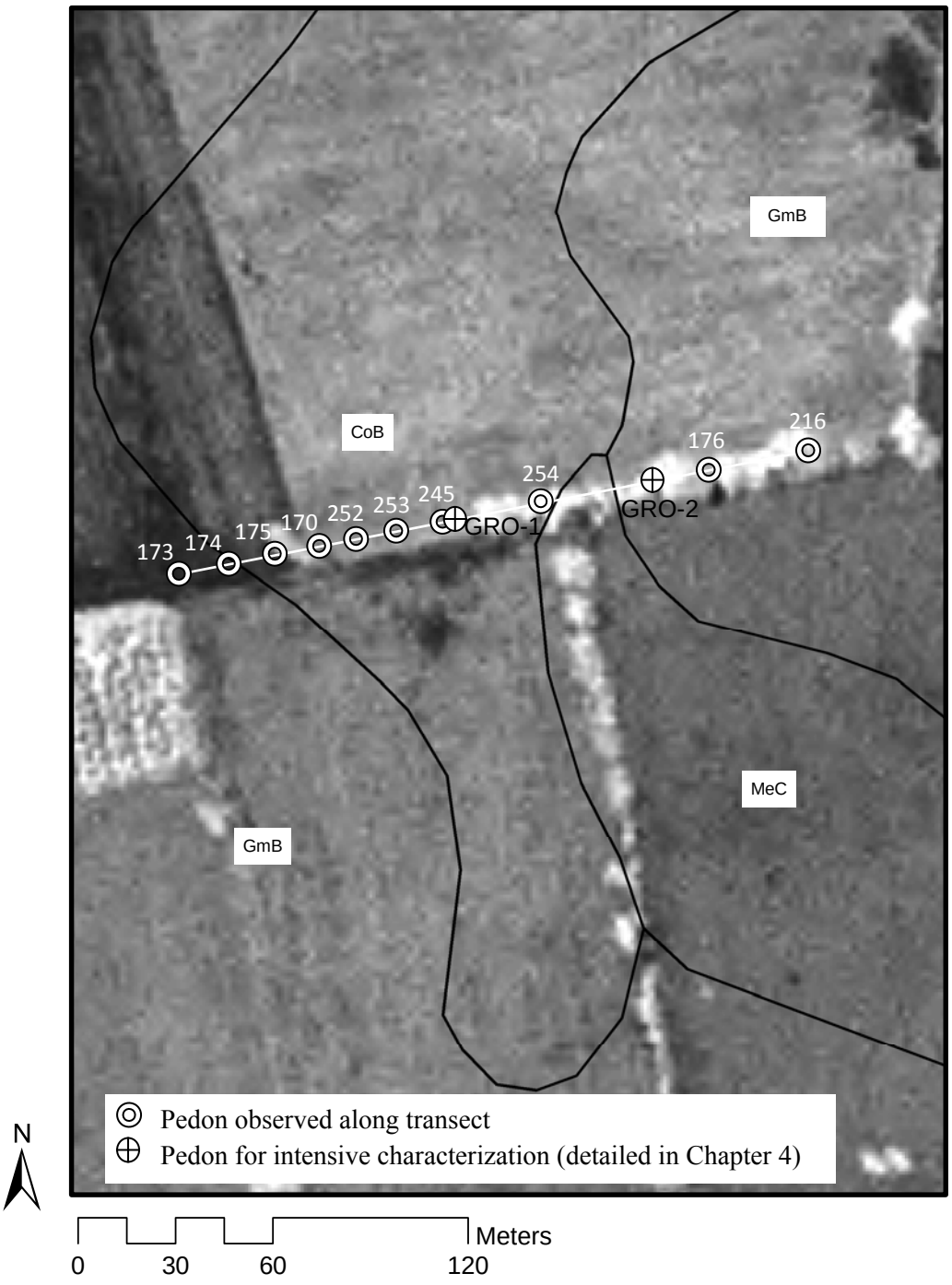

Fig. 3-7. Soil survey map (from the Frederick County Soil Survey, NRCS, 2002) of the Grossnickle site showing location of transect. CoB=Conestoga and Letort silt loams, 3 to 8% slopes; GmB=Glenelg-Mt. Airy channery loams, 3 to 8% slopes; MeC=Mt. Airy channery loam, 8 to 15% slopes.

The Grossnickle transect (Fig. 3-8) shows a thick, localized accumulation of black, Mn-enriched soil up to 7 m deep, much like the Dotterer site. The black (5YR 1/1) material which is observed in pedons 253, 245, and 254 shows a lateral gradation into lighter shades (value/ chroma of 3/3) at the edges (pedons 170, 252, 176, and 216). The light-colored soils rich in phyllite fragments which border the black lens of manganiferous material and this site correspond with the area mapped as Glenelg-Mt. Airy in the soil survey (Fig. 3-7). Manganiferous soils at this site extend from the summit down to the footslope, although the strongest expression of the manganiferous soil runs from the summit through the backslope. All of the manganiferous pedons would probably be considered to fall within the mapping concept of Letort-type soils used by the NRCS for soil mapping purposes because of their dark color and loamy textures. However, these soils really do not fit the Letort series description because they are darker than Munsell value/ chroma of 3/2 and may have a different parent material. Although a perpendicular transect was not made at the GRO site, visual observations of the soil surface indicate that the area of manganiferous soils at this site is approximately 1 ha or less.

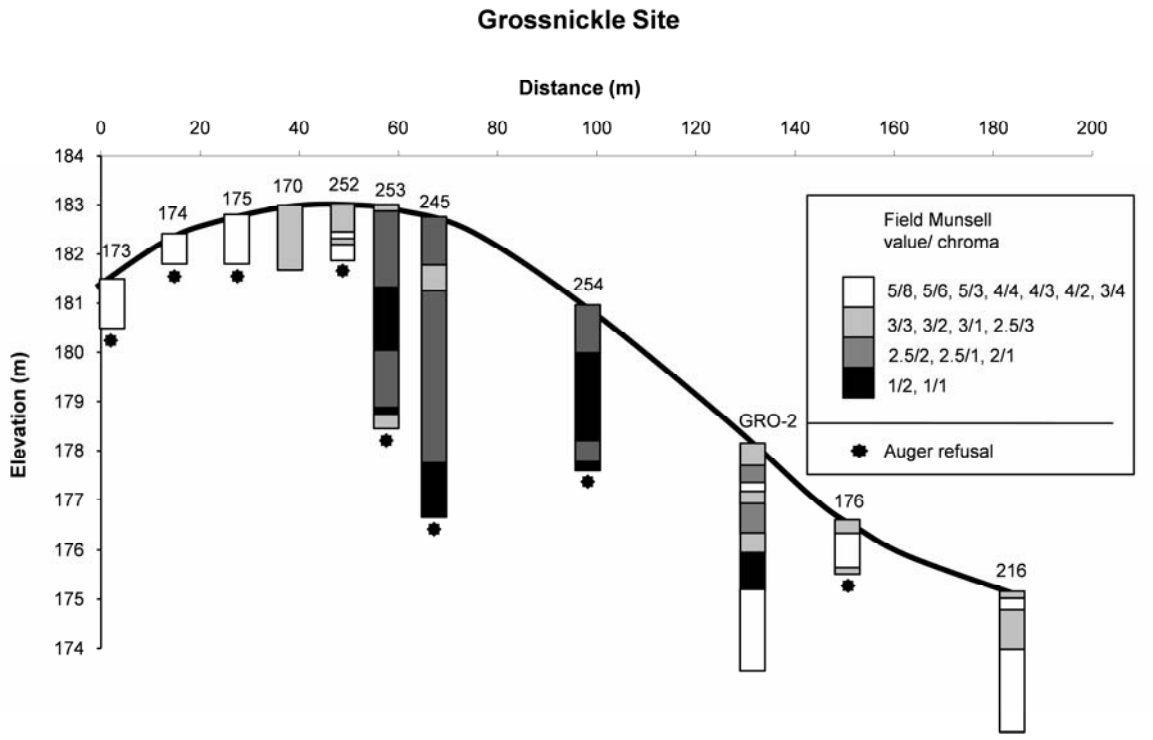

Fig. 3-8. Vertical cross-section of the Grossnickle transect, summarizing the matrix colors of the pedons. (Accompanying morphological descriptions may be found in Appendix A; morphological description of GRO-2 pedon may be found in Table 4-4.)

Flickinger Site

The Flickinger (FLI) site is located approximately 2.5 km south of Union Bridge, MD (Fig. 3-3). The area is underlain by the Sams Creek Formation, with folds creating alternating north-south-trending bands of Sams Creek Phyllite and Wakefield Marble (Fig. 3-9). Wakefield Marble is quarried to the east of the Flickinger site by Lehigh Cement Co. (Fig. 3-9). The FLI site occurs mainly within a delineation of the Conestoga and Letort mapping unit. A delineation of the Benevola mapping unit also occurs nearby (Fig. 3-10).

Flickinger Site Geology

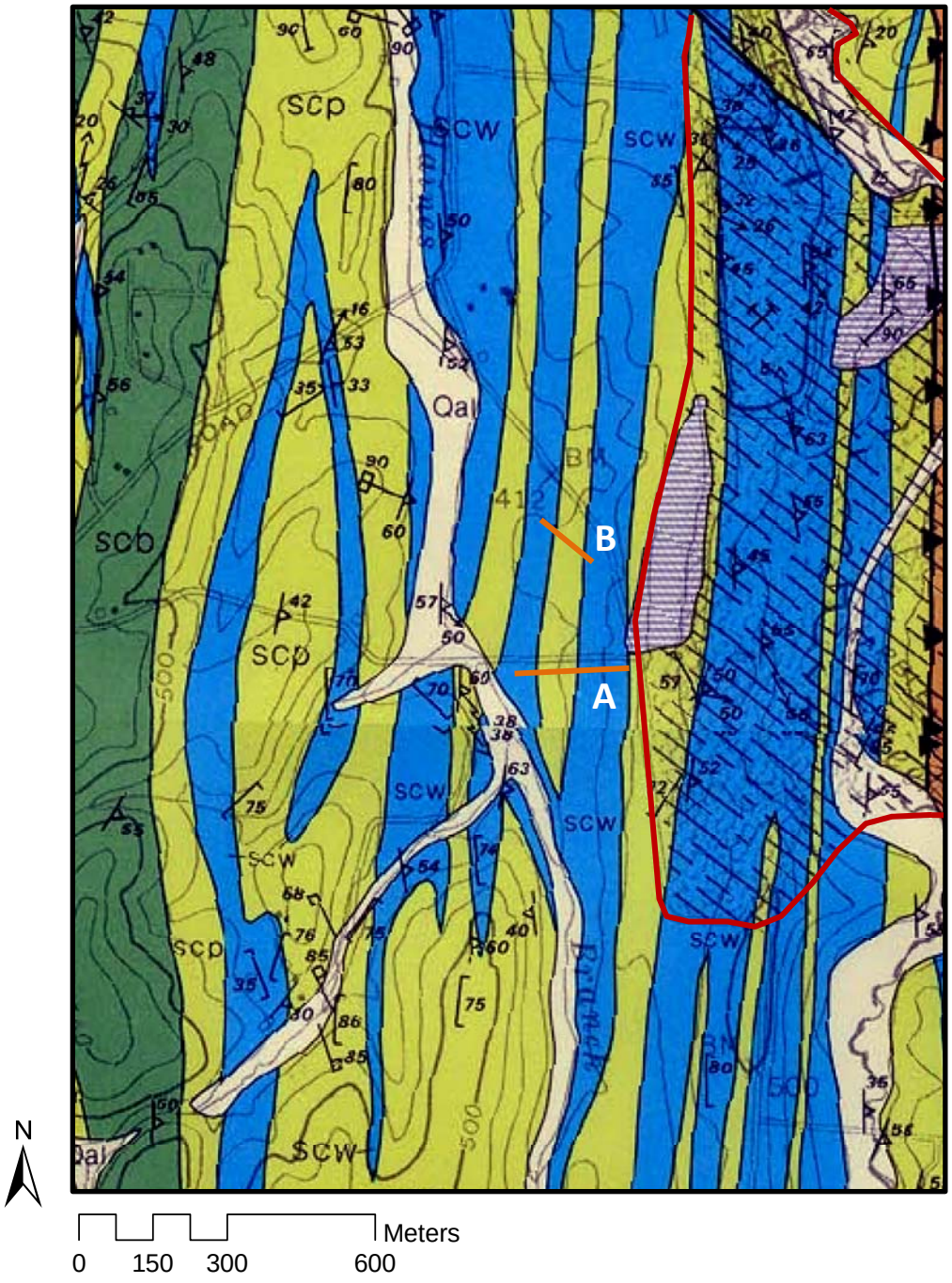

Fig. 3-9. Geology map of the Flickinger site, from the Geologic Map of the Union Bridge Quadrangle (Maryland Geological Survey, 1986). The blue (scw) areas are Wakefield marble, the light green (scp) areas are Sams Creek phyllite, and the dark green (scb) areas are Sams Creek metabasalt (greenstone). All are part of the Sams Creek Formation. Hatched area outlined in red on east side of map is Lehigh Cement quarry. Locations of Transects A and B are shown in orange.

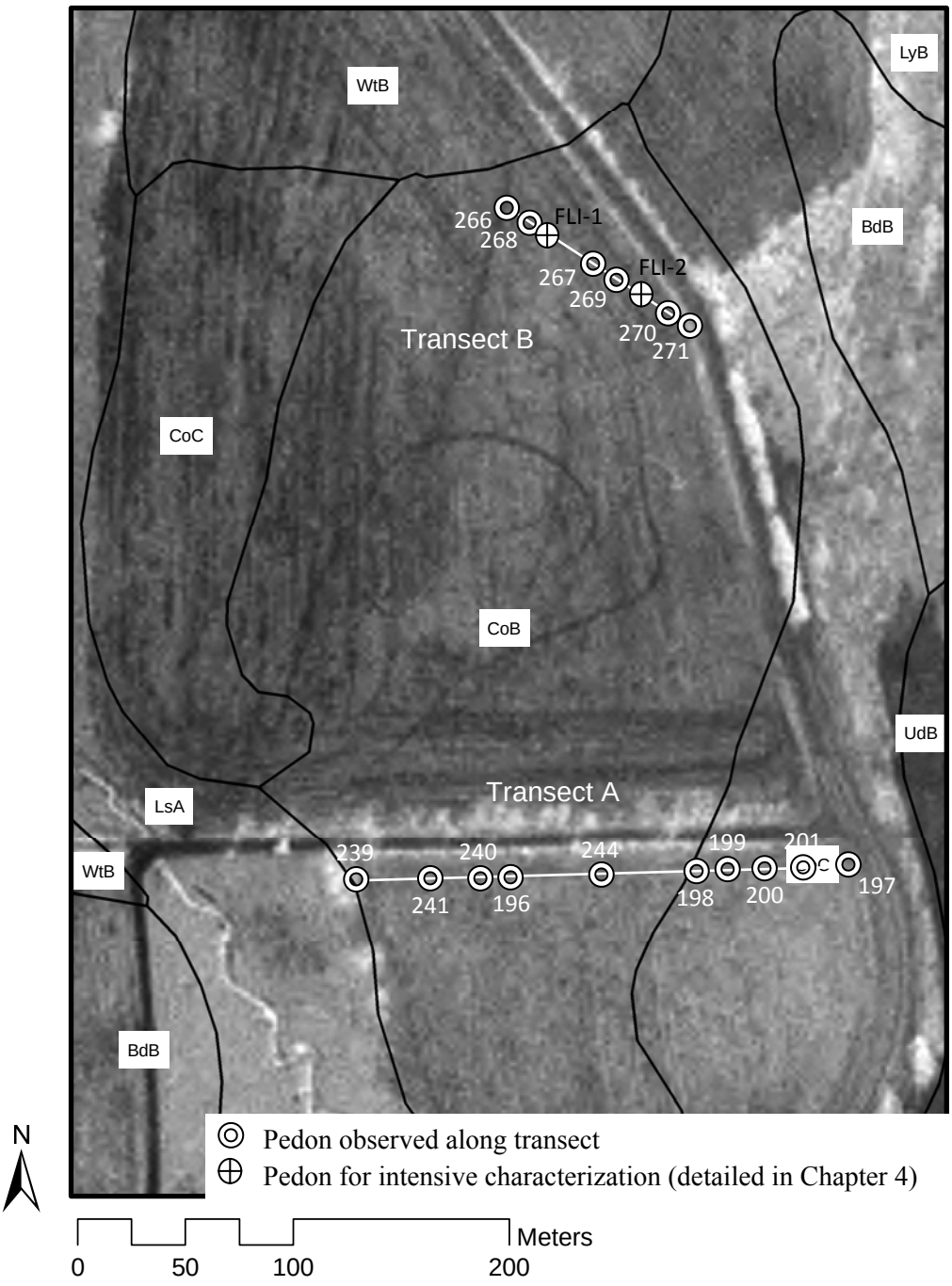

Fig. 3-10. Soil survey map (from the Frederick County Soil Survey, NRCS, 2002) of the Flickinger site. Locations of Transects A and B are shown. BdB= Benevola silty clay loam, 0 to 8% slopes; CoB= Conestoga and Letort silt loams, 5 to 8% slopes; CoC= Conestoga and Letort silt loams, 8 to 15% slopes; LyB= Linganore-Hyattstown channery silt loams, 3 to 8% slopes; LsA= Lindside silt loam, 0 to 3% slopes; UdB=Udorthents, smooth, 0 to 8% slopes; WtB= Wiltshire-Funkstown complex, 0 to 8% slopes.

The middle part of Flickinger Transect A (Fig. 3-11) has black, loamy, Mn-rich material with low bulk density in the lower part of the profiles (BC horizons). This black color is lost gradually downslope, especially in pedons 239 and 241. The auger was usually refused within a few meters at this transect, probably due to the presence of shallow marble bedrock (observed outcropping at surface near pedon 244). In all of the pedons along Transect A, soil with a much lighter color and finer texture overlies the black, Mn-rich material. These soils might be closest to the Benevola series because of their black C horizons, fine textures and marble bedrock.

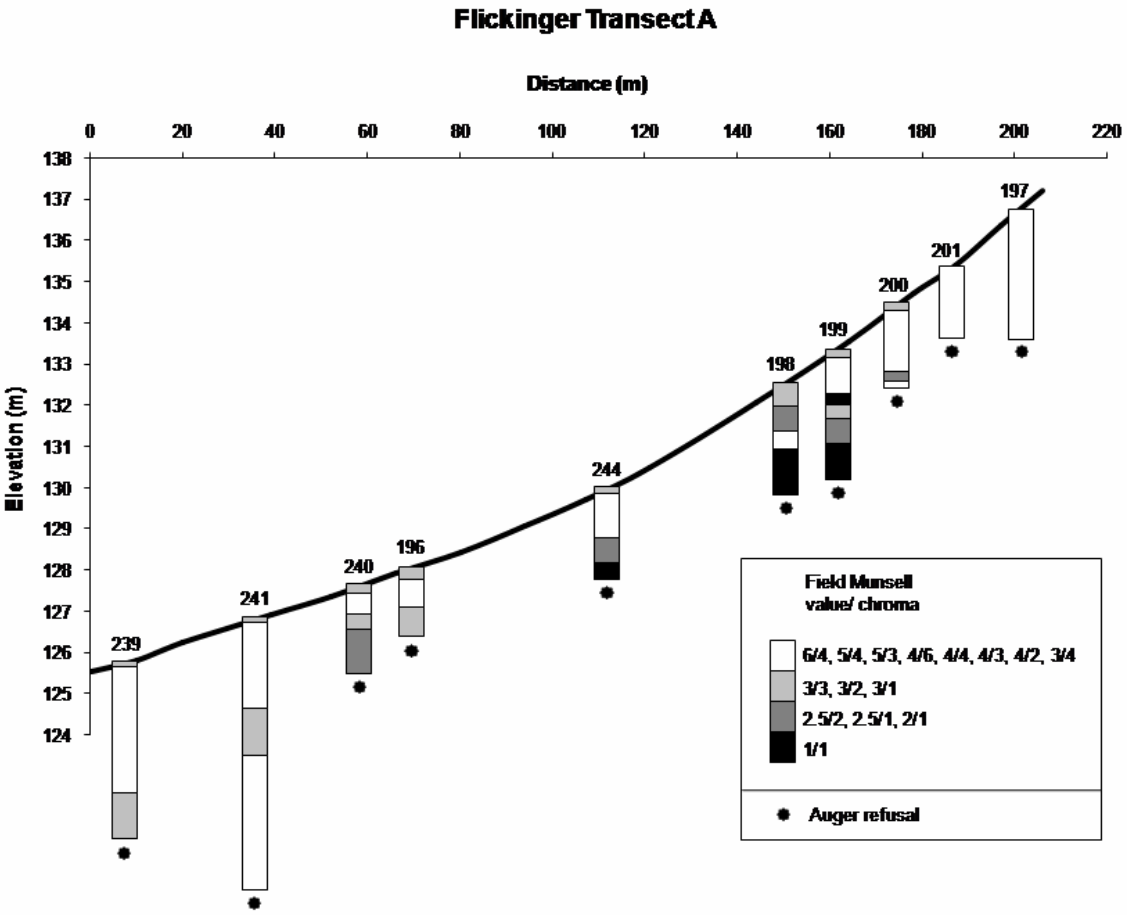

Fig. 3-11. Vertical cross-section of Flickinger Transect A, summarizing the matrix colors of the pedons. (Accompanying morphological descriptions may be found in Appendix A.)

Flickinger Transect B (Fig. 3-12) was constructed on another field on the property (Fig. 3-10), and shows an irregular, heterogeneous accumulation of Mn oxides. The only pedon in this transect with value and chroma of 1/1 is number 270, but the remainder of the pedons show very dark material in the lower part with light-colored horizons in the upper part, and an abrupt boundary (color change) between the brighter Bt horizons and

the very dark BC horizons. The location of manganiferous soils in this transect shows no relation to the landforms.

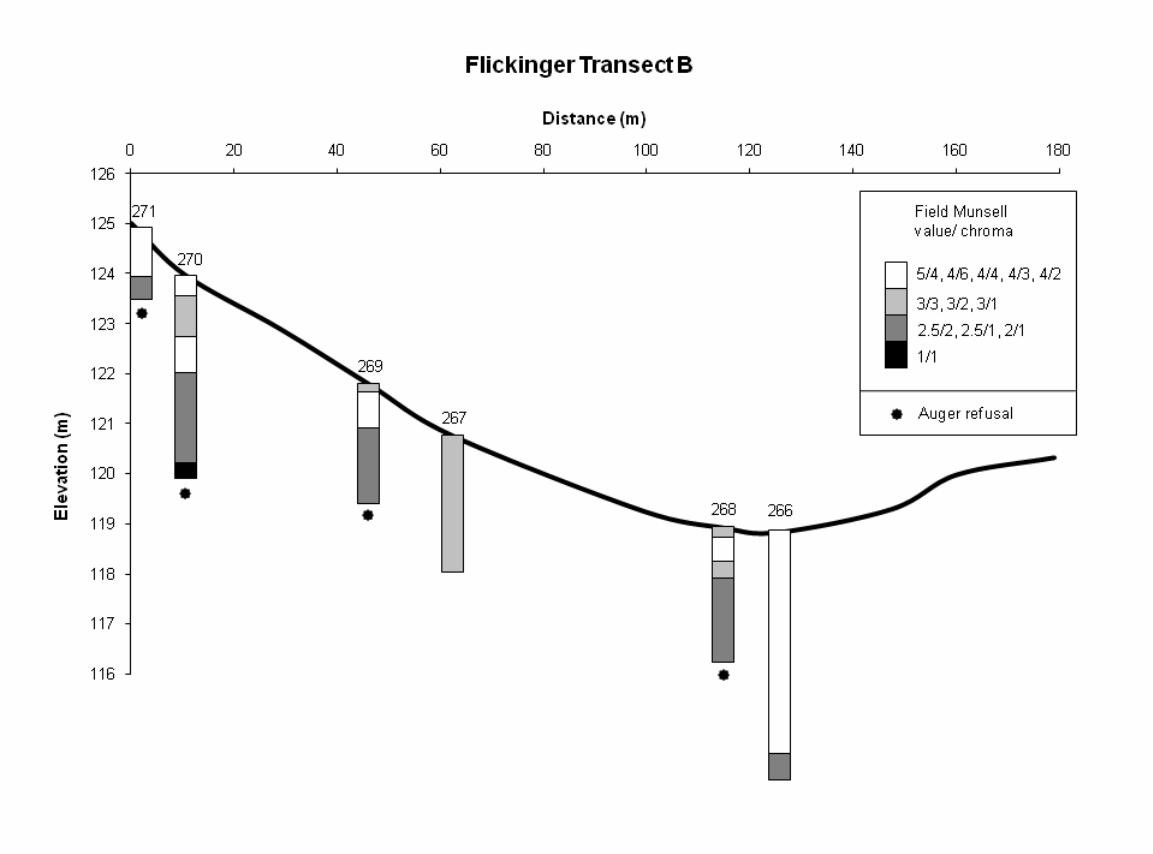

Fig. 3-12. Vertical cross-section of Flickinger Transect B, summarizing the matrix colors of the pedons. (Accompanying morphological descriptions may be found in Appendix A.)

Observations of the vertical cross-sections of FLI Transects A and B (Figs. 3-11 and 3-12), as well as visual observations of the soil surface, indicate that the area of manganiferous soils at the FLI site may be up to a few ha, which is larger than the areas of manganiferous soils at the DOT and GRO sites.

Clemsonville Road Site

The Clemsonville Road (CR) site is located approximately 4 km south of Union Bridge, MD (Fig. 3-3). The CR site has very similar geology to the Flickinger site (similar to that seen in Fig. 3-9) and occurs mainly within delineations of the Conestoga and Letort and Benevola mapping units. The pedons examined along the CR transect show subsoil horizon colors as dark as Munsell value/ chroma of 3/3, and black (1/1) nodules are present throughout (Fig. 3-13, Appendix A). At the CR site, manganiferous nodules and coatings were found at all landscape positions (from summit to footslope) across undulating topography. This site has one of the few areas observed where the darker soil material overlies lighter soil material (at pedons 179 and 178). The GRO-2 pedon shows a similar pattern of darker soil over lighter soil (Fig. 3-8).

Fig. 3-13. Vertical cross-section of Clemsonville Road Transect, summarizing the matrix colors of the pedons. (Accompanying morphological descriptions may be found in Appendix A.)

Pearre Road Site

The Pearre Road (PR) site is located approximately 4.5 km south of Union Bridge, MD (Fig. 3-3). The PR site has very similar geology to the Flickinger site (similar to that seen in Fig. 3-9) and also occurs mainly within delineations of the Conestoga and Letort and Benevola mapping units. The PR site shows some black, loamy material below the argillic horizon, similar to the DOT, GRO, and FLI sites, but its occurrence is only documented in two non-adjacent pedons (Appendix A). Manganiferous soil materials were found at all landscape positions at the PR transect,

although the most Mn-rich material (with a black matrix color) occurs at a summit/ shoulder position.

Emerson Burrier Road Site

The Emerson Burrier Road (EB) site is located approximately 5 km southeast of Libertytown, MD (Fig. 3-3). The EB transect occurs within a delineation of Sams Creek marble, which is surrounded by the phyllitic Marburg Formation (Maryland Geological Survey, 1986). The soils at the EB site occur mainly within delineations of the Conestoga and Letort and Benevola mapping units. The pedons examined along the EB transects show subsoil horizon colors as dark as Munsell value/ chroma of 3/3, and black (1/1) nodules are present throughout (Appendix A). The EB site is in a valley, and the topography is relatively flat compared to the other sites, but manganiferous nodules and coatings occur at all landscape positions.

Summary of Soil-Landscape Studies

The soils of the Piedmont region are quite varied due to the area's complex metamorphic geology and topography, so it is perhaps not surprising that manganiferous soils are heterogeneous within and between the sites observed. A continuum of manganiferous properties was documented. Some soil materials at the transect sites had soil colors typical of non-manganiferous soils of the area, and trace quantities of Mn, confirmed by little or no reaction with 10% H_2O_2 (0-1 on scale in Table 3-1). Other soil

materials had a high amount of Mn, confirmed by stronger reaction with 10% H_2O_2 (2-3 on scale in Table 3-1), and contained either ferromanganiferous nodules or had a moderately dark soil matrix color, with value and chroma of approximately 3/3. At the DOT, GRO, FLI, and PR sites, soil materials were found that had the maximum expression of manganiferous morphology, with a very dark or black soil matrix color (value and chroma of 2/1 or estimated to be 1/1 and reaction of 4-5 with 10% H_2O_2 on scale in Table 3-1). In most cases, the manganiferous soils were darkest (most Mn-enriched) lower in the profile, just above the bedrock, and lighter-colored materials were found overlying the dark horizons. However, lighter-colored materials were found underneath black, Mn-rich horizons at the Grossnickle site at pedons 252, GRO-2, and 216 (Fig. 3-8) and at the Clemsonville Road site at pedons 179 and 178 (Fig. 3-13). The lighter-colored soil materials are presumably derived from phyllite or greenstone of the Sams Creek formation, reflecting the complicated, folded geology of the area.

Soil colors vary among the six sites observed. At the DOT and GRO sites, soil colors are relatively dark to the surface, while at the FLI and PR sites there is relatively lighter/ brighter colored soil material overlying the black, Mn-rich soil. At the CR and EB sites, manganiferous morphology is relatively weakly expressed, and the black, loamy material is absent. At the PR, CR, and EB sites, soil matrix colors are generally lighter, but black, soft masses of Mn and ferromanganiferous nodules are abundant.

Soil textures vary among the sites as well. The soils at the FLI, PR, and EB sites seem to have better-expressed argillic horizons with finer textures, and may come closest to fitting within the range of characteristics of the Benevola series. In contrast, the DOT

and GRO sites generally have soils with more loamy textures and more weakly expressed argillic horizons, which are more similar to the Letort series.

The area and depth of manganiferous soil horizons varies. The DOT and GRO sites show the thickest manganiferous soils (>7 m), but these occupy only about 1 ha and appear to exist in isolated pods or lenses. At the FLI site, the depth to bedrock is shallower, and manganiferous soil horizons are spread out more thinly over the bedrock, occupying possibly a few ha. The depth of Mn-rich material varies widely over short distances, and there appears to be an abrupt boundary between manganiferous and non-manganiferous soils. Therefore, manganiferous soils may be thought of as small islands surrounded by contrasting, lighter-colored soils.

In soils with typical, trace concentrations of Mn, manganese oxides are very sensitive to changes in oxidation-reduction potential and may become mobile. Under reducing conditions, which are facilitated by acidity and/ or waterlogging, insoluble Mn(III) and (IV) in Mn(III,IV)(hydr)oxides may become reduced to soluble Mn(II), which may travel in soil solution, and be re-concentrated under oxidizing conditions. For example, in Ultisols and Alfisols formed in gneiss residuum in the North Carolina Piedmont, accumulation of Mn is related to interactions between landscape position and associated redox potential rather than mineralogy of soil parent material (McDaniel and Buol, 1991). The location of Mn oxides may therefore be controlled by topography where Mn concentrations are typical. The manganiferous soils of this study, however, are far from typical. There is no common landscape position among the sites that is associated with the location of black, Mn-rich soil material. The surface topography is relatively variable among the sites, and manganiferous soil materials are found at summit, shoulder,

backslope, and footslope positions. Also, there is no evidence of redox processes in the manganiferous pedons observed. There are manganiferous nodules present in many upper horizons, but there are no Fe concentrations or depletions. This evidence suggests that the location of manganiferous soils is governed by bedrock geology rather than by some relocation process such as colluviation or mobilization/ concentration via reduction-oxidation. This finding corresponds well with observations of Dowding and Fey (2007) of black manganiferous oxisols formed in dolomite residuum in South Africa, which were observed to have little correlation with landscape position, and therefore their location was most likely related to variation in parent material composition.

Four of the six transected sites are mapped (according to the MD Geological Survey, 1986) as being underlain by the Sams Creek Formation. Interestingly, the sites with the thickest manganiferous soils (DOT and GRO) are mapped within the Ijamsville Formation, which is not described as having a marble member. However, since marble exists in this region as small lenses, it is most likely that the DOT and GRO transects are underlain or derived from marble lenses that were simply overlooked in the geologic survey, or could not be easily identified at the scale at which the mapping was done.

All of the transects occur within, or in close proximity to, delineations of Conestoga and Letort, or Benevola soil map units. Manganiferous soils may have C horizons estimated to be as dark as Munsell value/ chroma of 1/1, so they are too dark to fit the color requirements for the Letort series. Manganiferous soils fit in the range of colors for the Benevola series (formed in marble residuum), but many of the pedons observed had fine-loamy rather than fine family particle-size control sections (loam/ clay

loam textures in Bt horizons). Therefore, a case may be made for proposing a new soil series to accommodate these unique soils.

Electromagnetic Induction Surveys

Since hand augering is so labor intensive, a non-invasive and efficient method for locating and delineating manganiferous soils was sought. Electromagnetic Induction (EMI) was tested for this purpose. During initial observations in November 2006, the EMI meter tended to produce very low (negative) apparent electrical conductivity (EC_a) readings over dark areas of soil that were known to be manganiferous, and the readings increased as the instrument was moved from the darker areas onto lighter-colored soils. This empirical relationship was quantified by comparing the weighted mean Mn content of each pedon (to a maximum depth of 150 cm, the depth measured by the EMI instrument) along the Grossnickle transect, to the average EC_a of the four nearest EMI readings (Fig. 3-14). Because soil color (low value and chroma) was strongly related to Mn content (Fig. 4-10, Table 4-13), the Mn content of these soils was estimated from color measurements made using a digital colorimeter. A strong relationship was identified between EC_a and the estimated weighted Mn content (Fig. 3-14). Therefore, we proceeded to evaluate three of the sites (Dotterer, Grossnickle, and Flickinger) using EMI in March 2007.

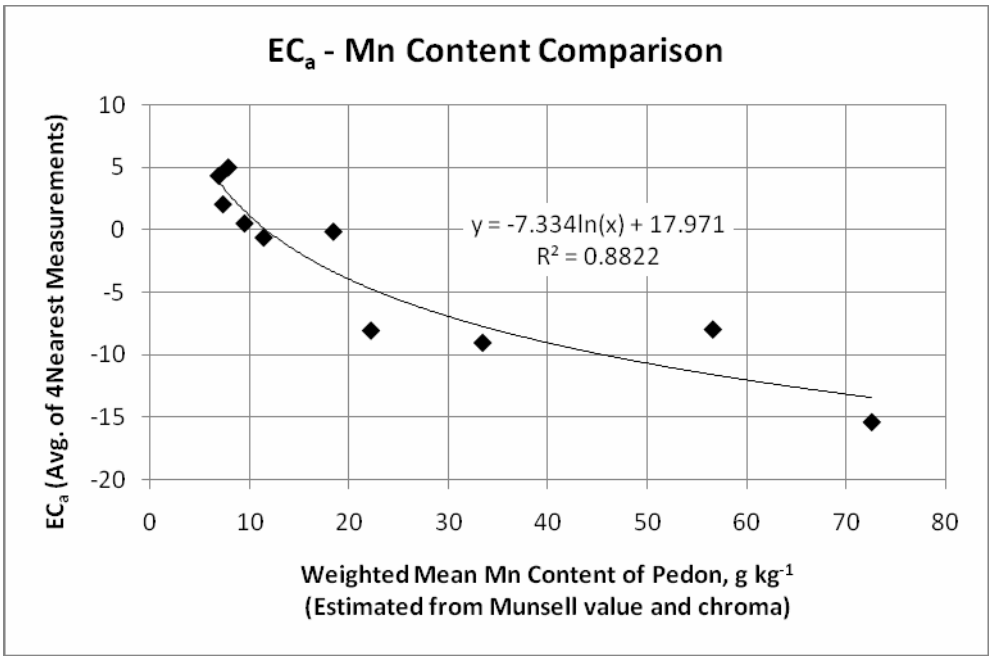

Fig. 3-14. Relationship between apparent electrical conductivity (EC_a) of the soil (measured over 150 cm using an EMI instrument) and weighted mean Mn content of the soil to a maximum depth of 150 cm. Mn content was predicted using its relationship to moist value and chroma (Table 4-13).

In the following EMI survey maps (Figs. 3-15, 3-16, and 3-17), the darker shades of grey represent lower EC_a and, therefore, likely areas of manganiferous soil. The figures show the results of readings made in the vertical dipole orientation, which supposedly sense soil properties to a depth of 150 cm. Because the EC_a readings are affected by various soil properties, such as texture, moisture, clay mineralogy, salts, etc., and the readings are also affected by instrument calibration and battery power, the distribution and range of actual EC_a values generated for each field varied considerably. Therefore, the scale developed for each field is specific to that field and cannot be compared among different fields. Maps generated using EC_a data measured in the horizontal dipole orientation (sensing to a depth of 75 cm) did not seem to provide any

useful information, and thus they are not presented. This is likely due to the fact that black, Mn-rich soil horizons generally occur below 75 cm.

The EMI survey of the Dotterer site is shown in Fig. 3-15. DOT-2 and DOT-3 represent the locations of pedons selected for intensive sampling (in Chapter 4). These pedons contain black, Mn-rich soil horizons, and have corresponding low EC_a readings surrounding them. In the future, it may be worth revisiting the site to observe the area of low readings in the northeast part of Field 1, but, unfortunately, this was not done in this study. The EMI survey predicted manganiferous soils in this area, but this was not confirmed in the field. There are less than 2 ha of low EC_a readings, which predict the extent of manganiferous soils at this site.

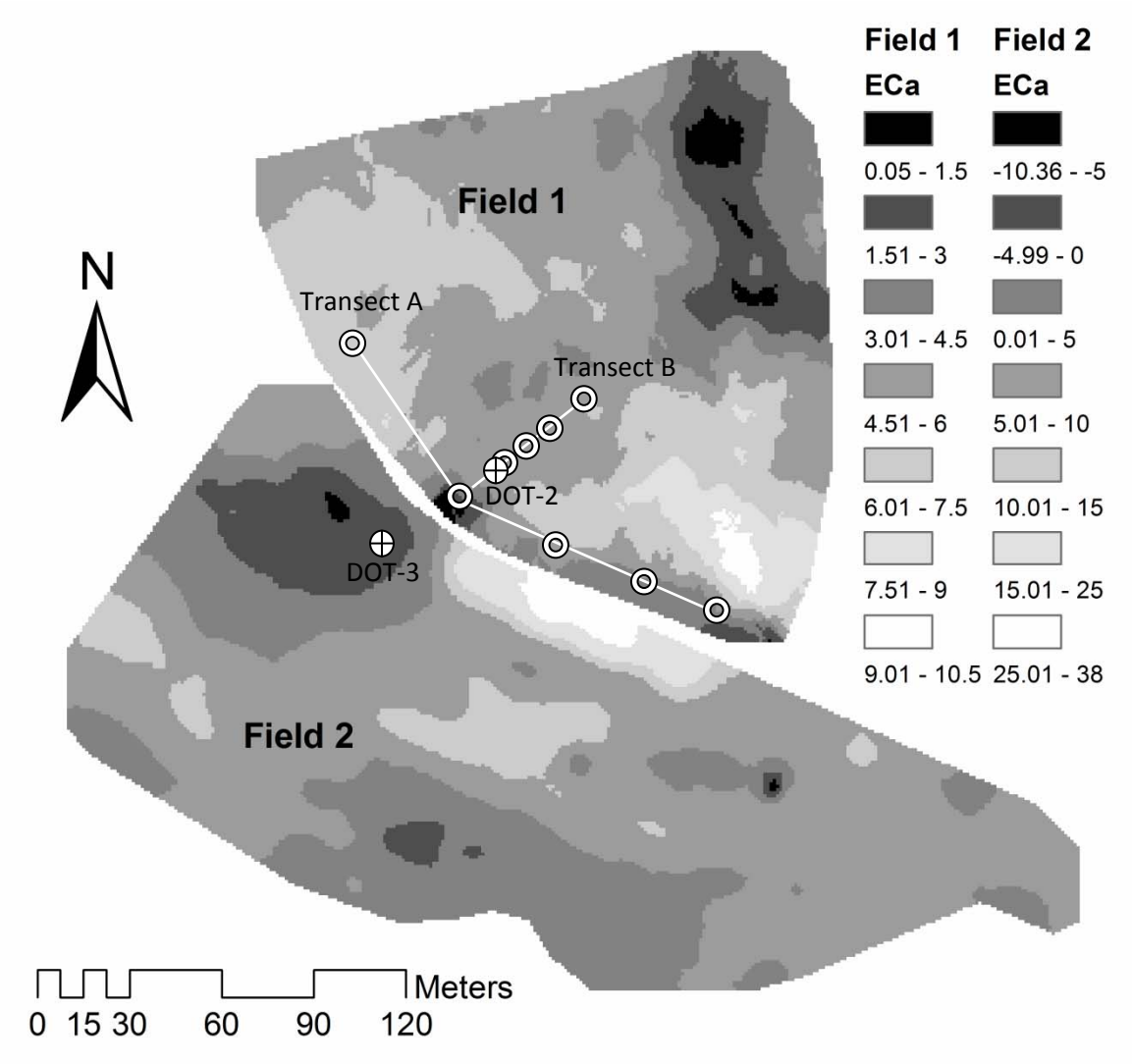

Fig. 3-15. Kriged map of apparent electrical conductivity (EC_a) data collected at the Dotterer site, measured with an EMI (Electromagnetic Induction) meter. Readings were collected in the vertical dipole orientation, sensing to a depth of 150 cm. An empirical relationship was established between low EC_a readings and the location of manganiferous soils. Fields 1 and 2 were surveyed at different times, thus legends, which are empirical, should be considered entirely independent.

The EMI survey of the Grossnickle site (Fig. 3-16) has perhaps the most obvious match to field observations. The delineation of a manganiferous soil unit is similar to that seen while visually observing the dark surface at this site, and it matches very well with the cross-section generated from the transect work (Fig. 3-8). The thickest, blackest Mn-rich soil material was observed in pedons 253, 245, and 254, and the EMI survey shows the lowest readings between these points. There is less than 1 ha of low EC_a readings, which may be interpreted as the area of manganiferous soils predicted with this EMI survey.

In the initial pedestrian EMI survey conducted at the Grossnickle site in November 2006, the EC_a data collected have a range of approximately 60 units. However, in the mobile EMI survey conducted in March 2007 (from which the data are presented in Fig. 3-16), the data collected have a range of approximately 20 units. This difference in range of EC_a is believed to be attributed to the difference in soil moisture content between the two survey times. Because soil moisture can increase EC_a, it is possible that moister soil conditions in March suppressed the extremely low negative readings observed for the high-Mn soils in October (J. Doolittle, personal communication).

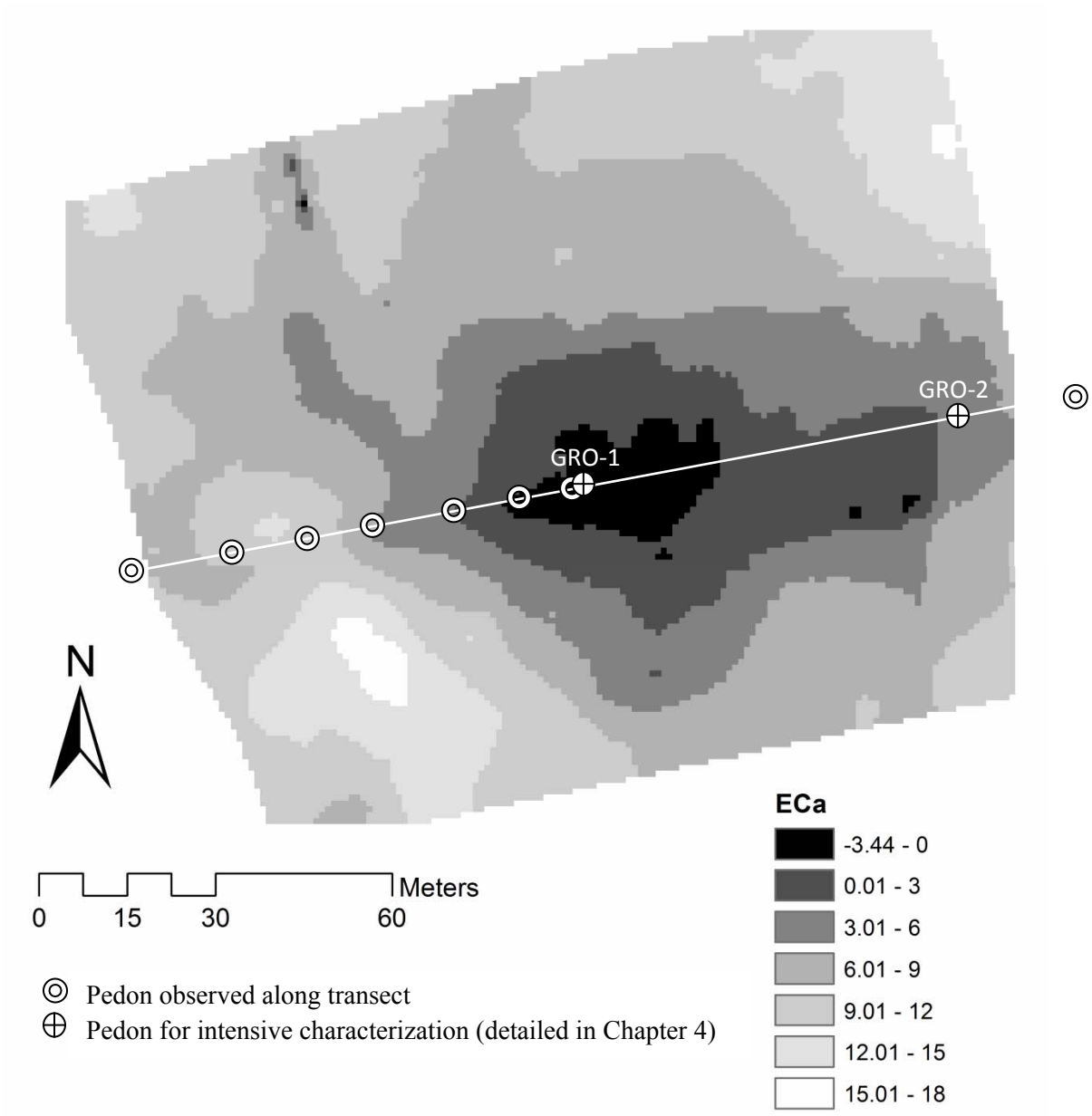

Fig. 3-16. Kriged map of apparent electrical conductivity (EC_a) data collected at the Grossnickle site, measured with an EMI (Electromagnetic Induction) meter. Readings were collected in the vertical dipole orientation, sensing to a depth of 150 cm. An empirical relationship was established between low EC_a readings and the location of manganiferous soils.

The EMI survey of the Flickinger site is shown in Fig. 3-17. Transect B lies along the edge of an area of low EC_a measurements, which predicts approximately 2 ha of

manganiferous soils. Unfortunately, we were not able to survey the field containing Flickinger Transect A because it was planted with alfalfa at the time.

Flickinger Site EMI Survey

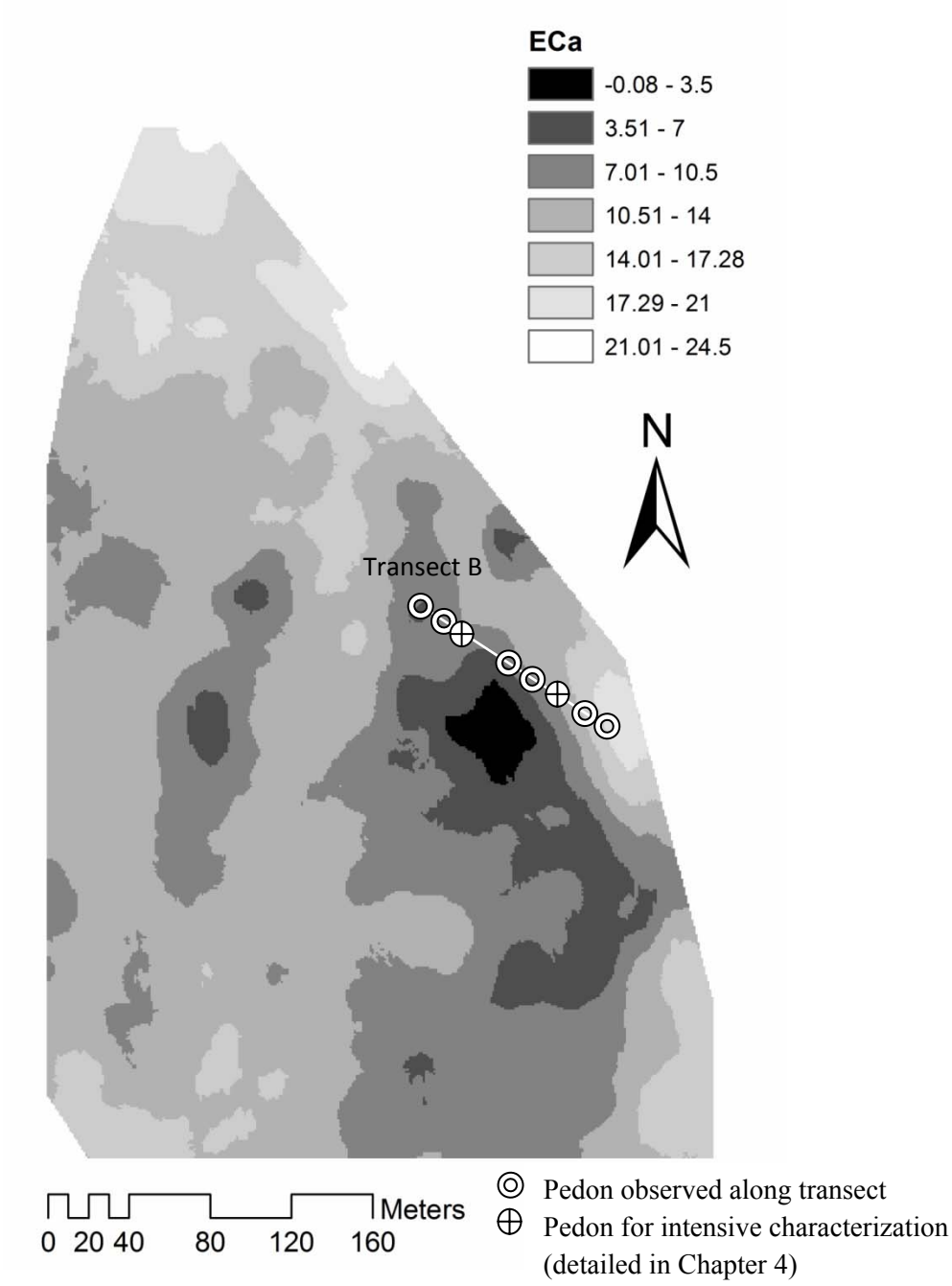

Fig. 3-17. Kriged map of apparent electrical conductivity (EC_a) data collected at the Flickinger site, measured with an EMI (Electromagnetic Induction) meter. Readings were collected in the vertical dipole orientation, sensing to a depth of 150 cm. An empirical relationship was established between low EC_a readings and the location of manganiferous soils.

This is the first time that EMI has been used to survey manganiferous soils. At all three of the sites surveyed, EC_a readings were generally lower over areas of soil which

were known to be manganiferous, as observed during the soil-landscape studies. A possible explanation for the low readings results directly from the high levels of Mn and Fe oxides, which have higher magnetic susceptibility than silicate minerals. EMI sensors are not specifically designed to measure magnetic susceptibility, but their response may be affected by variations in this property (J. Doolittle, personal communication, 2006).

EMI may be used to delineate or approximate the location of manganiferous soils in a field where they are known to occur. This method did identify areas in the field where EC_a was low and thus where one might predict that manganiferous soils were present. At each site, the area of manganiferous soils predicted with EMI is approximately 1-2 ha. These estimates were consistent with visual observations of the soil surface, and descriptions of pedons in our soil-landscape studies. Although EMI seems useful for delineating manganiferous soils in this case, it is unlikely one could discover these soils using only EMI, since EC_a readings vary based on so many different soil properties.

CONCLUSIONS

The manganiferous soils of the Maryland Piedmont appear to exist in a limited area of 200 km^2 in eastern Frederick County and western Carroll County. The manganiferous soils appear to be associated with marble components of the Sams Creek Formation. The NRCS soil surveys for Frederick and Carroll Counties do not explicitly mention manganiferous soils. Nevertheless, the soil surveys were still useful in assisting us in locating them, because the Benevola and Letort series were used by NRCS soil

scientists to represent some of the manganiferous soils, where they were found. However, it is apparent that the Letort series is not an appropriate classification of manganiferous soils because they are darker than the true Letort series, and have a different parent material.

Although they are most likely rare and occupy relatively small areas, manganiferous soils may warrant their own new soil series due to their unique characteristics (to be explored in detail in the following chapter). The general region where the soils seem to occur (based on our reconnaissance assessment) is approximately 200 km^2. However, based on our field observations and EMI surveys, it appears that the manganiferous soils seem to be restricted to isolated "pods" <2 ha in size. Manganiferous soils are heterogeneous over short distances, and their properties vary between sites. Some pedons show modest to moderate Mn enrichment in the form of black nodules or coatings, while some pedons show extreme Mn enrichment in the form of black, loamy material up to several meters deep.

An Electromagnetic Induction (EMI) instrument was used in an attempt to help delineate manganiferous soils. Our observations suggest that EC_a readings are affected by extreme soil Mn/ Fe content, and therefore EMI proved useful in helping to delineate the extent of the soils on these landscapes.

CHAPTER 4

Characterization of Manganiferous Soils:
Morphology, Chemical Properties, Physical Properties, and Mineralogy

INTRODUCTION

Manganese is found in most soils worldwide, but it is considered a trace element, as it is normally found in soils in concentrations of less than 1 g kg^{-1} (Dixon and White, 2002). A search of the Natural Resources Conservation Service (NRCS) characterization database of soils in the U.S. reveals that the highest documented concentrations of Mn are 30-50 g kg^{-1}, and these occur in Ap horizons of oxisols in Puerto Rico and Hawaii (Soil Survey Staff, 2008). However, manganiferous soils were recently discovered in Frederick County, MD, containing as much as 120 g kg^{-1} Mn (Rabenhorst, personal communication). In South Africa, manganiferous oxisols with as much as 58.3 g kg^{-1} Mn in B horizons have been reported (Dowding and Fey, 2007).

Manganese oxides are found in oxidizing soil conditions, where Mn(III) and Mn(IV) are stable. When concentrated, Mn(III) and Mn(IV) are visible as brown-black nodules/ concretions or soft masses of Mn(III, IV) (hydr)oxides, often in close association with Fe(III) (hydr)oxides. Red/ orange, oxidized Fe is normally found in higher concentrations, up to 30-50 g kg^{-1} in this region (Foss et al., 1969), and so usually has more influence on soil color than Mn. However, because Mn is a stronger pigmenting agent than Fe, it may mask the Fe and cause the color of soil materials to be black even when there is less than one-fifth as much Mn present as Fe (Schwertmann and Fanning, 1976). Manganiferous soils in South Africa are so enriched in Mn oxides that whole soil

horizons may be colored black (Dowding and Fey, 2007). This phenomenon is also observed in the manganiferous soils of Maryland.

Manganese oxide minerals are difficult to identify in soils due to their typically low concentrations and poor crystallinity. X-Ray Diffraction (XRD) may be used to identify them when naturally concentrated in nodules, coatings, or soft masses, but Mn oxide peaks tend to be broad, and coincide with other common soil minerals such as kaolinite. This usually makes pre-treatment necessary to remove phyllosilicates in order to allow Mn oxide peaks to be visible on an X-ray diffractogram. Selective extraction procedures such as those of Tokashiki et al. (2003) may be used in conjunction with differential XRD in order to identify Mn oxides (and Fe oxides) in ferromanganiferous nodules. An alternative to XRD is Fourier Transform Infrared Spectroscopy (FTIR), which is more useful in identifying poorly crystalline or amorphous minerals. Potter and Rossman (1979) identified peaks for several common Mn oxide minerals using FTIR.

Under reducing conditions, Mn(III) and Mn(IV) in Mn oxide minerals are transformed to Mn(II), which is soluble, mobile, and hence bioavailable. Excessive Mn(II) uptake by plants on soils enriched in Mn may cause phytotoxicity, such as in Hawaii (Hue et al., 1999) where soil Mn concentrations are 10 to 40 g kg^{-1} (Fujimoto and Sherman, 1948). However, since Mn oxides are insoluble, it is the soil redox state which controls the bioavailability of Mn. Therefore, it was the occurrence of reducing conditions in conjunction with the high Mn concentration which led to phytotoxicity in Hawaii (Hue et al., 1999).

Because of their chemically reactive nature, Mn oxides are important components of soils in spite of their normally small concentrations. Mn oxides have a large specific surface area, and adsorb certain divalent cations such as Co^{2+} and Pb^{2+}. Retention of heavy metals is so extreme in South African manganiferous oxisols that they may be considered contaminated; for example, there is up to 560 mg kg^{-1} Ni and up to 412 mg kg^{-1} Pb in some B horizons (Dowding and Fey, 2007). Mn oxides are also the main oxidants of inert Cr(III) to its toxic form, Cr(VI) (Bartlett and James, 1988).

The extremely high amounts of Mn in the manganiferous soils of Maryland has likely affected their fundamental characteristics. These soils have not been previously characterized in detail, so documenting their properties is crucial for classification, to begin to understand their origin, and to best understand their utility and limitations. Therefore, our objective was to observe and document the morphology and the chemical, physical, and mineralogical properties of manganiferous soils found in the Maryland Piedmont.

MATERIALS AND METHODS

Field Morphology and Sampling

Based on information gathered from earlier reconnaissance and transect work, three sites were chosen for detailed analysis and are herein named for their landowners Dotterer (DOT), Grossnickle (GRO), and Flickinger (FLI). At each site, two pedons were exposed via excavation to a depth of approximately 2 m, and then a bucket auger was used to examine the soil below the excavated pit (until refusal). Sites were selected such

that one of the pedons would represent the maximum expression of manganiferous properties at that site, i.e., a pedon with the thickest and darkest soil material found. The other pedon was selected to represent some intermediate expression of manganiferous properties, i.e., thinner and/ or lighter-colored soil material. This was intended to give some indication of the range and variability of morphological, chemical, and physical properties at each site and among the three sites.

Each pedon selected for study was described in the field according to standard NRCS procedures (Schoeneberger et al., 2002), where morphological data were recorded for each horizon. Data recorded included horizon depth and boundary type, field moist Munsell color, texture class and percent clay by feel, coarse fragments by visual estimation, structure, mottles or clay films if present, moist consistence, and any other features of note. In addition, a digital colorimeter was used in the lab on crushed, homogenized samples to measure soil color in both moist and air-dry states. Duplicate colorimeter measurements were made (recorded to 0.1 units of hue, value, and chroma) and averaged in order to account for variability; duplicate measurements generally varied by only 0.1-0.2 units.

From each pedon, two types of samples were collected by horizon (except in some especially thick horizons that were sampled by depth in order to assess variations within the horizon). First, bulk samples were collected from each horizon, which were air-dried, crushed, and sieved to 2 mm to separate coarse fragments from the fine earth fraction. These bulk samples were used for physical, chemical, and mineralogical characterization. In addition, oriented clod samples were extracted from each horizon for bulk density measurements and thin section preparation. For the horizons below the base

of the pit (sampled via augering), only bulk samples were collected because it was not possible to retrieve undisturbed clod samples using an auger.

Chemical Properties

Concentrations of Mn and Fe oxides and oxyhydroxides were measured on all samples using a modification of the dithionite-citrate-bicarbonate (DCB) extraction procedure of Mehra and Jackson (1960). Due to the extremely high concentrations of Mn and Fe in the soils, we used a smaller ratio of soil to extractant (1/4 that suggested by Mehra and Jackson (1960)). To ensure full reductive dissolution of Mn and Fe oxides, we used 0.25 g soil per 14 mL citrate buffer and increased the heating time from 15 min to 45 min. As per Mehra and Jackson (1960), samples were typically extracted two times. Some very dark samples, however, were extracted 2-3 additional times until the residues were gray, indicating full removal of Mn and Fe oxides. Extracts were brought to 100 mL volume, and measurements were then made on 1:101 dilutions using atomic absorption spectrophotometry (AAS). All extractions were made in duplicate for each sample, and each extract was diluted in duplicate before AAS analysis. In addition, twelve of these DCB extracts were selected for Ni, Co, and Zn analysis using AAS. From each of the three sites (DOT, GRO, and FLI), the two samples with the highest Mn content were chosen, and, from the same pedon, the two samples with the lowest Mn content were measured for comparison.

Soil pH was measured using a 1:1 soil/ water slurry (Thomas, 1986). Ten milliliters of distilled water were added to 10 g of air-dried sample, and the mixture was

allowed to equilibrate for approximately 15 min. Measurements were made using a glass electrode.

Total organic carbon was measured by dry combustion at 950°C using a Leco Corp. CHN-2000 Elemental Analyzer. Three samples suspected to contain carbonates were combusted at 990°C to ensure full carbonate removal, treated with a 5% sulfurous acid solution to remove carbonates, and measured for organic C (Piper, 1942; Nelson and Sommers, 1982).

Physical Properties

Particle size analysis was performed using the pipet method (Gee and Bauder, 1986). Bulk density (D_b) was measured by the clod method (Blake and Hartge, 1986) on two to three replicate clods from each horizon for the portion of the pedon exposed by excavation (generally the upper 1.5 m). Five samples representing a range in Mn/ Fe oxide content were chosen for determination of particle density (D_p), which was done in duplicate using a slight modification of the pycnometer method (Blake and Hartge, 1986). Typically, D_p is determined by using 10 g soil in a 25 mL pycnometer, but the low bulk density of the manganiferous soils made this impossible, so only 3-5 g soil were used. Porosity for the horizons represented by the five samples was calculated based on measured bulk density and particle density.

Mineralogical Characterization

X-Ray Diffraction

Two horizons were selected from each of three pedons selected to represent the modal expression of the manganiferous soils. In each pedon, a Bt and deeper BC horizon were chosen to compare a vertical weathering sequence through the soil profile.

A 30-60 g portion of each of the six soil samples was fractionated into sand (0.05-2 mm), silt (0.002-0.05 mm), and clay (<0.002 mm) by sieving and centrifugation. Portions of the sand fractions were ground in a spex mill. The sand and silt fractions were scanned from 4 to 60°2θ at a speed of 50 s per degree 2θ using a randomly oriented powder mount on a Phillips X-Ray Diffractometer with Cu-Kα radiation. Samples of the clay fraction were saturated either with Mg followed by glycolation, or with K (Jackson, 1974). Each of these saturated samples was oriented using a filter apparatus and applied to a glass slide using the method of Drever (1973). The K- or Mg-saturated clay slides were scanned from 2 to 30°2θ at a speed of 50 s per degree 2θ under the following conditions: Mg-saturated and glycolated at 25°C; K-saturated and air-dry at 25°C; K-saturated and heated to 300°C for 2 hours; K-saturated and heated to 550°C for 2 hours. Semi-quantitative assessments were performed by peak height and area analysis (visual estimation of the sum of the area under the XRD peaks for each mineral identified).

Fourier Transform Infrared Spectroscopy

To aid in identification of the Mn oxide mineral (or minerals) present in the black, Mn-rich soil materials, samples from three pedons (DOT-3, GRO-1, and FLI-1) were selected for Fourier Transform Infrared Spectroscopy (FTIR). These three pedons represented the maximum expression of manganiferous properties at each site, and were chosen for FTIR because their excessively high concentrations of Mn oxides would presumably make identification easier.

FTIR spectra were collected at the University of Delaware with a Thermo Nicolet Nexus spectrometer using single bounce ATR-FTIR spectroscopy with a diamond internal reflection element at ambient temperature (23º C). Spectra were collected using 128 scans at 4 cm^{-1} and a DTGS detector with the Omnic 7.0 software package.

RESULTS AND DISCUSSION

Morphology

DOT-2 represents a pedon with intermediate expression of manganiferous morphology at the Dotterer site (Fig. 4-1, Table 4-1). It is located at 39.5310°N/ 77.2266°W (see Fig. 3-4). DOT-2 has developed an argillic horizon above the black, highly manganiferous silt loam material, which begins at around 185 cm. Although the Bt horizons are relatively dark compared to other non-manganiferous soils in the vicinity (value/ chroma of 4/3 or darker), they are not as dark as DOT-3, which represents a pedon with maximum expression of manganiferous morphology at the Dotterer site (Fig.

4-2, Table 4-2). DOT-3 is located at 39.53087N°/ 77.22688°W (see Fig. 3-4). DOT-3 lacks an argillic horizon, and instead has a cambic horizon which is relatively lighter in color than the underlying BC material, but this profile has colors darker than 3/2 even in the B horizons. The BC horizons are especially dark, with colors of approximately 7.5YR 2/1. Colors with value/ chroma of 2/1 are not normally seen in mineral subsoil horizons. In non-manganiferous soils, such dark colors are often the result of organic C accumulation (usually in O and A horizons). The black, highly manganiferous BC material has a sandy loam texture in this pedon, and it first comes in at 95 cm. The DOT-2 and DOT-3 pedons show a similar mixing of dark brown/ black material in the transition between the B and BC horizons.

GRO-1 (Fig. 4-3, Table 4-3) represents a pedon with the maximum expression of manganiferous morphology at the Grossnickle site. It is located at 39.5372°N/ 77.2272°W (see Fig 3-7). The GRO-1 pedon is very dark throughout the entire profile (matrix value/ chroma less than 2/2). There is an argillic horizon, but it has 17% clay, which is relatively coarse-textured for an argillic horizon in the Piedmont. The profile has black sandy loam material with only 2-3% clay from 155 to 850 cm. This is assumed to be a thick accumulation of relatively unaltered, manganiferous marble residuum. GRO-1 shows some interesting features that are not present in any of the other pedons. There is some cementation in the BC and CB horizons, with shiny, possibly micaceous coatings on many of the ped faces. There is also an angular blocky structure, which appears to be remnant rock structure. GRO-1 is the deepest profile observed, with bedrock occurring at 8.5 m, and there is approximately 6.7 m of black, Mn-rich soil material overlying the bedrock at this spot. GRO-2 (Fig. 4-4, Table 4-4) represents a pedon with intermediate

expression of manganiferous properties at the Grossnickle site (located at 39.53743°N/ 77.22635°W, see Fig. 3-7). The GRO-2 pedon is unique because it is the only one of the six sampled profiles which shows a lithologic discontinuity below the black Mn-rich material. There was no marble bedrock found below this pedon. Rather, an abrupt color change was observed below the BC5 horizon. It is thought that this lighter-colored residuum (Fig. 4-4b) represents soil derived from a different type of bedrock, probably metabasalt.

The FLI-1 pedon represents the maximum expression of manganiferous morphology at the Flickinger site (Fig. 4-5, Table 4-5), and is located at 39.54805°N/ 77.17803°W (see Fig. 3-10). The FLI-1 pedon has well-developed Bt horizons with value/ chroma of around 4/4. These B horizons are lighter in color than those observed in the DOT and GRO pedons; these colors are more typical for soils of the Piedmont region. However, there is an abrupt boundary between the Bt material and the black, Mn-rich BC material. The BC horizons have matrix colors of approximately 5YR 2/1. These colors are similar to those seen in the BC horizons at the DOT and GRO sites; however, the BC material at the FLI site has a much finer texture than the BC horizons at the other two sites. Since bedrock was too deep to be seen at the DOT and GRO sites, the FLI site was instrumental in confirming the parent material of the soils, which was marble. The contact with marble bedrock at 189 cm in the FLI-1 pedon shows a clear weathering front or "halo" of black (<2/1), low-bulk density residuum (Fig. 4-5b). The FLI-2 profile (39.54842°N/ 77.17847°W) (Fig. 4-6, Table 4-6), although it also has marble bedrock within 2 m, does not show as much accumulation of Mn oxides as FLI-1, and so this pedon represents an intermediate expression of manganiferous morphology. Below 69

cm, the soil matrix colors have value and chroma of approximately 3/3 to 2/2, and the dark BC material has a very irregular shape and varies in thickness across the pit (Fig. 4-6b).

The morphology of these manganiferous soils is quite varied, but there are some general trends among the six pedons. The A and B horizons are lighter in color (although still quite dark), and many have phyllite channers and show pedogenic features such as clay films and ferromanganiferous nodules. The lower parts of the profiles (BC and C horizons) consist of the Mn- and Fe-rich marble residuum, and have a much more striking morphology. These horizons show the darkest colors, have little clay, are mostly devoid of coarse fragments, and some have prominent red mottles.

Because the colors of these soils are so dark, it is often challenging to estimate hue, value, and chroma visually using Munsell color charts. In many cases, manganiferous horizons are darker than the darkest chips in the Munsell soil color book. There is also little distinction in color between horizons with these visual estimations, because they are not very precise. Therefore, a digital colorimeter was used to measure color more precisely. In most cases, the visual estimations were very close to the colorimeter measurements.

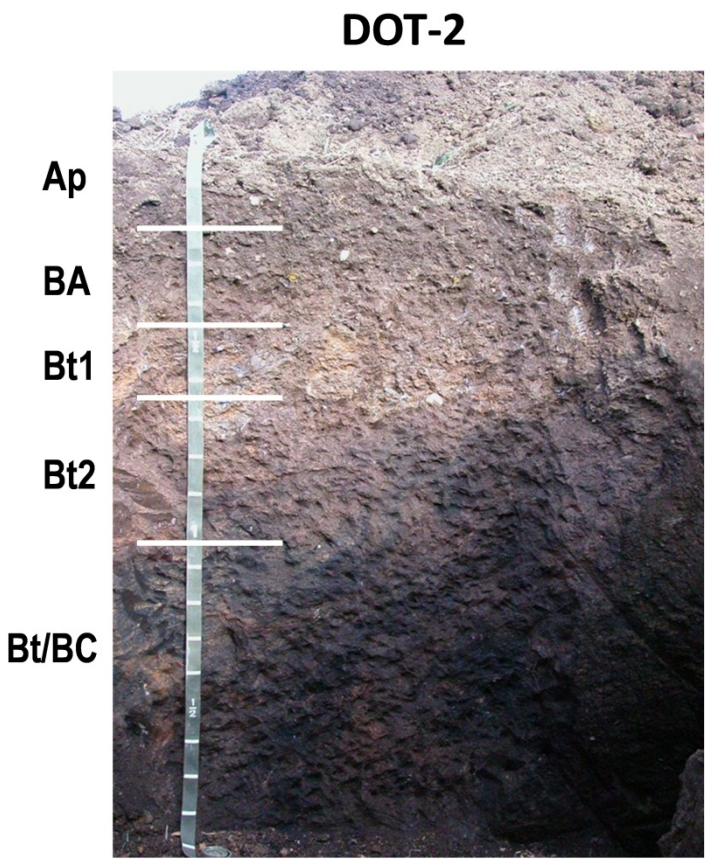

Fig. 4-1. Photograph of the DOT-2 pedon, which shows an intermediate expression of manganiferous morphology at the Dotterer site. The Bt1 and Bt2 horizons had colors of 7.5YR 4/4 and 5YR 3/2, respectively.

Table 4-1. Morphological description of the DOT-2 pedon. ch=channery; cl=clay loam; comp=component; fr=friable; frags=fragments; l=loam; med=medium; mod=moderate; PT=parting to; sbk=subangular blocky; sil=silt loam; vfr=very friable; wk=weak.

Horizon	Lower depth (cm)	Matrix color (moist, field Munsell)	Matrix color (moist, digital colorimeter)	Matrix color (dry, digital colorimeter)	Structure	Moist consist-ence	% Coarse frags by volume (PSA)	Texture class PSA/ (by feel)	% Clay PSA/ (by feel)	Other features
Ap	24	7.5YR 3/2	7.9YR 2.7/2.0	9.5YR 3.9/3.1	mod fine sbk	fr	17	ch sil (sil)	13.4 (17)	
BA	45	7.5YR 3/3	7.6YR 2.8/2.3	9.3YR 4.1/3.1	mod med sbk	fr	15	l (l)	21.3 (23)	
Bt1	65	7.5YR 4/4	8.0YR 3.7/2.8	9.4YR 5.1/3.4	wk to mod med and coarse sbk	fr	30	ch l (ch cl)	26.1 (29)	thin clay films on ped faces
Bt2	104	5YR 3/2	6.8YR 2.4/1.8	8.2YR 3.3/2.6	wk to mod med and coarse sbk; also mod platy	fr	5	cl (cl)	29.2 (30)	thick clay films on ped faces; 10% 7.5YR 4/3 fine and medium mottles; 15% black (7.5YR 2/1) medium and coarse mottles
Bt/BC (Bt comp, 55% of horizon)	185	5YR 2.5/2	6.3YR 2.4/1.5	7.9YR 3.0/2.3	wk med and coarse sbk	fr	2	cl (cl)	34.3 (30)	Brown Bt zones are 10-30 cm wide, inclined @45 degrees; other mottles: 5% (of horizon) 2.5YR 4/4 medium and coarse mottles
Bt/BC (BC comp, 40% of horizon)		5YR 1/1	6.1YR 2.1/0.9	7.2YR 2.3/1.6	wk med platy PT wk med sbk	vfr	7	cl (l)	29.2 (18)	5% 7.5YR 4/4 pore linings
BC1	330	5YR 1/1	5.8YR 1.8/1.0	7.1YR 2.5/1.6			2	sil	20.0	5% 10YR 7/4 fine mottles; 2% 2.5YR 4/6 mottles

BC2	388	10YR 4/4	7.2YR 2.9/1.6	8.8YR 4.0/2.1	20% black Mn zones
BC3 (sampled by depth)	500	5YR 1/1	4.3YR 1.2/0.8	4.1YR 1.4/1.3	
	600		2.9YR 1.4/0.7	3.3YR 1.7/1.4	
	720		2.3YR 1.5/0.5	4.5YR 1.1/1.4	
BC4	775	5YR 1/1	5.1YR 1.7/1.1	5.9YR 1.9/1.8	30% 5YR 4/8 mottles in upper part, disappearing halfway down horizon

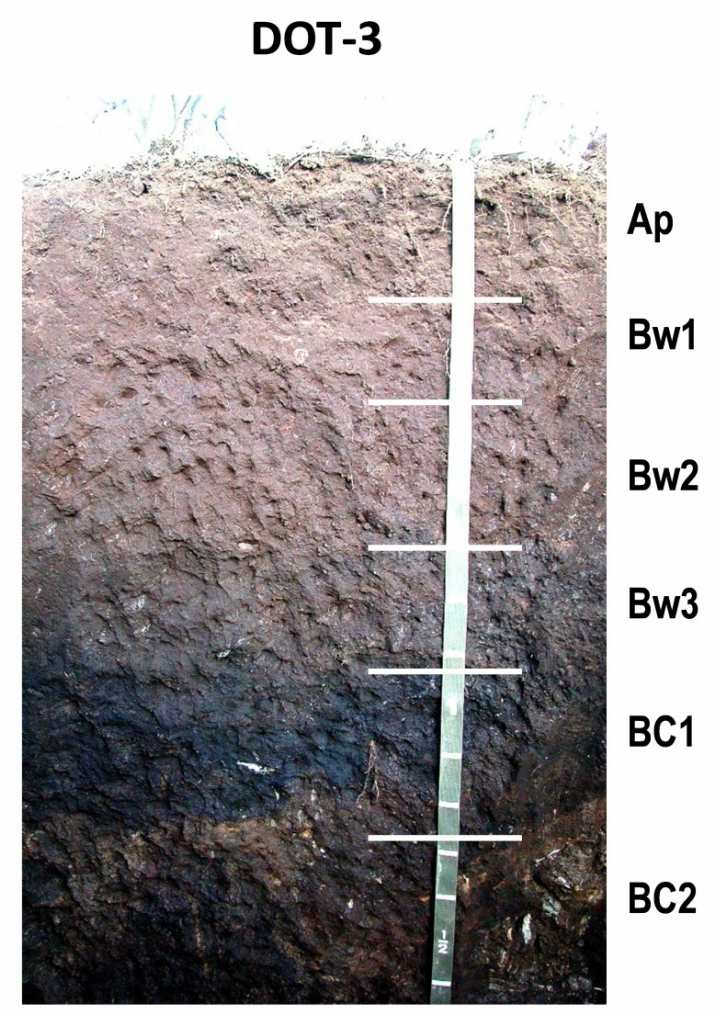

Fig. 4-2. Photograph of the DOT-3 pedon, which shows the maximum expression of manganiferous morphology observed at the Dotterer site.

Table 4-2. Morphological description of the DOT-3 pedon. ch=channery; comp=component; fr=friable; frags=fragments; l=loam; med=medium; mod=moderate; PT=parting to; sbk=subangular blocky; sl=sandy loam; vfr=very friable; wk=weak.

Horizon	Lower depth (cm)	Matrix color (moist, field Munsell)	Matrix color (moist, digital colorimeter)	Matrix color (dry, digital colorimeter)	Structure	Moist consis-tence	% Coarse frags by volume (PSA)	Texture class PSA/ (by feel)	% clay PSA/ (by feel)	Other features
Ap	27	7.5YR 2.5/2	6.7YR 1.9/1.7	8.3YR 2.8/2.8	very wk med and coarse sbk PT wk to mod fine granular	vfr	6	l (l)	8.9 (16)	
Bw1	46	7.5YR 2.5/2	6.2YR 2.1/1.8	7.9YR 3.1/3.1	wk med to coarse sbk	fr	7	l (l)	14.0 (18)	
Bw2	70	7.5YR 2.5/2	6.1YR 2.8/1.6	7.8YR 2.9/3.1	wk coarse sbk	fr	6	l (l)	15.2 (18)	
Bw3	95	7.5YR 1/2	6.2YR 2.0/1.3	7.5YR 2.5/2.6	very wk med to coarse sbk	vfr	3	l (l)	12.8 (20)	
BC1 (brown comp, 60% of horizon)	127	5YR 2.5/1	5.8YR 1.7/0.9	5.7YR 1.7/1.3	mod fine and med sbk	vfr	7	sl (l)	9.0 (15)	nodules present
BC1 (black comp, 40% of horizon)		5YR 1/1								
BC2	180	10YR 2.5/2	7.3YR 2.5/1.5	8.9YR 2.9/2.7	mod fine to med sbk	vfr	2	l (l)	19.4 (12)	10% 7.5YR 5/6 stringers (mottles); 20% black (5YR 1/1) zones
BC3 (sampled by depth)	300	5YR 2/1	6.4YR 1.8/1.0	7.7YR 2.7/1.6				(sl)	(13)	5Y 5/3 weathered phyllite ghosts; horizon has very low bulk density
	400		7.7YR 2.0/1.1	8.5YR 2.8/1.6						

BC4 (sampled by depth)	500	5YR 1/1	6.9YR 1.5/0.8	7.3YR 2.0/1.3		(sl)	(8)
	630		6.0YR 1.4/0.8	7.6YR 2.1/1.3			
BC5	665	5YR 2/1	7.8YR 1.9/1.2	9.1YR 2.9/1.8		(sl)	(11)
Cr	710	5YR 1/1	6.5YR 1.7/0.9	6.3YR 2.4/1.4	3% phy ch	sl (ch sl)	3.3 (8)

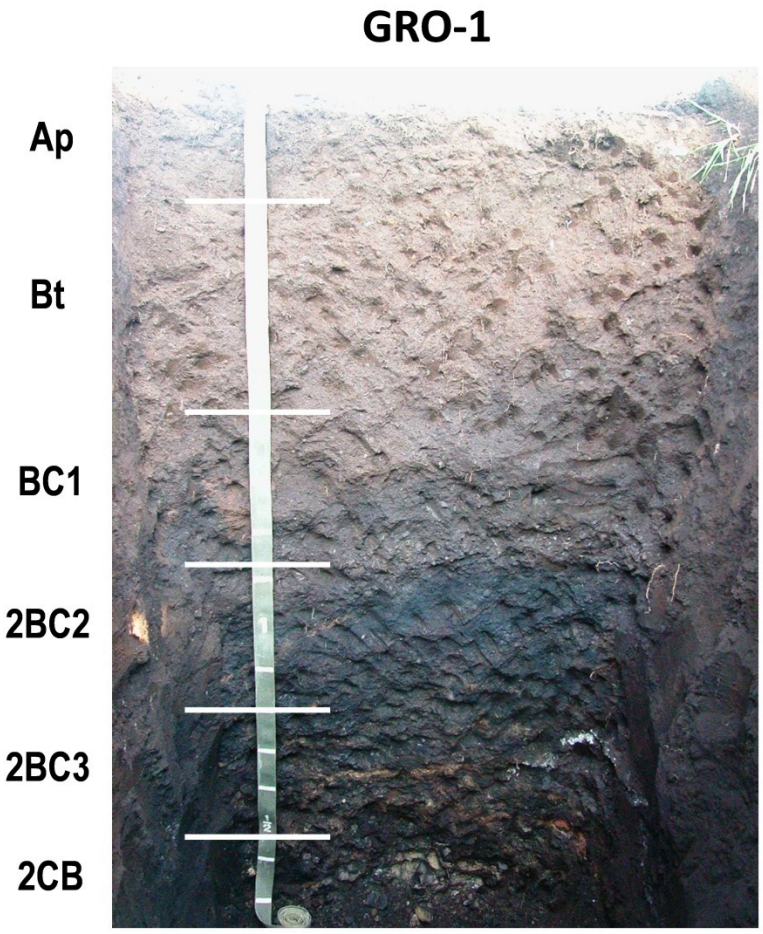

Fig. 4-3. Photograph of the GRO-1 pedon, which shows the maximum expression of manganiferous morphology observed at the Grossnickle site. Ap and Bt colors were 7.5YR 2.5/2.

Table 4-3. Morphological description of the GRO-1 pedon. abk=angular blocky; fr=friable; frags=fragments; grad=gradual; l=loam; med=medium; mod=moderate; PT=parting to; sbk=subangular blocky; sil=silt loam; sl=sandy loam; vfr=very friable; wk=weak.

Horizon	Lower depth (cm)	Boundary type	Matrix color (field, moist, Munsell)	Matrix color (moist, digital colorimeter)	Matrix color (dry, digital colorimeter)	Structure	Moist consis-tence	% Coarse frags by volume (PSA)	Texture class PSA/ (by feel)	% Clay PSA/ (by feel)	Other features
Ap	26	clear smooth	7.5YR 2.5/2	6.7YR 2.0/1.6	8.2YR 2.9/2.7	wk fine and med sbk	fr	11	sl (l)	7 (19)	
Bt	63	clear wavy	7.5YR 2.5/2	6.0YR 2.1/1.4	7.6YR 2.6/2.5	wk med prismatic PT mod med and coarse sbk	vfr	8	l (l)	17.4 (23)	Few, faint clay films
BC1	88	abrupt wavy	5YR 2/1.5	5.5YR 1.7/1.1	6.6YR 2.0/2.0	wk coarse sbk PT fine mod sbk	vfr	3	l (1)	10.7 (17)	
2BC2	121	clear wavy	5YR 1/1	4.0YR 1.5/0.8	3.9YR 1.8/1.4	wk to mod coarse and med sbk	vfr with some cemented zones	3	sl (l)	6.2 (15)	10% prominent (5YR 4/6) fine and medium mottles
2BC3	155	grad smooth	5YR 1/1	6.0YR 1.7/1.2	7.0YR 2.1/1.9	mod and strong, fine and med sbk and abk	vfr with some firm cemented zones	8	sl (sil)	15.5 (10)	5% prominent (5YR 4/6) mottles; 10% prominent (10YR 5/6) mottles; some ped faces are shiny (micaceous?) and are 10YR 4/1

2CB	180		5YR 2/2	6.3YR 2.0/1.0	7.4YR 2.6/1.8	strong, med and coarse abk	firm, slightly cemented	9	sl (sil)	2.6 (<10)	5YR 2/2 interior of peds; almost all ped faces have shiny (micaceous?) coatings that are 10YR 4/2, 2.5Y 4/2 and 2.5Y 5/2
*	255		<5YR 1/1	4.1YR 1.4/0.8	4.3YR 1.4/1.4						
	290		<5YR 1/1	5.7YR 1.5/0.6	7.1YR 1.5/1.2						
	410		<5YR 1/1	5.4YR 1.5/0.8	7.2YR 1.4/1.3						5% 5YR 5/6 mottles; 1% 10YR 6/6 mottles
	540		<5YR 1/1	3.0YR 1.6/0.6	4.5YR 1.7/1.3						
	600		<5YR 1/1	4.1YR 1.6/0.7	4.6YR 1.5/1.5						
	700		<5YR 1/1	5.5YR 1.5/0.7	5.7YR 1.7/1.4						
	800		<5YR 1/1	2.7YR 1.5/0.7	4.0YR 1.7/1.6						water saturation? @ 700
	850		<5YR 1/1	2.8YR 1.5/0.8	3.3YR 1.7/1.5			3	sl	2.4	at bottom: carbonates (white, react w/ HCl); hit hard rock

*Horizonation not evident; sampled by depth.

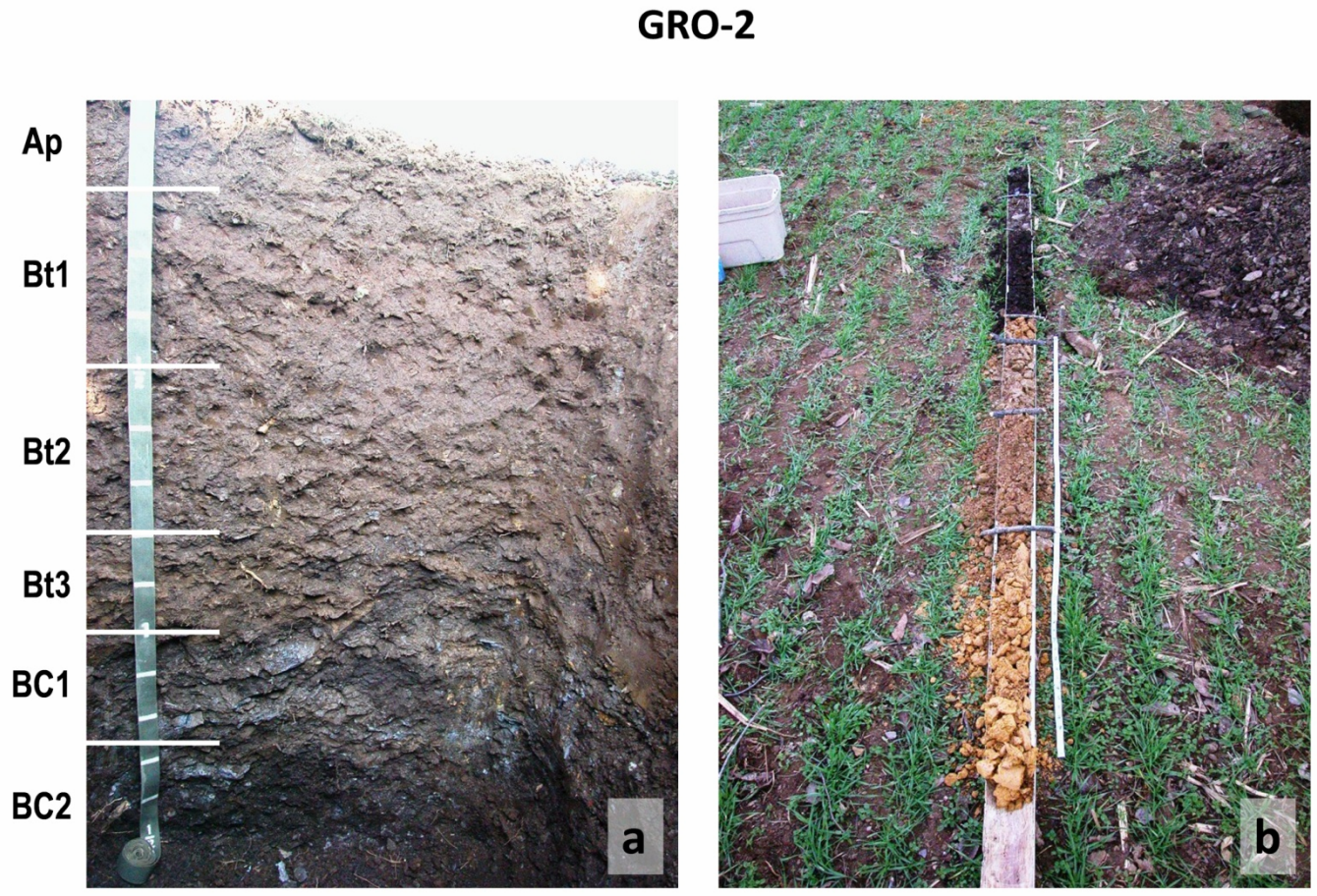

Fig. 4-4. Photographs of the GRO-2 pedon, which shows an intermediate expression of manganiferous morphology at the Grossnickle site. (a) pedon exposed via excavation and (b) soil material augered to a depth of 470 cm, showing the abrupt lithologic discontinuity between black manganiferous material (BC5 horizon) and lighter-colored residuum below (2BC6 horizon).

Table 4-4. Morphological description of the GRO-2 pedon. ch=channery; fr=friable; frags=fragments; grad=gradual; l=loam; med=medium; mod=moderate; sbk=subangular blocky; sil=silt loam; vfr=very friable; vch=very channery; wk=weak.

Horizon	Lower depth (cm)	Boundary type	Matrix color (field, moist, Munsell)	Matrix color (moist, digital colorimeter)	Matrix color (dry, digital colorimeter)	Structure	Moist consis-tence	% Coarse frags by volume (PSA)	Texture class PSA/ (by feel)	% clay PSA/ (by feel)	Other features
Ap	23	clear smooth	7.5YR 2.5/3	7.6YR 2.0/2.0	8.9YR 3.3/3.1	mod fine sbk	fr	16	ch l (l)	12.8 (17)	
Bt1	48	grad smooth	7.5YR 2.5/3	6.6YR 2.2/1.9	8.4YR 3.5/3.1	wk to mod med and coarse sbk	fr	10	l (l)	22.7 (26)	thin clay films on ped faces
Bt2	78	clear smooth	7.5YR 2.5/2	7.4YR 2.3/2.1	8.9YR 3.7/3.4	wk to mod coarse sbk	fr	15	l (l)	21.3 (24)	thin clay films on ped faces
Bt3	100	clear wavy	7.5YR 3/4	7.9YR 2.9/2.4	9.4YR 4.2/3.3	wk med and coarse sbk	vfr	10	l (l)	21.3 (23)	15% pockets of 7.5YR 2.5/2, 5% zones of 7.5YR 4/4
BC1	127	clear wavy	5YR 3/3	7.6YR 2.5/1.6	9.1YR 3.6/2.8	wk fine and med sbk	fr	49	vch l (vch l)	14.7 (20)	
BC2	152		5YR 2.5/1	7.4YR 2.3/1.1	8.6YR 3.3/2.6	mod fine and very fine sbk	vfr	38	vch l (ch l)	12.0 (16)	
BC3	190		5YR 2.5/1	7.7YR 2.2/1.2	8.5YR 3.0/2.3			25†	(ch l)	(16)	
BC4	228		7.5YR 3/2	8.4YR 2.4/1.7	9.4YR 3.9/2.7			55†	(vch l)	(18)	
BC5	298		5YR 1/2	6.7YR 2.2/1.3	8.3YR 2.6/2.7			5†	(l)	(16)	
2BC6	314		7.5YR 5/6	8.3YR 4.2/4.3	9.4YR 5.6/4.5				(l/sil)	(25)	

2BC7	352	10YR 4/3	8.9YR 4.3/3.5	0.1Y 5.8/3.6	(l)	(12)
2BC8	400	7.5YR 4/4	9.0YR 3.8/3.6	0.1Y 5.2/3.7	(l)	(20)
2BC9	470+	7.5YR 5/8	9.1YR 5.3/5.5	0.1Y 6.6/5.6	(sil)	(22)

† Estimated in the field.

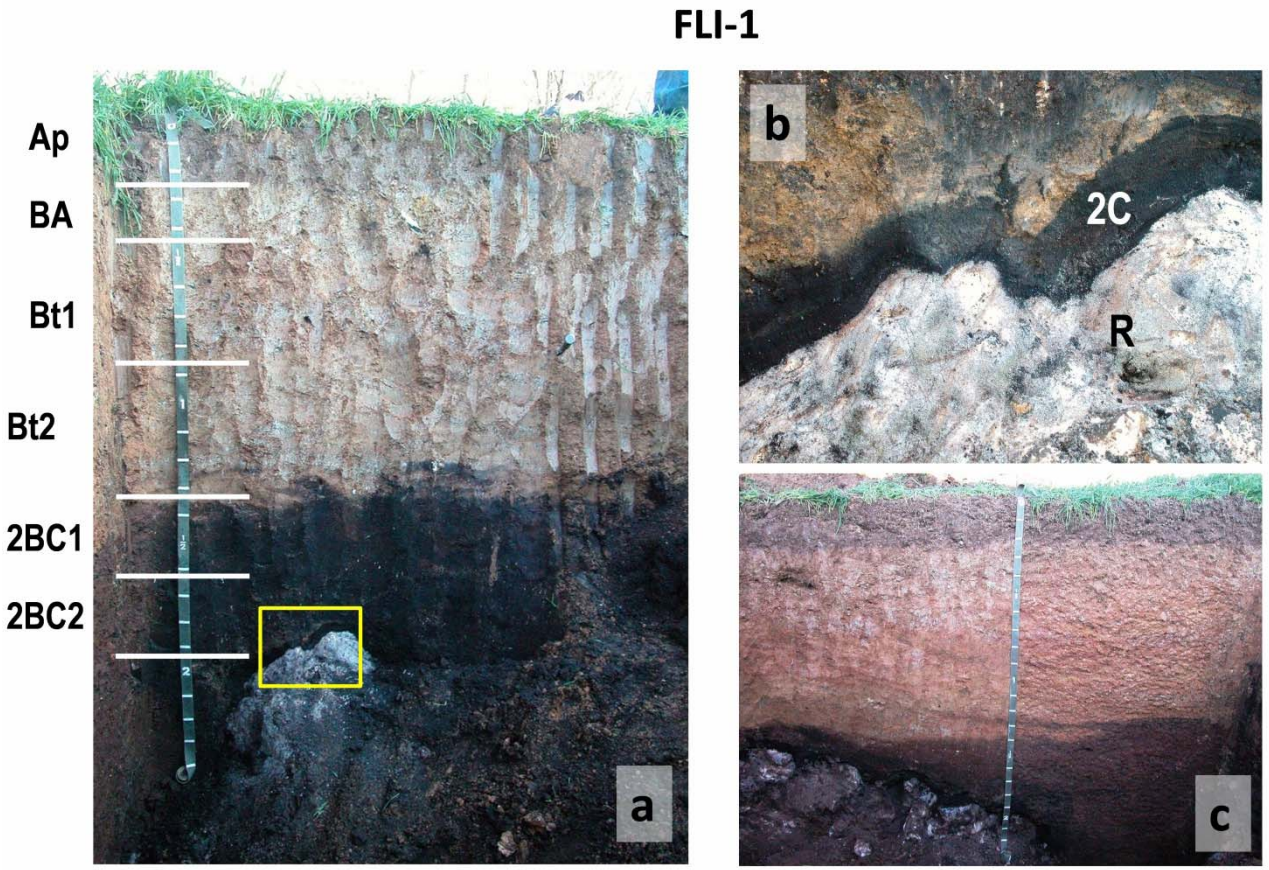

Fig. 4-5. Photographs of the FLI-1 pedon, which shows the maximum expression of manganiferous morphology observed at the Flickinger site. (a) pedon described; yellow rectangle is area depicted in Fig. 4-5b, (b) closeup of contact with marble bedrock and 2C horizon, and (c) another view of pit showing irregular rock contact and irregular boundary between Bt (lighter-colored) horizons and BC (black, Mn-rich) horizons.

Table 4-5. Morphological description of the FLI-1 pedon. c=clay; cl=clay loam; fr=friable; frags=fragments; grad=gradual; irreg=irregular; l=loam; med=medium; mod=moderate; PT=parting to; sbk=subangular blocky; sicl=silty clay loam; sil=silt loam; vfr=very friable; wk=weak

Horizon	Lower depth (cm)	Boundary type	Matrix color (field, moist, Munsell)	Matrix color (moist, digital colorimeter)	Matrix color (dry, digital colorimeter)	Structure	Moist consis-tence	% Coarse frags by vol. (PSA)	Texture class PSA/ (by feel)	% Clay PSA/ (by feel)	Other features
Ap	28	abrupt smooth	10YR 3/4	8.8YR 2.8/2.6	0.1Y 4.3/3.5	wk coarse sbk PT wk to mod med granular	fr	6	sil (sil)	13.6 (20)	
BA	42	clear smooth	7.5YR 4/4	8.8YR 3.6/3.8	0.1Y 5.1/3.8	wk to mod med and coarse sbk	fr	16	ch l (l)	23.6 (25)	
Bt1	87	grad	7.5YR 4/6	7.9YR 3.5/4.0	9.1YR 5.0/4.4	mod coarse sbk	fr	11	l (cl)	24.3 (29)	
Bt2	135	abrupt irreg	7.5YR 4/6	8.4YR 3.8/4.1	9.3YR 5.3/4.5	wk to mod, coarse and very coarse sbk	fr to firm	7	l (sicl)	24.4 (27)	
2BC1	162	clear wavy	5YR 1/1	6.2YR 2.0/1.1	6.5YR 1.9/2.1	wk to mod med sbk	fr	2	c (sil)	41.5 (22)	4% 5YR 4/4 fine and med mottles
2BC2	185	abrupt wavy	N1	6.3YR 2.0/1.1	6.7YR 2.1/2.0	mod coarse and med sbk	fr	4	cl (sil)	27.4 (15)	4% 7.5YR 4/4 fine mottles
2C	189		N1	5.6YR 1.8/0.9	6.4YR 1.8/1.6	structureless massive	vfr	0	l (sil)	22.8 (5)	Halo surrounding marble bedrock. At contact with overlying horizon, there is a zone (halo) of 0.5-1 cm that is 7.5YR 3/2.

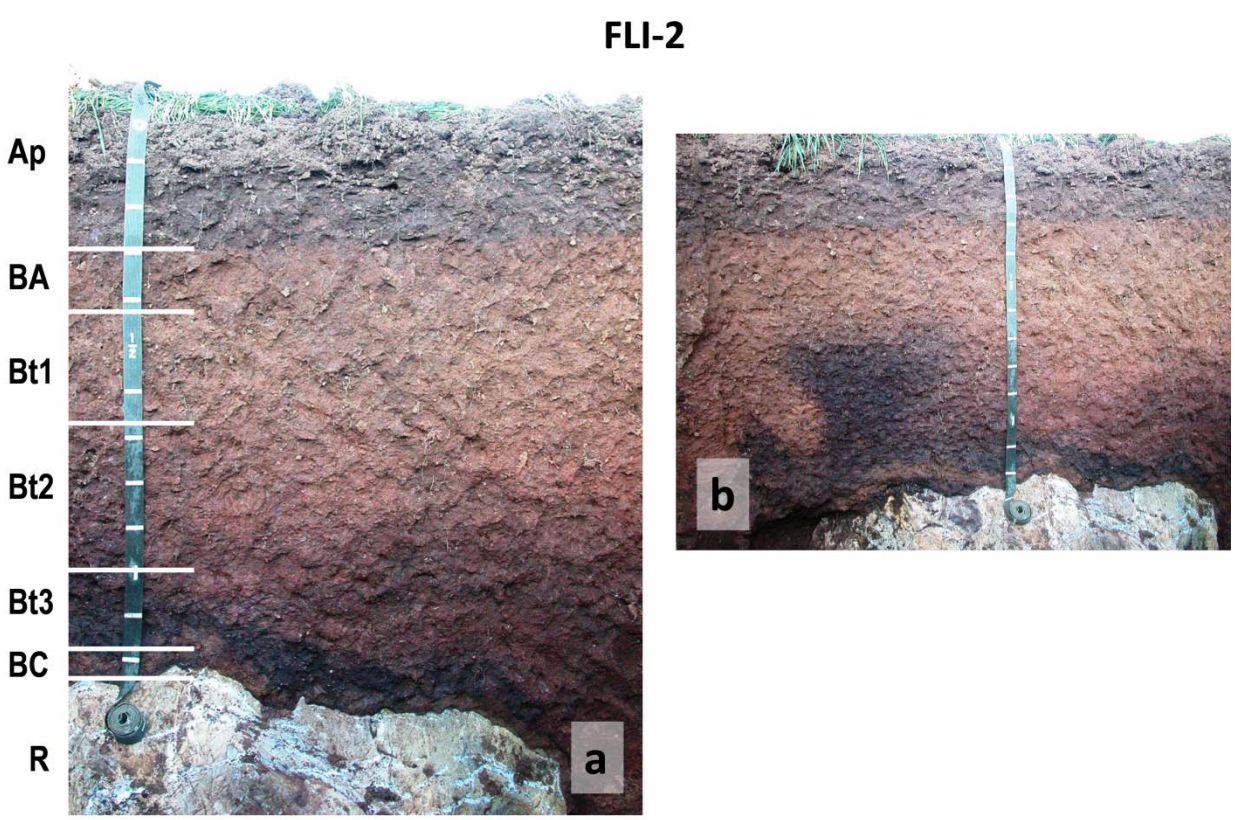

Fig. 4-6. Photographs of the FLI-2 pedon, which shows an intermediate expression of manganiferous morphology at the Flickinger site. (a) pedon described and (b) another view of pit showing irregular shape of black, Mn-rich horizon (BC).

Table 4-6. Morphological description of the FLI-2 pedon. c=clay; ch=channery; cl=clay loam; comp=component; fr=friable; frags=fragments; irreg=irregular; l=loam; med=medium; mod=moderate; sbk=subangular blocky; sicl=silty clay loam; sil=silt loam; wk=weak.

Horizon	Lower depth (cm)	Boundary type	Matrix color (field, moist, Munsell)	Matrix color (moist, digital colorimeter)	Matrix color (dry, digital colorimeter)	Structure	Moist consis-tence	% Coarse frags by vol. (PSA)	Texture class (PSA)	% Clay (PSA)	Other features
Ap	27	abrupt smooth	10YR 3/3	8.5YR 2.7/2.5	9.9YR 4.3/3.6	wk coarse sbk	fr to firm	3	sil (sil)	16.8 (18)	
BA	42	clear smooth	7.5YR 4/4	7.9YR 3.2/3.4	9.3YR 4.8/4.0	wk coarse sbk	fr	1	sil (sil)	22.7 (21)	
Bt1	69	clear smooth	7.5YR 4/5	8.1YR 3.3/3.6	9.5YR 4.6/4.0	mod, med and coarse sbk	firm	2	sicl (sil)	30.8 (25)	
Bt2	100	clear irreg	7.5YR 3/2	6.3YR 2.6/3.2	8.0YR 3.8/4.0	mod, coarse and med sbk	fr to firm	5	cl (cl)	35.0 (28)	
Bt3	118	abrupt wavy	7.5YR 2.5/2	6.5YR 2.2/1.8	7.9YR 2.7/3.0	mod, fine and med platy	fr	7	cl (l)	27.3 (25)	
BC (brown comp)	123	abrupt wavy to irreg	7.5YR 4/4 or 3/4	7.7YR 2.4/2.9	8.5YR 3.1/3.2			0†	(sil)	(17)	
BC (black comp)			7.5YR 2.5/2	8.4YR 2.0/2.0	9.5YR 3.0/2.7				(sil)	(11)	
R											marble bedrock - in some parts of pit, R is deeper than 190 cm.

†Estimated in field.

Chemical Properties

Soil Acidity

Soil mineral transformations, redox processes, and bioavailability of elements such as Mn are all controlled by pH. The manganiferous soils, though formed from marble residuum, are non-calcareous, and because they are part of the highly weathered Piedmont, one would expect them to be acidic throughout. The manganiferous soils were acidic below 1.5 m, with pH of around 5 (Fig. 4-7). Oxidation of Mn^{2+} yields H^{+} ions which could aid in acidification of the soils. However, the measured soil pH was near 7 to a depth of approximately 1 m in all of the profiles. Agricultural lime added to reduce acidity may have some influence on the pH of Ap horizons, but normally it should not influence soil acidity to depths as great as 1 m. In these manganiferous soils, the upper 1 m of soil is usually formed from a rock layer other than marble, but it is not clear why the pH was near-neutral in the upper 1 m. At near-neutral or slightly alkaline pH, Mn(III) and Mn(IV) in oxides are less likely to be reduced to soluble, bioavailable Mn(II). The Eh-pH stability line for Mn has a negative slope, indicating that for a given Eh, oxidized Mn is more thermodynamically stable at a higher pH. Anecdotal evidence from the landowners reveals no significant toxicity or effect on crop yield of corn and soybeans grown on the manganiferous soils. Although the high levels of Mn might suggest that there is a large potential for toxicity, the well-drained conditions and relatively high surface pH probably prevent any significant reduction of Mn(III) and Mn(IV), and movement of Mn(II) through soil solution.

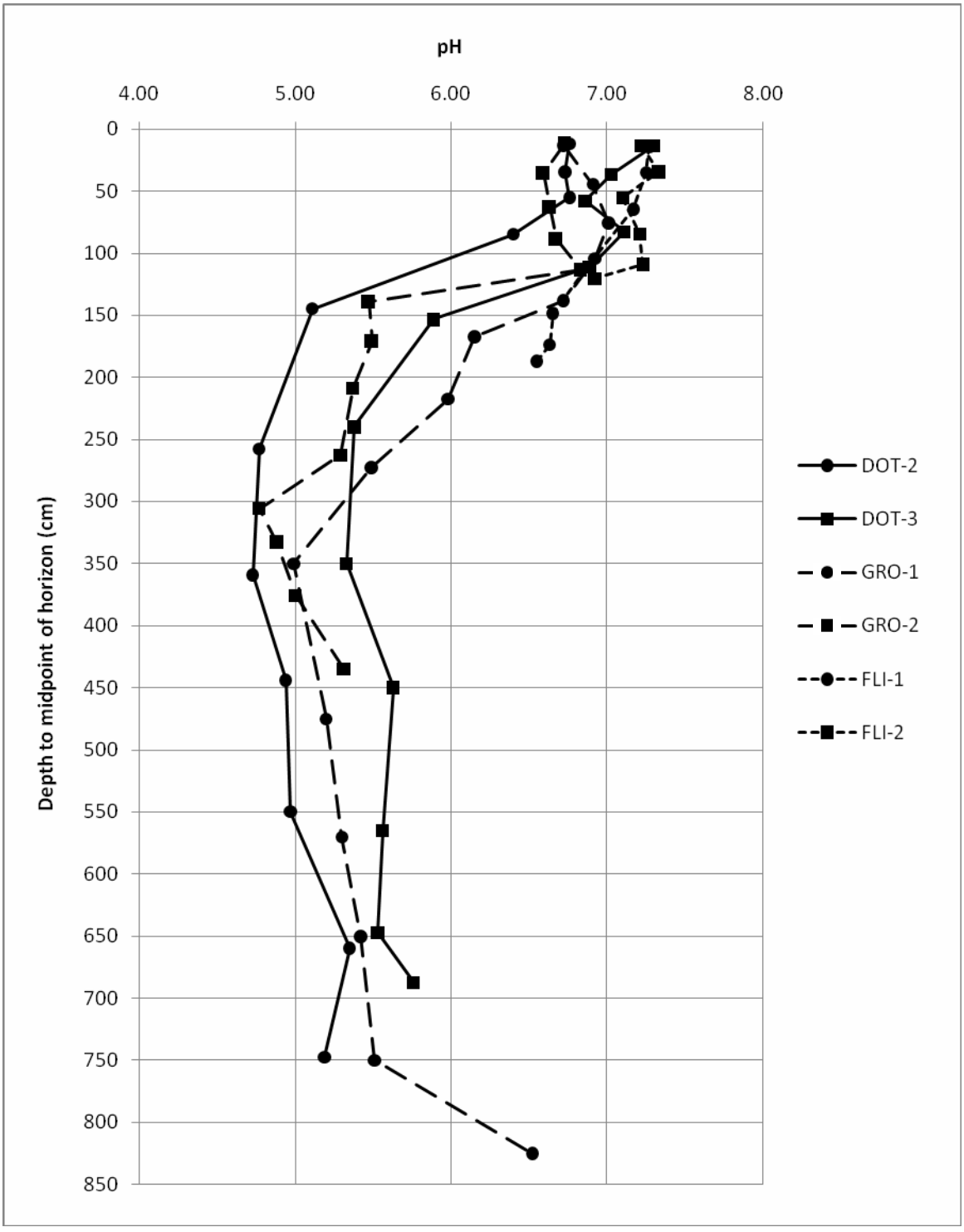

Fig. 4-7. pH of all six pedons by horizon.

Total Organic Carbon

The organic C distribution was similar among the six profiles. In general, there was 3 to 20 g kg^{-1} C in the upper 0.5 m and less than 3 g kg^{-1} C from 0.5 to 2 m. Below 2 m, there was less than 1 g kg^{-1} C (Fig. 4-8). These low values are typical for well-drained agricultural soils of the region (Soil Survey Staff, 2008). The FLI-2 profile showed an atypical increase in C in the deepest (BC) horizon (below 100 cm), and the DOT-2 profile showed an increase in C in the deepest (BC4) horizon (around 750 cm). It is unlikely for organic C to accumulate in mineral BC horizons. In the FLI-2 profile, the pH of the BC horizon was near 7 (Fig. 4-7), so it was suspected that the measured increase could be due to the presence of carbonates derived from the underlying marble bedrock. However, the pH of the DOT-2 BC4 horizon was 5.2 (Fig. 4-7), and under these acidic conditions, it would be far less likely for carbonates to be present. In order to determine if carbonates actually were present, these outliers (FLI-2 BC and DOT-2 BC4 horizons) were treated with sulfurous acid to remove any potential carbonates and re-measured for organic C. The data (not shown) suggest that there may be a few percent of carbonates present. However, the soil material did not show any reaction with 10% hydrochloric acid when examined under a microscope, so it is still not clear whether there are carbonates present.

The colors of the Ap horizons are influenced by organic matter, as shown by the relatively darker surface and higher C content compared with the B horizons. However, it is obvious that the black colors of deeper manganiferous subsoil are not related to organic matter. Black, manganiferous horizons generally occur below 100 cm, where concentrations of C were less than 2 g kg^{-1} (and many had less than 1 g kg^{-1}). These low concentrations of C would not be enough to impart a black color to the soil material.

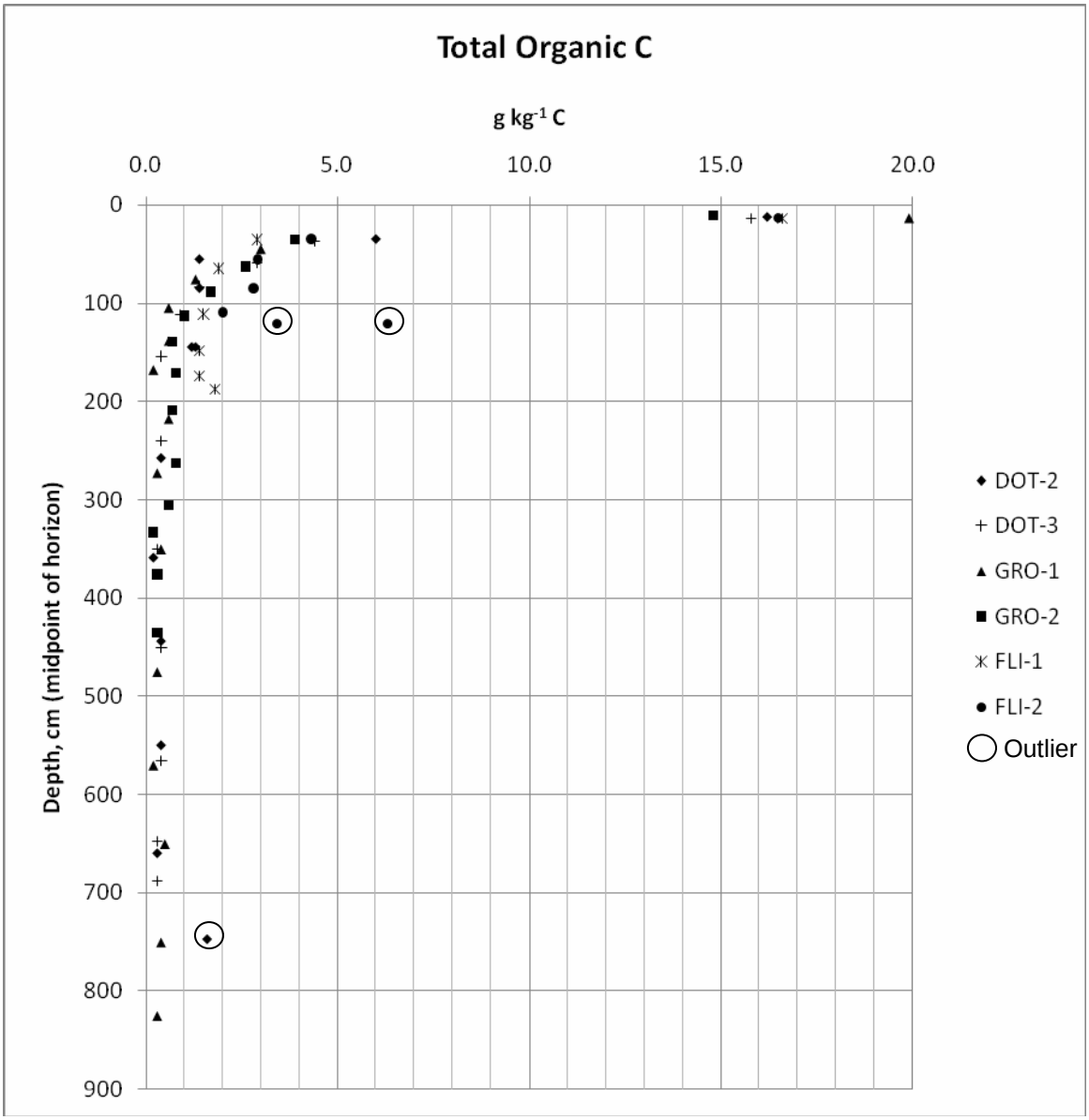

Fig. 4-8. Total organic carbon measured by horizon. Trend is typical for well-drained soils in the region, providing evidence that the black color of manganiferous soils is not derived from organic matter. The three outliers are from samples that came from the deepest horizons of the DOT-2 and FLI-2 pedons.

Manganese Oxides and Iron Oxides

The defining feature of manganiferous soils is their extraordinarily high concentrations of Mn oxides and associated Fe oxides (Tables 4-7, 4-8, 4-9, 4-10, 4-11, and 4-12). The dark, sometimes black matrix colors and manganiferous nodules and coatings result from the presence of such high concentrations of Mn. Although there is a larger amount of Fe present than Mn, Mn oxides have a stronger pigmenting ability and mask the red/ orange Fe oxides. Manganese and Fe levels tend to be lowest in the A and B horizons, where matrix colors have relatively higher value and chroma. However, the quantities of Mn in the A and B horizons are still much greater than 1 g kg^{-1}, so all profiles are highly enriched in Mn beginning at the soil surface. The BC and C horizons have the highest quantities of Mn and Fe (up to 141 g kg^{-1} Mn and 169 g kg^{-1} Fe in DOT-2, Table 4-7) because these consist of the Mn- and Fe-rich marble residuum. Iron concentration is positively correlated with Mn concentration (r=0.89) (Fig. 4-9) because Fe and Mn are associated chemically and are likely derived from the same source (marble bedrock).

Table 4-7. Concentrations of Fe and Mn in the DOT-2 profile, determined by dithionite-citrate-bicarbonate extraction (means of duplicate dilutions and duplicate measurements).

Horizon	Lower Depth	Fe	Mn
		g kg^{-1}	
Ap	24	49.4	11.0
BA	45	52.5	9.2
Bt1	65	42.1	3.4
Bt2	104	90.0	28.4
Bt/BC brown	185	88.9	39.5
Bt/BC black	185	101.0	75.0
BC1	330	117.2	61.9
BC2	388	68.7	21.3
BC3	500	159.8	113.0
BC3	600	167.0	130.2
BC3	720	169.2	141.0
BC4	775	157.8	102.5

Table 4-8. Concentrations of Fe and Mn in the DOT-3 profile, determined by dithionite-citrate-bicarbonate extraction (means of duplicate dilutions and duplicate measurements).

Horizon	Lower Depth	Fe	Mn
		g kg^{-1}	
Ap	27	69.0	30.8
Bw1	46	87.4	31.4
Bw2	70	117.8	34.3
Bw3	95	108.2	45.3
BC1	127	159.0	95.4
BC2	180	113.8	44.1
BC3	300	91.2	52.0
BC3	400	109.9	63.0
BC4	500	148.2	101.8
BC4	630	149.5	90.7
BC5	665	77.2	35.2
Cr	710	99.7	71.5

Table 4-9. Concentrations of Fe and Mn in the GRO-1 profile, determined by dithionite-citrate-bicarbonate extraction (means of duplicate dilutions and duplicate measurements).

Horizon	Lower Depth (cm)	Fe	Mn
		g kg^{-1}	
Ap	26	66.0	30.7
Bt	63	90.5	40.0
BC1	88	136.4	62.5
2BC2	121	111.1	112.7
2BC3	155	127.4	76.5
2CB1	180	71.8	41.5
3CB2	255	131.6	105.6
"	290	128.6	140.1
"	410	160.9	130.7
"	540	110.6	78.3
"	600	114.0	101.0
"	700	126.4	113.0
"	800	117.2	109.0
"	850	103.8	85.5

Table 4-10. Concentrations of Fe and Mn in the GRO-2 profile, determined by dithionite-citrate-bicarbonate extraction (means of duplicate dilutions and duplicate measurements).

Horizon	Lower Depth	Fe	Mn
		g kg^{-1}	
Ap	23	49.9	17.3
Bt1	48	60.6	16.8
Bt2	78	62.6	19.4
Bt3	100	60.9	19.4
BC1	127	70.3	20.4
BC2	152	82.1	28.3
BC3	190	115.4	50.5
BC4	228	67.8	19.2
BC5	298	130.0	65.7
2BC6	314	60.5	3.3
2BC7	352	53.9	3.2
2BC8	400	51.8	1.6
2BC9	470+	48.3	0.8

Table 4-11. Concentrations of Fe and Mn in the FLI-1 profile, determined by dithionite-citrate-bicarbonate extraction (means of duplicate dilutions and duplicate measurements).

Horizon	Lower Depth	Fe	Mn
		g kg^{-1}	
Ap	28	34.4	4.9
BA	42	52.0	1.5
Bt1	87	68.1	2.2
Bt2	135	84.5	2.2
2BC1	162	100.2	75.9
2BC2	185	93.7	79.1
2C	189	108.3	121.2

Table 4-12. Concentrations of Fe and Mn in the FLI-2 profile, determined by dithionite-citrate-bicarbonate extraction (means of duplicate dilutions and duplicate measurements).

Horizon	Lower Depth	Fe	Mn
		g kg^{-1}	
Ap	27	32.5	6.4
BA	42	30.3	4.1
Bt1	69	39.0	3.3
Bt2	100	54.2	12.4
Bt3	118	75.0	26.1
BC brown	123	43.5	6.9
BC black	123	61.4	10.5

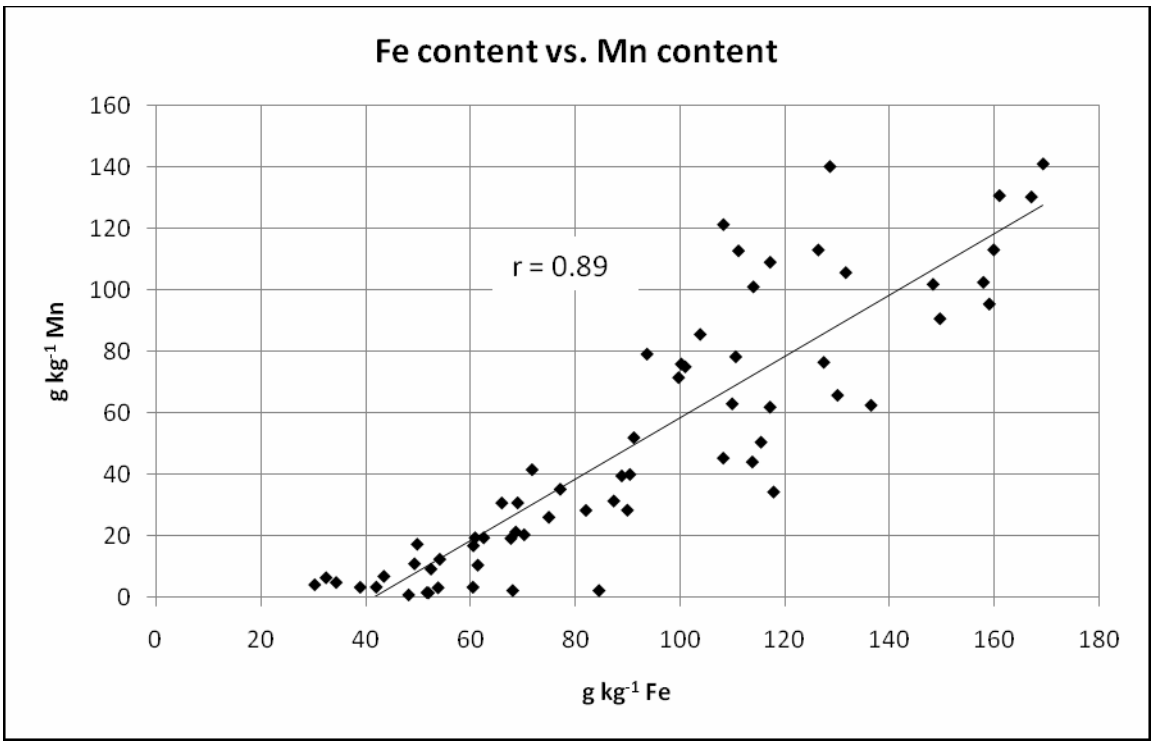

Fig. 4-9. Association between Fe content (DCB-extractable, as oxides) and Mn content (DCB-extractable, as oxides) in all soil horizon samples. Concentration of Fe is positively correlated with concentration of Mn in manganiferous soils (r (correlation coefficient) = 0.89).

The concentration of Mn in these soils exceeds that of all soils characterized by the NRCS Soil Survey Lab (Soil Survey Staff, 2008). Similar concentrations have been documented in ferromanganiferous nodules found in the Benchley soil from Texas, with 123 g kg^{-1} Mn in nodules, and the Decatur soil from Alabama, with 133 g kg^{-1} Mn in nodules (Uzochukwu and Dixon, 1986). But, the only known soils in the world which have similar Mn oxide concentrations in the whole soil matrix are manganiferous oxisols in South Africa. They have as much as 58.3 g kg^{-1} Mn and 89.0 g kg^{-1} Fe (DCB-extractable) in B horizons that are colored black (5YR 2.5/1) as a result these of large

amounts of finely disseminated Mn (Dowding and Fey, 2007). The manganiferous oxisols in South Africa also have been reported to have as much as 287 g kg^{-1} Mn in the black dolomite residuum (Hawker and Thompson, 1988).

There are strong relationships between Mn content and field Munsell value and chroma (Figs. 4-10 and 4-11). Visual estimates using the Munsell color charts are therefore useful for a rough estimation of Mn content for manganiferous soils. For example, based on the data in Figs. 4-10 and 4-11, in the field, one may assume that if the color of the manganiferous soil is estimated to have value/ chroma of 2.5/2 or darker, then there is probably a minimum of 20-30 g kg^{-1} Mn (Fig. 4-10).

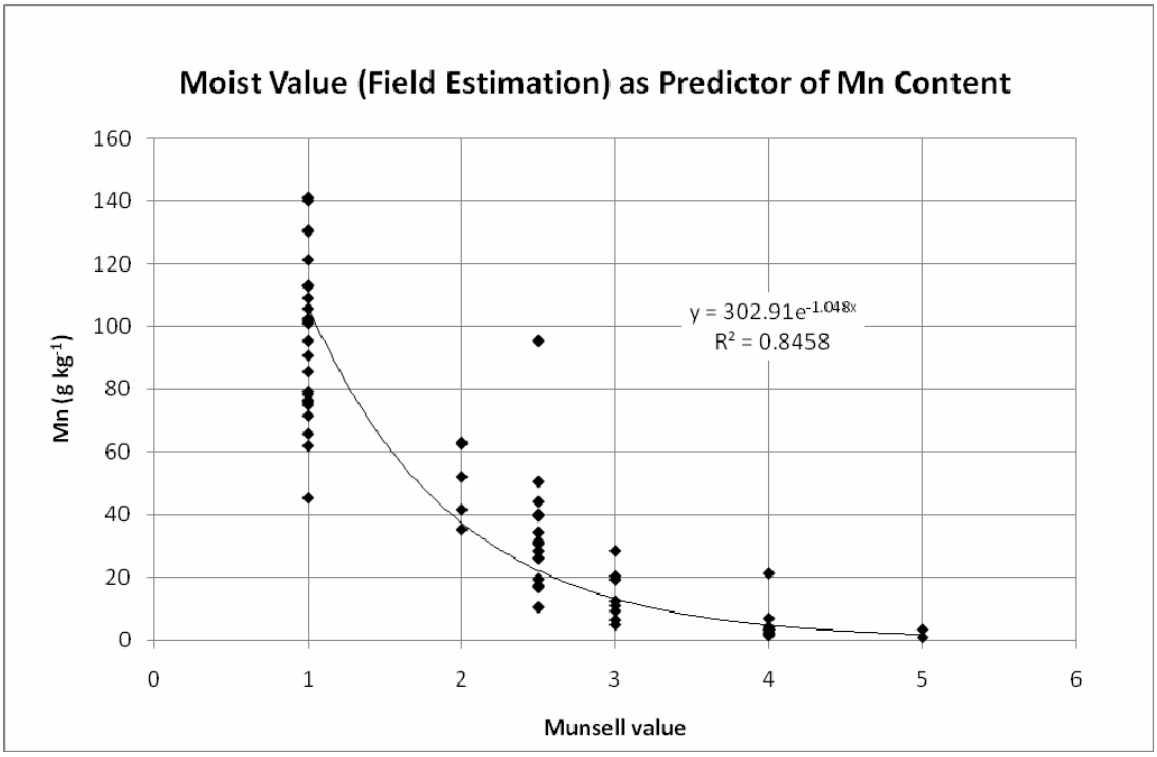

Fig. 4-10. Relationship between moist Munsell value (as measured in the field with soil color charts) and Mn content.

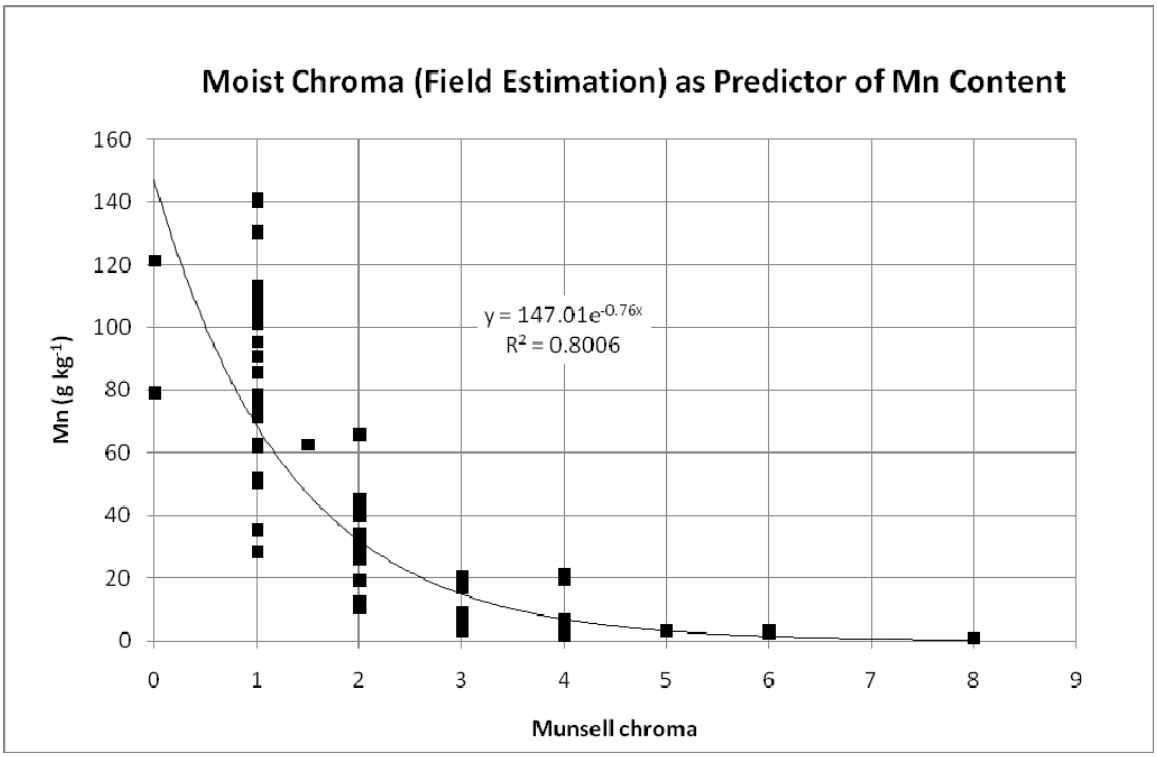

Fig. 4-11. Relationship between moist Munsell chroma (as measured in the field with soil color charts) and Mn content.

It was advantageous to also measure the color of manganiferous soils using a digital colorimeter, for a few reasons. The human eye can estimate Munsell value and chroma only to the nearest 1 or 0.5 units, and it is often difficult to visually assess very dark colors. In addition, the Munsell soil color charts usually do not have standard color chips dark enough to accommodate the manganiferous soils. The digital colorimeter measures value and chroma to the nearest 0.1 unit, so the relationship between soil color and Mn content was documented more precisely than with field estimations (Figs. 4-12 and 4-13). The exponential nature of the relationship may be explained by the strong pigmenting ability of Mn oxides. Small amounts of Mn oxides greatly affect the soil value and chroma. However, once there is a large amount of Mn oxides present, and the

soil is nearly black (value and chroma are low), then the addition of more Mn oxides will not make the soil much darker.

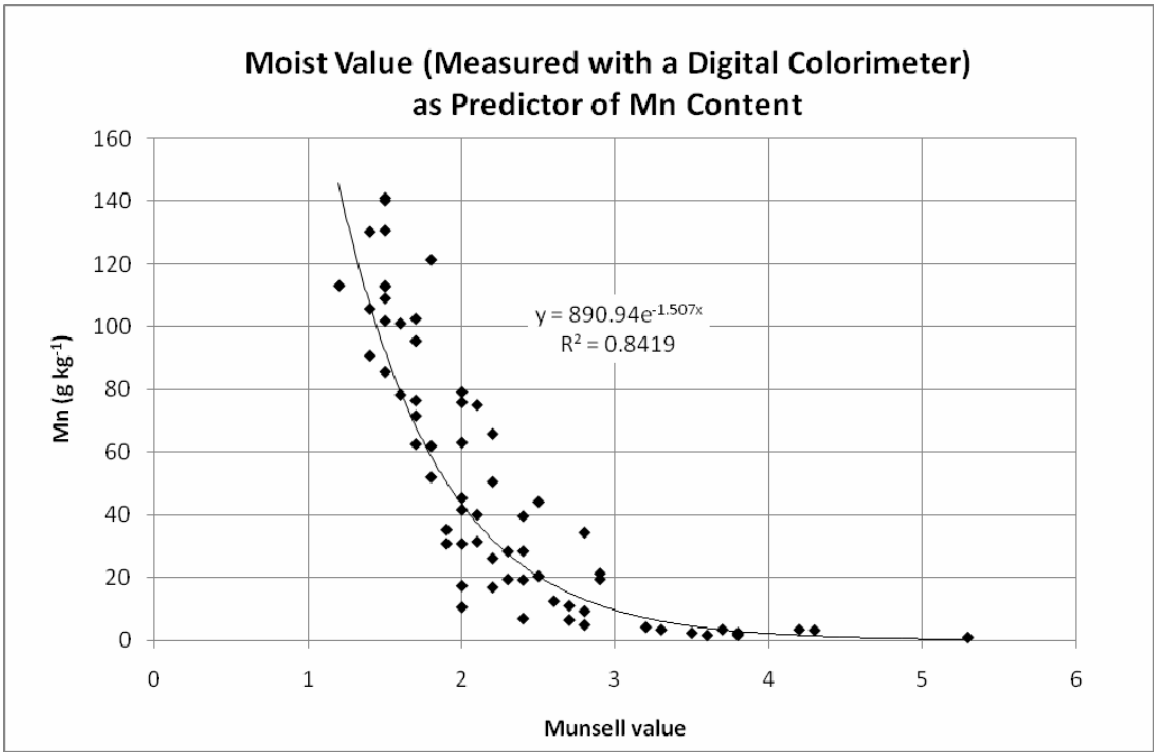

Fig. 4-12. Relationship between moist Munsell value (as measured in the lab with a digital colorimeter) and Mn content.

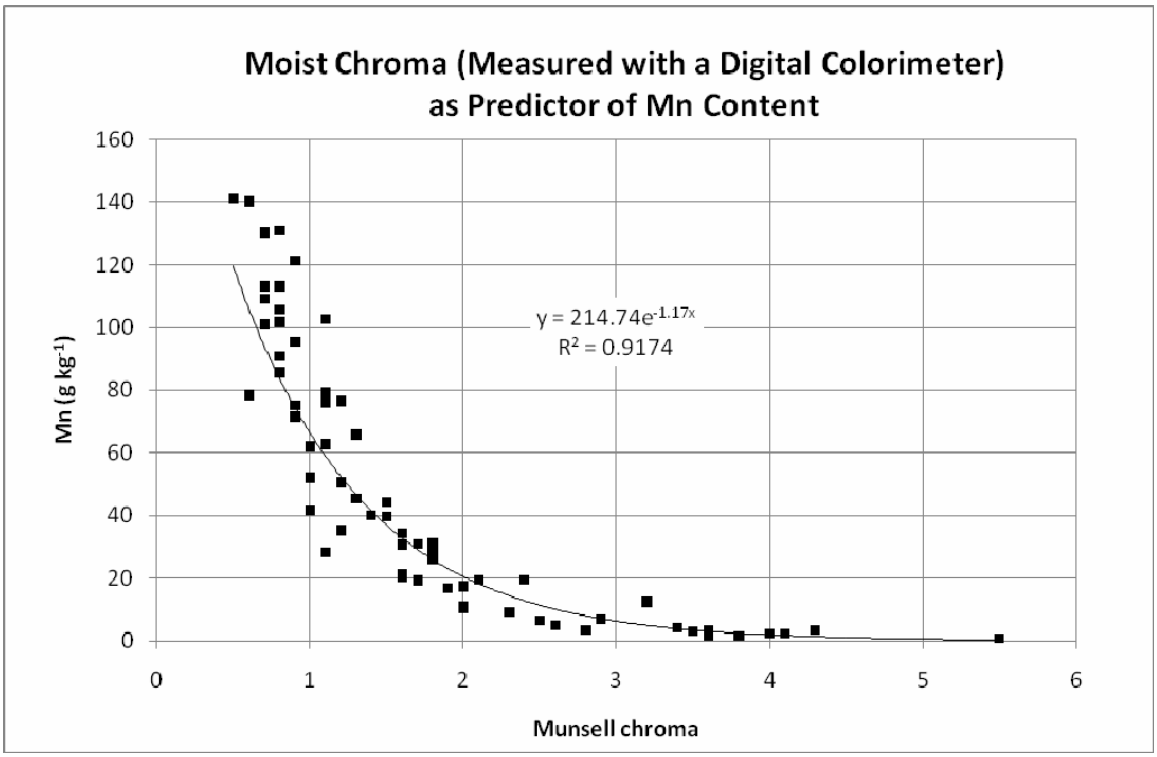

Fig. 4-13. Relationship between moist Munsell chroma (as measured in the lab with a digital colorimeter) and Mn content.

Since value and chroma (as measured with a digital colorimeter) are both very good predictors of Mn content, multiple linear regression analysis was performed to show the relationship of both variables to Mn content. There is an exponential relationship between value and Mn content, and between chroma and Mn content. Therefore, the data were transformed before analysis using the natural log (ln). The results of the regression analysis are summarized in Table 4-13. The regression model has an adjusted R^2 value of 0.92, meaning that 92% of the variation in soil color (value and chroma) can be explained by the Mn content. The P-values for value (0.002) and chroma ($1.1x10^{-10}$) are both highly significant. Therefore, digital colorimeter measurements of value and chroma may be used in place of DCB extractions to predict Mn content of manganiferous soils quickly and easily.

Table 4-13. Summary of multiple linear regression analysis of Munsell value and chroma (predictor variables) and Mn content of manganiferous soils (g kg^{-1}).

Regression Statistics	
Multiple R	0.96
R^2	0.92
Adjusted R^2	0.92
Standard Error	0.38
Observations	66

ANOVA

	df	SS	MS	F
Regression	2	109.1564	54.5782	373.4980
Residual	63	9.2060	0.1461	
Total	65	118.3624		

	Coefficients	Standard Error	t-Statistic	P-value
Intercept	4.87	0.2251	21.6423	7.17456E-31
Value (x_1)	-1.19	0.3745	-3.2018	0.002141851
Chroma (x_2)	-1.60	0.2077	-7.7105	1.14533E-10

Manganophilic Elements: Nickel, Cobalt, and Zinc

Certain trace divalent metals have a high affinity for Mn oxides. These manganophilic elements may accumulate in association with Mn oxides during weathering (Dixon and White, 2002). For example, the manganiferous soils in South Africa are naturally enriched in divalent Ni, Co, Zn, Cu, and Pb (Dowding and Fey, 2007). We performed a quick assessment of the concentrations of selected metals (Ni, Co and Zn) in the soils to explore the possibility that the manganiferous soils in Maryland are similarly enriched in trace divalent metals (Table 4-14).

Table 4-14. Some DCB-extractable metal concentrations of selected soil samples.

Pedon/ Horizon	Depth	Mn	Ni	Co	Zn
	cm	g kg^{-1}	mg kg^{-1}		
DOT-2 BA	24-45	9	150	195	58
DOT-2 Bt1	45-65	3	160	174	38
DOT-2 BC3	500-600	130	188	195	65
DOT-2 BC3	600-720	141	329	246	47
GRO-1 Ap	0-26	31	160	195	58
GRO-1 Bt	26-63	40	178	226	88
GRO-1 2CB	255-290	140	169	205	77
GRO-1 2CB	290-410	131	225	103	136
FLI-1 BA	28-42	1	141	41	38
FLI-1 Bt1	42-87	2	150	174	39
FLI-1 2BC2	162-185	79	263	62	223
FLI-1 2C	185-189	121	291	103	515
		Mean	200	160	115

Soils of the U.S. have Ni concentrations of <5-150 mg kg^{-1}, with a mean of 19 mg kg^{-1} (Shacklette and Boerngen, 1984). The manganiferous soils in this study have 150-329 mg kg^{-1} Ni and mean of 200 mg kg^{-1} Ni, which is very high. Nickel and manganese concentrations were positively correlated (Fig. 4-14).

Soils of the U.S. have Co concentrations ranging from 3-50 mg kg^{-1}, with a mean of 10.5 mg kg^{-1} (Shacklette and Boerngen, 1984). The manganiferous soils have 41-246 mg kg^{-1} Co, with a mean of 160 mg kg^{-1} Co, which is also very high. Cobalt did not show any correlation with Mn content, however (Fig. 4-15).

Soils of the U.S. have Zn concentrations ranging from 13-300 mg kg^{-1}, with a mean of 73.5 mg kg^{-1} (Shacklette and Boerngen, 1984). The manganiferous soils have 38-

515 mg kg^{-1} Zn, and a mean of 115 mg kg^{-1} Zn, which mostly falls within the normal range. Zinc content did not show much correlation with Mn content (Fig. 4-16).

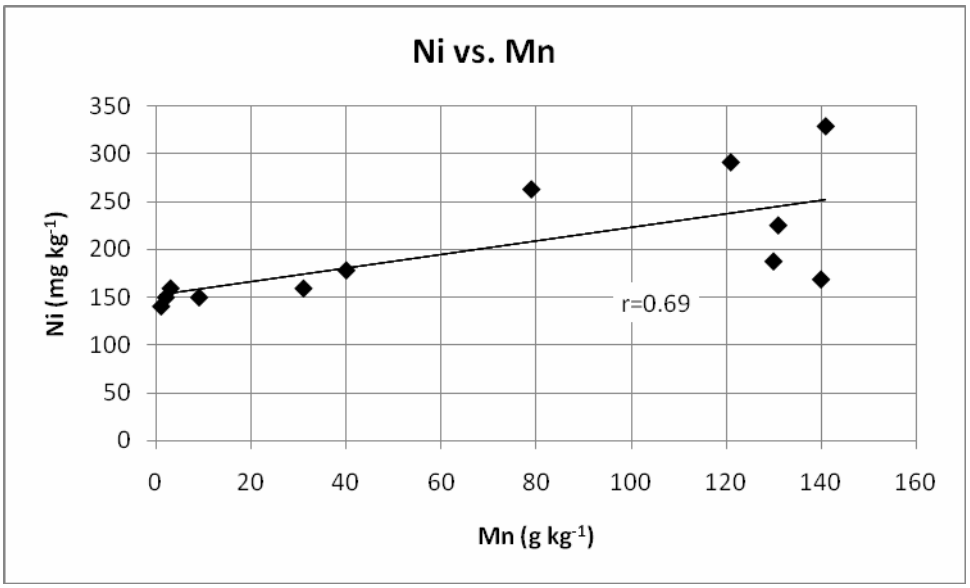

Fig. 4-14. Graph showing association between Ni content and Mn content in manganiferous soils.

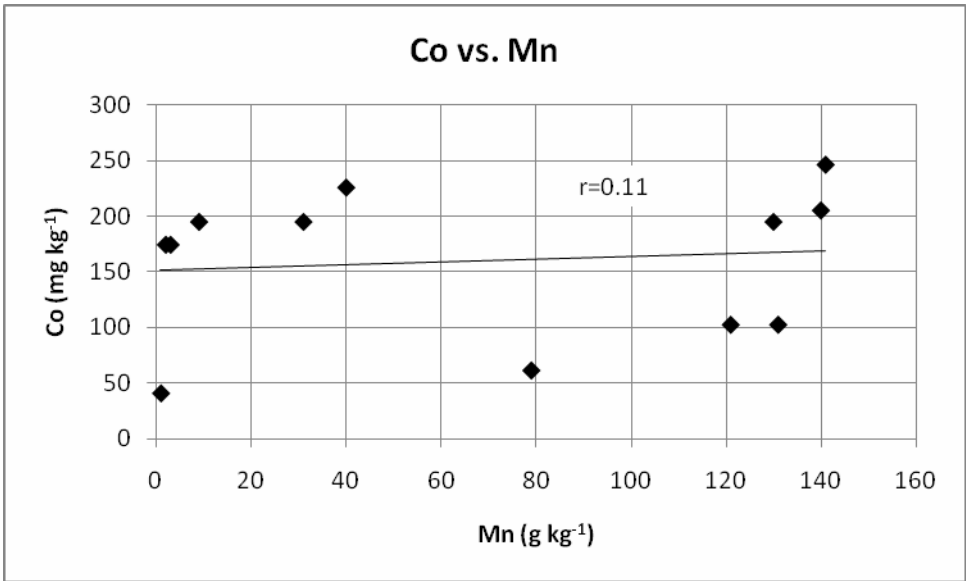

Fig. 4-15. Graph showing association between Co content and Mn content in manganiferous soils.

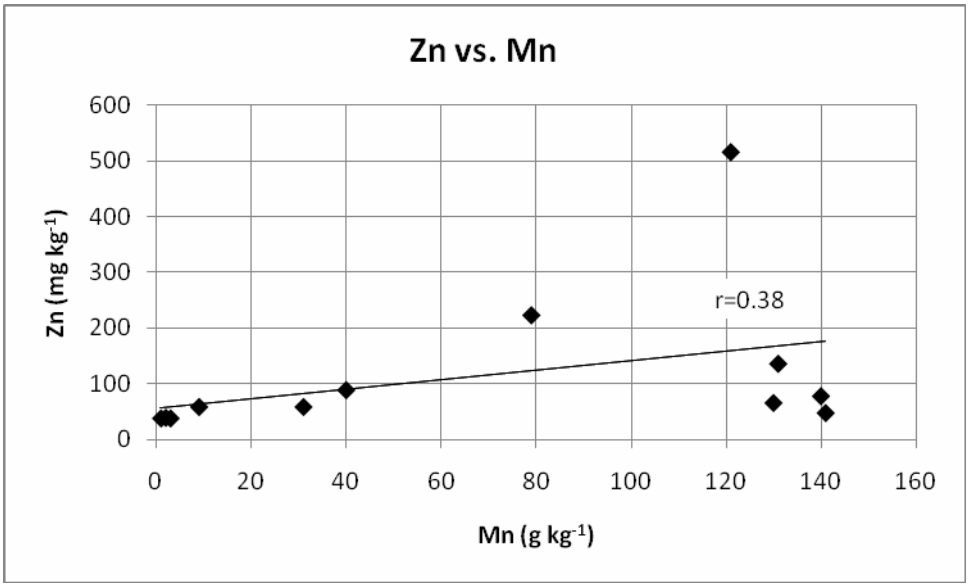

Fig. 4-16. Graph showing association between Zn content and Mn content in manganiferous soils.

The manganiferous soils of South Africa have 212-560 mg kg^{-1} Ni, 81-200 mg kg^{-1} Co in the soil matrix, and concentrations of Cu and Pb high enough for the soils to be technically considered "contaminated" (metals soluble in aqua regia) (Dowding and Fey, 2007). The manganiferous soils in Maryland have similarly high concentrations of Ni and Co, and although they are natural in origin, could potentially be of concern for crop production and groundwater quality. Ni and Co are readily taken up by plants; however, the strong affinity of these elements for Mn and the relatively high pH of the soils may prevent much phytotoxicity in this case.

Physical Properties

Bulk Density

In a typical mineral soil profile, bulk density (D_b) tends to increase with depth (Brady and Weil, 2007). This is primarily because of the influence of organic matter in the surface, which lowers bulk density, and also due to greater compaction in the subsoil from the weight of overlying soil material. The manganiferous soils show the opposite trend, where bulk density decreases dramatically with depth (Fig. 4-17). The horizons most enriched in Mn, which occur deeper in the profiles, have the lowest bulk density. Indeed, there is an inverse relationship between Mn content and D_b (Fig. 4-18). Horizons with bulk density of approximately 1.0 or less tend to contain approximately 40 g kg^{-1} or more Mn (Fig. 4-18) and are therefore black in color (Munsell value and chroma of 2/1 or darker) (Figs. 4-10 and 4-11). Horizons with less Mn and lighter colors (overlying the black Mn-rich material) have more typical, higher bulk density values. This is especially apparent in the FLI-1 profile (Fig. 4-5, Table 4-5), where there is an abrupt boundary between the Bt2 and 2BC1 horizons at 135 cm, and the horizons above this boundary are brown and have less than 5 g kg^{-1} Mn. The bulk density of these horizons is >1.4 g cm^{-3}, which is fairly typical of mineral soils in this region (Soil Survey Staff, 2008). Below the boundary, the soil is black and has >75 g kg^{-1} Mn, and the bulk densities of these horizons are <1.1 g cm^{-3}. Such low values are uncommon for mineral soils, especially for subsoil horizons, and are more common for Andisols and Histosols (Brady and Weil, 2007). The low D_b measurements corroborate field observations that some of the black, Mn-rich soil materials were obviously lightweight and porous.

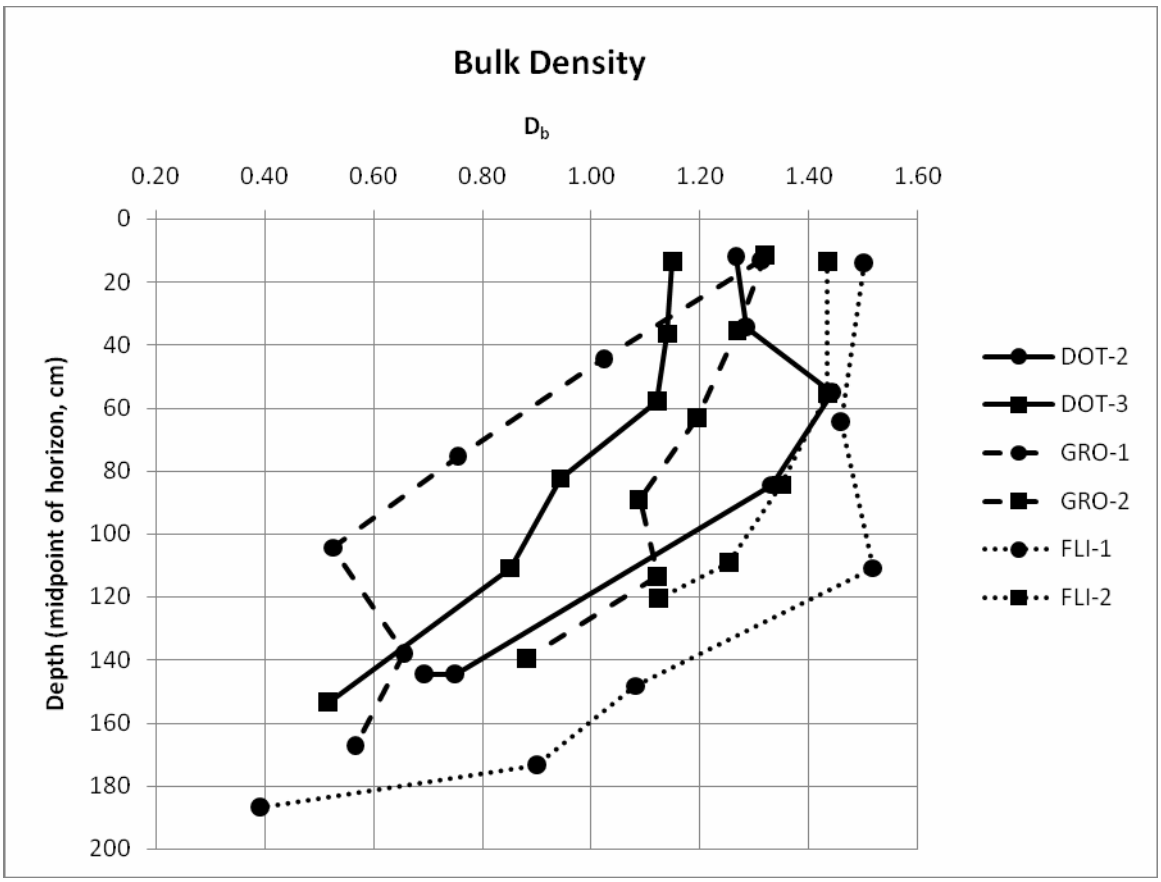

Fig. 4-17. Bulk density by horizon for all pedons. Manganiferous soils show a decrease in bulk density with depth, which is the opposite trend expected for a mineral soil.

.

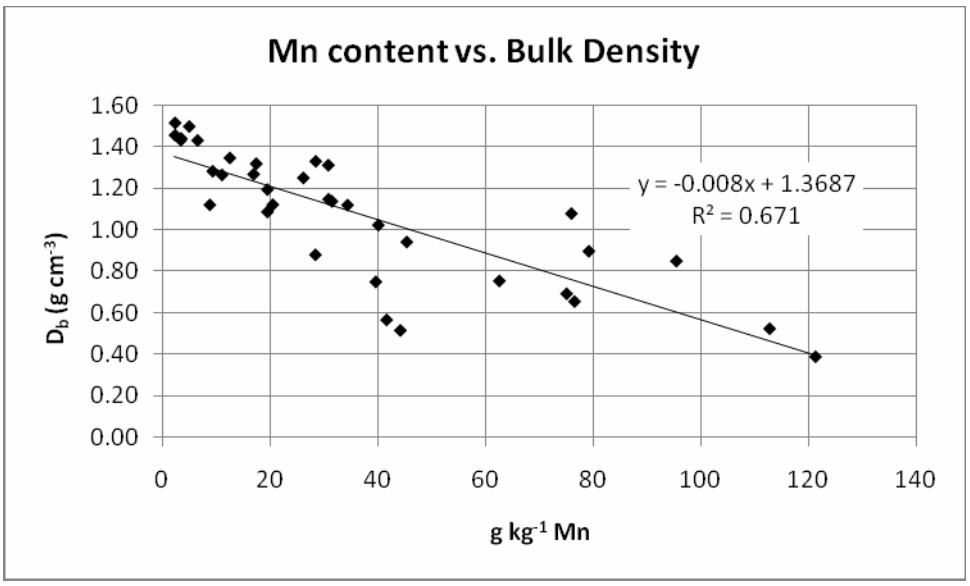

Fig. 4-18. Graph showing relationship between soil Mn content and bulk density.

Particle Density

The bulk mineralogy of most soils is dominated by quartz, with far lesser amounts of other minerals such as feldspars, micas, clays, and Fe oxides. Therefore, the particle density (D_p) of most soils is usually assumed to be close to that of quartz (2.65 g cm^{-3}) (Gee and Bauder, 1986). The particle density of manganiferous soils was suspected to be higher than average due to the influence of large amounts of the denser Mn and Fe oxide minerals. (Lithiophorite has a density of 3.3 g cm^{-3}, and hematite has a density of 5.3 g cm^{-3}.) Five representative samples with a range in Mn content from 5 to 121 g kg^{-1} and a range in Fe content from 30 to 140 g kg^{-1} were chosen for D_p determination.

The manganiferous soils have D_p that is significantly higher than 2.65 g cm^{-3} ($P<0.0005$), the highest recorded being 3.25 g cm^{-3} (Table 4-15). There is a marginal relationship between D_p and Mn content ($P=0.065$, $R^2=0.73$) (Fig. 4-19), but there is a

significant relationship between D_p and Fe content (P=0.008, R^2=0.93) (Fig. 4-20). It is likely that Fe has more of an effect than Mn on particle density because hematite has a substantially higher density than lithiophorite, and Fe is more abundant than Mn in these soils.

Table 4-15. Physical properties of selected soil horizon samples. Means of duplicate analyses.

Sample	Bulk Density	Particle Density	Porosity
	----------g cm^{-3}----------		%
FLI-1 Ap	1.50	2.74	45.3
FLI-1 Bt1	1.46	2.81	48.1
DOT-3 Bw2	1.12	2.95	62.0
GRO-1 2BC3	0.66	3.25	79.7
FLI-1 2C	0.39	3.13	87.5

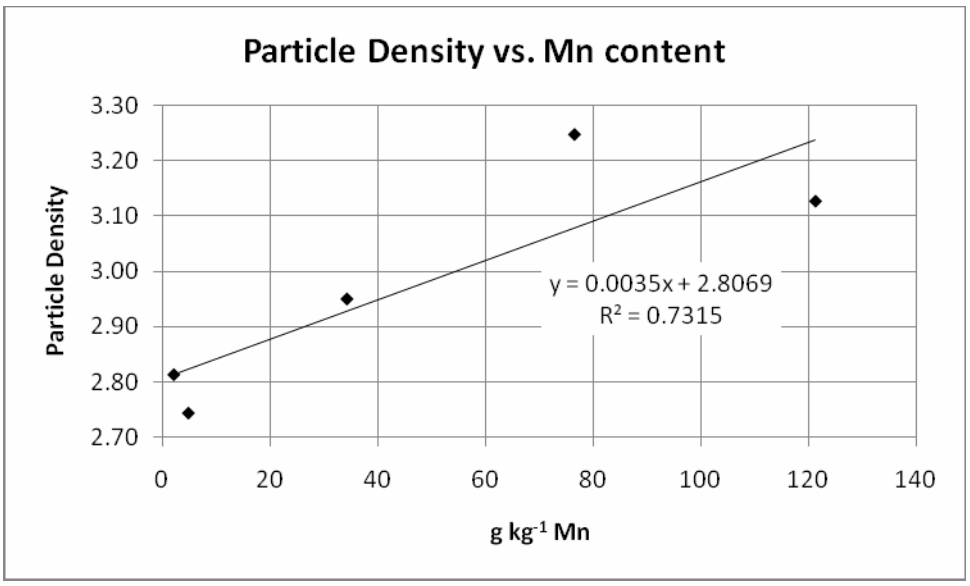

Fig. 4-19. Graph showing relationship between particle density and Mn content and corresponding linear regression equation.

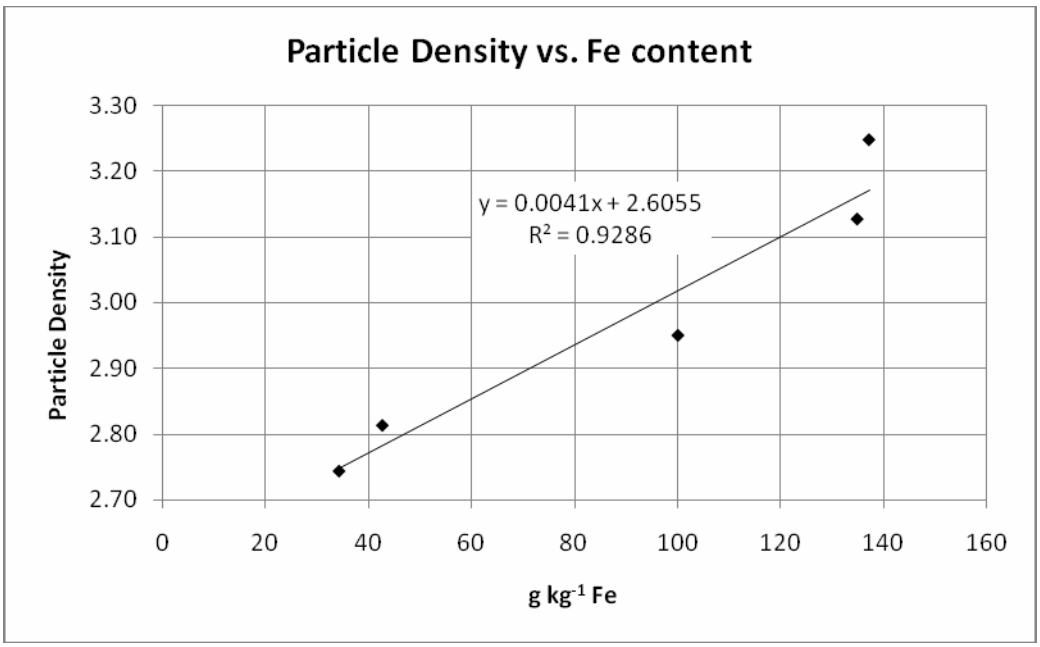

Fig. 4-20. Graph showing relationship between particle density and Fe content and corresponding linear regression equation.

Porosity

In comparing particle density with bulk density, it is surprising that there is a negative relationship between D_b and D_p, i.e., horizons with lower D_b have higher D_p ($P=0.023$, $R^2=0.84$) (Fig. 4-21). The combination of low D_b and high D_p implies that there is a tremendous amount of pore space in manganiferous soil horizons. Porosity of mineral soils is usually around 50% by volume. Of the samples measured, horizons which have less Mn and Fe and brighter colors show typical D_b and somewhat high D_p, with typical porosity (FLI-1 Ap and FLI-1 Bt1 shown in Table 4-15). Manganiferous soil horizons, however, have a porosity of up to 88% (FLI-1 2C horizon), although this is an extreme case due to the very low bulk density (0.39 g cm^{-3}) of this horizon. Because of the pore size distribution, these soils must have very large water-holding capacity. Hawker and Thompson (1988) describe the black, Mn-rich soil materials in South Africa (with as much as 287 g kg^{-1} Mn) as being "porous" and "sponge-like." These descriptions suggest that these South African manganiferous soils have similarly low D_b and high D_p, although these properties were not actually reported.

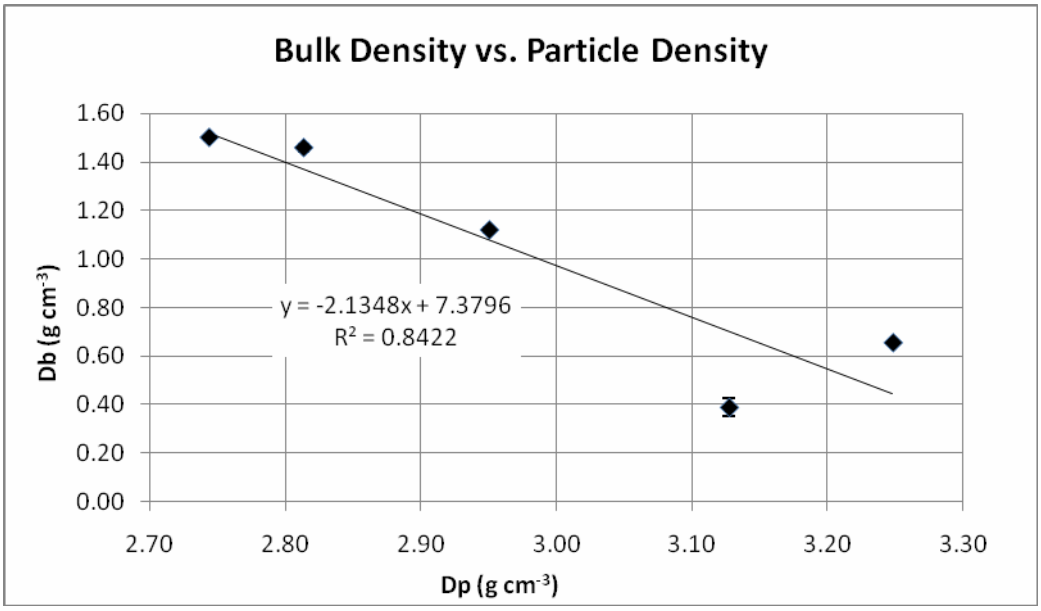

Fig. 4-21. Graph showing relationship between bulk density and particle density and corresponding linear regression equation.

Particle Size Analysis

Particle size data for each of the six pedons are reported in the morphological descriptions (Tables 4-1, 4-2, 4-3, 4-4, 4-5, and 4-6). There was initially some concern about the assumptions of the pipet method for PSA (Gee and Bauder, 1986) because of the high particle density of the manganiferous soils. The pipet method assumes a particle density of the coarse clay fraction of 2.65 g cm^{-3}, whereas the particle density of the manganiferous soils (whole soil) may be as high as 3.25 g cm^{-3}. However, it was observed that, in the PSA cylinder, the darkest particles settled quickly, and the clay remaining in suspension was much lighter brown in color. A dried sample of this suspension did not react with hydrogen peroxide. This suggests that Mn oxides are

minimal in the clay fraction, so associated Fe oxides are likely less abundant than in the whole soil. Therefore, the assumption of a particle density of 2.65 g cm^{-3} for the clay fraction of manganiferous soils is probably reasonable. Uzochukwu and Dixon (1986) also found that the majority of the Mn oxides in nodules (from two soils) were found in the sand and silt fractions.

The particle size analyses performed in the laboratory generally agree with field textures, except in a few particular cases. For several of the BC and C horizons, the PSA results show considerably higher clay contents than estimated in the field. This discrepancy is particularly extreme in the FLI-1 pedon (Table 4-5), where the BC and C horizons have clay contents measured in the lab that are 12-20% higher than those estimated in the field. The black manganiferous residuum generally feels like silt loam, but it is possible that it contains silt-sized micro-aggregates that are broken down to clay-sized particles during PSA in the lab.

Mineralogy

X-Ray Diffraction

The sand and silt fractions of the DOT-2 pedon were dominated by quartz, with lesser amounts of mica and hematite, and possibly lithiophorite (Table 4-16, Appendix B). There was also some kaolinite present in the Bt1 silt fraction. The clay fractions showed mixed mineralogy, with kaolinite and mica most abundant, and smaller amounts of vermiculite (Bt1) or hydroxy-interlayered vermiculite (HIV) (BC1), goethite, and possibly lithiophorite present. It appeared from the PSA work that the majority of the Mn

oxides were sand- and silt-sized. However, the oriented nature of the clay fraction may allow relatively smaller amounts of lithiophorite to produce XRD peaks.

Table 4-16. Semi-quantitative analysis of mineralogy of DOT-2 pedon based on peak height analysis of XRD patterns shown in Appendix B. Q=quartz; M=mica; K=kaolinite; H=hematite; G=goethite; L=lithiophorite; Ca=calcite; D=dolomite; HIV=hydroxy-interlayered vermiculite; F=feldspar; XXXX= >70%; XXX= 30-70%; XX= 10-30%; X= 5-10%; x=<5%; tr= trace.

Horizon/ Fraction	Q	M	K	H	G	L	HIV	F	V
Bt1 sand	XXX	XX		XX					
BC1 sand	XXXX			XX		x			
Bt1 silt	XXX	XX	X	XX	x				
BC1 silt	XXX	X		XX		x			
Bt1 clay	X	XXX	XXX		X			x	XX
BC1 clay		XXX	XXX		x	X	X	x	

In the FLI-1 pedon, whereas the sand and silt fractions of the Bt1 horizon contained mica, hematite, and kaolinite in addition to the quartz, the 2BC2 sand and silt fractions were nearly pure quartz (Table 4-17, Appendix B). The Bt1 clay fraction was dominated by kaolinite, mica, and HIV, with smaller amounts of chlorite, quartz, and goethite. The 2BC2 clay fraction was mostly comprised of kaolinite and an interstratified smectite-like mineral, with small amounts of mica, goethite, and lithiophorite as well.

Table 4-17. Semi-quantitative analysis of mineralogy of FLI-1 pedon based on peak height analysis of XRD patterns shown in Appendix B. Q=quartz; M=mica; K=kaolinite; H=hematite; G=goethite; L=lithiophorite; HIV=hydroxy-interlayered vermiculite; Ch=chlorite; S=smectite. XXXX= >70%; XXX= 30-70%; XX= 10-30%; X= 5-10%; x= <5%; tr=trace.

Horizon/ Fraction	Q	M	K	H	G	L	HIV	Ch	S
Bt1 sand	XXX	XX	XX	XX					
2BC2 sand	XXXX			X					
Bt1 silt	XXXX	Xx	Xx	X					
2BC2 silt	XXXX	X		x					
Bt1 clay	x	XX	XXX		x		XXx	X	
2BC2 clay	tr	X	XXX		X	x			XXX

The samples from the FLI-2 pedon were mainly quartz in the sand fractions, with lesser amounts of hematite and mica, and there was some chlorite in the BC sand fraction. The silt fractions were also mostly quartz, with lesser amounts of mica, chlorite, and hematite (Table 4-18, Appendix B). The BC clay fraction was mostly chlorite, kaolinite, and mica, with lesser amounts of vermiculite and HIV, and minor quartz and goethite. The Bt2 clay fraction had similar mineralogy to the BC, except chlorite was absent, and there was more vermiculite present.

Table 4-18. Semi-quantitative analysis of mineralogy of FLI-2 pedon based on peak height analysis of XRD patterns shown in Appendix B. Q=quartz; M=mica; K=kaolinite; H=hematite; G=goethite; L=lithiophorite; HIV=hydroxy-interlayered vermiculite; V=vermiculite; Ch=chlorite; XXXX= >70%; XXX= 30-70%; XX= 10-30%; X= 5-10%; x=<5%; tr=trace.

Horizon/ Fraction	Q	M	K	H	G	L	HIV	V	Ch
Bt2 sand	XXX	XX		X					
BC sand	XXXX	x		x		x			XX
Bt2 silt	XXXX	X		X					x
BC silt	XXX	XX		x		x			XX
Bt2 clay	x	X	XXX		x		X	XXx	
BC clay	tr	XX	XXx		x		X	X	XXX

The silicate minerals identified in the manganiferous soils (quartz, kaolinite, mica, hydroxy-interlayered vermiculite, vermiculite, chlorite, and smectite) are common in soils of the region, and therefore the silicate mineral assemblage of manganiferous soils may be considered typical and similar to many other soils of Maryland. However, the presence of Fe oxide (hematite and goethite) and possible Mn oxide (lithiophorite) peaks in some of the fractions is unusual for soils in this region. Iron and Mn oxides are typically not easily identified using XRD on whole soils (as opposed to ferromanganiferous nodules or concentrations), yet the manganiferous soils have enough hematite and goethite, and possibly lithiophorite, to produce some significant peaks. The hematite (Fe_2O_3) peaks at 1.69Å and 2.69 Å are sharp, since hematite is a well-crystalline mineral. Hematite has high thermodynamic stability and is resistant to weathering in acidic, oxidizing conditions. In temperate climates, hematite is most commonly found in

well-drained soils formed from porous, calcareous parent materials (Bigham et al., 2002). Goethite (α-FeOOH) is identifiable by its characteristic broad peak at 4.17 Å and collapse of the peak with heating to 300°C. Goethite is the most common of the Fe oxides, and is found in a wide variety of soil environments (Bigham et al., 2002). The identification of small lithiophorite ($Al_2LiMn_2^{4+}Mn^{3+}O_6(OH)_6$) peaks at 4.71 Å and 9.47 Å in some of the fractions suggests that this Mn oxide may be abundant; however, the confirmation of lithiophorite cannot be dependent upon XRD alone because of the coincidence of lithiophorite peaks with other common soil minerals such as kaolinite and chlorite. Differential XRD was attempted using a 1 M hydroxylamine hydrochloride extraction similar to the method of Neaman et al. (2004) to remove Mn oxides, and a subsequent dithionite-citrate-bicarbonate extraction to remove Fe oxides (Mehra and Jackson, 1960; Tokashiki et al. 2003). However, this method was unsuccessful at providing any additional information about the Fe or Mn mineralogy of the soils, probably because we were using a Cu X-ray source, for which Mn and Fe have a very high absorption.

Fourier Transform Infrared Spectroscopy

FTIR proved useful in identifying the dominant Mn oxide mineral present in the manganiferous soils. Figures 4-19 and 4-20 show the FTIR spectra of two Mn-rich samples which were also characterized using XRD. (The remaining spectra may be found in Appendix C.) Several characteristic lithiophorite peaks were observed (around 1004, 912, 691, 524, and 460 cm^{-1}) based on the work of Potter and Rossman (1979). Lithiophorite ($LiAl_2(Mn_2^{4+}Mn^{3+})O_6(OH)_6$) has an Al interlayer, so it likely grows and

persists under acid conditions (Golden et al., 1993). The presence of lithiophorite is not unexpected in the manganiferous soils of Maryland, given that the soils are generally below pH 6-7 in subsoil horizons (Fig. 4-13). Lithiophorite is considered to be the end product in Mn oxide weathering (Dixon, 1988), with the only further weathering being to gibbsite through reductive dissolution (Golden et al., 1993). Lithiophorite is more crystalline, has a lower specific surface and is weathered more slowly than other Mn oxides (Vodyanitskii, 2003). Lithiophorite was also identified as the dominant Mn oxide in the manganiferous soils formed in dolomite residuum in South Africa (Dowding and Fey, 2007), the Decatur soil formed from limestone residuum in Alabama (Uzochukwu and Dixon, 1986), and the acid, Mn-rich soils formed on basalt in Hawaii (Golden et al., 1993). There does not appear to be any birnessite or other soil Mn oxides present in the samples.

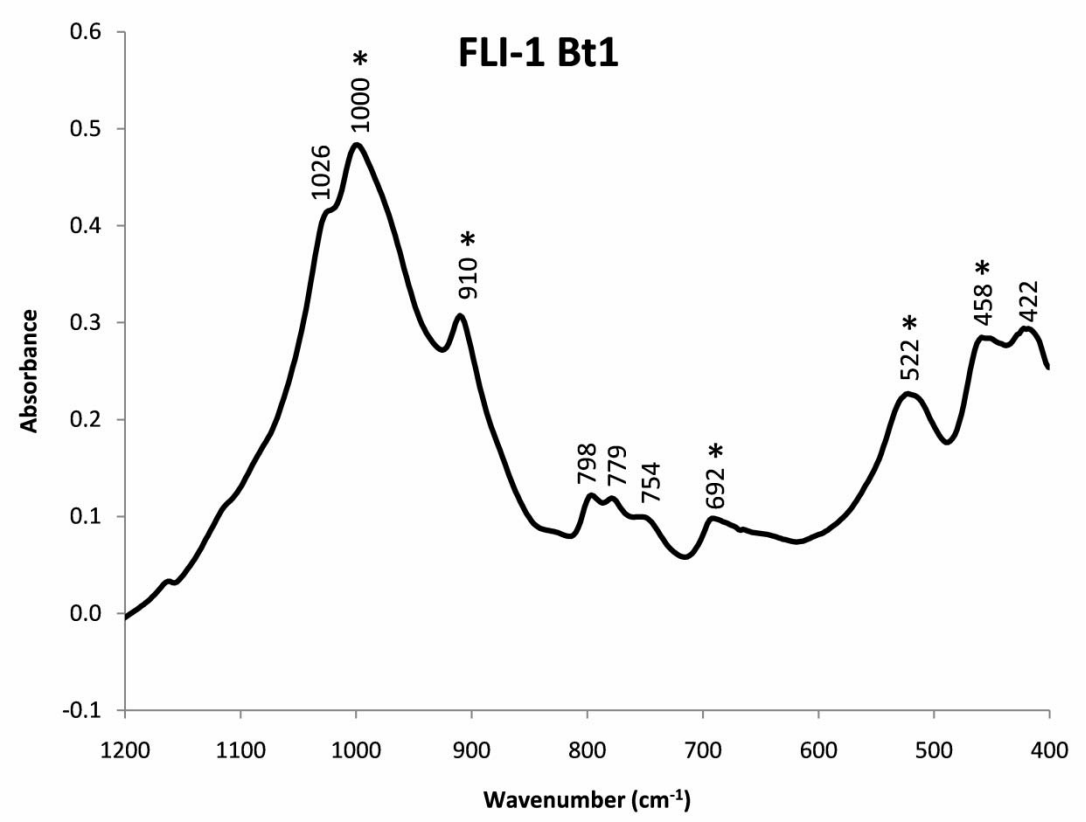

Fig. 4-22. Fourier Transform Infrared spectrum of the Bt1 horizon from the FLI-1 pedon, which has 2.2 g kg^{-1} Mn. The region of 400 to 1200 cm^{-1} is normally used for identification of characteristic Mn oxide peaks. Peaks labeled with an asterisk (*) were identified as lithiophorite based on the work of Potter and Rossman (1979).

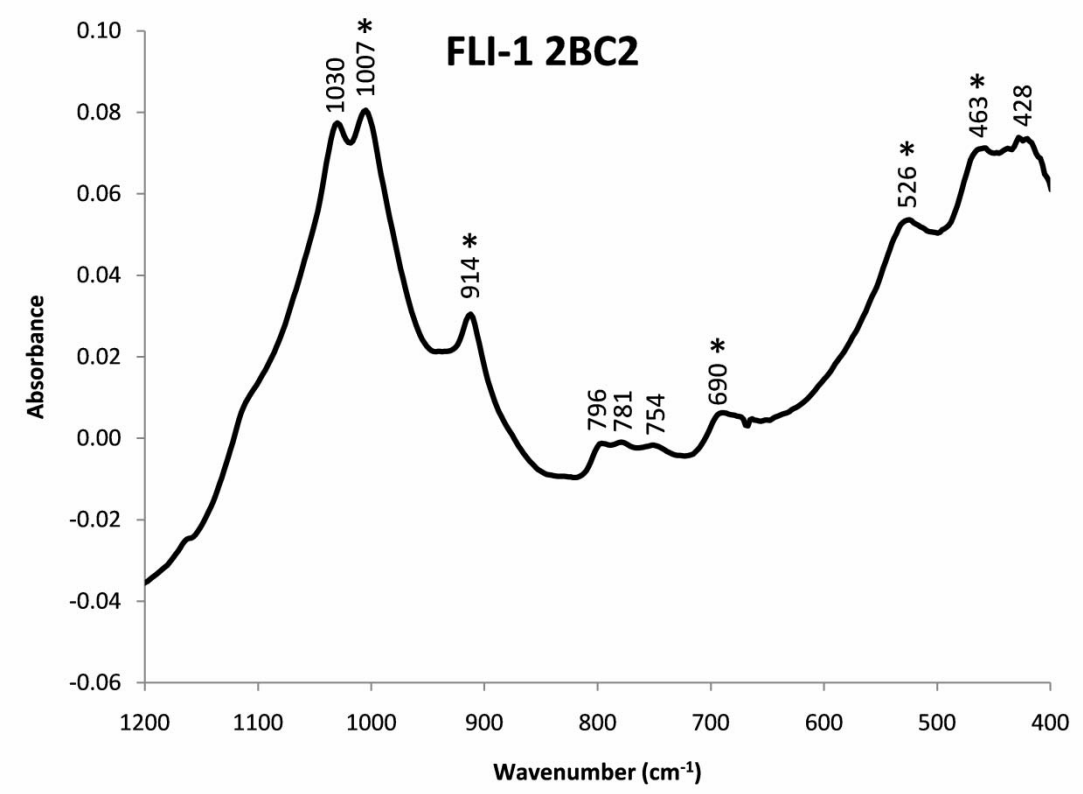

Fig. 4-23. Fourier Transform Infrared spectrum of the 2BC2 horizon from the FLI-1 pedon, which has 79 g kg^{-1} Mn. The region of 400 to 1200 cm^{-1} is normally used for identification of characteristic Mn oxide peaks. Peaks labeled with an asterisk (*) were identified as lithiophorite based on the work of Potter and Rossman (1979).

CONCLUSIONS

The fundamental properties of manganiferous soils in MD, which are unlike any other known soils in the country, were documented for the first time. The morphology of these soils is varied, with a large range thickness of manganiferous soil material (from several cm to several m). Their morphology is very distinctive, since they are so dark, often having a matrix with Munsell value/ chroma of 2/1, especially in the BC horizons

formed in the Mn-rich marble residuum. This color is not related to organic matter, as organic C concentrations are low. The black color results instead from the presence of Mn oxides that can be as high as 141 g (DCB-extractable) Mn kg^{-1} soil. There are no known soils in the U.S. which have such high concentrations of Mn. Concentrations of Fe oxides (as much as 169 g kg^{-1} Fe) are positively correlated with the Mn oxides, but their reddish color is masked by the more strongly pigmenting Mn oxides. Trace metals Ni and Co, which are known to have a strong affinity for Mn oxides, are also found in very high concentrations in the manganiferous soils. The mineralogy of the manganiferous soils is dominated by typical assemblages of quartz, mica, kaolinite, and hydroxy-interlayered vermiculite, but concentrations of Fe oxides (hematite and goethite) and possibly Mn oxides (lithiophorite) are high enough to produce XRD peaks in some samples. The presence of lithiophorite was confirmed by FTIR analysis. Hematite and lithiophorite grow and persist in acidic, well-drained conditions. The high pH of the soils (near 7) in the upper 1 m, combined with well-drained conditions, likely inhibits much reduction of Mn(III) and Mn(IV) to Mn(II), preventing phytotoxicity. The manganiferous soils also have very unusual physical properties, with a high particle density from enrichment in Fe (and Mn) oxides, but surprisingly, the most Fe- and Mn-rich horizons are highly porous, with very low bulk density.

CHAPTER 5

Pedogenesis of Manganiferous Soils

INTRODUCTION

Some unusual soils with extremely high amounts of Mn oxides have been discovered in Frederick County, Maryland. These soils have up to 140 g kg^{-1} Mn as oxides (see Table 4-9). These high concentrations of brown-black Mn oxides cause some subsoil horizons to be essentially black in color, giving these manganiferous soils a very striking and characteristic morphology. Typically, Mn is found in very low amounts in most soils worldwide, or less than 1 g kg^{-1} in the Mid-Atlantic region (Foss et al., 1969). Therefore, the manganiferous soils in MD are rare and unique. The only other known soils in the world which have similar amounts of Mn oxides (and similar morphology) occur over dolomite bedrock in South Africa, near Graskop, Mpumalanga Province (Hawker and Thompson, 1988; Dowding and Fey, 2007).

The geology of Maryland is very diverse and, as a result, there are many different types of soils and soil parent materials in the state. The manganiferous soils observed in this study are found in eastern Frederick County and western Carroll County. This area is part of the Western Division of the Piedmont physiographic province, and is characterized by rolling topography and weakly metamorphosed Precambrian bedrock, comprised mainly of metamorphosed sedimentary rocks (phyllite, slate, quartzite, limestone and marble), with some areas of metamorphosed volcanic rocks (metabasalt

and metarhyolite). Most of the soils in the Piedmont are Ultisols and Alfisols formed in residuum from these rocks.

Soils formed from calcareous rocks are of limited extent in the state, but are significant because of their unique properties. These soils are sometimes called terra rossa ("red earth"), because they often have a reddish color which is derived from high amounts of Fe oxides (usually hematite). Manganese oxides are often elevated in terrae rossae as well, since Mn(III, IV) tends to be associated with Fe(III). Limestone-derived soils in MD such as those of the Hagerstown series may have as much as 6 g kg^{-1} Mn and 78 g kg^{-1} Fe (Soil Survey Staff, 2008) and commonly have black manganiferous concentrations resulting from reduction and re-oxidation of Mn.

The genesis of terra rossa- type soils is somewhat controversial. The most widely accepted theory, called the "residual theory," holds that these soils are formed from the dissolution of carbonates and in situ accumulation of non-carbonate residue from within the rock (Leinigen, 1929). Since carbonate rocks (limestone, dolostone, and marble) tend to be relatively pure (low in non-carbonate residues), the residual theory implies that a large amount of rock would have to be dissolved in order for a soil to be formed from the residues. For example, Foster and Chittleborough (2003) estimated that approximately 150 m of rock (a certain nearly pure dolomite in Australia) would need to be dissolved in order to leave behind 40 cm of residual soil. Several authors have shown that soils overlying carbonate rocks are related to the residues collected from acid dissolution of the parent rock (e.g., Bronger et al., 1984; Moresi and Mongelli, 1988). Other authors have rejected the residual theory, showing that input of allochthonous materials may make up the major part of soils overlying carbonate bedrock (e.g., Olson et al., 1980).

Still, other authors have shown that a combination of both processes may be important factors in terra rossa genesis. For example, Foster et al. (2004) showed that the deeper soil horizons at their study sites were likely derived from non-carbonate residue from marble, but that the upper soil horizons appeared to have substantial input of colluvium.

There is little known about the manganiferous soils of Maryland and their pedogenesis. Therefore, our objectives are 1) to determine why they are so enriched in Fe and Mn oxides, and 2) to develop a general theory of their origin.

MATERIALS AND METHODS

Selection of Study Sites, Soil Sampling, and Soil Analyses

Using information from our previous reconnaissance and transect work, three sites containing manganiferous soils were chosen for intensive analysis, and are herein named for their landowners Dotterer (DOT), Grossnickle (GRO), and Flickinger (FLI). The locations of the sites are shown in Fig. 3-3, and the locations where pedons were sampled are shown in Figs. 3-4, 3-7, and 3-10. At each of the three sites, two pedons were exposed via excavation. The morphology of the pedons was described according to standard NRCS procedures (Schoeneberger et al., 2002). Bulk soil samples were collected from each horizon in all six pedons. Bedrock samples were collected from two pedons (FLI-1 and FLI-2) where the bedrock was exposed during excavation. Soils were air-dried, crushed, and sieved to pass through a 2 mm sieve in order to separate coarse fragments from the fine earth fraction. These samples were characterized in detail, and the results of the characterization are reported in Chapter 4. Quantities of Fe and Mn

oxides were measured on these samples using a modified dithionite-citrate-bicarbonate extraction (Mehra and Jackson, 1960). In addition, oriented clods were extracted from each horizon for thin section preparation (described later).

Four horizons were selected for standard X-ray diffraction (XRD) analysis from the two pedons from which bedrock samples were able to be collected (FLI-1 and FLI-2 profiles). From each of the two profiles, a B horizon and BC horizon were chosen for analysis. This choice of samples would allow us to examine mineral transformations, by comparing mineralogy vertically through the soil profile, and comparing the soil mineralogy to the mineralogy of the non-carbonate rock residues. A 30-60 g portion of each of the selected soil samples was fractionated into sand (0.05-2 mm), silt (0.002-0.05 mm), and clay (<0.002 mm) by sieving and centrifugation. Portions of the sand fractions were ground in a spex mill. The sand and silt fractions were prepared using a randomly oriented powder mount and scanned from 4 to 60°2θ at a speed of 50 s per degree 2θ using a Phillips X-Ray Diffractometer and Cu-Kα radiation filtered with a graphite crystal monochronometer. Samples of the clay fraction were saturated either with Mg followed by glycolation, or with K (Jackson, 1974). Each of these saturated samples was oriented using a filter apparatus and applied to a glass slide using the method of Drever (1973). The K- or Mg-saturated clay slides were scanned from 2 to 30°2θ at a speed of 50 s per degree 2θ under the following conditions: Mg-saturated and glycolated at 25°C; K-saturated and air-dry at 25°C; K-saturated and heated to 300°C for 2 hours; K-saturated and heated to 550°C for 2 hours. Semi-quantitative assessments were performed by visual estimations of peak height and area.

Sampling and Composition of Parent Rock

At the Flickinger (FLI) site, bedrock was shallow enough to be exposed during excavation of soil pits. Four large samples of this bedrock (several kg each) were collected for analysis; one sample was taken from the FLI-1 pit (sample R1), and the other three were taken from the FLI-2 pit (samples R9, R10, and R11). Since only one large sample was able to be collected from the FLI-1 pit, four smaller rock samples were collected (R2, R3, R4, and R6) for comparison to R1. Mineralogy of the eight rock samples was determined using XRD. Samples were scanned from 4 to 60°2θ at a speed of 50 s per degree 2θ using a randomly oriented powder mount on a Phillips X-Ray Diffractometer with Cu-Kα radiation and a graphite monochrometer.

Concentrations of Fe and Mn in the rock samples were measured using an acid extraction on small subsamples. Duplicate subsamples were collected from each of the four large rock samples (R1, R9, R10, and R11). These subsamples were ground to a fine powder in a spex mill, and then duplicate 0.5 g samples were extracted with 50 mL of 6 M HCl at room temperature (approx. 25°C) for approximately 1 h. For the four smaller rock samples (R2, R3, R4, and R6), duplicate 5 g samples were extracted with 500 mL of 6 M HCl at 25°C for 2 h. The extractions were filtered through Whatman no. 1 filter paper to remove any non-carbonate residue, and Fe and Mn were measured in the supernatant using atomic absorption spectrophotometry.

Collection and Analyses of Non-Carbonate Residues

Non-carbonate residues were collected via acid dissolution of the rock samples using the method of Rabenhorst and Wilding (1984). One kilogram of each of the four rock samples (R1, R9, R10, and R11) was crushed to pass through a 5 mm sieve before adding acetic acid buffered to pH 4.5. The method had to be modified for the dissolution of sample R1. Because R1 is mainly dolomite, it would not dissolve in acetic acid. Therefore, hydrochloric acid was added to lower the pH of the solution to approximately 1. After 3 d at pH 1, sample R1 had completely dissolved. Then, the residue was washed with distilled water until the solution was approximately pH 4.5, in an effort to prevent mineralogical alteration. The material remaining after acid dissolution of each sample was washed and weighed to determine the quantity of non-carbonate residue in the rock. This non-carbonate residue was fractionated by sieving and centrifugation to determine its particle-size distribution and to separate the sand (0.05-2 mm), silt (0.002-0.05 mm), and clay (<0.002 mm) fractions for mineralogical analysis.

Mineralogy of the non-carbonate residues was determined on each size fraction using standard XRD techniques. Portions of the sand fractions were ground in a spex mill. The sand and silt fractions were scanned from 4 to 60 degrees 2θ at a speed of 50 s per degree 2θ using a randomly oriented powder mount on a Phillips X-Ray Diffractometer and Cu-Kα radiation filtered with a graphite crystal monochrometer. Samples of the clay fraction were prepared and analyzed in the same manner as the soil samples.

Thin Section Preparation and Soil Micromorphology

Thin sections were prepared from oriented soil clods in our lab. Each clod was placed in a plastic cup (maintaining its orientation) and air-dried, and then oven-dried at 95°C overnight before being impregnated with Scotchcast #3 Electrical Resin under vacuum to release trapped air. The resin was cured in an oven at 95°C for 24 h. Each cured, impregnated clod was cut into a block, and one side was polished before being mounted onto a glass slide (previously ground to uniform thickness with a Micro-Trim thin section machine) using epoxy, and pressure was applied with a jig during the curing process to ensure complete adhesion of the impregnated soil to the slide. The block of impregnated soil was trimmed and ground down to a thickness of approximately 100 μm using the Micro-Trim. Final polishing to a thickness of approximately 30 μm was achieved by hand polishing with a series of silicon carbide grits and cutting oil on a textured glass plate. Thin sections were examined and photographed using a petrographic microscope under both plane- and cross-polarized light.

RESULTS AND DISCUSSION

Soil Parent Materials

Soil Morphological Evidence

In Chapter 3, the manganiferous soils were shown to be associated with areas mapped as the Sams Creek geologic formation. Observations of the marble bedrock (at the FLI site) are consistent with descriptions of the Wakefield Marble member of the

Sams Creek formation, which is mapped at the site. The FLI-1 profile (Fig. 4-5, Table 4-5) shows a clear weathering rind or "halo" of black residuum surrounding the marble bedrock, providing morphological evidence that the manganiferous soils are derived from marble residuum.

The soil morphology documented in Chapter 4 also suggests that there are lithologic discontinuities in some of the profiles. Three of the pedons described in Chapter 4, DOT-2, GRO-1 and FLI-1, show abundant phyllite channers and lighter colors in the upper part, with distinctly darker, highly manganiferous BC horizons underneath, which are devoid of phyllite channers. The DOT-2 profile has lighter colors, and only 17-30% coarse fragments by volume (mainly phyllite channers) in the upper three horizons (Ap, BA, and Bt1), and there are colors of 3/2 or darker and only 2-7% quartzite gravels in the horizons below (Table 5-1). Although we did not describe a lithologic discontinuity in DOT-2 in the field, it now appears that there is a lithologic discontinuity at 65 cm. The FLI-1 profile has 6-16% coarse fragments (phyllite channers) and lighter colors in the upper part, and below the lithologic discontinuity at 135 cm, there are colors estimated to be 1/1 or darker, and only 0-4% quartzite gravels (Table 5-2). The GRO-1 profile has dark colors (2.5/2 or darker) throughout, but there is 8-11% coarse fragments (mainly phyllite channers) in the upper two horizons (Ap and Bt), and 3-9% quartzite gravels below the lithologic discontinuity at 88 cm (Table 5-3). The GRO-2 profile is the only pedon documented that has a lithologic discontinuity beneath the black, Mn-rich residuum. Below approximately 3 m, there is a much lighter-colored residuum present (Table 5-4). The brown colors, loam and silt loam textures, and the absence of phyllite fragments suggest that this second parent material might be Sams

Creek metabasalt (greenstone). The presence of these lithologic discontinuities is consistent with the complex nature of the Sams Creek formation, which was folded during the Appalachian Orogeny approximately 300 to 350 million years ago, resulting in interbedding of the marble with green (chlorite-rich) and purple (hematite-rich) phyllites and metabasalt.

Table 5-1. DOT-2 abbreviated morphological description.

Horizon	Lower depth	Matrix color (moist, field Munsell)	Coarse fragments by volume (PSA)	Texture class PSA/ (by feel)	Clay PSA/ (by feel)
	cm		%		%
Ap	24	7.5YR 3/2	17	ch sil (sil)	13.4 (17)
BA	45	7.5YR 3/3	15	l (l)	21.3 (23)
Bt1	65	7.5YR 4/4	30	ch l (ch cl)	26.1 (29)
Bt2	104	5YR 3/2	5	cl (cl)	29.2 (30)
Bt/BC (Bt component, 55% of horizon)	185	5YR 2.5/2	2	cl (cl)	34.3 (30)
Bt/BC (BC component, 40% of horizon)		5YR 1/1	7	cl (l)	29.2 (18)
BC1	330	5YR 1/1	2	sil	20.0
BC2	388	10YR 4/4			
BC3 (sampled by depth)	500	5YR 1/1			
	600				
	720				
BC4	775	5YR 1/1			

Table 5-2. FLI-1 abbreviated morphological description.

Horizon	Lower depth	Matrix color (moist, field Munsell)	Coarse fragments by volume (PSA)	Texture class PSA/ (by feel)	Clay PSA/ (by feel)
	cm		%		%
Ap	28	10YR 3/4	6	sil (sil)	13.6 (20)
BA	42	7.5YR 4/4	16	ch l (l)	23.6 (25)
Bt1	87	7.5YR 4/6	11	l (cl)	24.3 (29)
Bt2	135	7.5YR 4/6	7	l (sicl)	24.4 (27)
2BC1	162	5YR 1/1	2	c (sil)	41.5 (22)
2BC2	185	N1	4	cl (sil)	27.4 (15)
2C	189	N1	0	l (sil)	22.8 (5)

Table 5-3. GRO-1 abbreviated morphological description.

Horizon	Lower depth	Matrix color (moist, field Munsell)	Coarse fragments by volume (PSA)	Texture class PSA/ (by feel)	Clay PSA/ (by feel)
	cm		%		%
Ap	26	7.5YR 2.5/2	11	sl (l)	7 (19)
Bt	63	7.5YR 2.5/2	8	l (l)	17.4 (23)
BC1	88	5YR 2/1.5	3	l (1)	10.7 (17)
2BC2	121	5YR 1/1	3	sl (l)	6.2 (15)
2BC3	155	5YR 1/1	8	sl (sil)	15.5 (10)
2CB	180	5YR 2/1	9	sl (sil)	2.6 (<10)
*	255 290 410 540 600 700 800 850	5YR 1/1	3	sl	2.4

*Horizonation not evident; sampled by depth.

Table 5-4. GRO-2 abbreviated morphological description.

Horizon	Lower depth	Matrix color (field, moist, Munsell)	% Coarse frags by volume (PSA)	Texture class PSA/ (by feel)	% clay PSA/ (by feel)
	cm		%		%
Ap	23	7.5YR 2.5/3	16	ch l (l)	12.8 (17)
Bt1	48	7.5YR 2.5/3	10	l (l)	22.7 (26)
Bt2	78	7.5YR 2.5/2	15	l (l)	21.3 (24)
Bt3	100	7.5YR 3/4	10	l (l)	21.3 (23)
BC1	127	5YR 3/3	49	vch l (vch l)	14.7 (20)
BC2	152	5YR 2.5/1	38	vch l (ch l)	12.0 (16)
BC3	190	5YR 2.5/1	25†	(ch l)	(16)
BC4	228	7.5YR 3/2	55†	(vch l)	(18)
BC5	298	5YR 1/2	5†	(l)	(16)
2BC6	314	7.5YR 5/6		(l/sil)	(25)
2BC7	352	10YR 4/3		(l)	(12)
2BC8	400	7.5YR 4/4		(l)	(20)
2BC9	470+	7.5YR 5/8		(sil)	(22)

†Estimated in field.

Mineralogical Evidence

Composition of the Bedrock

The X-ray diffractograms of the large rock samples (which were dissolved for analysis of non-carbonate residue) collected at the Flickinger (FLI) site are shown in Fig. 5-1. Sample R1, collected from the FLI-1 pedon, is primarily dolomite, with small amounts of quartz and calcite (Fig. 5-1). However, samples R9, R10, and R11, which were collected from the FLI-2 pedon, are nearly pure calcite (Fig. 5-1). Because R1 was the only large sample collected from the FLI-1 pedon, and because it differed mineralogically from the rock samples collected from the FLI-2 pedon, some smaller FLI-1 rock samples were analyzed for comparison. The smaller FLI-1 samples, R2, R3, and R4, are mainly dolomite, with minor calcite, similar to R1 (Fig. 5-2). Sample R6 is a mixture of dolomite and calcite. All of the smaller marble samples have substantially less quartz (chert) than R1.

These data (Figs. 5-1 and 5-2) confirm that the bedrock underlying the FLI pedons is marble. The mineralogy and morphology of the rock is consistent with the description of Wakefield Marble, which is indeed mapped at the site (see Fig. 3-9). The Wakefield Marble member occurs in the lower part of the Sams Creek Formation, which is mainly comprised of greenish metamorphosed basalt. The white to grey Wakefield Marble is late Precambrian in age. Some zones of the marble are primarily calcitic, while other zones are primarily dolomitic, because it was formed as a result of metamorphism of limestones and dolostones (Maryland Geological Survey, 1986).

Bedrock from FLI-1 and FLI-2

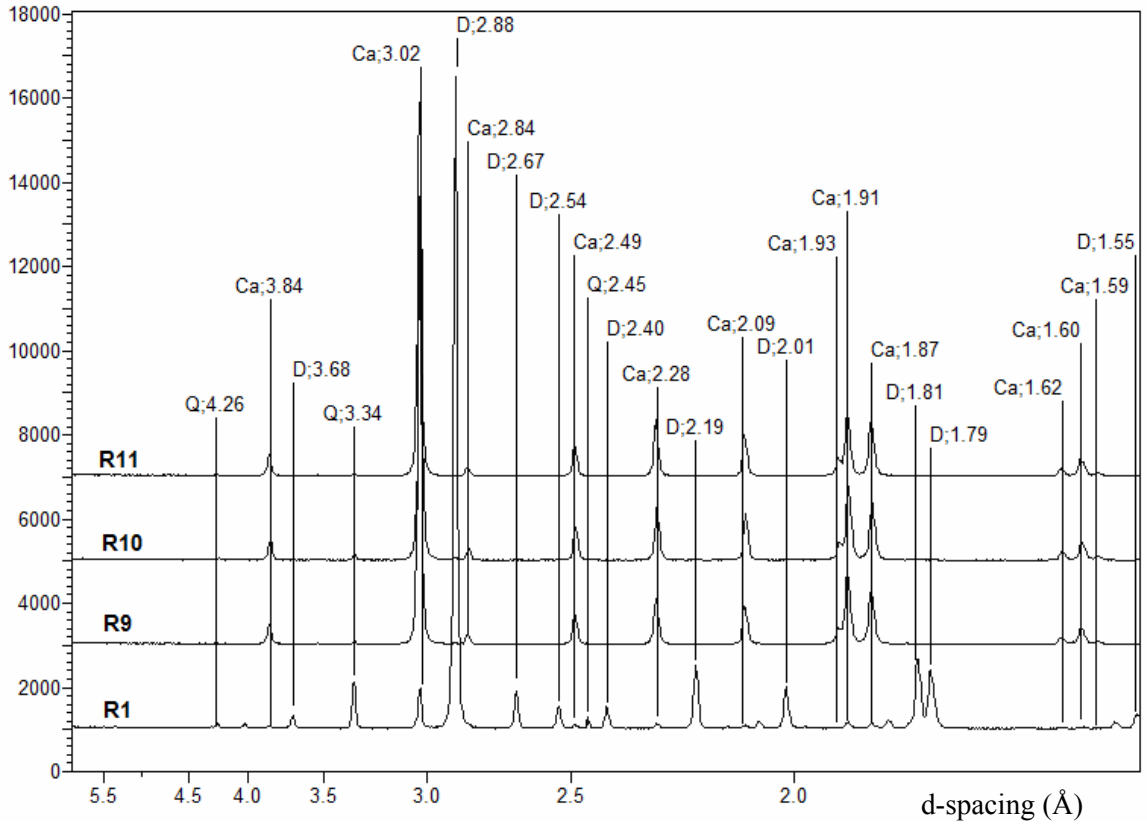

Fig. 5-1. X-ray diffractograms of four marble bedrock samples from the FLI site. Sample R1 (mainly dolomite) was taken from the FLI-1 pedon, and samples R9, R10, and R11 (all mainly calcite) were taken from the FLI-2 pedon. Ca=calcite; D=dolomite; Q=quartz.

FLI-1 Bedrock (Samples for Comparison to R1)

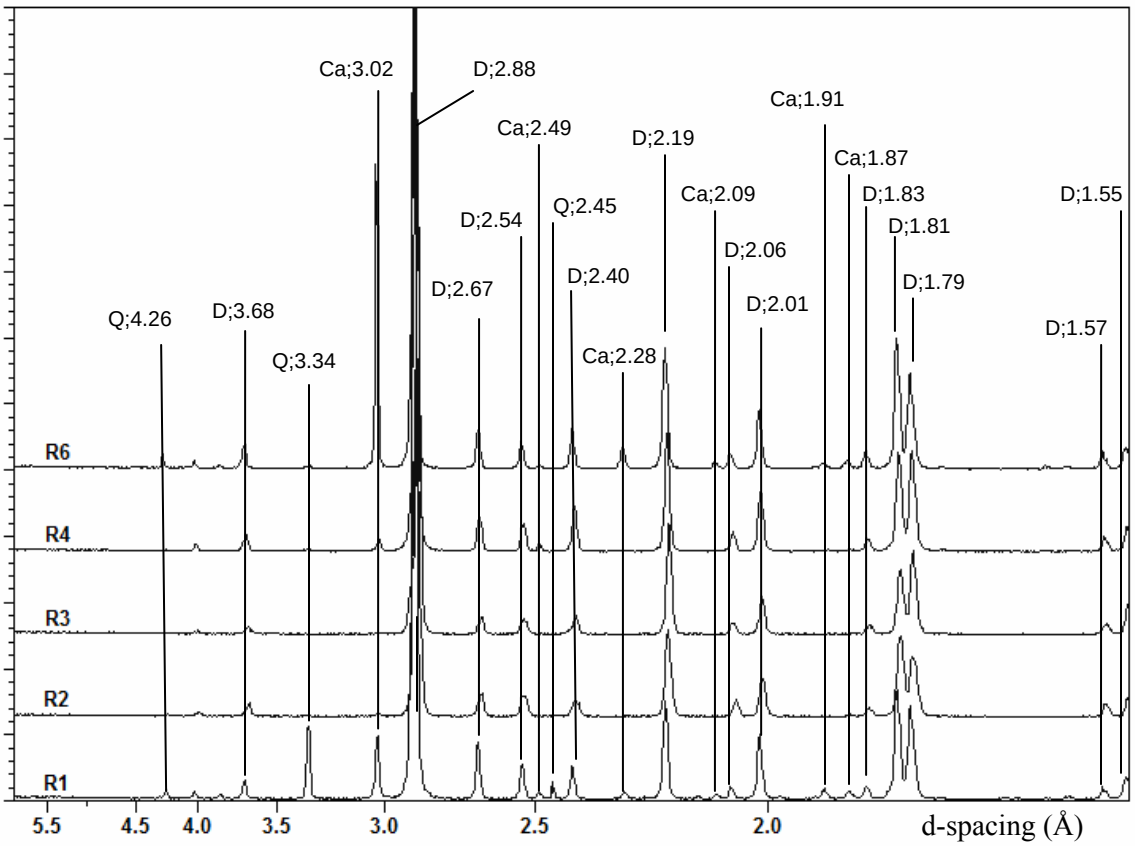

Fig. 5-2. X-ray diffractograms of marble bedrock samples collected from beneath the FLI-1 pedon. One kg of rock sample R1 was dissolved and the non-carbonate residue was collected for mineralogical analysis. R2, R3, R4, and R6, though not characterized in detail, were scanned to compare to R1 (to determine if dolomitic marble is typical for the FLI-1 pedon). Ca=calcite; D=dolomite; Q=quartz.

During the formation of the original limestones and dolostones that were later metamorphosed into the Wakefield Marble, there was some input of non-carbonate materials, which is typical of sedimentary carbonates. Siliclastic sediments were mixed in with the carbonate sediments, and became physically bound during lithification. Divalent Fe and Mn may have been incorporated into the crystal lattice of the calcite and dolomite. Fe^{2+} and Mn^{2+} can substitute for Ca^{2+} and Mg^{2+} in calcite ($CaCO_3$) and dolomite

($CaMg(CO_3)_2$). Fe and Mn may also occur as distinct carbonate minerals (siderite, $Fe(CO_3)_2$ and rhodochrosite, $Mn(CO_3)_2$). Manganese may occur in calcite as part of the solid solution between $CaCO_3$ and $Mn(CO_3)_2$ (Eriksson et al., 1975). However, little Fe occurs in calcite as a result of the immiscibility gap between $CaCO_3$ and $CaMg(CO_3)_2$ and between $CaCO_3$ and $CaFe(CO_3)_2$ (ankerite) (Wolf et al., 1967). Calcites in South Africa contain 10 g kg^{-1} FeO and 30 g kg^{-1} MnO (Eriksson et al., 1975). Dolomite crystals may contain a greater proportion of Fe and Mn than calcite, or up to 30 g kg^{-1} FeO and 100 g kg^{-1} MnO, since there may exist a solid solution between dolomite ($CaMg(CO_3)_2$), ankerite ($CaFe(CO_3)_2$), and kutnahorite ($CaMn(CO_3)_2$) (Eriksson et al., 1975).

Typically, Fe and Mn are found in concentrations on the order of approximately 4 g kg^{-1} Fe and 1 g kg^{-1} Mn in carbonate rocks (Krauskopf, 1972, as cited in Stevenson and Cole, 1999). The calcitic marble samples (R9, R10, and R11) collected from beneath the FLI-2 profile have an average of 1.59 g kg^{-1} Fe and 0.35 g kg^{-1} Mn, and may therefore be considered to have typical or low concentrations of Fe and Mn. The dolomite marble samples (R1, R2, R3, R4, and R6) collected from beneath the FLI-1 pedon have an average of 3.99 g kg^{-1} Fe and 4.23 g kg^{-1} Mn, so these rocks have higher than average concentrations of Mn (Table 5-5). For comparison, the dolomite bedrock underlying the manganiferous soils of South Africa has an average of 5.6 g kg^{-1} Fe and 13.3 g kg^{-1} Mn (Hawker and Thompson, 1988).

Table 5-5. Fe and Mn content of marble bedrock samples as determined by extraction with 6M HCl.

Sample	Source pedon	Dominant mineralogy	Fe	Mn
			g kg^{-1}	
R1	FLI-1	dolomite	4.48	3.89
R2	FLI-1	dolomite	5.06	5.81
R3	FLI-1	dolomite	3.35	3.32
R4	FLI-1	dolomite	3.93	4.29
R6	FLI-1	dolomite	3.13	3.83
R9	FLI-2	calcite	2.12	0.52
R10	FLI-2	calcite	1.41	0.27
R11	FLI-2	calcite	1.25	0.27

Weathering of Marble Bedrock and Formation of Saprolite and Residuum

Subsequent to the Appalachian Orogeny roughly 300 to 350 million years ago, the Wakefield marble has been weathered and altered since the beginning of the evolution of the Piedmont landscape. Calcite and dolomite, the major components of the marble, are typically weathered by congruent dissolution, i.e. dissolution into simple ionic constituents without formation of secondary minerals. Calcite and dolomite are both soluble in acidic conditions. In the region where the manganiferous soils are found, the udic soil moisture regime favors leaching and acidic soil conditions. Therefore, carbonate rocks are weathered easily, the Ca^{2+}, Mg^{2+}, and CO_3^{2-} are leached, and soils derived from carbonate rocks are usually non-calcareous. The actively weathering nature of the dolomitic marble directly underlying the black manganiferous residuum of the FLI-1

pedon is shown in Fig. 5-3. The jagged crystal edges are indicative of dissolution. Dissolution of the edges of the carbonate crystals is the first step in the formation of manganiferous soils from the underlying marble bedrock.

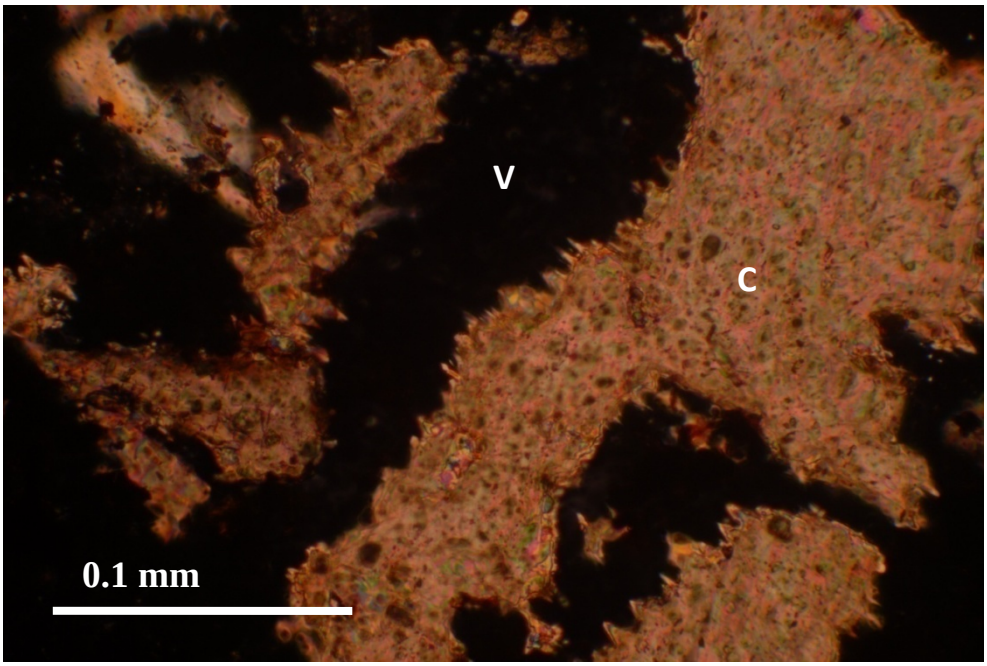

Fig. 5-3. FLI-1 bedrock contact at approximately 189 cm. XPL. Actively weathering marble; note the jagged crystal edges. C=carbonate (calcite or dolomite); V=void (black areas not to be confused with Mn oxides).

Figures 5-4 and 5-5 also show dissolution of the marble, which is causing the crystals to become unconsolidated into sand-sized particles, forming a weathered rock, or saprolite. The FLI-1 profile has a zone of marble saprolite several cm thick overlying the marble bedrock. (It is unusual to find weathered marble of any substantial thickness, because it usually dissolves completely along a thin weathering front.) During the weathering process, a red and black rind is visible around the carbonate grains, especially

in Fig. 5-4, which shows the initial stages of alteration. This indicates that Fe^{2+} and Mn^{2+} (previously tied up in the crystal structure of the carbonates) are released and oxidized, and accumulate along the edges of the dissolving carbonate grains. Oxidation of Fe^{2+} and Mn^{2+} releases H^{+} ions which may enhance dissolution of the carbonates. Non-carbonate (silicate) residues are also presumably released, left intact, and accumulate with the Fe and Mn oxides around the dissolving carbonate crystals, although they are not clearly visible because they must be pigmented by the Fe and Mn oxides.

Figure 5-5 shows a more advanced stage of alteration of the marble, which leads to formation of porous ferromanganiferous material (shown in Figs. 5-6, 5-7, and 5-8) that remains after dissolution of the carbonate crystals. This is strong evidence that the manganiferous soils are derived from marble residuum.

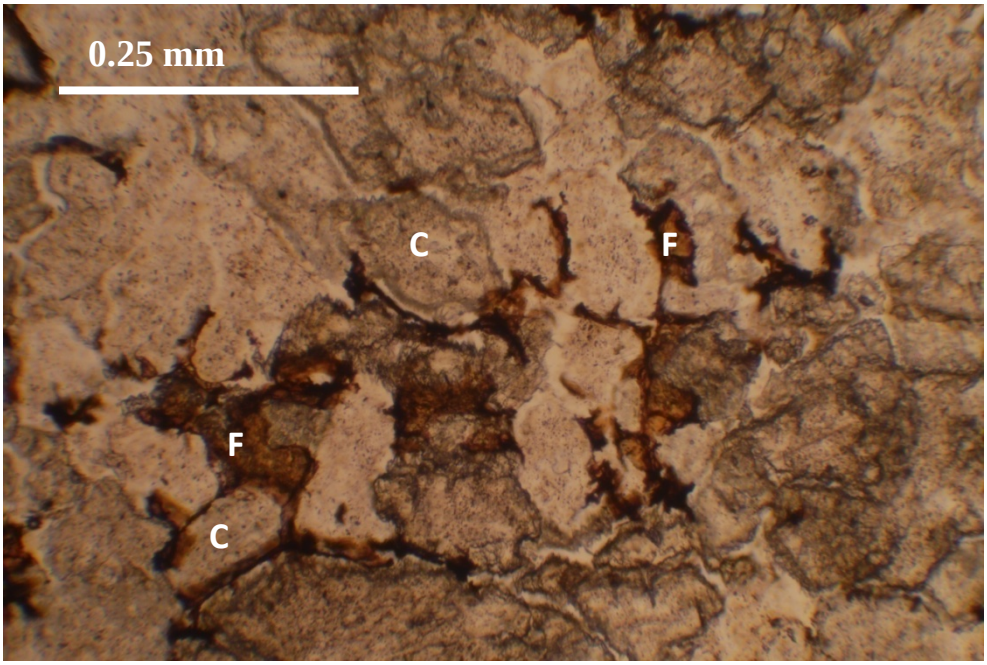

Fig. 5-4. FLI-1 marble saprolite. PPL. Note the beginning of the formation of the ferromanganiferous "framework" in between the carbonate grains. C=carbonate (likely dolomite); F=Fe- and Mn-rich material released during weathering.

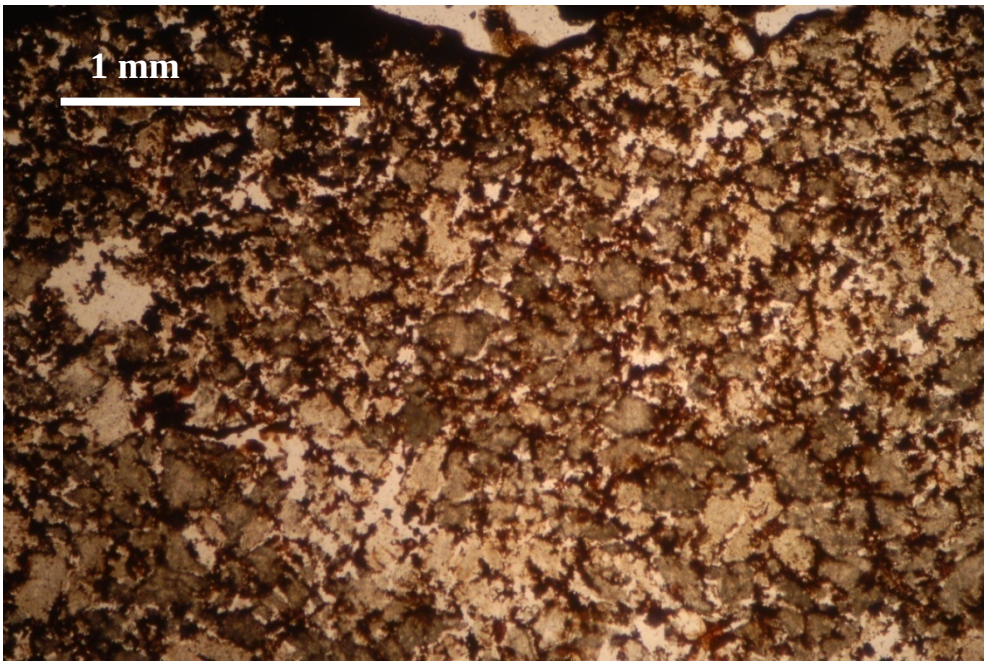

Fig. 5-5. FLI-1 marble saprolite. PPL. Note the presence of ferromanganiferous micro-aggregates beginning to form in between the carbonate grains. Grey areas are carbonate (calcite or dolomite) grains; red/ black areas are Fe- and Mn-rich material released and precipitated during weathering.

The manganiferous and carbonate-free marble residuum has very unusual physical properties. In Chapter 4, it was shown that this material has very low bulk density, very high particle density, and therefore very high porosity. A micrograph of the FLI-1 2C horizon (the black "halo" overlying the marble bedrock) is shown in Fig. 5-6. This horizon has 121 g kg^{-1} Mn, 108 g kg^{-1} Fe (Table 4-11), loam texture (Table 4-5), bulk density of 0.39 g cm^{-3}, particle density of 3.13, and porosity of 87.5% (Table 4-15). The microaggregates are nearly all manganiferous, so they are opaque. A "spongy" microstructure is apparent.

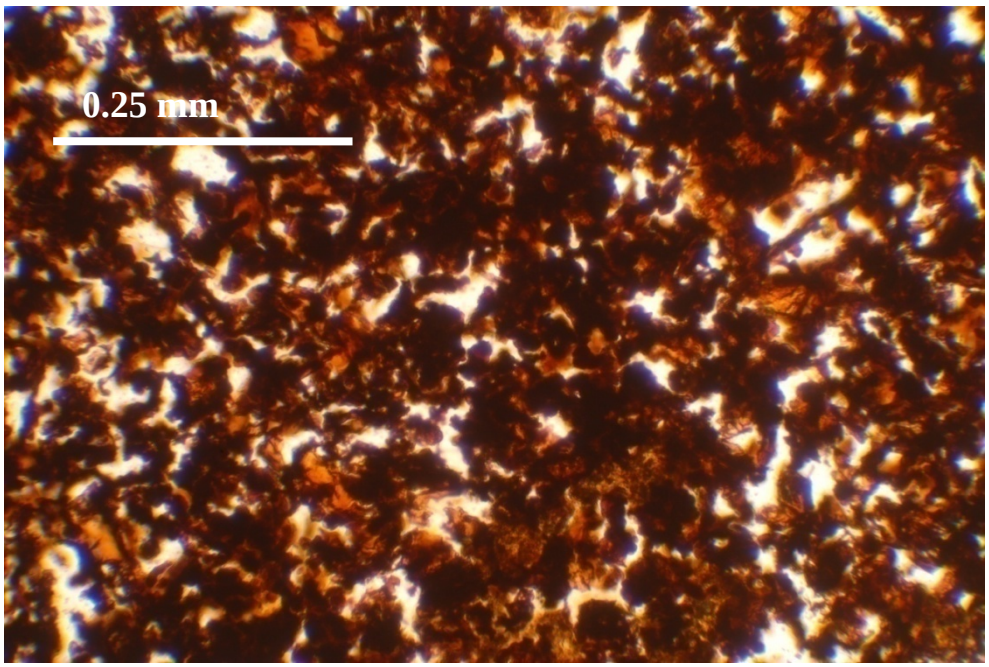

Fig. 5-6. FLI-1 2C horizon. PPL. Note the opacity of the soil and the highly porous microstructure.

The sponge-like, porous structure of manganiferous marble residuum is also documented visually in Figs. 5-7 and 5-8, which show micrographs of the BC1 horizon from the DOT-2 pedon. Hawker and Thompson (1988) reported a very similar sponge-like microstructure in manganiferous dolomite residuum in South Africa. The authors speculated that after the original dolomite crystals in the parent rock had dissolved, they were "replaced" by a highly porous framework of manganiferous material. It seems reasonable that Hawker and Thompson's (1988) explanation for the porous structure would also apply to the manganiferous soils in Maryland.

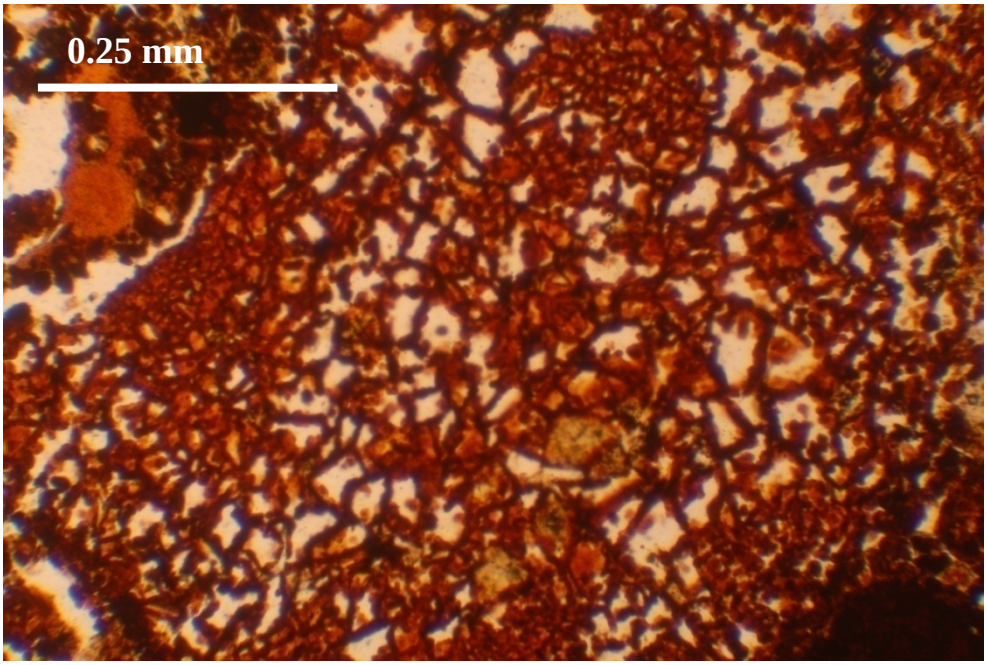

Fig. 5-7. DOT-2 BC1. PPL. Note the sponge-like structure (high porosity) and voids which were presumably left after the dissolution of carbonate (calcite and/ or dolomite) crystals.

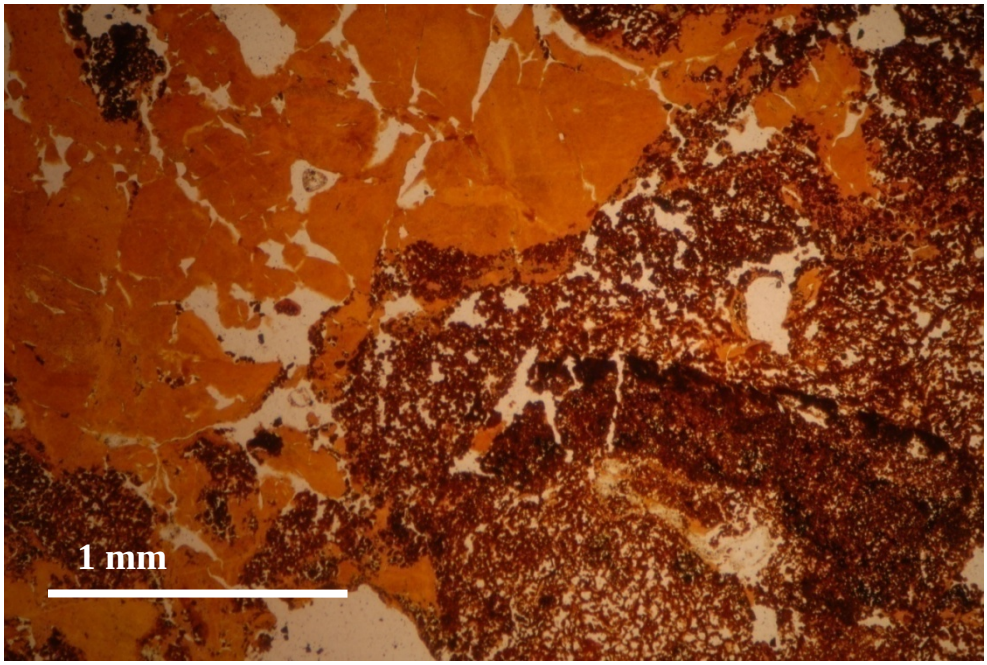

Fig. 5-8. DOT-2 BC1. PPL. Note the high porosity of the black manganiferous material, and the red-orange Fe oxide clay accumulation (mottle).

Quantity and Particle Size of Non-Carbonate Residues

If the residual theory of terra rossa pedogenesis (Leinigen, 1929) applies to Maryland soils, then these manganiferous soils are formed as a result of the accumulation of non-carbonate residue left after dissolution of carbonates in the marble bedrock. This non-carbonate residue would be largely composed of the siliclastic sediments which were added to the original sedimentary limestones and dolostones that were later metamorphosed into the Wakefield marble, and the Fe and Mn oxides discussed previously. In order to determine the possibility that the marble bedrock is in fact the parent material of manganiferous soils, we examined the residue remaining after acid dissolution of the marble in the laboratory.

The residue left after dissolution of the dolomitic marble sample (R1, from FLI-1) in the laboratory was very different than the residue left after dissolution of the calcitic marble samples (R9, R10, and R11, from FLI-2). The R1 residue was mainly gravel- and sand-sized chert, with very little silt and clay (Table 5-6). Chert is a secondary quartz mineral which may result from the replacement of carbonates with silica. The R9, R10, and R11 residues had very few coarse fragments, and had silt loam textures. The texture of the calcitic residues more closely matched the texture of the BC and C material found at the FLI site (loam/ clay loam/ silt loam textures, see Tables 4-5 and 4-6). The chert extracted from R1 is probably not typical for the dolomite component of the Wakefield Marble. The X-ray diffraction patterns in Fig. 5-2 show that the other dolomitic rock samples collected have very little chert, so the chert most likely occurs in irregular zones throughout the marble. It is possible that the manganiferous soils may be derived from the non-carbonate residue of some component of the marble bedrock.

In order to determine the possibility that there was originally enough rock to produce the thickness of soils observed, the amount of rock necessary to produce a fixed amount of soil was calculated using the following assumptions: 1) the soil is derived completely from the non-carbonate residues; 2) the bulk density of the marble bedrock is 3.0; and 3) the bulk density of the residuum is 1.0 (Table 5-6).

Table 5-6. Quantity and particle size of non-carbonate residues from rock samples, collected via acid dissolution. Calculations of the quantity of rock needed to produce a fixed amount of soil is based on quantity of residue in rock, assuming a bulk density of 3.0 for marble samples, and a bulk density of 1.0 for soils. vgr=very gravelly.

Sample	Quantity of residue in rock	Gravel	Sand	Silt	Clay	Texture class of residue	Quantity of rock needed to produce soil of volume or thickness x
	----------%----------						
R1	3.34	39.14	90.17	8.73	1.10	vgr sand	10.0x
R9	2.29	0.00	23.82	62.31	13.87	silt loam	14.6x
R10	2.42	0.79	33.82	55.73	10.46	silt loam	13.8x
R11	2.47	1.02	29.47	59.59	10.94	silt loam	13.5x

Our calculations show that the amount of marble bedrock weathered to form these soils would need to be approximately 13 times the volume or thickness of soil observed. The black, Mn-rich portion of these soils ranged from 5 cm (FLI-2 pedon, Table 4-6) to 8.5 m (GRO-1 pedon, Table 4-3). According to our calculations, these thicknesses of soil would require that 65 cm to 110.5 m of marble be dissolved. The thickness of the Wakefield Marble member is reported to range between 1 and 150 m (Maryland Geological Survey, 1986).

As mentioned earlier, sample R1 was mainly comprised of gravel- and sand-sized chert. The horizon above this rock, however, the FLI-1 2C horizon, had a loam texture, with 0% coarse fragments and 34% sand. If we were to assume that the coarse chert was precipitated as a secondary mineral and segregated into lenses (confirmed by the very low quartz content of other marble samples collected from the FLI-1 pedon, Fig. 5-2), we could recalculate to account for this. If the gravel and excess sand are subtracted from the non-carbonate residue extracted from R1, then the equivalent amount of soil-producing residue in R1 is only 0.9%, and the quantity of rock needed to produce soil is 37x rather than 10x (as shown in Table 5-6). In the FLI-1 pedon, the thickness of black, Mn-rich soil material is 54 cm, which would therefore require approximately 20 m of marble to have dissolved, if the gravel and excess sand portions are excluded from the calculation. Therefore, with regard to the soil thickness and quantity of non-carbonate residues, it is feasible and reasonable to speculate that the manganiferous soils could be derived mainly from residuum of both the calcitic and dolomitic components of the Wakefield Marble.

Quantities of Manganese and Iron in Rock Related to Quantity of Residue

When the concentrations of Fe and Mn within the marble are calculated in terms of the quantity of non-carbonate residue present, they are very similar to the concentrations of Fe and Mn in the black soil material directly overlying the marble (Table 5-7). The FLI-1 2C horizon, which directly overlies marble bedrock (from which sample R1 was taken), has 108 g kg^{-1} Fe and 121 g kg^{-1} Mn (see Table 4-11). The marble underlying the FLI-1 pedon is dolomitic, so it may accommodate more Fe and Mn in its

crystal structure than calcite. The FLI-2 BC horizon (directly overlying the bedrock from which samples R9, R10, and R11 were taken) has 61 g kg^{-1} Fe and 11 g kg^{-1} Mn (see Table 4-12). These quantities of Fe are more typical of other soils derived from carbonate rock, and these quantities of Mn, while still very high (high enough to produce soil colors of 3/3, 3/2 or darker), are low relative to the FLI-1 pedon. The marble underlying the FLI-2 pedon is calcitic. Since calcite cannot accommodate much Fe and Mn in its crystal lattice, this may account for the difference in Mn content between the marble samples and between the soils. The ionic radii of Mg^{2+}, Fe^{2+}, and Mn^{2+} are similar, so Fe^{2+} and Mn^{2+} may easily substitute for Mg^{2+} in dolomite. The soil zones which are highest in Mn may therefore be derived from dolomite components of the Wakefield marble. If this were the case, they could be similar to the manganiferous soils of South Africa that are derived from dolomite (Hawker and Thompson, 1988; Dowding and Fey, 2007).

Table 5-7. Quantity of Fe and Mn in rock samples calculated in terms of the quantity of non-carbonate residue.

Sample	Fe	Mn
	g kg^{-1}	
R1	134	116
R9	92	22
R10	58	11
R11	51	11

For sample R1, if the gravel and excess sand are subtracted for the reasons described earlier, and a residue content of 0.9% is therefore assumed, then the quantities of Fe and Mn calculated in terms of the non-carbonate residue increase to 498 g kg^{-1} and

342 g kg^{-1}, respectively. These concentrations are much higher than those in the soils. Therefore, the estimate of 0.9% soil-producing residue in the rock may be too low, and the chert component of R1 may be uncharacteristic of the parent marble. Figure 5-2 shows that R1 has substantially more chert than the other marble samples collected from FLI-1.

These results indicate that all of the Fe and Mn present in the manganiferous soils can be explained as being derived directly from the parent rock. Therefore, it is reasonable to assume that the soils are comprised of the non-carbonate residue plus Fe and Mn released during dissolution of the calcite and dolomite, which were previously tied up in the crystal structure.

Observations of the marble bedrock, saprolite, and residuum indicate that the black manganiferous soil material is derived directly from weathering of the marble bedrock. Sometimes these black horizons are below horizons that are derived from another parent material (such as in the DOT-2, GRO-1, and FLI-1 profiles), and sometimes they are above another type of residuum (such as in the GRO-2 profile). These lithologic discontinuities are presumably related to how the rock layers were originally deposited and subsequently folded.

Mineral Weathering in Manganiferous Soils

Since it appears that the black horizons of manganiferous soils are derived from marble, then the soils should reflect the mineralogy and weathering of the non-carbonate residues of the marble. The mineralogy of soil samples from the FLI-1 and FLI-2 profiles

were characterized for comparison to the non-carbonate residues of the underlying marble (since these were the only profiles from which marble bedrock samples were able to be collected). One Bt horizon and one BC horizon from each profile were selected in order to compare a vertical sequence in each pedon.

The FLI-1 Pedon

In the non-carbonate residue of the marble collected from FLI-1 (R1), quartz is dominant in the sand fraction, and there is a lesser amount of chlorite (Fig. 5-9, Table 5-8). It is likely that the chlorite, a primary mineral, was formed from clays occurring in the sediments within the marble during metamorphism. The sand fraction from the FLI-1 2BC2 horizon (which overlies marble sample R1) is mainly quartz, with a lesser amount of hematite (Fig. 5-10, Table 5-8). The sand fraction of the Bt1 horizon is also mainly quartz, but it contains significant amounts of mica, kaolinite, and hematite (Fig. 5-10, Table 5-8). Quartz is very resistant to weathering, tends to remain stable and is inherited directly from the parent material. The mica present in the Bt1 horizon is likely derived from the phyllite component in the upper part of the soils. This is evidenced by the fact that there is mica (a primary mineral) present in the Bt1, and it is absent in the R1 marble residue and the 2BC2 horizon. This mineralogy supports our field description of a lithologic discontinuity in FLI-1 (Table 4-5). Chlorite is not found in the sand fraction of either of the FLI-1 soil horizons. Therefore, much of the original sand-sized chlorite present in the non-carbonate residues has likely weathered to clay minerals in the soils.

The silt fraction of the non-carbonate residue of R1 is mostly quartz, with significantly more chlorite than in the sand fraction of the R1 residue (Fig. 5-11, Table 5-9). In the silt fractions of the Bt1 and 2BC2 horizons, quartz is still the primary mineral present, but there are also small amounts of kaolinite and mica, and minor amounts of hematite (Fig. 5-12, Table 5-9). Kaolinite in the Bt1 horizon could be formed from the weathering of mica or other minerals. There is more mica present in the Bt1 than in the 2BC2 horizon, and there is no mica in the silt fraction of the R1 residue. This is further evidence that there is a lithologic discontinuity between the two horizons.

The clay fraction of the non-carbonate residue from R1 (collected from the FLI-1 pedon) is mostly chlorite, with some quartz, mica, goethite, and minor amounts of feldspar and hematite (Fig. 5-13, Table 5-10). The FLI-1 2BC2 horizon, which directly overlies R1, has no chlorite, but abundant kaolinite and smectite, and some mica, goethite, and quartz (Fig. 5-14, Table 5-10). Chlorite weathers easily to vermiculite or smectite in acid soils upon dissolution of the interlayer hydroxide sheet (Kohut and Warren, 2002). Chlorite has completely weathered to form smectite and kaolinite in the 2BC2 clay fraction, while the mica has remained stable. In the FLI-1 Bt1 horizon, there is some chlorite present, but most of it has weathered to form HIV (Fig. 5-15, Table 5-10).

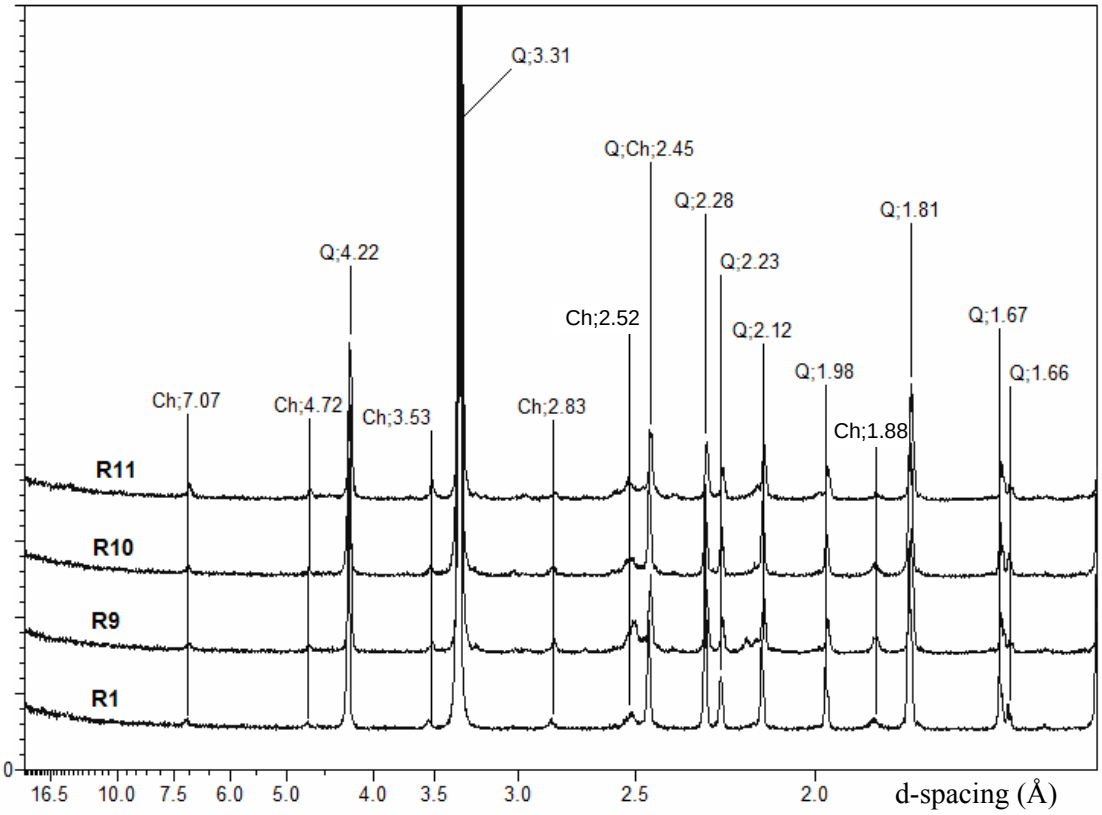

Fig. 5-9. X-ray diffractograms of the sand fractions of the non-carbonate residues (collected via acid dissolution) from the four marble samples. Ch=chlorite; Q=quartz.

FLI-1 Sand Fractions

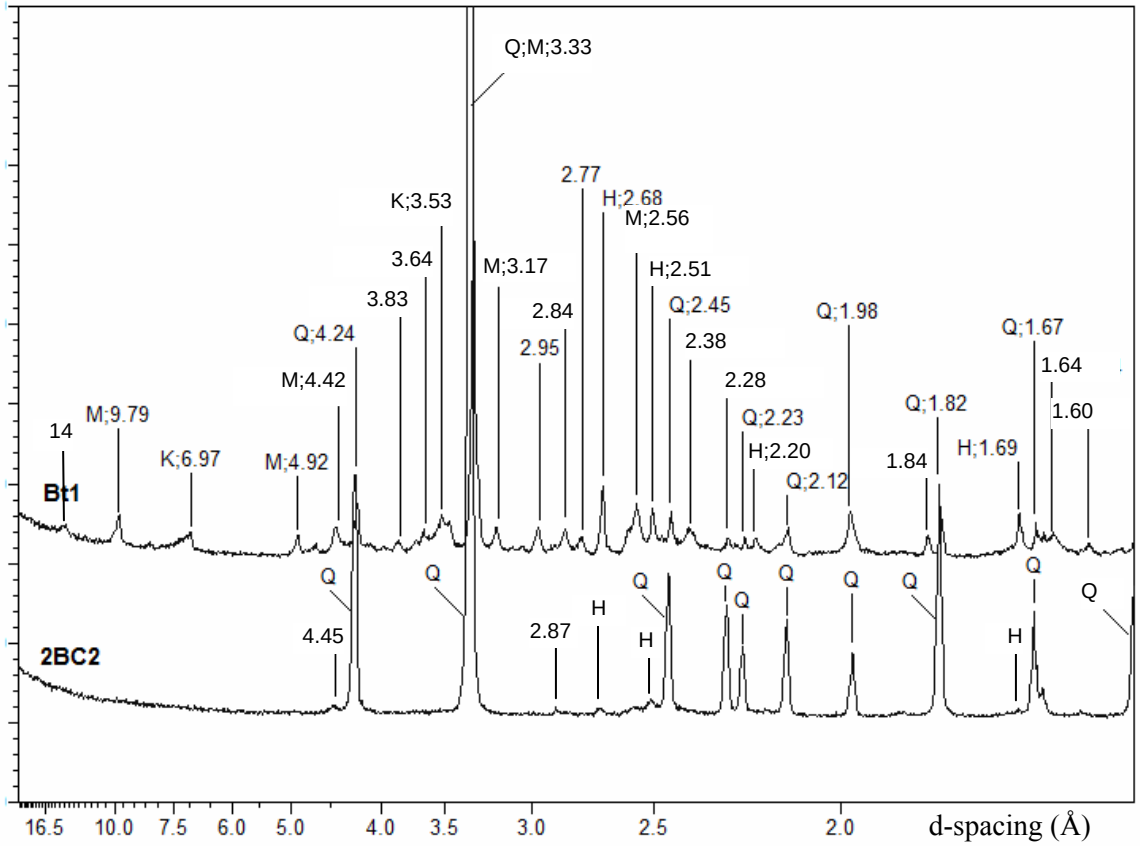

Fig. 5-10. X-ray diffractograms of sand fractions of two horizons from the FLI-1 pedon. H=hematite; K=kaolinite; M=mica; Q=quartz.

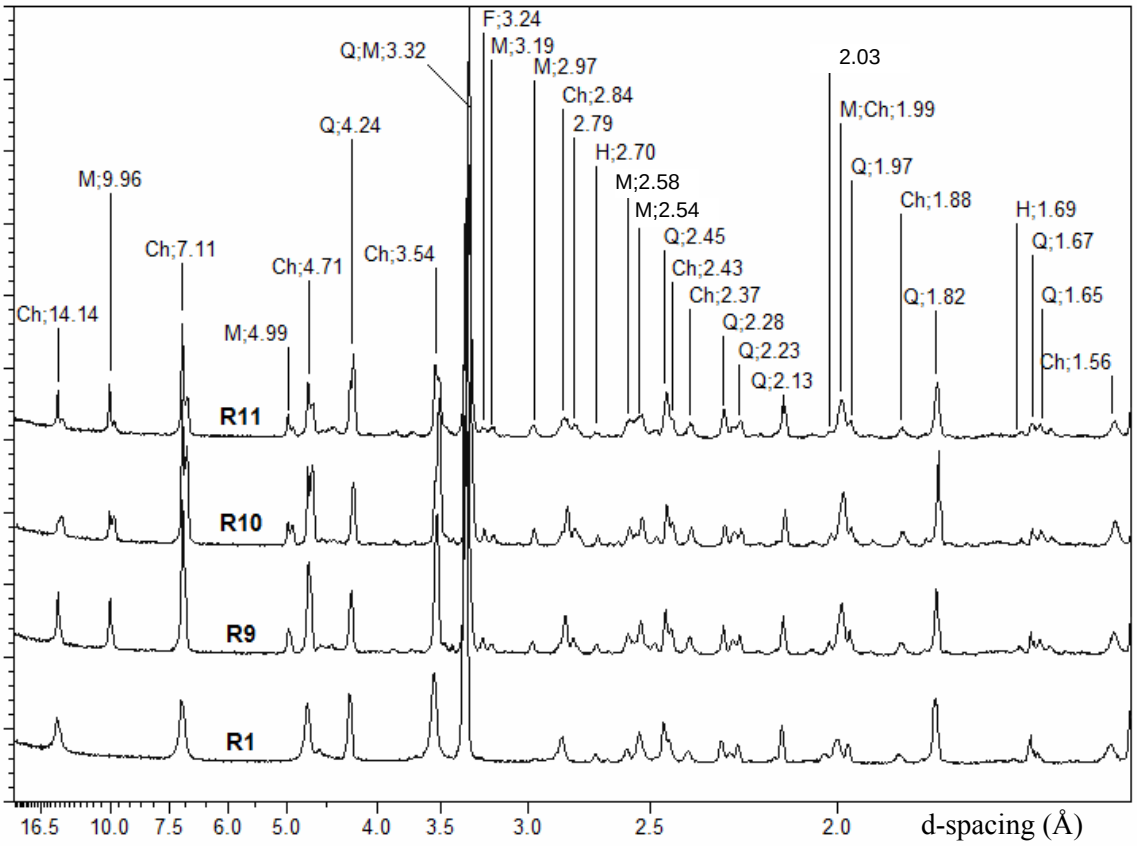

Fig. 5-11. X-ray diffractograms of the silt fractions of the non-carbonate residues (collected via acid dissolution) from the four marble samples. Ch=chlorite; F=feldspar; H=hematite; M=mica; Q=quartz.

FLI-1 Silt Fractions

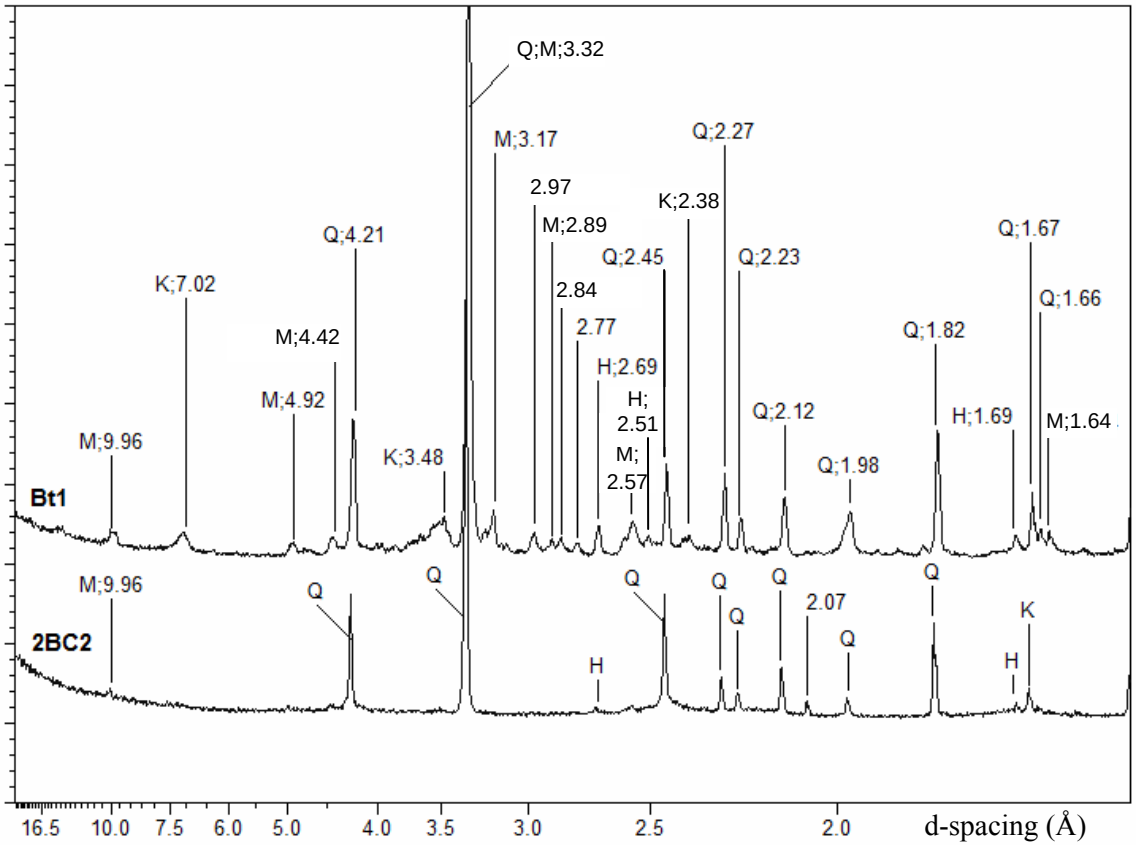

Fig. 5-12. X-ray diffractograms of silt fractions of two horizons from the FLI-1 pedon. H=hematite; K=kaolinite; M=mica; Q=quartz.

R1 Non-carbonate Residue: Clay Fraction

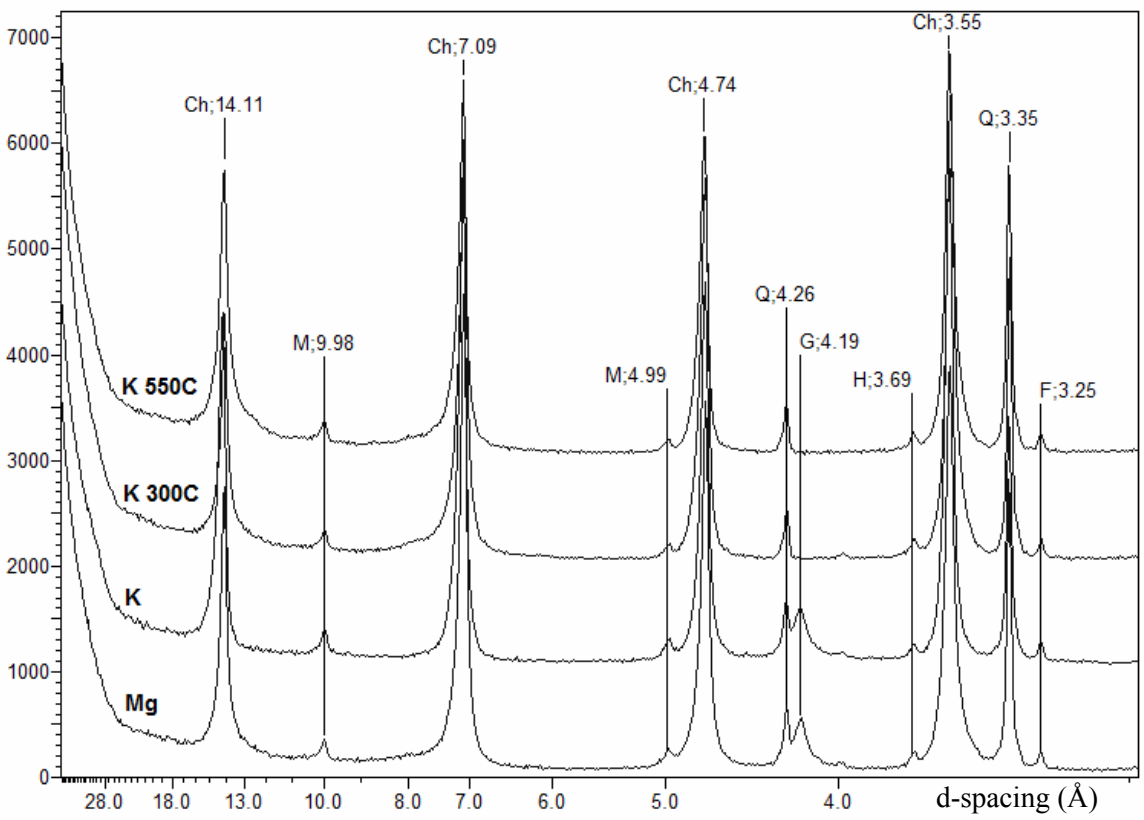

Fig. 5-13. X-ray diffractograms of clay fraction of non-carbonate residue (collected via acid dissolution) from the R1 dolomitic marble sample. Ch=chlorite; F=feldspar; G=goethite; Q=quartz; H=hematite; M=mica.

FLI-1 2BC2 Clay Fraction

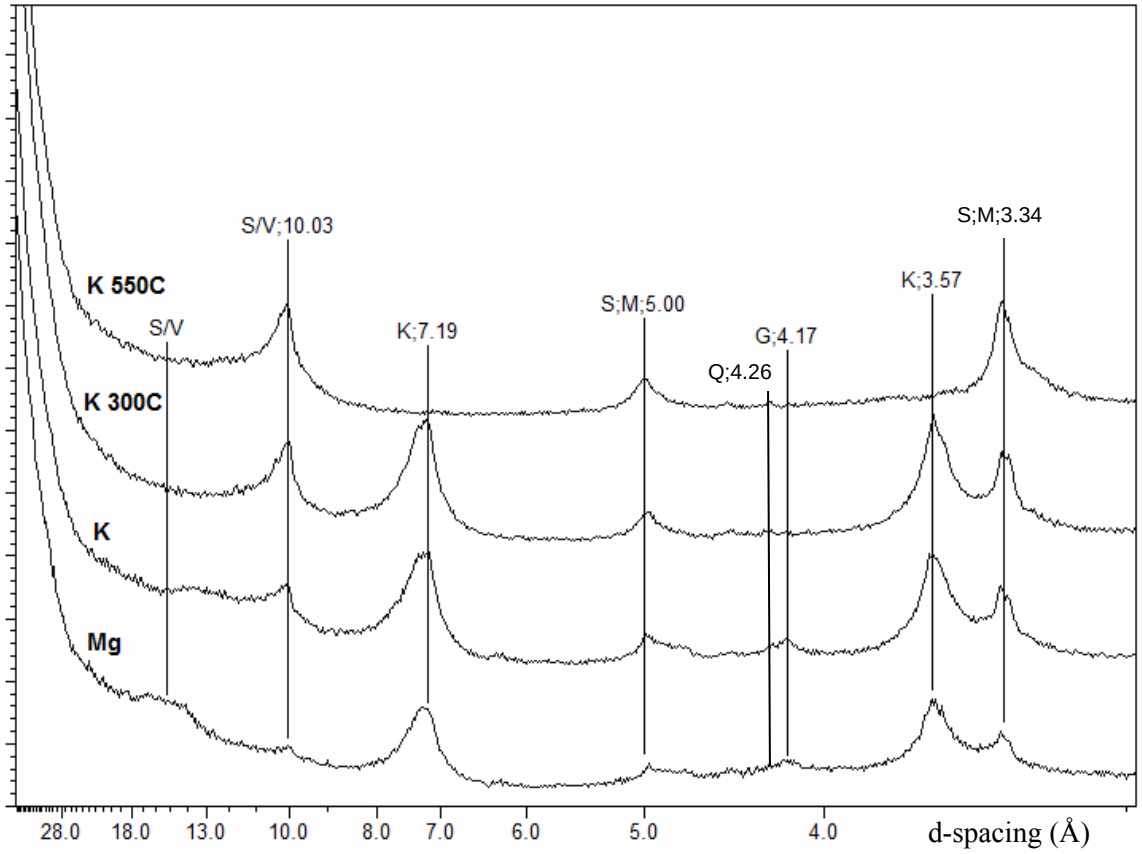

Fig. 5-14. X-ray diffractograms of clay fraction of 2BC2 horizon from the FLI-1 pedon. G=goethite; K=kaolinite; M=mica; Q=quartz; S=smectite; V=vermiculite.

FLI-1 Bt1 Clay Fraction

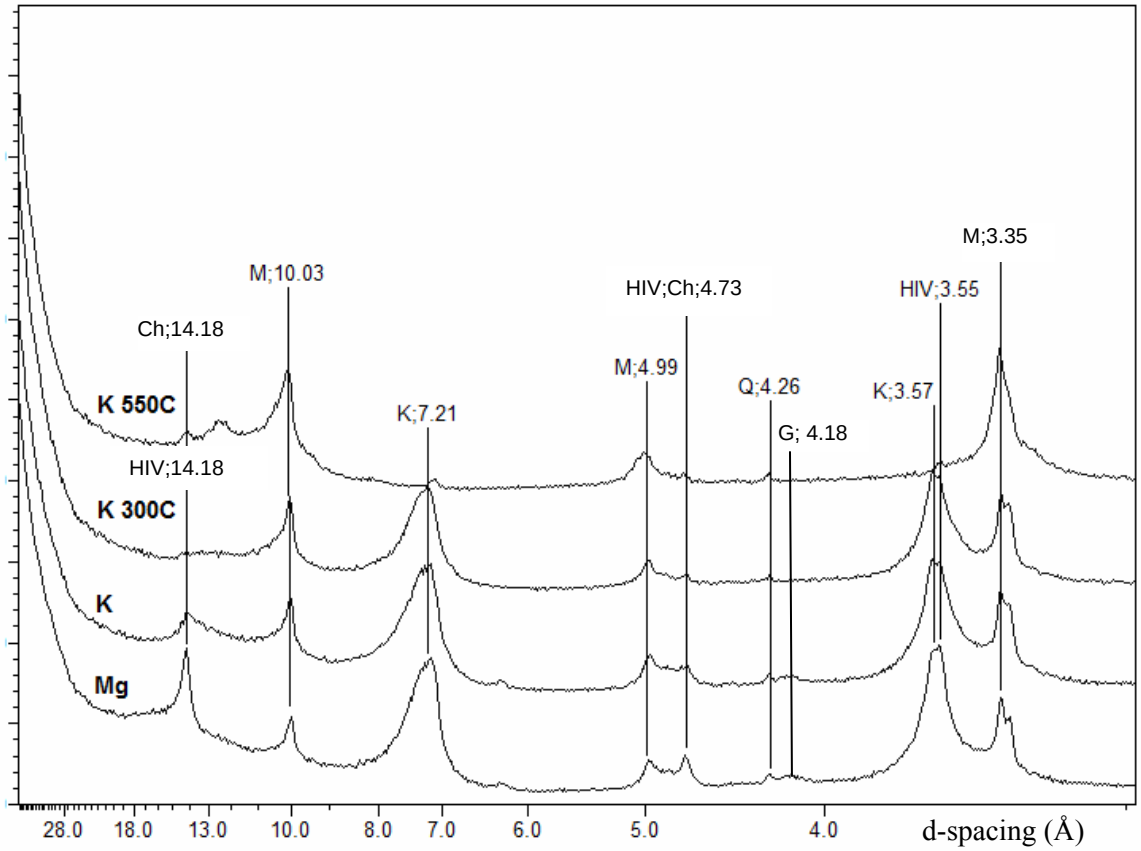

Fig. 5-15. X-ray diffractograms of clay fraction of Bt1 horizon from the FLI-1 pedon. G=goethite; HIV=hydroxy-interlayered vermiculite; K=kaolinite; M=mica; Q=quartz.

Table 5-8. Semi-quantitative mineralogy of FLI-1 sand fractions, based on XRD patterns in Figs. 5-8 and 5-9. XXXX= >70%; XXX= 30-70%; XX= 10-30%; X= 5-10%; x= <5%; tr=trace. Ch=chlorite; H=hematite; K=kaolinite; L=lithiophorite; M=mica; Q=quartz.

Sample (Sand Fraction)	Ch	Q	M	K	H	L
FLI-1 Bt1		XXX	XX	XX	XX	
FLI-1 2BC2		XXXX			X	
R1	X	XXXX				

Table 5-9. Semi-quantitative mineralogy of FLI-1 silt fractions, based on XRD patterns in Figs. 5-10 and 5-11. XXXX= >70%; XXX= 30-70%; XX= 10-30%; X= 5-10%; x= <5%; tr=trace. Ch=chlorite; F=feldspar; H=hematite; K=kaolinite; L=lithiophorite; M=mica; Q=quartz.

Sample (Silt Fraction)	Ch	Q	M	K	F	H	L
FLI-1 Bt1		XXXX	Xx	Xx		X	
FLI-1 2BC2		XXXX	X			x	
R1	XX	XXX				x	

Table 5-10. Semi-quantitative mineralogy of FLI-1 clay fractions, based on XRD patterns in Figs. 5-12, 5-13, and 5-14. XXXX= >70%; XXX= 30-70%; XX= 10-30%; X= 5-10%; x= <5%; tr=trace. A=amphibole; Ch=chlorite; Cr=cristobalite; F=feldspar; G=goethite; H=hematite; HIV=hydroxy-interlayered vermiculite; K=kaolinite; M=mica; Q=quartz; S=smectite; V=vermiculite.

Sample (Clay Fraction)	Ch	Q	M	K	HIV	V	S	F	H	G	A	Cr
FLI-1 Bt1	X	x	XX	XXX	XXx					x		
FLI-1 2BC2		tr	X	XXX			XXX			X		
R1	XXXX	X	X					x	x	X		

The FLI-2 Pedon

The sand fractions of the non-carbonate residues of R9, R10, and R11 (collected from underneath the FLI-2 pedon) are mostly quartz, with a small amount of chlorite (Fig. 5-9, Table 5-11). The sand fractions of the FLI-2 soils are mostly quartz, with some mica and hematite (Fig. 5-16, Table 5-11). However, there is a possible lithiophorite peak detected in the FLI-2 BC sand fraction, which could result from the abundance of this Mn oxide. Lithiophorite is one of the more well-crystalline Mn oxide minerals, but its peak at 4.71 Å overlaps with a chlorite peak. The presence of lithiophorite was confirmed using Fourier Transform Infrared spectroscopy (results presented in Chapter 4). Chlorite remains in the FLI-2 BC horizon sand fraction, so there appears to be minimal change in the sand mineralogy of the BC horizon compared to the non-carbonate residues. A lithologic discontinuity was not described in the field for the FLI-2 pedon, but there is mica present in the Bt sand fraction and not in the BC sand fraction, so there is likely a lithologic discontinuity present.

The silt fractions of the non-carbonate residues of R9, R10, and R11 (collected from FLI-2) are mostly quartz, with significant amounts of chlorite and mica present (Fig. 5-11, Table 5-12). The silt fraction of the FLI-2 BC horizon (Fig. 5-17, Table 5-12) is very similar to the silt fractions of the underlying rock residues, so there has not been substantial mineralogical alteration. The silt fraction of the FLI-2 Bt2 horizon (Fig. 5-17, Table 5-12) has the same suite of minerals, but there is less chlorite, which has presumably weathered to form clay minerals. Also, there is a possible lithiophorite peak at 4.71 Å in the BC horizon, like the sand fraction of this horizon. Although the sand fractions indicate that there is more mica present in the Bt2 horizon than in the BC

horizon, there is a similar amount of mica in the silt fractions of the FLI-2 rock residues and soils.

The clay fractions of the non-carbonate residues from R9, R10, and R11 (collected from the FLI-2 pedon) are similar to the residue from R1, except the FLI-2 samples (R9, R10, and R11) have very small amounts of amphibole (as evidenced by a small but persistent peak around 8.1 Å) and cristobalite (as evidenced by a peak around 4.05 Å) (Figs. 5-18, 5-19, and 5-20, Table 5-13). Also, there is considerably more mica in the FLI-2 rock samples (R9, R10, and R11) than the FLI-1 rock sample (R1). The residue from R9 had a reddish color and is the only residue collected from a FLI-2 calcitic sample which shows a hematite peak (Fig. 5-18, Table 5-13). The FLI-2 BC horizon, which directly overlies samples R9, R10, and R11, is still high in chlorite, but much has been altered to kaolinite, HIV, and vermiculite due to mineral weathering (Fig. 5-21, Table 5-13). In the Bt2 horizon, chlorite has weathered completely to form vermiculite and some HIV (Fig. 5-22, Table 5-13). Mica makes up a substantial component of the non-carbonate residues of the marble, and clay-sized mica persists throughout the FLI-2 Bt2 and BC horizons, which does not indicate a lithologic discontinuity.

FLI-2 Sand Fractions

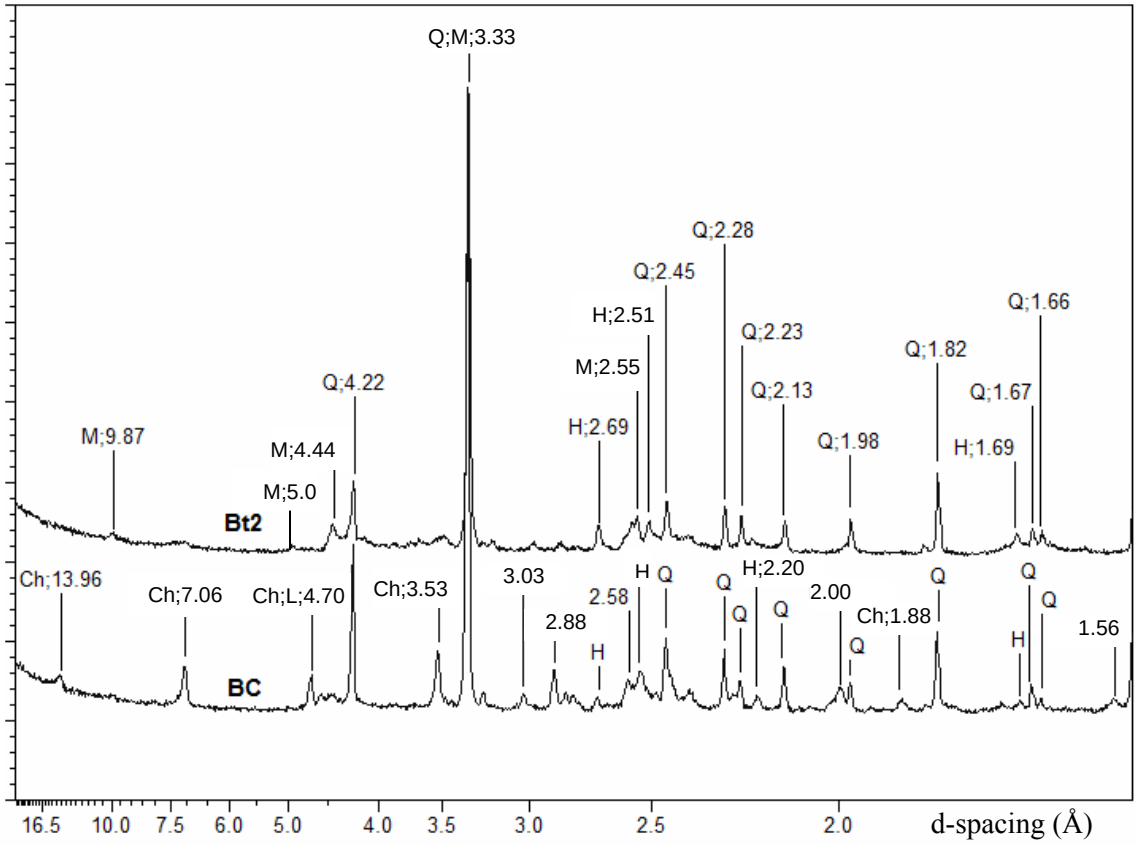

Fig. 5-16. X-ray diffractograms of sand fractions of two horizons from the FLI-2 pedon. Ch=chlorite; Q=quartz; H=hematite; K=kaolinite; L=lithiophorite; M=mica.

FLI-2 Silt Fractions

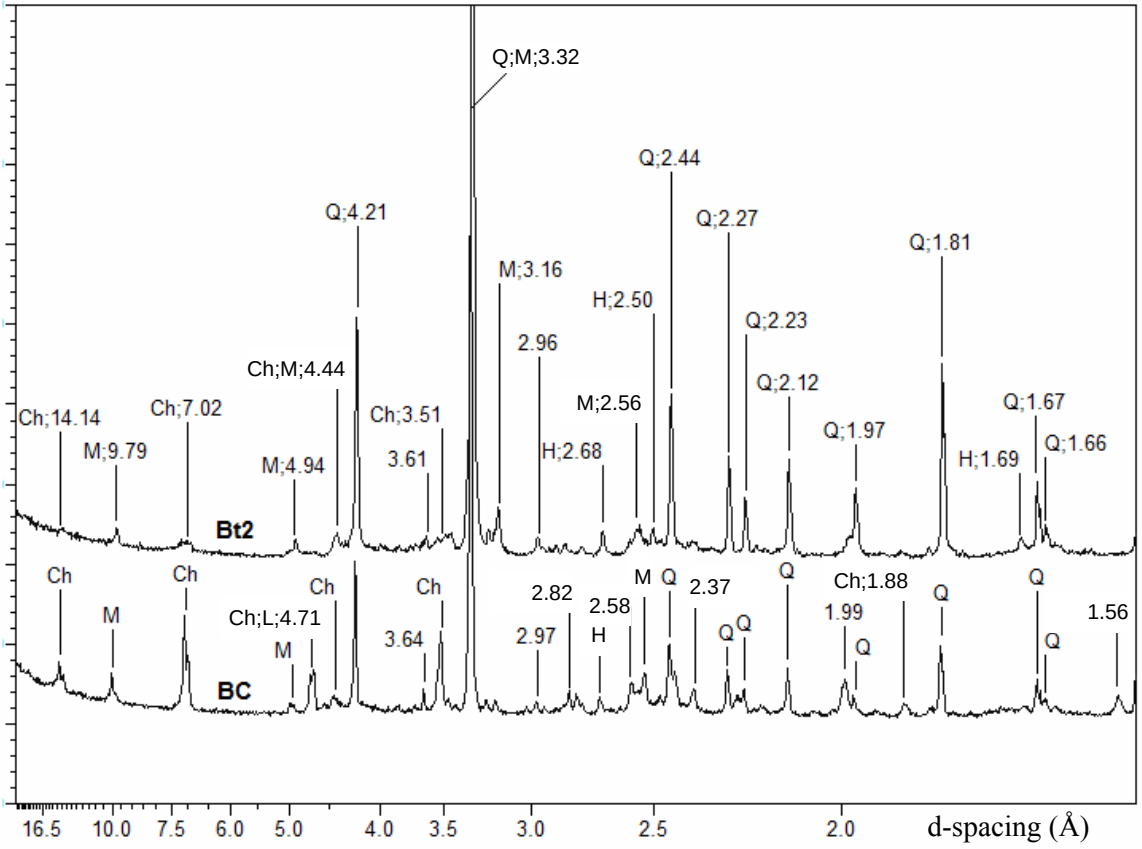

Fig. 5-17. X-ray diffractograms of silt fractions of two horizons from the FLI-2 pedon. Ch=chlorite; H=hematite; K=kaolinite; L=lithiophorite; M=mica; Q=quartz.

R9 Non-carbonate Residue: Clay Fraction

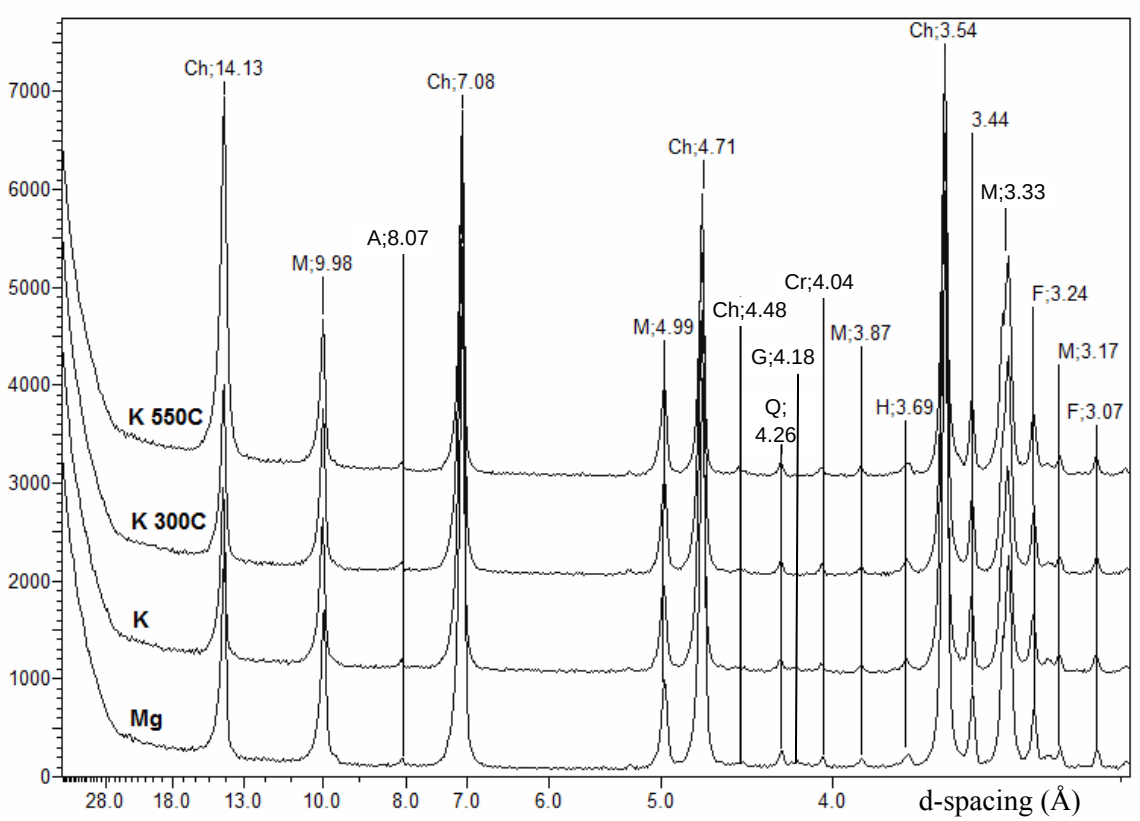

Fig. 5-18. X-ray diffractograms of clay fraction of non-carbonate residue (collected via acid dissolution) from the R9 calcitic marble sample. A=amphibole; Ch=chlorite; Cr=cristobalite; F=feldspar; G=goethite; H=hematite; Q=quartz; M=mica.

R10 Non-carbonate Residue: Clay Fraction

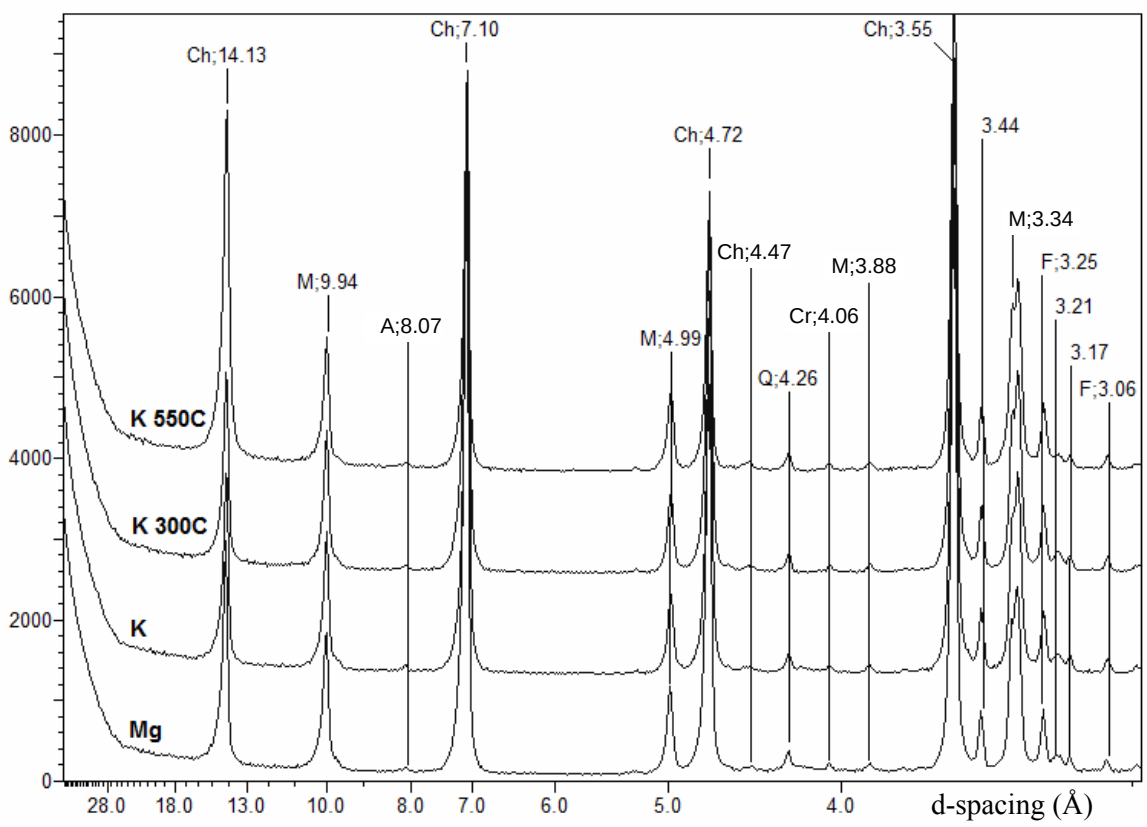

Fig. 5-19. X-ray diffractograms of clay fraction of non-carbonate residue (collected via acid dissolution) from the R10 calcitic marble sample. A=amphibole; Ch=chlorite; Cr=cristobalite; F=feldspar; Q=quartz; M=mica.

R11 Non-carbonate Residue: Clay Fraction

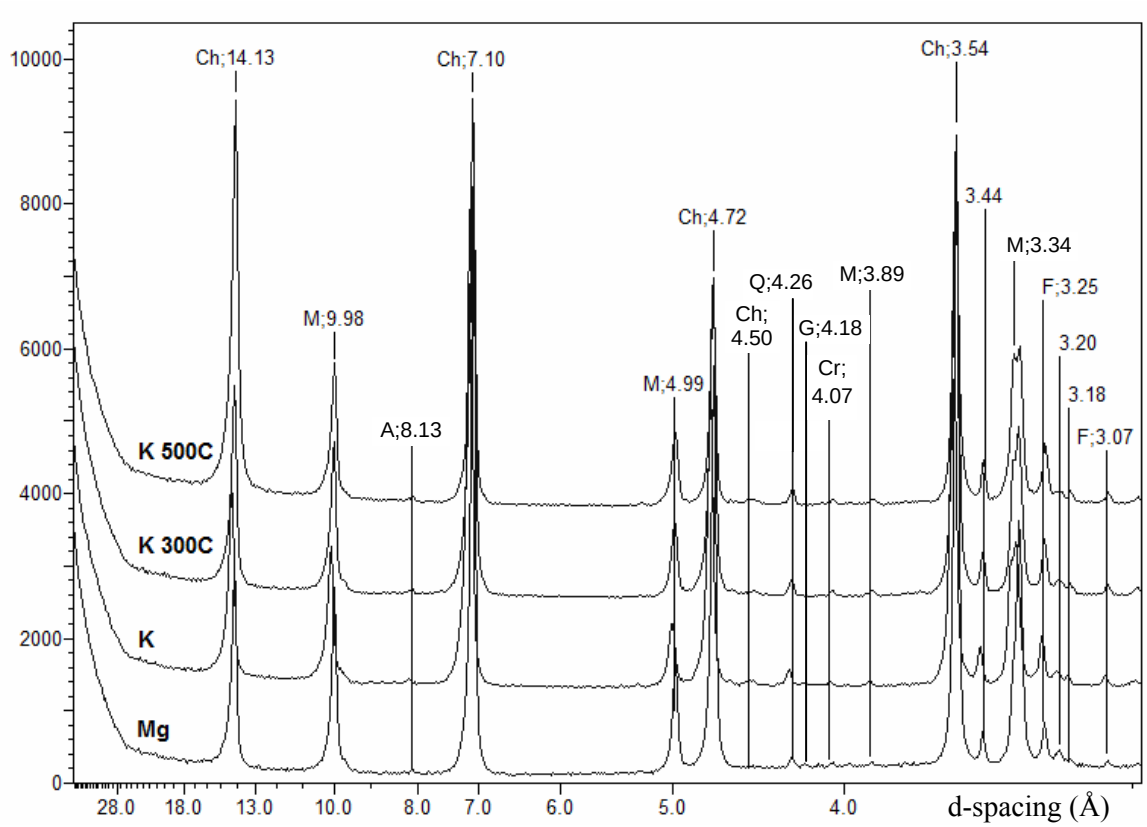

Fig. 5-20. X-ray diffractograms of clay fraction of non-carbonate residue (collected via acid dissolution) from the R11 calcitic marble sample. A=amphibole; Ch=chlorite; Cr=cristobalite; F=feldspar; G=goethite; M=mica; Q=quartz.

FLI-2 BC Clay Fraction

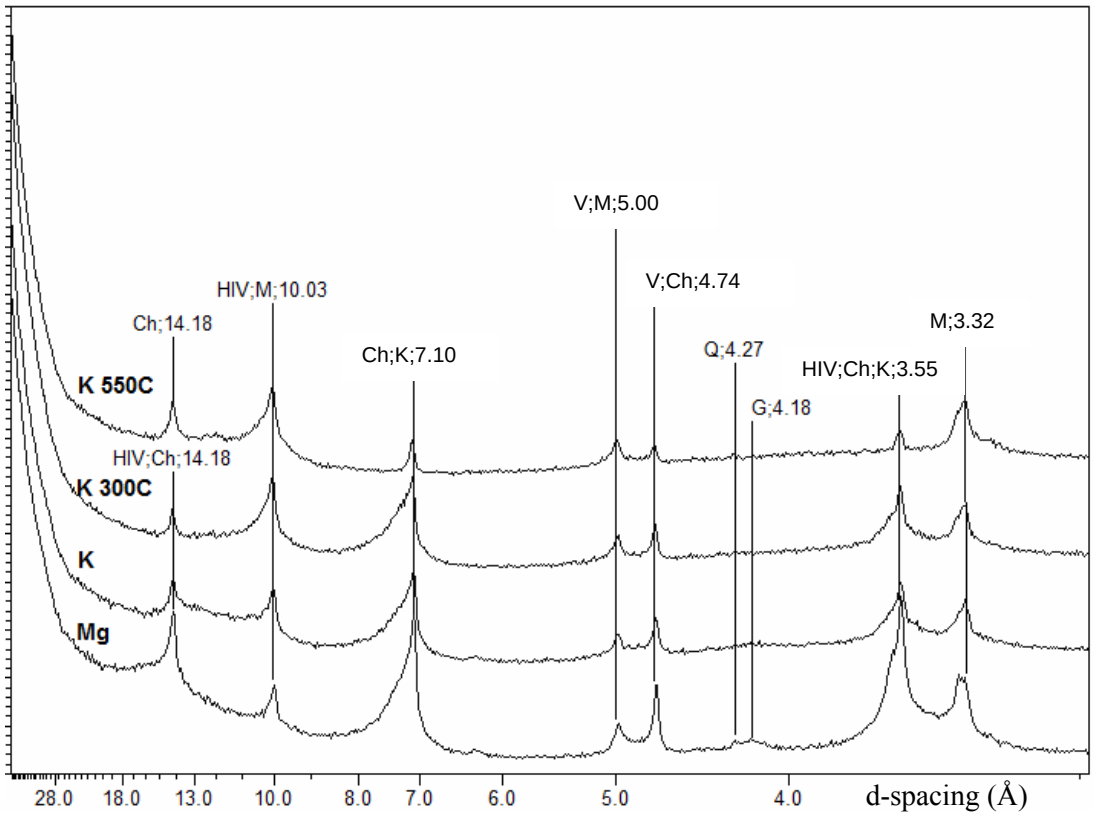

Fig. 5-21. X-ray diffractograms of clay fraction of BC horizon from the FLI-1 pedon. Ch=chlorite; G=goethite; HIV=hydroxy-interlayered vermiculite; K=kaolinite; M=mica Q=quartz; V=vermiculite.

FLI-2 Bt2 Clay Fraction

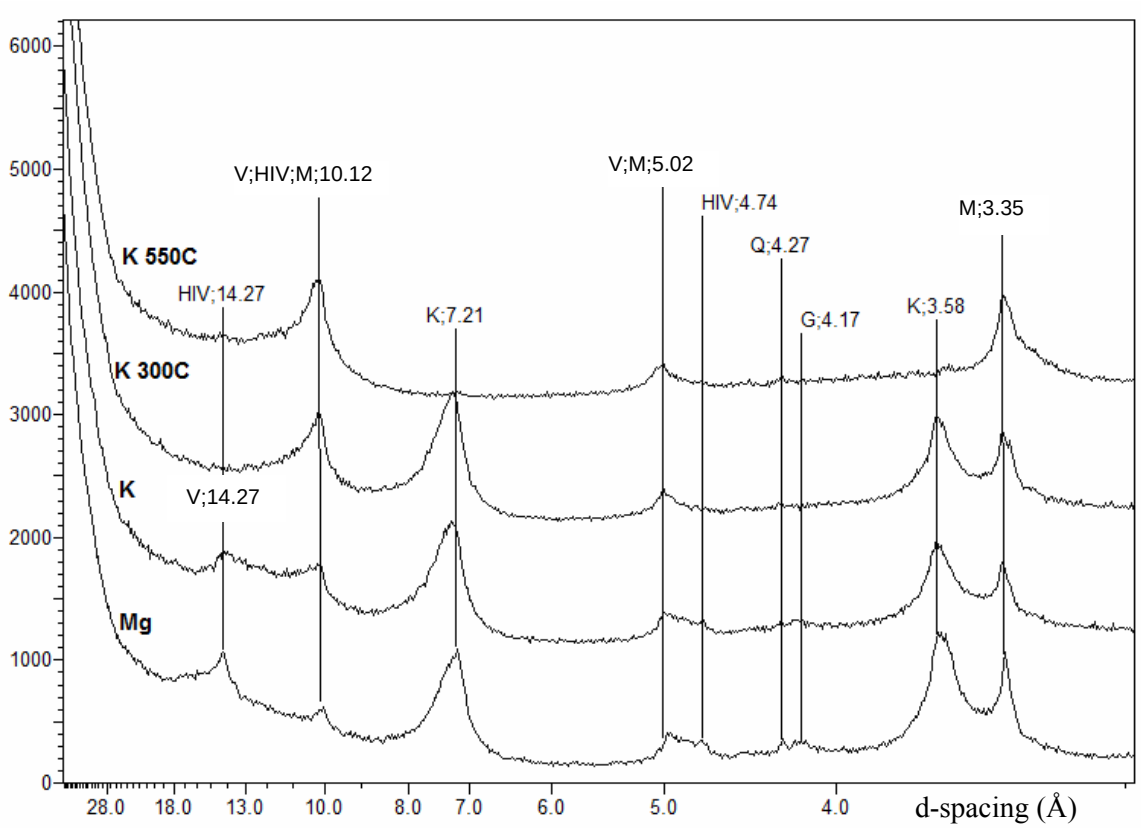

Fig. 5-22. X-ray diffractograms of clay fraction of Bt2 horizon from the FLI-2 pedon. G=goethite; HIV=hydroxy-interlayered vermiculite; K=kaolinite; M=mica; Q=quartz.

Table 5-11. Semi-quantitative mineralogy of FLI-2 sand fractions, based on XRD patterns in Figs. 5-8 and 5-15. XXXX= >70%; XXX= 30-70%; XX= 10-30%; X= 5-10%; x= <5%; tr=trace. Ch=chlorite; H=hematite; K=kaolinite; L=lithiophorite; M=mica; Q=quartz.

Sample (Sand Fraction)	Ch	Q	M	K	H	L
FLI-2 Bt2		XXX	XX		X	
FLI-2 BC	X	XXXX	x		x	X
R9	X	XXXX				
R10	X	XXXX				
R11	X	XXXX				

Table 5-12. Semi-quantitative mineralogy of FLI-2 silt fractions, based on XRD patterns in Figs. 5-10 and 5-16. XXXX= >70%; XXX= 30-70%; XX= 10-30%; X= 5-10%; x= <5%; tr=trace. Ch=chlorite; F=feldspar; H=hematite; K=kaolinite; L=lithiophorite; M=mica; Q=quartz.

Sample (Silt Fraction)	Ch	Q	M	K	F	H	L
FLI-2 Bt2	x	XXXX	X			X	
FLI-2 BC	XX	XXX	XX			x	X
R9	XX	XX	XX		x	x	
R10	XX	XX	XX		x	x	
R11	XX	XX	XX		x	x	

Table 5-13. Semi-quantitative mineralogy of FLI-2 clay fractions, based on XRD patterns in Figs. 5-17, 5-18, 5-19, 5-20, and 5-21. XXXX= >70%; XXX= 30-70%; XX= 10-30%; X= 5-10%; x= <5%; tr=trace. A=amphibole; Ch=chlorite; Cr=cristobalite; F=feldspar; G=goethite; H=hematite; HIV=hydroxy-interlayered vermiculite; K=kaolinite; M=mica; Q=quartz; S=smectite; V=vermiculite.

Sample (Clay Fraction)	Ch	Q	M	K	HIV	V	S	F	H	G	A	Cr
FLI-2 Bt2		x	X	XXX	X	XXx				x		
FLI-2 BC	XXX	tr	XX	XXx	X	X				x		
R9	XXX	X	XX					X	x	tr	x	x
R10	XXX	X	XX					X			x	tr
R11	XXX	X	XX					X		tr	x	tr

Other Pedogenic Processes and Features in Manganiferous Soils

Clay Illuviation

In the manganiferous soils, clay illuviation is a major pedogenic process leading to the development of argillic horizons and other features in most of the profiles. Illuvial clay was commonly observed throughout the manganiferous soils, and many profiles have Bt horizons. Argillic horizons are typical for soils of the region, but manganiferous soils also show considerable clay illuviation below the Bt horizons, in BC or C horizons. Figures 5-23 and 5-24 show an extraordinary example of a complex compound illuvial clay coating in the FLI-1 2BC2 horizon, just above the contact with marble bedrock. Another clay film is shown in Figs. 5-25 and 5-26 that shows strong evidence of laminations typical of illuvial clay. The red-orange color of the illuvial clay coatings suggests that they are rich in Fe oxides. It is thought that clay illuviation is facilitated by the highly porous nature of the manganiferous materials, which allows free movement of water and suspended clay particles.

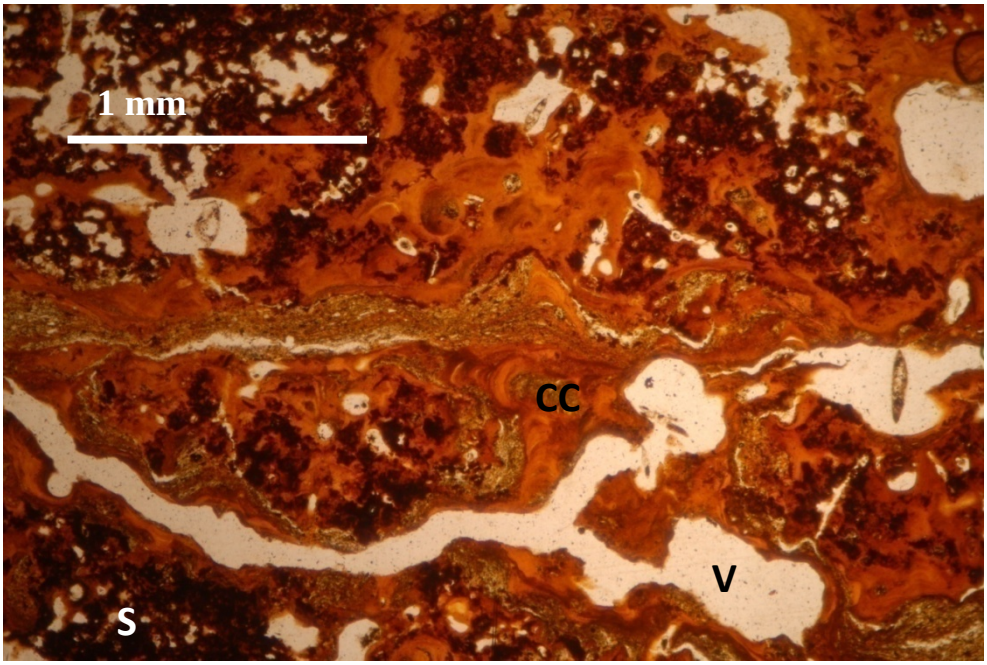

Fig. 5-23. FLI-1 2BC2, a few cm above marble bedrock contact. PPL. Note the complex compound illuvial clay coating nearly filling a void. CC=clay coating; S=spongy manganiferous residuum; V=void.

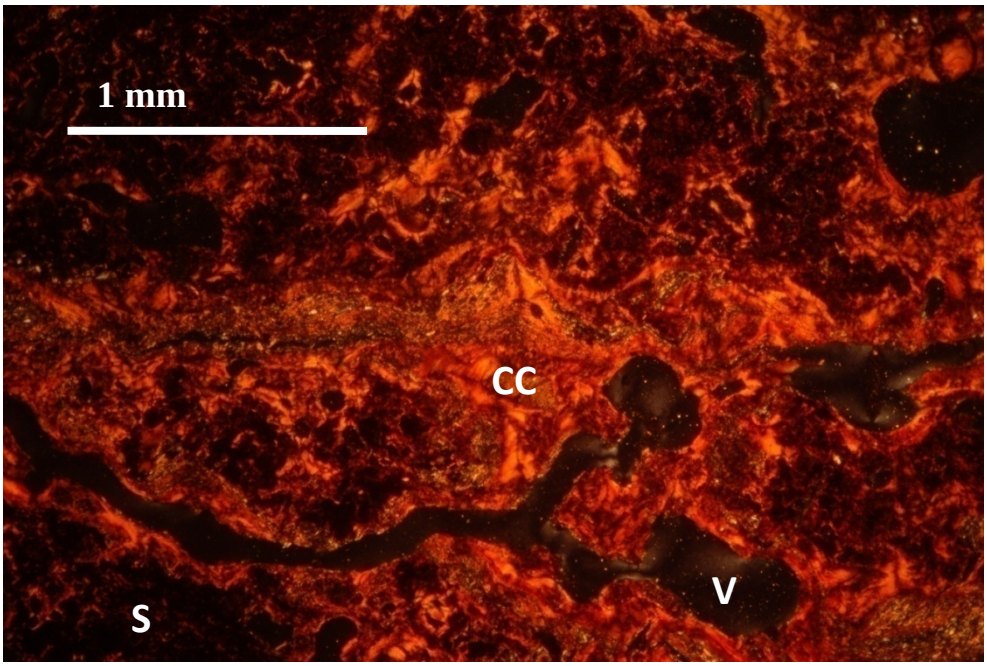

Fig. 5-24. FLI-1 2BC2, a few cm above marble bedrock contact. XPL. Same view as in Fig. 5-22. CC=clay coating; S=spongy manganiferous residuum; V=void.

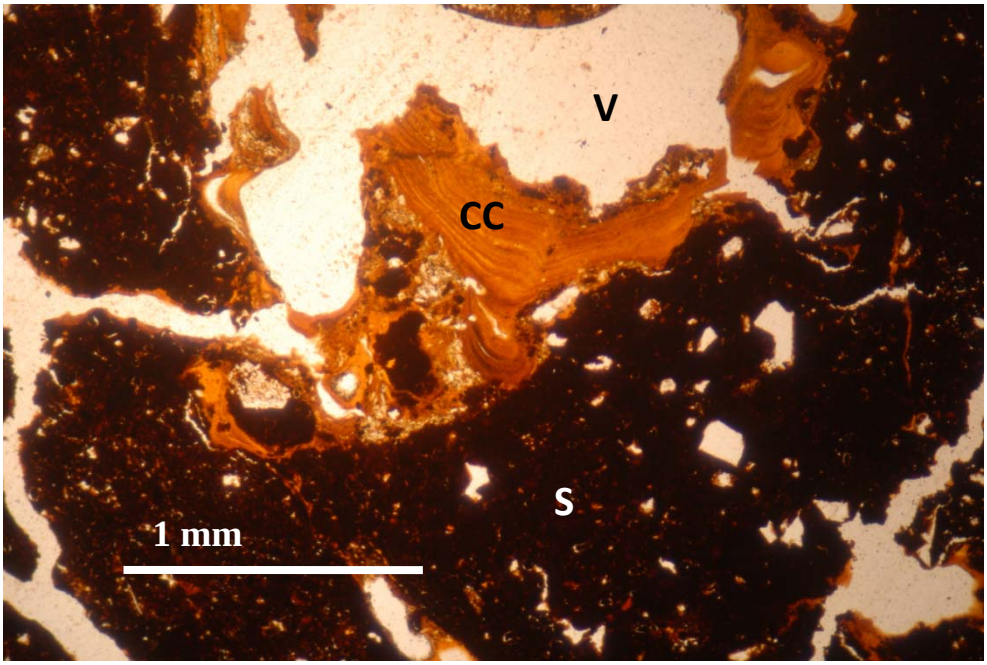

Fig. 5-25. FLI-1, 2BC1 horizon. PPL. Clay film, rich in Fe oxides, is especially thick and laminated. CC=clay coating; S=spongy manganiferous residuum; V=void.

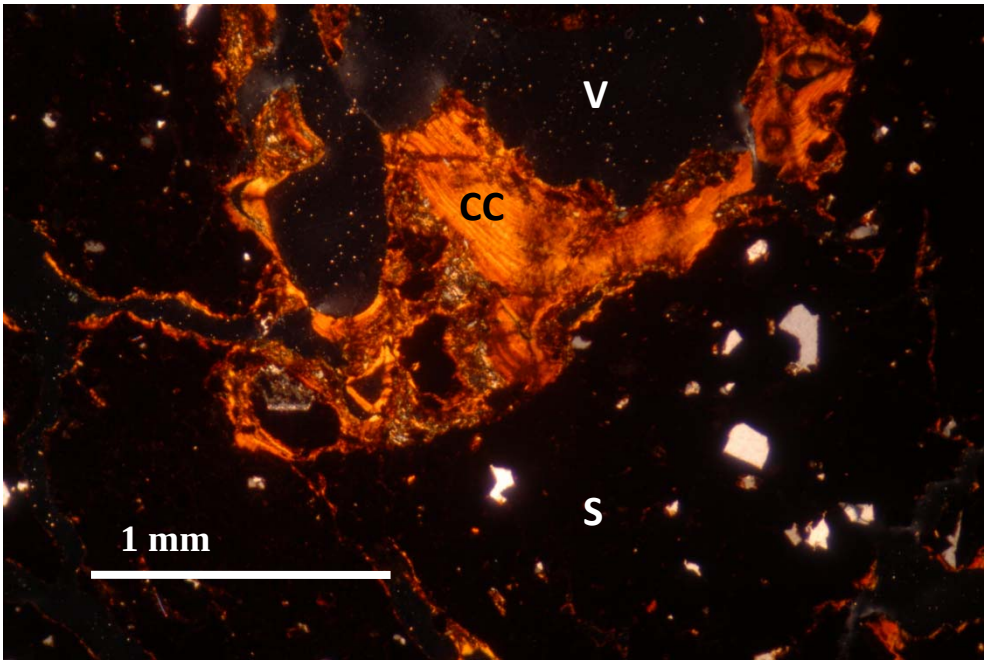

Fig. 5-26. FLI-1, 2BC1 horizon. XPL. Same view as in Fig. 5-24. CC=clay coating; S=spongy manganiferous residuum; V=void.

Manganiferous Nodules and Coarse Fragments

Manganiferous nodules and coarse fragments represent a significant component of the current morphology of manganiferous soils. The upper horizons of some of the manganiferous pedons are lighter in color and contain phyllite channers, indicating that they have had input of residuum or colluvium from a different parent rock. However, these horizons still have high amounts of Mn oxides (relative to other, non-manganiferous soils of the region), often visible as manganiferous nodules. Sand-sized manganiferous nodules are shown in Fig. 5-27. Nodules are ubiquitous throughout A and B horizons of manganiferous soils, and they tend to show diffuse boundaries and irregular shapes, indicating that they formed in place. Typically, manganiferous nodules are associated with seasonal reducing conditions caused by a perched water table. However, there is no indication either of a moisture-inhibiting layer or of seasonal reducing conditions in the manganiferous soils observed. In fine-textured terra rossa-type soils such as those of the Hagerstown series, there can be mobilization and re-oxidation of Mn without a perched water table. This is because the low hydraulic conductivity of these soils allows near-saturated conditions during rain events, leading to periodic reducing conditions, and formation of manganiferous coatings. However, it is not likely that this same process is occurring in the manganiferous soils, due to the more loamy textures and the fact that nodules, rather than coatings, are present.

It is possible that the manganiferous nodules could be formed by similar processes to those which formed the black horizons underneath (in situ accumulation after dissolution of carbonate rock), but that the Mn originated from a different layer of rock containing a mixture of phyllite and a Mn-rich calcareous component. Evidence for this

may be seen in Fig. 5-27, which shows a coarse fragment of calcareous phyllite in the FLI-1 Bt2 horizon. The very high order birefringence colors (seen in Fig. 5-28) confirm that this fragment contains a significant component of a carbonate mineral. These calcareous phyllite fragments are found in the underlying BC material also, and they are full of opaque mineral grains which could possibly be rich in Fe and Mn. The presence of these fragments supports the idea that the upper part of the soils originated from calcareous parent material. The presence and persistence of calcareous materials, which could be physically protected by the micaceous foliation in the rock fragment, may also be the reason for the relatively high pH (6.6 to 7.3) at the FLI site (see Fig. 4-7).

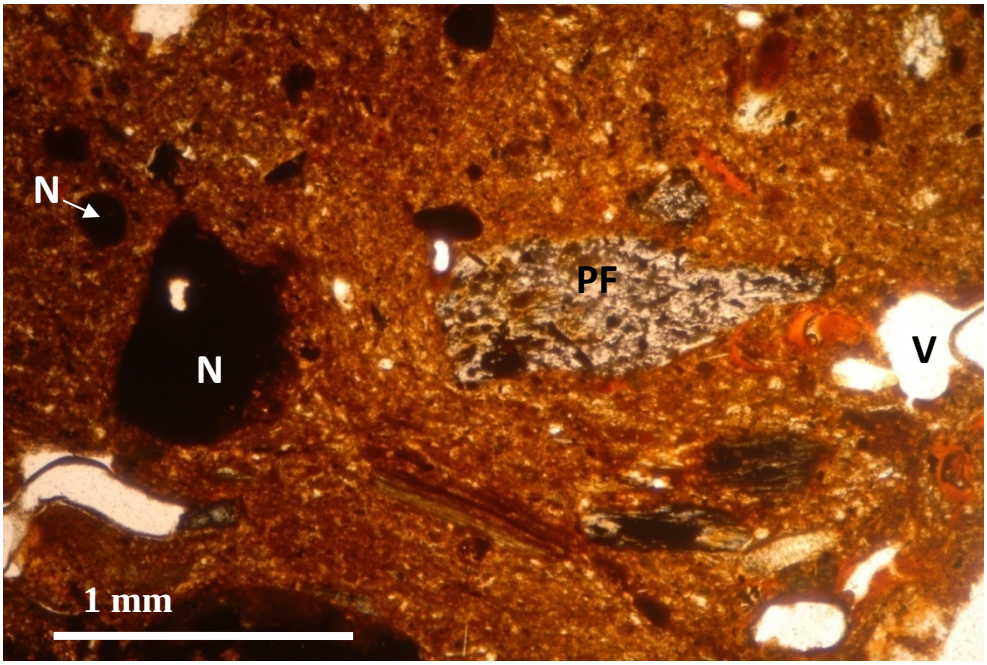

Fig. 5-27. FLI-1 Bt2-2BC1 transition. Plane-polarized light (PPL). Note the calcareous phyllite fragment and ferromanganiferous nodules. PF=calcareous phyllite fragment; N=nodule; V=void.

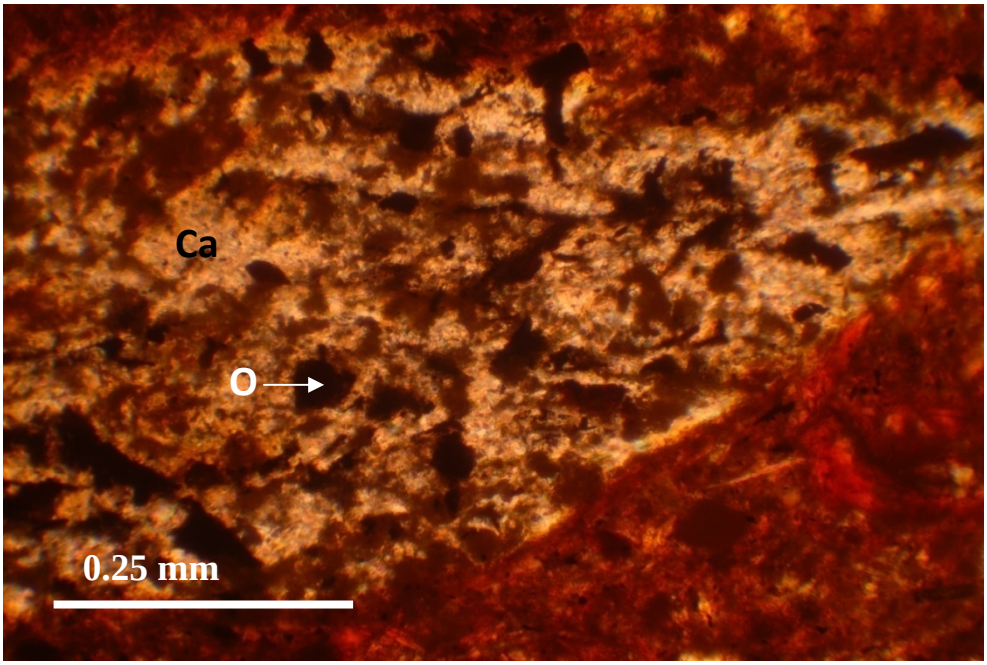

Fig. 5-28. FLI-1 Bt2-2BC1 transition. Cross-polarized light (XPL). Closeup of calcareous phyllite fragment seen in Fig. 5-1, with opaque minerals which may be manganiferous. Ca=carbonate; O=opaque mineral.

CONCLUSIONS

The black, Mn-rich horizons of the manganiferous soils of Maryland have formed in situ from marble, specifically the Precambrian Wakefield Marble member of the Sams Creek formation. The black horizons may be found either above or below other, lighter-colored soil materials. The lighter-colored residual soil materials are presumably derived from other types of rock, such as phyllite or metabasalt, and their positions are related to how the rocks were emplaced during, and subsequent to, the Appalachian Orogeny.

When the original sedimentary limestones and dolostones were formed (which were later metamorphosed into the Wakefield marble), Fe^{2+} and Mn^{2+} became bound within the crystal structure of with the carbonates, especially in the dolomite component, because dolomite can accommodate more Fe^{2+} and Mn^{2+} in its crystal structure than calcite. Some siliclastic sediments with detrital clays were also added during carbonate deposition, comprising a few percent of the rock.

During the time of the evolution of the Piedmont landscape (since the Appalachian Orogeny), calcite and dolomite were solubilized from the Wakefield marble, and Fe and Mn were released from within the crystal structure, accumulating as oxides along with the silicate residues. Calculations of the amount of rock needed to produce the thickness of soils observed (assuming that the soils are made up completely of the non-carbonate residue) are consistent with the estimated thickness of the Wakefield Marble. When calculated in proportion to the non-carbonate residue present, the amount of Fe and Mn within the marble are similar to the concentrations of Fe and Mn in the soils. Therefore, all of the Fe and Mn present in the manganiferous soils can be explained as

being derived from the marble. Fe oxides, Mn oxides, and silicate minerals accumulated along the edges of the dissolving carbonate grains, leaving behind a black, porous framework of oxide-rich residuum.

Following the loss of carbonates and accumulation of the non-carbonate residues, the chlorite common in the clay fraction weathered to form 2:1 clay minerals, particularly vermiculite, HIV, and, less commonly, smectite. In some cases, the greater abundance of mica in the Bt horizon than in the underlying BC horizon provides further evidence that there is a lithologic discontinuity between the lighter-colored horizons (presumably derived from more phyllitic materials) and the black horizons which are extremely enriched in Mn (derived from the marble). Clay illuviation is greatly facilitated by the high porosity of the manganiferous soils, so that many of the soils have developed argillic horizons and red, Fe-rich clay films in BC and C horizons. In the lighter-colored horizons found in manganiferous soils, black nodules are abundant. These nodules are not likely derived from seasonal redox processes. Instead, they are possibly formed from similar processes to those which formed the black horizons, but from a different, partially calcareous rock layer.

CHAPTER 6

Thesis Conclusions

The manganiferous soils investigated in this study are found in a limited area in eastern Frederick and western Carroll Counties, Maryland. This area lies within the Western Division of the Piedmont of Maryland, which has very complex, folded and interbedded metamorphic geology. The soils appear to be associated with areas mapped as the Wakefield Marble member of the Sams Creek formation, which is mainly comprised of metabasalt (greenstone) and phyllite. The Frederick County Soil Survey (2002) may be used as a guide in assisting to locate manganiferous soils, because NRCS soil scientists included them in the Benevola mapping unit and the Conestoga and Letort mapping unit in some cases. Some of the manganiferous soils are close to fitting within the range of characteristics of the Benevola series, which is formed in marble residuum and may have a black (N1) C horizon. The Benevola series is described as having a fine texture in the family particle-size control section. However, many of the pedons observed in this study had more loamy textures, and could not be properly classified within the Benevola series. These loamy manganiferous soils were included within the mapping concept of the Letort series, which has a fine-loamy particle size and a relatively dark (Munsell value/ chroma of 3/2) C horizon, but the manganiferous soils often have colors in BC and C horizons which are darker than 3/2. Therefore, there is no soil series which adequately accommodates the manganiferous soils.

Based on an empirical relationship between Mn content and apparent electrical conductivity measured by an Electromagnetic Induction (EMI) instrument, EMI was successfully used to help delineate the extent of manganiferous soils at three sites. The soils occur in small pods or lenses, <1 to 2 ha at each site. There is no evidence that the soils occur beyond the general areas where the Benevola and Conestoga and Letort mapping units are found, which is approximately 200 km^2.

Manganiferous soils are found at all landscape positions, and this suggests that their location is related more to bedrock geology than to some relocation process tied to landform. The manganiferous soils vary in morphological properties between sites. Some sites have only modest enrichment in Mn, visible only as black coatings or nodules, while other sites have black, loamy horizons that range from several centimeters up to several meters deep.

The fundamental morphological, chemical, physical, and mineralogical properties of manganiferous soils are unlike those of any other known soils in the United States. The soils have a striking morphology, with black colors (often Munsell value/ chroma of 2/1) in subsoil horizons, which makes them appear morphologically similar to organic soils. However, organic C concentrations in the soils are too low to produce such black colors. Instead, extremely high amounts of Mn oxides have pigmented the soils black. Manganese is normally considered a trace element, as it is found in most soils in concentrations of less than 1 g kg^{-1} (Dixon and White, 2002). Black horizons in the soils studied may have as much as 141 g kg^{-1} DCB-extractable Mn. There are no known soils in the country (in the NRCS characterization database) that are close to having such high concentrations of Mn. The only other known soils in the world that have similar black,

Mn-enriched soils exist in South Africa over dolomite bedrock (Dowding and Fey, 2007). Concentrations of Fe oxides in the manganiferous soils of MD are high (up to 169 g kg^{-1} DCB-extractable Fe), and are positively correlated with Mn concentration. However, the strongly pigmenting black color of the Mn oxides masks most of the red color of the Fe oxides. The trace elements nickel and cobalt, which are known to have a strong affinity for Mn oxides, are elevated in the manganiferous soils. There is a large potential for phytotoxicity due to the extremely high concentrations of Mn, Fe, Ni, and Co in these soils. However, the pH of the manganiferous soils is relatively high (near 7) especially in the upper 1 m, and the soils are well-drained. These conditions probably keep the elements in insoluble, oxidized forms, preventing much phytotoxicity, and this is confirmed by anecdotal evidence from the landowners.

The manganiferous soils have unusual physical properties. The bulk density decreases with Mn content (lowest measured was 0.39 g cm^{-3}), but the horizons with lower bulk density have higher particle density (highest measured was 3.25 g cm^{-3}) due to the influence of Fe and Mn oxides, which have higher densities than silicate minerals. This combination of low bulk density and high particle density produces a very large amount of pore space (maximum calculated was 88%). This high porosity, combined with relatively large pore size (loam/ silt loam textures), implies a high water-holding capacity for the soils.

The mineral suite in the manganiferous soils shares a number of commonalities with other soils of the region, since it is dominated by typical silicate assemblages of quartz, mica, kaolinite, and 2:1 clays such as hydroxy-interlayered vermiculite. However, the soils can have greater than 20% Fe and Mn oxides by weight. Although Fe and Mn

oxides are usually difficult to identify using standard X-ray diffraction, hematite, goethite, and lithiophorite peaks are evident in some of the samples due to the unusually high concentrations of these oxides. The presence of the Mn oxide lithiophorite, which forms and persists in acid, well-drained conditions (such as those in which the manganiferous soils are found) was confirmed using FTIR.

The geologic origin of manganiferous soils was first recognized based on observations of soil morphology. The FLI-1 pedon has a "halo" or weathering rind of black, manganiferous residuum following the contour along the surface of the marble bedrock, which shows that the black material is derived from the marble. However, there are often lithologic discontinuities in the soils. Where a lithologic discontinuity was noted, the black horizons were usually found lower in the profile, underneath soil horizons which were lighter in color and contained many phyllite channers. But occasionally, the black horizons were found overlying lighter-colored soil materials. Presumably, the lighter-colored materials are derived from a layer of bedrock other than the Wakefield marble, and the relative position of the darker and lighter soil materials is related to how the bedrock layers were emplaced during folding in the Appalachian Orogeny.

The marble collected from the FLI site has zones which are primarily calcite and zones which are primarily dolomite, which is consistent with the description of Wakefield Marble. The marble contains approximately 2-3% non-carbonate residue, which probably represents materials accumulated during formation of the original limestones and dolostones (which were later metamorphosed into marble). The non-carbonate residue of the dolomitic sample was mainly coarse fragments of chert (a

secondary quartz), but the non-carbonate residue of the calcitic samples had a silt loam texture. The Wakefield Marble is reported to range between 1 and 150 m (Maryland Geological Survey, 1986), and by our estimations, 65 cm to 110.5 m of marble would have to be dissolved in order to produce the thickness of soils observed (by dissolution of carbonates and accumulation of non-carbonate residues). The non-carbonate residues were mainly comprised of quartz, which is a very stable mineral, and chlorite, an easily weathered mineral which was presumably formed from other clay minerals during diagenesis or metamorphism. In the soils overlying the marble bedrock at the FLI site, quartz has remained stable, but most of the chlorite has weathered to hydroxy-interlayered vermiculite and other 2:1 clays. There is substantially more mica in the Bt horizons of the soils, where phyllite channers are also abundant. Presumably, these horizons formed from a phyllitic parent material rather than from (or in addition to) marble.

Based on the quantities of Fe and Mn measured in the marble samples, it appears that the Fe and Mn in the soils is derived from the parent marble. In the Precambrian time period, waters were rich with Fe^{2+} and Mn^{2+} due to the more reducing conditions caused by lower levels of atmospheric O_2. During deposition of the original carbonates, Fe^{2+} and Mn^{2+} were likely included in the crystal structure of the calcite and dolomite. However, the crystal structure of dolomite can accommodate more Fe and Mn than calcite, so it is more likely that the more Mn-rich zones of the manganiferous soils are derived from the dolomitic component of the Wakefield Marble. Observations of thin sections of the marble saprolite and residuum show that the Fe and Mn are released during the weathering of the marble and then oxidized following carbonate dissolution, and are

accumulating along the edges of the dissolving carbonate grains. Non-carbonate (silicate) residues are presumably accumulating as well, but they are pigmented by the black Mn oxides. After the carbonates have dissolved completely, a spongy, black, ferromanganiferous framework of residuum remains. This explains the high porosity and low bulk density of the soils. This highly porous microstructure allows free movement of water and suspended clay particles, leading to the more recent formation of argillic horizons and Fe-rich, red clay films deeper in the profiles.

Manganiferous nodules are abundant in lighter-colored A and B horizons of manganiferous soils, but they are probably not formed as a result of seasonal reducing conditions because the manganiferous soils are well-drained. The nodules are found in horizons containing many phyllite fragments. These lighter-colored horizons presumably are formed from a phyllitic rock layer, and not from marble. It appears that the phyllitic rock layer included a calcareous component, as evidenced by the presence of calcareous phyllite fragments in the horizons. Therefore, these nodules may be formed by processes similar to those which formed the black horizons underneath.

In this study, much was discovered about the fundamental nature and origin of manganiferous soils in Maryland. However, some basic questions have inevitably arisen which were beyond the scope of this study. Since the soils are formed from dolomite marble, one may wonder if manganiferous soils occur in other, undiscovered locations which have similar bedrock geology. And if this is not the case, then perhaps there is something unusual about the Wakefield marble itself, or perhaps there is something special about the conditions in which the rock has weathered and the soils have formed, which have allowed Mn and Fe oxides to accumulate and persist. These rare

manganiferous soils have provided us with some fascinating questions to be explored in the future.

APPENDIX A

Transect Morphological Descriptions

Dotterer Transect A

Waypoint Latitude Longitude	Hor-izon	Depth (cm)	Color (moist, field Munsell)	Texture class/ % clay by feel	Reaction w/ 10% H_2O_2	Other observations
WP221 39.5307N 77.2255W		30 (AR)	dark brown		3-4	very rocky, impossible to auger, large phyllite fragments
WP220 39.5307N 77.2259W	Ap	0-20	7.5YR 3/2	sil 20%	3	
	Bt1	20-64	7.5YR 3/2	cl 29%	3	
	Bt2	64-102	7.5YR 3/2;1% v. fine Mn conc	cl 34%	4	
	BC	102-127	5YR 3/2	cl 29%; 10% gravels	4+	
		(AR)				
WP219 39.5308N 77.2263W	Ap	0-10	7.5YR 3/2	sil 22%	2	
	Bt1	10-43	7.5YR 4/3	l 26%	3+	
	Bt2	43-71	7.5YR 3/2; 2% fine (7.5YR 1/1) Mn conc	l 26%	3+	
	Bt3	71-124	5YR 3/2	gr cl 34%	4	

	BC1	124-152	5YR 2.5/1	gr l 26%; 15-20% qtz & phyllite gravels & paragravels	5	
	BC2	152-196	5YR 2.5/1	l/sil 21%	5	
	sam-pled by depth	196-229	2.5YR 2/1	gr l 15% (15% nodules)	5	gradually gets darker w/ depth
	"	229-259	2.5YR 0.5/0.5	l/sil 10%; 5% qtz gravels	5	low bulk density; micaceous
	"	259-290	2.5YR 0.5/0.5	l/sil 10%; 5% qtz gravels	5	
	"	290-320	2.5YR 0.5/0.5	l/sil 10%; 5% qtz gravels	5	
	"	320-351	2.5YR 0.5/0.5	l/sil 10%; 5% qtz gravels	5	
	"	351-381	2.5YR 0.5/0.5	l/sil 10%; 5% qtz gravels	5	
WP207 39.5310N 77.2266W	Ap	0-20	7.5YR 3/1	l/ sil	4	
	Bw1	20-48	5YR 2.5/1	l	4+	
	Bw2	48-81	5YR 2.5/1	l	4+	
	Bw3	81-112	5YR 2.5/1; fine 5YR 1/1 Mn conc	l 17%	4	
	BC1	112-175	5YR 1/1	l	5	
	BC2	175-211	5YR 1/1	l	5	
	BC3	211-284	7.5YR 1/1	l	5	
	CB1	284-307	5YR 1/1 Coatings/ matrix; 5YR 3/3 interior of some peds	l	5	

	CB2	307-335	7.5YR 1/1	loam	5
	CB3	335-368	5YR 1/1	l 14%; with small nodules	5
	C1	368-411	5YR 1/1	gr loam 11% (30% small nodules and gravels)	5
	C2	411-508	5YR 0.5/0.5	gr loam 11% (30% small nodules and gravels)	5
	samp-led by depth	508-538	5YR 0.5/0.5	l 12%	5
	"	538-569	5YR 0.5/0.5	l 12%	5
	"	569-599	5YR 0.5/0.5	l 12%	5
	"	599-630	5YR 0.5/0.5	l 9%	5
	"	630-660	5YR 0.5/0.5	l 10% w/ nodules	5
	"	660-691	2.5YR 1/1	vgr l	5
	"	691+	2.5YR 1/1	vgr l (qtz gravels)	5
WP218 39.5315N 77.2270W	Ap	0-18	7.5YR 4/2	gr sil 19%	1+
	Bt1	18-61	7.5YR 4/4	ch cl 30%	0
	Bt2	61-91	7.5YR 5/4; 2% fine black Mn conc	ch cl 30%	1
	Bt3	91-114 (AR)	7.5YR 5/4	vch cl	0+

Dotterer Transect B

Waypoint Latitude Longitude	Hor-izon	Depth (cm)	Color (moist, field Munsell)	Texture class/ % clay by feel	Reaction w/ 10% H_2O_2	Other observations
WP207 39.5310N 77.2266W	Ap	0-20	7.5YR 3/1	l/ sil	4	
	Bw1	20-48	5YR 2.5/1	l	4+	
	Bw2	48-81	5YR 2.5/1	l	4+	
	Bw3	81-112	5YR 2.5/1; fine 5YR 1/1 Mn conc	l 17%	4	
	BC1	112-175	5YR 1/1	l	5	
	BC2	175-211	2.5YR 1/1	l	5	
	BC3	211-284	7.5YR 1/1	l	5	
	CB1	284-307	5YR 1/1 coatings/ matrix; 5YR 3/3 interior of some peds	l	5	
	CB2	307-335	7.5YR 1/1	l	5	
	CB3	335-368	5YR 1/1	l 14%; with small nodules	5	
	C1	368-411	5YR 1/1	gr loam 11% (30% small nodules and gravels)	5	
	C2	411-508	5YR 0.5/0.5	gr loam 11% (30% small nodules and gravels)	5	
	sam-pled by depth	508-538	5YR 0.5/0.5	l 12%	5	
	“	538-569	5YR 0.5/0.5	l 12%	5	
	“	569-599	5YR 0.5/0.5	l 12%	5	
	“	599-630	5YR 0.5/0.5	l 9%	5	
	“	630-660	5YR 0.5/0.5	l 10% w/ nodules	5	

	“	660-691	2.5YR 1/1	vgr l	5
	“	691+	2.5YR 1/1	vgr l (qtz gravels)	5
WP208 39.5311N 77.2265W	Ap	0-28	7.5YR 4/3	l	2
	Bt	28-76	7.5YR 5/4 matrix; 7.5YR 1/1 Mn conc	gravelly cl	matrix: 0; conc: 4
	BC1	76-124	7.5YR 3/2 matrix; 7.5YR 2.5/1 Mn conc	cl	3
	BC2	124-163	7.5YR 3/1 matrix; 7.5YR 2.5/1 Mn conc	cl	4
	C1	163-178	5YR 2.5/1 Mn matrix/ coatings; 2.5YR 6/3 and 7.5YR 5/4 Fe conc/ interior of peds	l	4
	C2	178-188	7.5YR 4/3 matrix; 7.5YR 2/1 Mn conc; 7.5YR 5/8 Fe conc; 7.5YR 6/4 depl	l/ sil	4
	C3	188-234	5YR 3/1	l/ sil	3
	C4	234-261	5YR 3/2	l	3+
	C5	261-300	7.5YR 3/2 matrix; 2.5YR 2.5/1 Mn conc; 7.5YR 4/6 Fe conc	sil	2
	C6	300-315	2.5YR 2.5/1 coatings; 2.5YR 3/3 interior of peds	l	4+
	C7	315-325+…	5YR 1/1	l	4+
	sam-pled by depth	325-356	2.5YR 2.5/1	sil 21%	4
	“	356-386	5YR 2.5/1	sil 17%	4
	“	386-417			

	“	417-447	5YR 3/2; 10% 2.5YR 4/2; 2% v. fine 5YR 1/1? Mn conc	l 18%	2	
	“	447-478	2.5YR 3/1	l/sil 14%	4	
	“	478-508	10R-2.5YR 3/1; 5% med 2.5YR 1/1? Mn conc	l/sil 18%	4+	
	“	508-538	10R-2.5YR 3/1 matrix; 2.5YR 2.5/1 and 2.5YR 3/2 conc	silt loam/ silt 8%	4	
	“	538-579	2.5YR 2.5/1; 5% 2.5YR 1/1? Fine Mn conc; 2% 2.5YR 2.5/2	silt loam/ silt 8%	4	
WP210 39.5312N 77.2264W	Ap	0-25	7.5YR 4/3	gr l	3	Rocky, difficult to auger.
	Bw1	25-64	7.5YR 4/2	l	4	
	Bw2	64-99	7.5YR 4/3	l 22%	3	
	BC	99-127	5YR 3/2 matrix; 7.5YR 1/1 Mn conc	l	3+	
	CB1	127-178	5YR 2.5/1	l	4	
	2CB2	178-239	5YR 4/2	l 18%	3	
	2CB3	239-254 (AR)	5YR 4/2	gr l 13%	3+	
WP209 39.5312N 77.2264W	Ap	0-15	7.5YR 4/2.5	silt loam	1	
	Bt	15-61	7.5YR 4/4	gravelly clay loam	0	
	Cr	61-79	Bluish phyllite saprolite			
WP206 39.5313N 77.2261W						phyllite saprolite; AR @ 60cm.; few Mn conc

Grossnickle Transect

Waypoint Latitude Longitude	Horizon	Depth (cm)	Color (moist, field Munsell)	Texture class/ % clay by feel	Reaction w/ 10% H_2O_2	Other observations
WP173 39.5371N 77.2280W	Ap	0-17cm	10YR 4/3	l	2	
	AB	17-41	10YR 4/3	l	1	
	Bt	41-69	7.5YR 4/3	cl	1	
	BC	69-99	7.5YR 4/3	gr sicl	1	
WP174 39.5372N 77.2277W	Ap	0-19	10YR 4/2	l/ sil	2	Similar to 173; red w/ silver phyllite
	Bt	19-38	10YR 4/3	cl/ sicl	1	
	BC	38-58	10YR 4/3	gr cl	2	
WP175 39.5372N 77.2276W	Ap	0-20	10YR 4/2	l/ sil	1	Less phyllite than 174
	Bt1	20-41	10YR 4/3	cl/ sicl	1	
	Bt2	41-71	10YR 4/3	cl/ sicl	1	
	CB	71-99	10YR 4/3	sil	1	
WP170 39.5372N 77.2255W	Ap	0-16cm	7.5YR 3/2	l	3	Rock frags: purple/white phyllite + quartzite
	AB	16-30	7.5YR 3/2	l	3	HCl: (-)
	Bt1	30-60	7.5YR 3/3	cl	3	
	Bt2	60-79	7.5YR 3/2	cl	4	

	Bt3	79-112	10YR 3/2	cl	4
	BC	112-130+	10YR 3/2	gr cl	3
WP252 39.5372N 77.2273W	Ap	0-18	7.5YR 3/2	l 17%	3
	BA	18-30	7.5YR 3/2-3	ch l 20%	3
	Bt1	30-38	7.5YR 3/1	l 22%	4+
	Bt2	38-58	7.5YR 3/2	ch l 22%	4
	Bt3	58-64	7.5YR 4/1-2	gr cl 28%	4
	Bt4	64-76	7.5YR 3/1	gr cl 28%	4
	BC1	76-102	7.5YR 4/1	vgr l 26% (talc phyllite)	2
	BC2	102-119	7.5YR 4/1	vgr l 23%	2
WP253 39.5372N 77.2272W	Ap	0-18	5YR 3/1	l 15%	4
	Bw1	18-38	5YR 2/1	l 16%	4
	Bw2	38-69	5YR 2/1	l 18%; 5% nodules (~3-4mm)	5
	BC	69-168	5YR 2/1; 2-5% of 7.5YR 6/6	gr l/sl; 20% nodules	5
	C1	168-216	5YR 1/1; 2% (2.5YR 4/6) Fe conc	gr l 15% w/ 10% black nodules	4+
	C2	216-295	5YR 1/1; 2% (2.5YR 3/2) Fe conc	l 15%	5
	C3	295-419	5YR 2/1	gr l 15%; 5-10% qtz gravels & 10% nodules	5
	C4	419-427	weathered rock, variegated w/ 25% 5YR 1/1 Mn	vgr l	4

	C5	427-445	5YR 3/1; silvery purple phyllite w/ black Mn conc on rock fragments	egr l	4
WP245 39.5372N 77.2272W	Ap	0-18	5YR 2.5/2	l 17%	4
	BA	18-51	5YR 2.5/1	l 19%	4
	Bt1	51-104	2.5YR 2.5/1	l 22%	5
	Bt2	104-150	5YR 3/2 matrix; 5-10% fine (5YR 1/1?) Mn conc; 5-10% (2.5YR 4/6) Fe conc	l 24%	4
	BC1	150-208	5YR 2.5/1 matrix; 5% med (5YR 1/1?) Mn conc; 3% med (2.5YR 4/6) Fe conc	l 21%	4
	BC2	208-394	2.5YR 2/1?	l 22%	4+
	CB	394-503	2.5YR 2/1?; 2% 2.5YR 4/4 Fe conc; 5% Mn conc	l 17%	5
	C	503-612	2.5YR 1/1?; 5% 2.5YR 2.5/2	sil 10%	5
WP254 39.5374N 77.2268W	Ap	0-15	5YR 2.5/2	sil 15%	4
	Bt1	15-58	2.5YR 2.5/1	l 20%	4+
	Bt2	58-79	2.5YR 2.5/1	cl 29%; 5% Mn nodules	4+
	Bt3	79-89	2.5YR 2.5/1	cl 29%	4+
	BC	89-94	5YR 2.5/2; 5% 5YR 1/1 nodules	gr l 22%	4+
	C1	94-241	2.5YR 1/1?	sil 12%	5
	C2	241-272	2.5YR 1/1?; 1-2% 2.5YR 4/6 very fine Fe conc	sil 14%	5

	C3	272-290	5YR 2.5/1; 10% 5YR 1/1 Mn conc	sil 13%	5
	C4	290-325	5YR 2/1?; 5% fine 2.5YR 4/4 Fe conc; 5% fine-med 5YR 1/1 Mn conc	sil 15%; 5% fine Mn nodules	5
	C5	325-335	2.5YR 1/1?; 5% 2.5YR 4/6 Fe conc	sil 16%	5
WP176 39.5374N 77.2261W	Ap	0-36	7.5YR 3/2	l	3
	Bt1	36-53	7.5YR 4/3	cl	3
	Bt2	53-71	7.5YR 4/3	cl	3
	Bt3	71-91	7.5YR 5/3	cl	2
	Bt4	91-104	7.5YR 5/3	cl	2
	BC	104-114	7.5YR 3/2	gr cl	4
WP216 39.5375N 77.2257W	Ap	0-18	7.5YR 3/2	l/sil 17%	3
	Bt1	18-43	7.5YR 4/3	cl 28%	3+
	Bt2	43-71	5YR 3/2; 2% fine (5YR 1/1) Mn conc	cl 28%	4
	Bt3	71-107	5YR 3/3	gr scl 29%	3+
	Bt4	107-124			
	Bt5	124-180	7.5YR 4/4 & 5YR 4/4	cl 30%; 10% gravels	3
	2BC	180-218	7.5YR 5/6	sicl 28%	1
	2CB	218-284+	7.5YR 5/6	sil 23%	0

Clemsonville Rd. Transect

Waypoint Latitude Longitude	Hor-izon	Depth (cm)	Color (moist, field Munsell)	Texture class/ % clay by feel	Reaction w/ 10% H_2O_2	Other observations
WP179 39.5297N 77.1747W	Ap	0-12	7.5YR 3/2	l	3+	
	Bt1	12-38	7.5YR 3/3	cl	3	
	Bt2	38-88	7.5YR 3/3 matrix; 5YR 2.5/1 Mn conc; 7.5YR 5/6 Fe conc	c	3	
	Bt3	88-103	7.5YR 4/6 matrix; large black Mn conc; 2.5YR 4/4 Fe conc	c	3	
	BC	103-121 (AR)	5YR 4/4 matrix; large black Mn conc	cl	2	
WP178 39.5297N 77.1745W	Ap	0-11	5YR 3/3	cl	3+	
	Bt1	11-29	5YR 3/3	c	3+	
	Bt2	29-44	5YR 4/4 matrix; 5YR 1/1? Mn conc	c	2	
	Bt3	44-75	5YR 4/4 matrix; 5YR 2.5/1 fine Mn conc	c	2	
	Bt4	75-112	5YR 4/4 matrix; 5YR 2.5/1 fine Mn conc	c	2	
	BC	112-150+	5YR 4/4 matrix; 5YR 2.5/1 Mn conc; 2.5YR 4/4 Fe coatings (clay skins?) and 7.5YR 5/6 Fe conc	c	matrix: 0; Mn conc: 4	

WP177 39.5296N 77.1743W	Ap	0-15	7.5YR 3/2	l	4	
	Bw1	15-42	7.5YR 3/2	l	4	
	Bw2	42-67	7.5YR 3/2	l	4	
	Bw3	67-117	7.5YR 3/2	l	4	
	BC	117-155+	7.5YR 3/3	l	4	
WP182 39.5296N 77.1740W	Ap	0-10	10YR 4/3	l	2	
	Bw1	10-32	10YR 4/3	l	2	
	Bw2	32-56	10YR 5/3	l	1	
	Bw3	56-75	7.5YR 4/3	l/ sil	1	
	BC1	75-96	7.5YR 5/4	l/ sil	1	
	CB1	96-133	7.5YR 4/3	cl	2	
	CB2	133-150+	7.5YR 4/3	channery cl	2	
WP180 39.5296N 77.1738W						AR @ 61cm; lt. brown, talc-rich phyllite; soybean field

Flickinger Transect A

Waypoint Latitude Longitude	Horizon	Depth (cm)	Color (moist, field Munsell)	Texture class/ % clay by feel	Reaction w/ 10% H_2O_2	Other observations
WP239 39.5456N 77.1794W	Ap	0-11 cm	2.5YR 3/2.5	sil 17%	3	
	AB	11-30	7.5YR 4/3	sil 19%	3	
	Bt1	30-71	7.5YR 4/4	sicl/ cl 29%	2	
	Bt2	71-107	5YR 4/3	cl 34%	1	
	Bt3	107-143	7.5YR - 10YR 4/4 matrix; 3% prominent (5YR 2.5/1) soft Mn masses/ coatings on ped faces	c 45%	2	
	BC1	143-165	7.5YR 4/4 matrix; 10-15% prominent (5YR 2.5/1) med-coarse soft Mn masses; 10% distinct (5YR 4/6) med-coarse soft Fe masses	c 50%	3	
	BC2	165-185	10YR 4/6 matrix; 5% soft Fe and Mn masses (7.5YR 2.5/2)	c 55%	3+	
	BC3	185-220	10YR 5/4 matrix; 15% faint (10YR 4/6) soft Fe masses; 10% distinct (7.5YR 3/4) soft Fe masses; 20% prominent (N 2.5) soft Mn masses	c 60%	4	
	BC4	220-247	10YR 4/6 matrix; 20% med distinct (7.5YR 3/4) Fe masses; 15% medium prominent (7.5YR 2.5/1) Mn coatings	c 65%	4	
	BC5	247-310	10YR 4/6 matrix; 25% distinct (10YR 5/3) depletions; 15% faint (7.5YR 4/6) soft Fe masses and nodules	c 60%; n-value <0.7	3	

	2BC6	310-420 (AR)	variegated matrix: 60% of 10YR 3/3; 20% of 10YR 5/6; 10% of 10YR 4/6; 10-15% is reddish black (10R 2.5/1) silt loam	c 60%; 5% gravels; n-value=0.7 (soft/ wet)		alluvial material
WP241 39.5457N 77.1792W	Ap	0-14 cm	7.5YR 3/2	sil 15%	3+	WT @ 3 m
	Bt1	14-66	7.5YR 4/6	cl 29%	3+	
	Bt2	66-119	7.5YR 4/6 matrix; 15% faint (7.5YR 3/3) Mn conc; 2% prominent (N2.5) Mn conc	c 42%	3	
	Bt3	119-163	5YR 3/4 matrix; 10% fine and medium prominent (5YR 2.5/1) soft Mn masses	cl/ c 40%	2	
	BC1	163-230	7.5YR 3/4 matrix; 15% fine prominent (5YR 2.5/1) soft masses of Mn	c 42%	4	
	2BC2	230-340	10YR 3/2 matrix - Rxn 4; 15% of 10YR 4/6 - Rxn 0; 10% of 10YR 2/1 - Rxn 5; 5% of 2.5YR 2.5/1 - Rxn 4 and 2.5YR 2.5/2 - Rxn 3.	sicl 39%	see color desc.	
	2BC3	340-665 (AR)	Black zones @ 420, 520, 590, 660 cm. Zones are 10-20cm thick, Rxn 5. Matrix is 10YR 5/4, Rxn 0; also 15% of 10YR 4/6; 4% of 2.5Y 6/2; 10% of 2.5Y 3/2; 2% of 10R 4/6; 6% of 2.5Y 5/3; 2% of 5YR 3/3.	sicl/ sic	Light zones: 0; black zones: 5	
WP240 39.5457N 77.1791W	Ap	0-14 cm	7.5YR 3/2	l 17%	3	
	AB	14-24	7.5YR 3/3	l 17%	3	
	BA	24-56	7.5YR 4/3	l/ sil 19%	2	
	Bt1	56-83	7.5YR 4/4 to 4/6 matrix; 5% prominent (7.5YR 2.5/2) soft Mn masses	cl 30%	2	
	Bt2	83-107	7.5YR 3/3 matrix; distinct (N2.5) soft Mn masses and pore linings	cl 33%	3+	

	BC/Bt	107-122	60% of 5YR 2.5/1 (BC mat'l); 40% of 7.5YR 4/6 (Bt mat'l); mottled: abrupt boundaries, intermixed.	cl 38%	4
	BC	122-210 (AR)	5YR 2.5/1 matrix; zones with 5-20% of 7.5YR 4/4	sicl 30%	5
WP196 39.5457N 77.1789W	Ap	0-30 cm	7.5YR 3/2	l	3+
	Bt1	30-69	7.5YR 4/4	l	3
	Bt2	69-100	7.5YR 4/4	cl	3
	2BC	100-150	5YR-7.5YR 3/3	gr cl 35%	3+
	2CB	150-175 (AR)	5YR 3/1	sil	5
WP244 39.5455N 77.1781W	Ap	0-10 cm	7.5YR 3/2	sil 17%	3
	BA	10-36	7.5YR 3/4	l 25%	3+
	Bt1	36-75	5YR 4/4	cl 38%	2
	Bt2	75-120	5YR 3/4	sc 36%	4
	2BC1	120-180	5YR 2.5/1	sil 25%	5
	2BC2	180-225 (AR)	5YR 1/1?	sil 17%	5
WP198 39.5458N 77.1775W	Ap	0-25	7.5YR 3/2	l	3
	Bt1	25-64	5YR 3/3	cl 29%	3+
	Bt2	64-122	5YR 2.5/2	cl	4
	Bt3	122-165	5YR 4/4 and 5YR 3/2	cl	4
	C	165-287 (AR)	5/YR 1/1?	sil	5

WP199 39.5257N 77.1774W	Ap	0-20	7.5YR 3/2	l/ sil	2
	Bt1	20-66	5YR 4/4 matrix; 5YR 1/1? fine black Mn conc	cl	3
	Bt2	66-109	2.5YR 4/6 and 7.5YR 6/6 Fe conc; 5YR 2.5/2 and 5YR 2.5/1 Mn conc	cl	4
	BC1	109-137	5YR 4/6 and 7.5YR 6/6 Fe conc (interior of peds); 5YR 1/1? Mn (matrix and coating of peds)	l/ cl	4+
	2BC2	137-183	5YR 3/3; 10% fine-med 5YR 1/1 Mn conc; 5YR 4/4 Fe conc	cl 35%	4+
	2BC3	183-234	5YR 2/1? Matrix; 5YR 5/6 Fe conc	cl	4+
	2CB1	234-267	5YR 1/1?	sil (sticky!)	5
	2CB2	267-300	7.5YR 1/1?	sil	5
	2C	300-320 (AR)	7.5YR 1/1?	sil	5
WP200 39.5458N 77.1772W	Ap	0-15	7.5YR 3/2	l	2
	AB	15-37	10YR 4/3	l	0
	Bt1	37-74	7.5YR 4/4 matrix; fine 5YR 2/1? Mn conc	gr cl 36%	1
	Bt2	74-114	7.5YR 4/4 matrix; 7.5YR 6/6 weathered rock depl?	cl	1
	Bt3	114-155	5YR 4/6 and 7.5YR 6/6	cl	1
	BC1	155-168	2.5YR 4/4 and 5YR 3/3	gr cl	0
	2BC2	168-180	2.5YR 2.5/1 matrix; 7.5YR 6/4 weathered rocks	gr l/ cl	4
	2BC3	180-191	7.5YR 2/1?	gr cl	4
	2BC4	191-206 (AR)	7.5YR 4/3	gr cl	4

WP201 39.5457N 77.1772W	Ap	0-18	10YR 4/2	l	1
	BA	18-36	10YR 4/3	l	0-1
	Bt1	36-64	10YR 4.5/4	gr cl	0
	Bt2	64-97	7.5YR 4/3	cl	0
	BC	97-114	7.5YR 4/3	gr cl	1
	CB1	114-158	7.5YR 4/3	l/ sil	1
	CB2	158-180	7.5YR 4/4 and 10YR 7/6 weathered rocks	gr cl	0
	CB3	180-198 (AR)	10YR 6/4 matrix; lt green saprolite (closest match: 10GY 6/0); 5YR 4/3 clay films	gr cl	0
WP197 39.5458N 77.1770W	Ap	0-15	10YR 4/3	l	2
	Bt1	15-53	10YR 5/4	cl	0
	Bt2	53-81	7.5YR-10YR 4/3	channery cl 28%	0
	BC1	81-131	10YR 4/3	gr cl	0
	BC2	131-170	7.5YR 4/3 matrix; 5YR 3/3 clay films	gr cl	0
	CB1	170-249	7.5YR 4/4 matrix; 7.5YR 4/2 clay films on weathered rock frags	l	0
	CB2	249-262	7.5YR 4/3 matrix; 5YR 3/3 conc; 10YR 6/6 depl (lithochromic)	gravelly cl	1
	CB3	262-292	10YR 5/3 matrix; 5YR 3/3 clay films	gr cl	1
	C	292-320 (AR)	10YR 5/3	l/ sil	1

Flickinger Transect B

Waypoint Latitude Longitude	Horizon	Depth (cm)	Color (moist, field Munsell)	Texture class/ % clay by feel	Reaction w/ 10% H_2O_2	Other Observations
WP271 39.54775N 77.17767W	Ap	0-21	7.5YR 4/3	l 22%	3	
	Bt1	21-62	5YR 4/4	cl 29%	3	
	Bt2	62-81	5YR 4/6	cl 37%	3	
	Bt3	81-99	5YR 4/6; <10% Mn conc	50% gravels; vgr clay 41%	3	clay films
	BC	99-145 (AR)	5YR 2/1 matrix; 5YR 4/6 Fe mottles (25%); soft marble frags (20%)	sicl 32%	5	
WP270 39.54788N 77.17775W	Ap	0-21	7.5YR 4/3	l 23%	3	
	Bt1	21-42	5YR-7.5YR 4/3	cl 30%	3	
	Bt2	42-70	5YR 3/2	cl 34%	4	
	BC1	70-125	5YR 3/3; Mn conc; increasing (5-10%) saprolitic frags w/ depth (7.5YR 6/8)	cl 35%	4	
	BC2	125-165	5YR 4/4 matrix; 30% of 7.5YR 6/8 material; <10% Mn conc	cl 35%	3	
	BC3	165-195	5YR 4/4 matrix; 45% of 7.5YR 6/8 material; 15% Mn conc	cl 28%	3	

	BC4	195-225	5YR 2.5/1 matrix; 15% of 7.5YR 6/8; 30% of 5YR 4/4	cl 29%	4	
	BC5	225-260	50% of 5YR 3/2; 50% of 5YR 2.5/1	l 26%	5	
	BC6	260-300	5YR 2/1 matrix; 15% of 7.5YR 6/8	cl 32%	5	
	CB1	300-325	5YR 2/1; qtz and weathered marble frags; <5% fine 7.5YR 6/8 mottles	l 22%	5	
	CB2	325-375	5YR 2/1; 2% of 5YR 4/4; 8-10% of 7.5YR 6/8	cl 29%	5	
	C1	375-400	5YR 1/1; 2% of 5YR 3/3	l 20%	5	
	C2	400-405 (AR)	5YR 1/1; low BD	l 17%	5+	low B.D.
WP269 39.54797N 77.17788W	Ap	0-20	7.5YR 3/2	l 20%	4	
	Bt1	20-75	7.5YR 4/4; fine few Mn conc	cl 35%	1	
	Bt2	75-92	5YR 4/4; few fine Mn conc and nodules	scl 28%	3	
	Bt3	92-174	5YR 2.5/1; 5-10% 7.5YR 5/6 mottles in upper part	cl 29%	5	
	BC	174-245 (AR)	5YR 2/1; marble saprolite (grey sand) sprinkled throughout; coarse 5YR 3/3 zones in lower part	l 22%	5+	

WP267 39.54805N 77.17803W	Ap	0-25	7.5YR 3/3	l 18%	3+
	Bt1	25-85	5YR 3/3; 2% Mn conc	cl 36%	3
	Bt2	85-170	5YR 3/3	cl 32%	3
	BC	170-270	5YR 3/3-4; 5-10% Mn conc and nodules	cl 31%	3
		2 auger lengths: bigger black zones			
WP268 39.54825N 77.17830W	Ap	0-26	7.5YR 3/2	l 18%	3+
	Bt1	26-65	7.5YR 4/4	l 26%	2
	Bt2	65-105	5YR 3/3	cl 37%	3
	BC	105-205	5YR 2.5/2; gradually gets darker top to bottom	cl 37%	4
	CB	205-270 (AR)	5YR 2.5/1; few cm transition zone brown/black zones mixed @205	l 23%	5
WP266 39.54842N 77.17847W	Ap	0-28	7.5YR 4/3	l 23%	3
	Bt1	28-78	7.5YR 4/4	cl 37%	2
	Bt2	78-156	5YR 4/4; 2% Mn nodules	cl 39%	2
	Bt3	156-226	5YR 4/4; 2% Mn conc	c 43%	2
	BC1	226-320	5YR-7.5YR 4/4; 5% fine 5YR 2.5/1 Mn conc	cl 32%	2

BC2	320-400	5YR 4/4; 5-10% fine-med 5YR 2.5/1 Mn conc	cl 39%	3
BC3	400-450	50% 5YR 4/6 and 50% 5YR 2.5/1	cl 38%	5
CB	450-500+	5YR 2.5/1 matrix; 20% of 5YR 4/6	cl 33%	5

Emerson Burrier Road

Waypoint Latitude Longitude	Horizon	Depth (cm)	Color (moist, field Munsell)	Texture class/ % clay by feel	Reaction w/ 10% H_2O_2	Other Observations
WP183 39.4491N 77.1988W						AR @ 40 cm; Reddish brown
WP185 39.4495N 77.1984W		grab sample	7.5YR 4/3			AR @ 30 cm; darker color
WP186 39.4502N 77.1978W		grab sample	5YR 4/4			AR @ 50 cm
WP187 39.4508N 77.1972W	Ap	0-13	7.5YR 3/3	l	3	
	Bt1	13-39	7.5YR 4/3	cl	2	
	Bt2	39-65	7.5YR 4/3	l/ cl	3	
	Bt3	65-110	5YR 3.5/4	cl	2	
	BC	110-138+	5YR 4/4 matrix; 5YR 2.5/2 Mn conc	cl/ scl	2	
WP188 39.4512N 77.1969W	Ap	0-21	7.5YR 3/3	l	3+	
	Bt1	21-64	2.5-5YR 3/4	cl	1	

	Bt2	64-114	2.5YR 3/4	cl	1
	BC1	114-130	7.5YR 3/3	l	4
	BC2	130-140+	5YR 3/4	l/ sl	2
WP189 39.4518N 77.1964W	Ap	0-7	7.5YR 3/2	l	2
	BA	7-24	7.5YR 3/2	l	3+
	Bt1	24-38	7.5YR 4/3	cl	3
	Bt2	38-74	7.5YR 4/4	cl	2
	BC1	74-92	5YR 4/3	gravelly l	3
	BC2	92-109	5YR 4/3 matrix; 5YR 3/2 Mn conc	gravelly l	4
	BC3	109-130+	7.5YR 4/4 matrix; 7.5YR 2.5/1 Mn conc	l	4
WP190 39.4520N 77.1966W	Ap	0-13	7.5YR 3/3	l	3
	BA	13-54	7.5YR 3/3	l	3
	Bt1	54-90	7.5YR 4/3	sicl	2
	BC	90-115+	7.5YR 4/3 matrix; 7.5YR 3/2 Mn conc	sicl	2
WP229 39.4538N 77.1960W	Ap	0-15	7.5YR 3/2-3	l 24%	3+

	Bt1	15-41	7.5YR 4/4 matrix; 5% med prominent (5YR 2.5/1) Mn conc	cl 33%	3
	Bt2	41-74	7.5YR 5/6 matrix; 2% fine prominent (7.5YR 3/1) Mn conc	cl 33%	matrix: 2
	Bt3	74-91	7.5YR 5/4; 2% fine 7.5YR 2.5/1 Mn conc	gr cl 32%	2
	BC1	91-107	7.5YR 5/6 and 6/6 (mottled); 5% 7.5YR 2.5/1 Mn conc	cl 35%; 5% nodules	3
	BC2	107-130	7.5YR 4/4; 5% 2.5YR 4/4 Fe conc; 10% 2.5YR 2.5/1 Mn conc	cl 30%	3
WP230 39.4540N 77.1962W	Ap	0-18	7.5YR 4/3	l 19%	3
	Bt1	18-74	7.5YR 5/4	cl 32%	3
	BC1	74-104	7.5YR 4/4; 2% fine Mn conc	cl/ scl 32%	3
	BC2	104-152	10YR 5/6; 5-10% very fine Mn conc	gr cl 36%	3
WP231 39.4536N 77.1956W	Ap	0-15	7.5YR 3-4/3	l/ sil 18%	2
	Bt1	15-36	7.5YR 4/4	l/cl 27%	2+
	Bt2	36-53	7.5YR 4/4	cl 31%	3

	Bt3	53-74	5YR-7.5YR 4/4	cl 30%	3
	BC	74-94	5YR 4/4; 2% 7.5YR 2.5/1 fine Mn nodules	scl 22%	3

Pearre Road

Waypoint	Horizon	Depth (cm)	Color (moist, field Munsell)	Texture class/ % clay by feel	Reaction w/ 10% H_2O_2	Other Observations
WP191 39.5251N 77.1722W	Ap	0-13	7.5YR 3/2	sil	1	
	BA	13-58	7.5YR 4/2	sil	3	
	Bt1	58-91	7.5YR 4/3	cl	3+	
	Bt2	91-109	7.5YR 4/3	cl	2	
	BC	109-140+	7.5YR 4/3	gravelly/ channery cl	2	
WP192 39.5250N 77.1740W	Ap	0-15	7.5YR 3/2	l	3+	
	BA	15-34	7.5YR 3/3	l	3	
	Bt1	34-53	7.5YR 4/3	cl	2	
	Bt2	53-77	7.5YR 4/3	sicl	1-2	
	BC	77-105	7.5YR 4/3	gravelly sicl	1	
	CB	105-140+	7.5YR 5/4	sil	1	
WP193 39.5247N 77.1765W	Ap	0-11	7.5YR 3/2	l	3	graphite phyllite
	Bt1	11-51	7.5YR 4/3	cl/ c	3	
	Bt2	51-93	5YR 4/3	c	3	
	Bt3	93-140+	5YR 4/3 matrix; fine black Mn conc	c	3	

WP194 39.5249N 77.1753W	Ap	0-14	7.5YR 3/2	l	3	
	Bw1	14-42	7.5YR 2.5/1	l	4+	
	Bw2	42-89	7.5YR 1/1	l	4+	
	2BC1	89-123	7.5YR 4/3 matrix; many black (1/1) Mn conc	c	4+	
	2BC2	123-142	7.5YR 3/3 matrix; black (1/1) Mn conc	c	4	
	2BC3	142-150+	7.5YR 3/3 matrix; black (1/1) Mn conc	c	2	
WP232 39.5247N 77.1756W	Ap	0-15	10YR 4/3	sil 23%	1	not manganiferous - blue phyllite
	Bt1	15-36	10YR 4/3	sil/ sicl 27%	1	
	Bt2	36-86	10YR 4/3	sicl 34%	0	
	Bt3	86-122	10YR 4/3	cl 34%	1	
	BC	122-178+	10YR 4/1; 2% Mn conc		matrix: 1	
WP058	Ap	0-15	7.5YR 3/2	l 17%	3+	
	BA	15-28	7.5YR 3/2	l 20%	3+	
	Bt1	28-79	7.5YR 3/2	cl 34%	4	
	Bt2	79-122	5YR 2.5/1; 2% 2.5YR 4/6 fine Fe conc	c 45%	4+	

BC1	122-180	5YR 2.5/1; 10% 2.5YR 4/4 med Fe conc	sil 25%	5
BC2	180-203	5YR 2.5/1; 10% med 2.5YR 4/6 Fe conc	sil 25%	5
CB1	203-295	5YR 2/1?; 5-10% 2.5YR 4/4 Fe conc	sil 19%	5
CB2	295-315	5YR 2/1?; 5% med 2.5YR 4/6 Fe conc	sil 20%	5
CB3	315-376	5YR 2/1?; 5% v. fine 5YR 4/4 Fe conc	sil 19%	5
CB4	376-467+	5YR 2/1?; 5% med 10R 4/6 Fe conc	sil 19%	5

APPENDIX B

X-Ray Diffraction Patterns of Selected Soil Fractions

Legend

Symbol	Mineral Name
Ch	chlorite
F	feldspar
G	goethite
H	hematite
HIV	hydroxy-interlayered vermiculite
K	kaolinite
L	lithiophorite
M	mica
Q	quartz
S	smectite
V	vermiculite

DOT-2 Sand Fractions

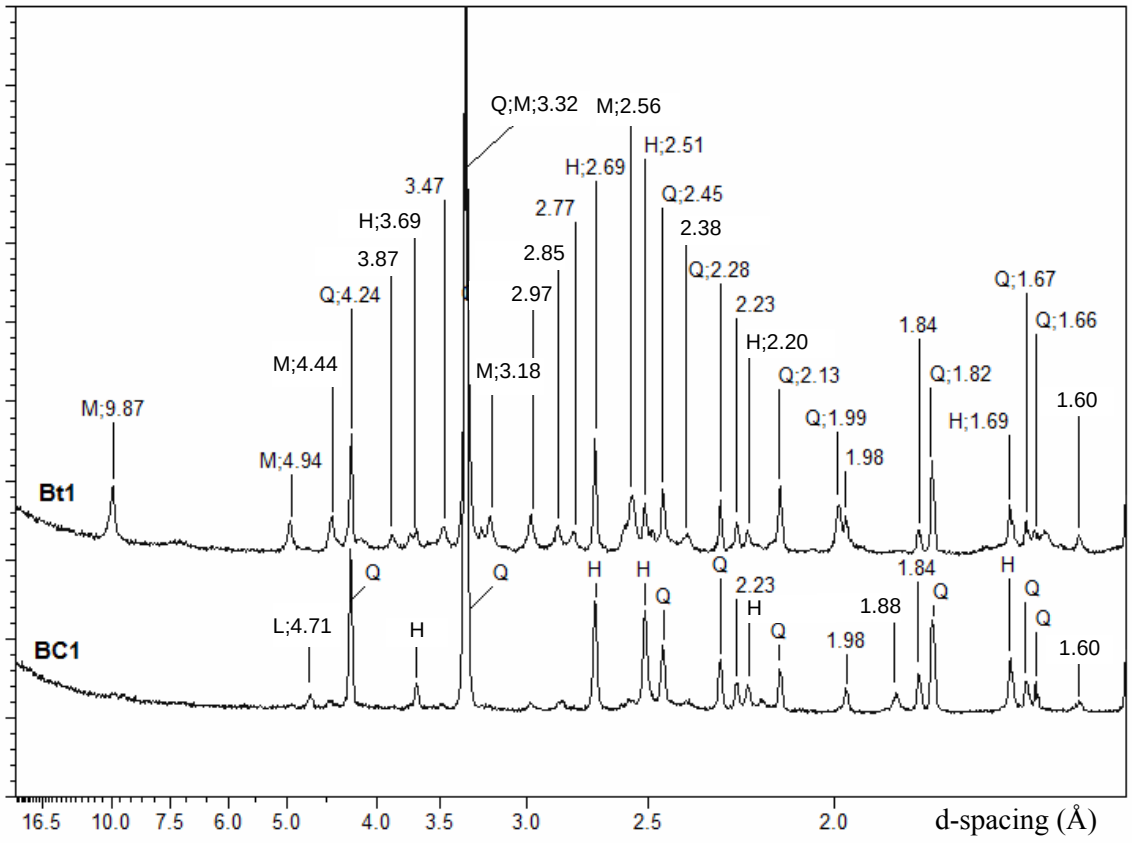

DOT-2 Silt Fractions

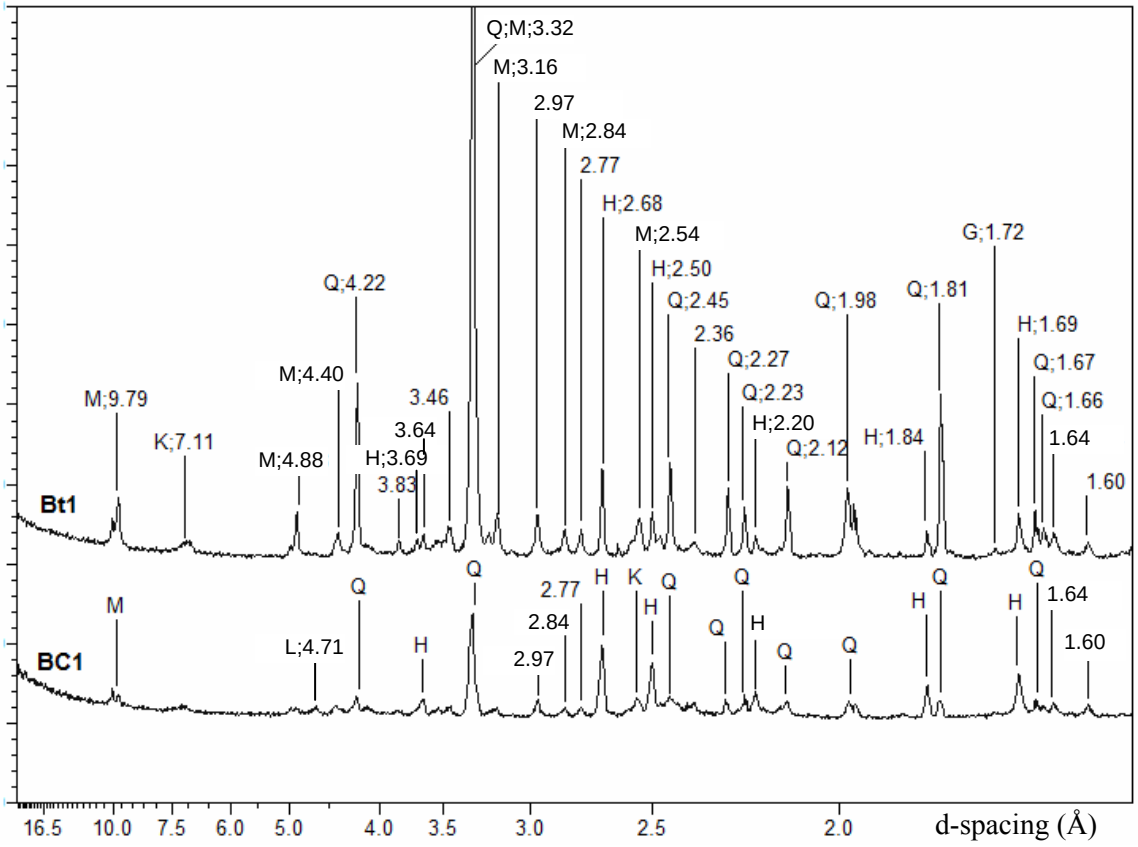

DOT-2 Bt1 Clay Fraction

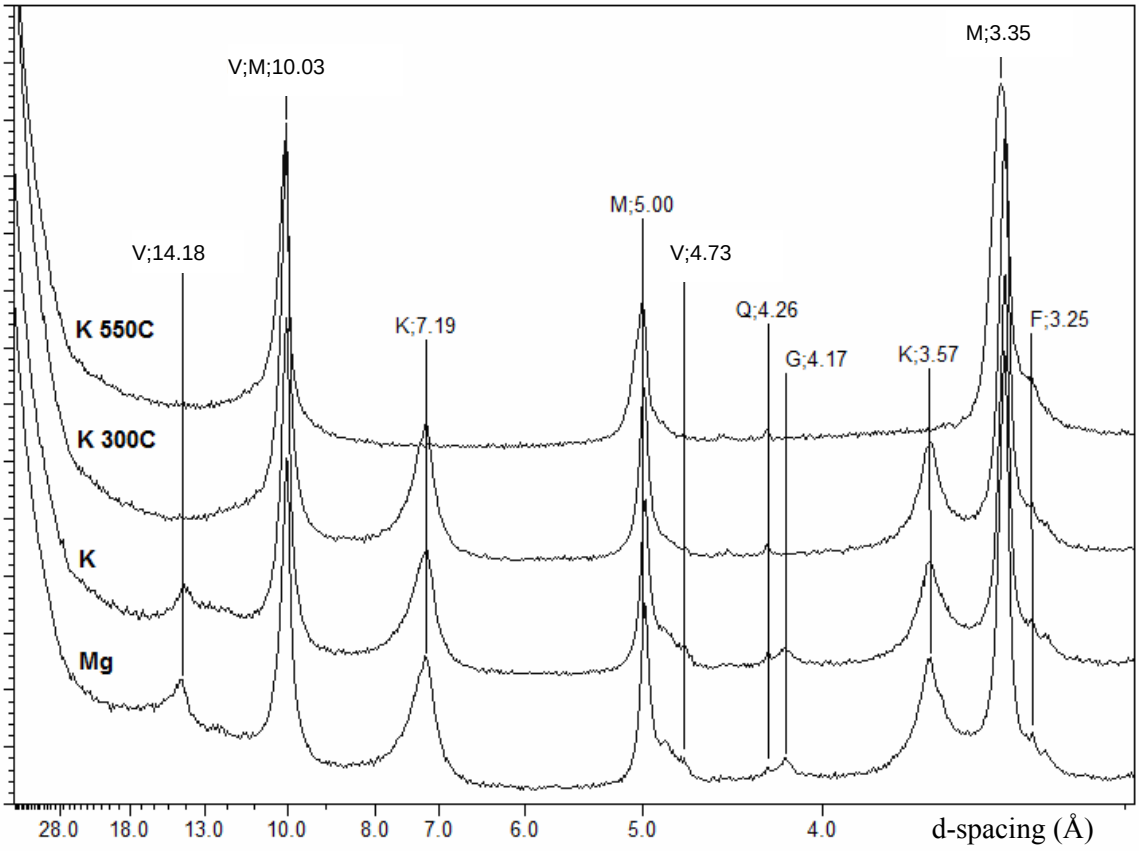

DOT-2 BC1 Clay Fraction

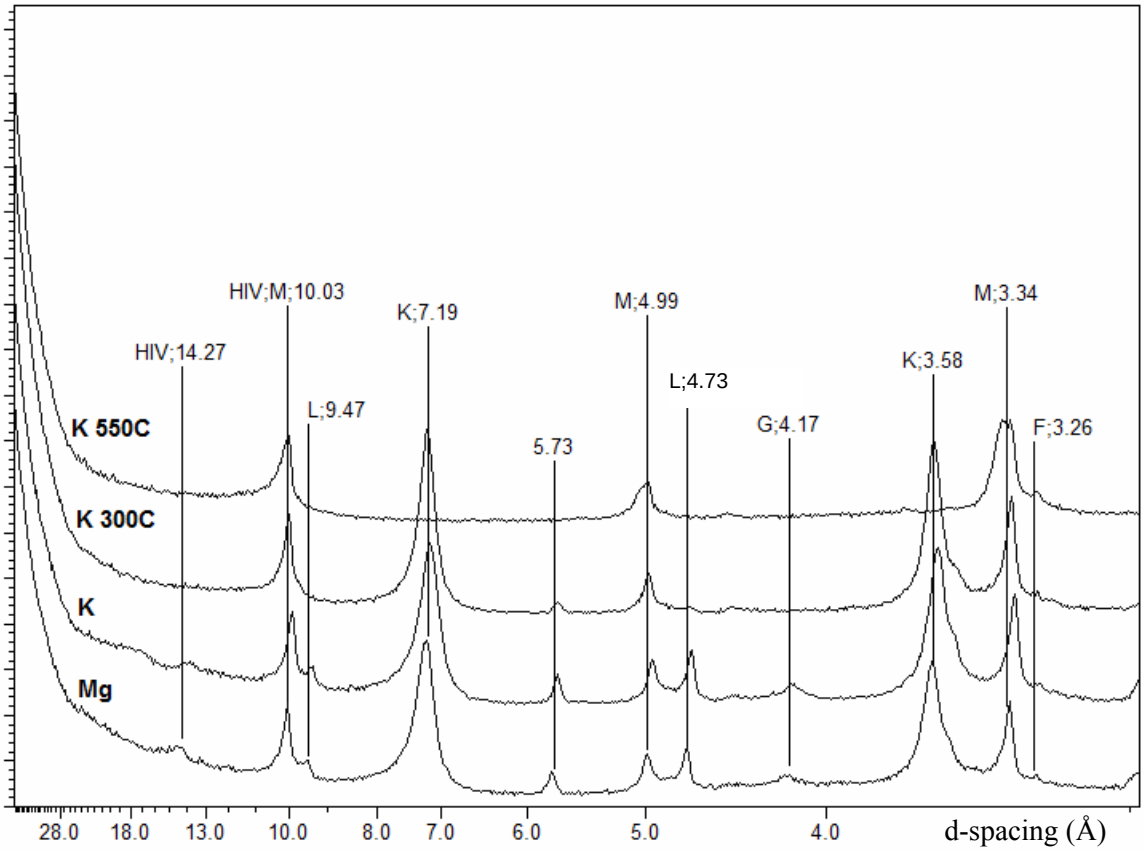

FLI-1 Sand Fractions

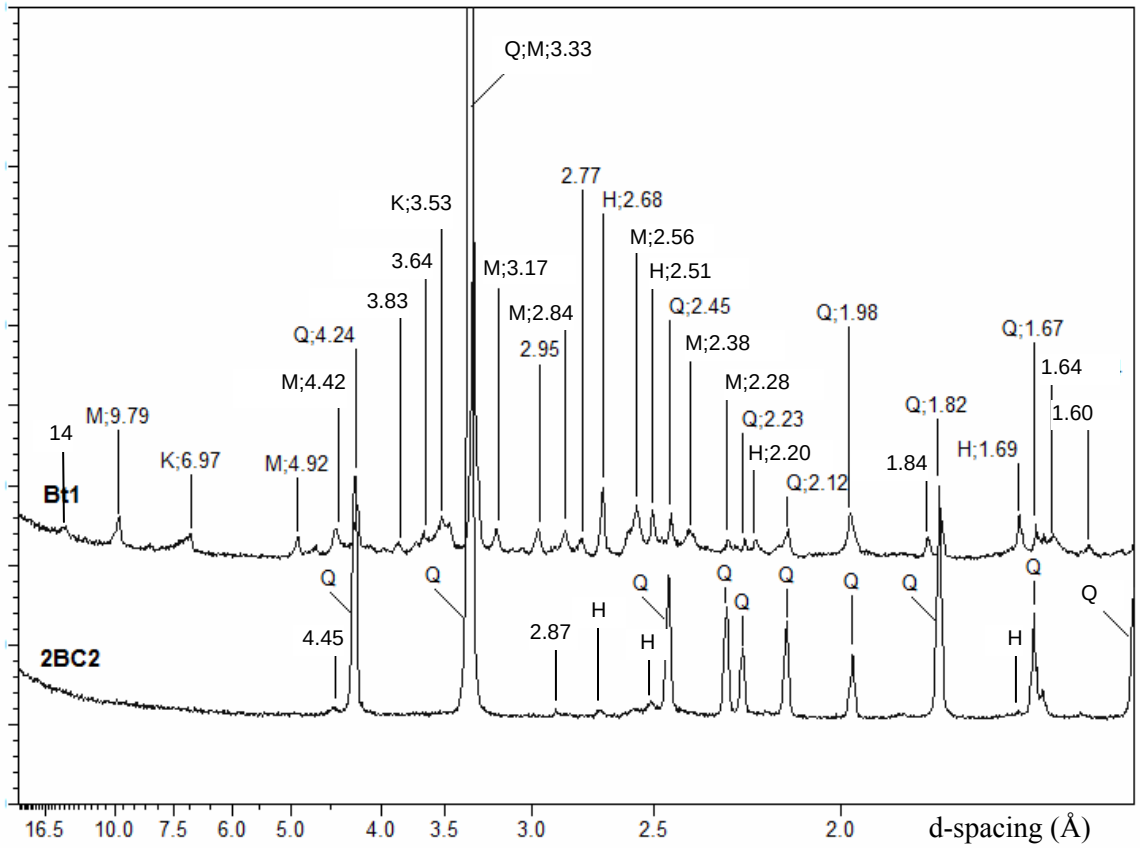

FLI-1 Silt Fractions

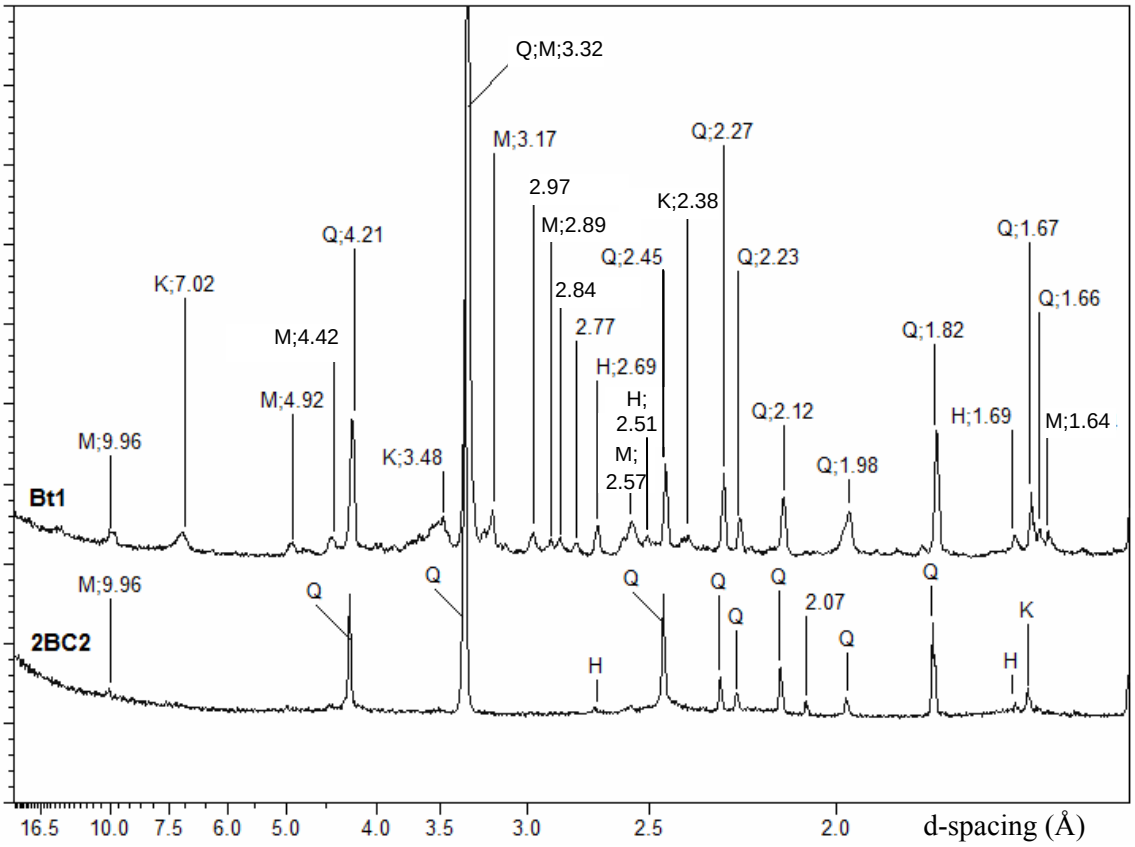

FLI-1 Bt1 Clay Fraction

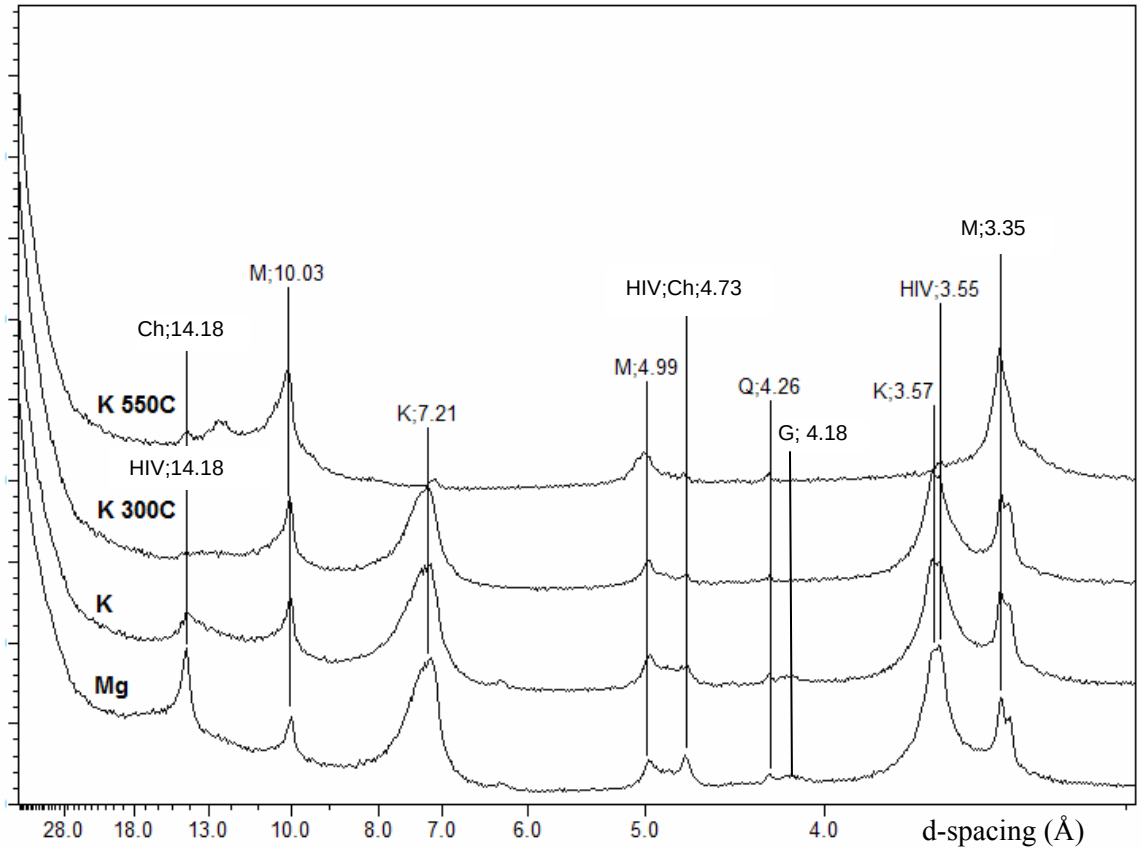

FLI-1 2BC2 Clay Fraction

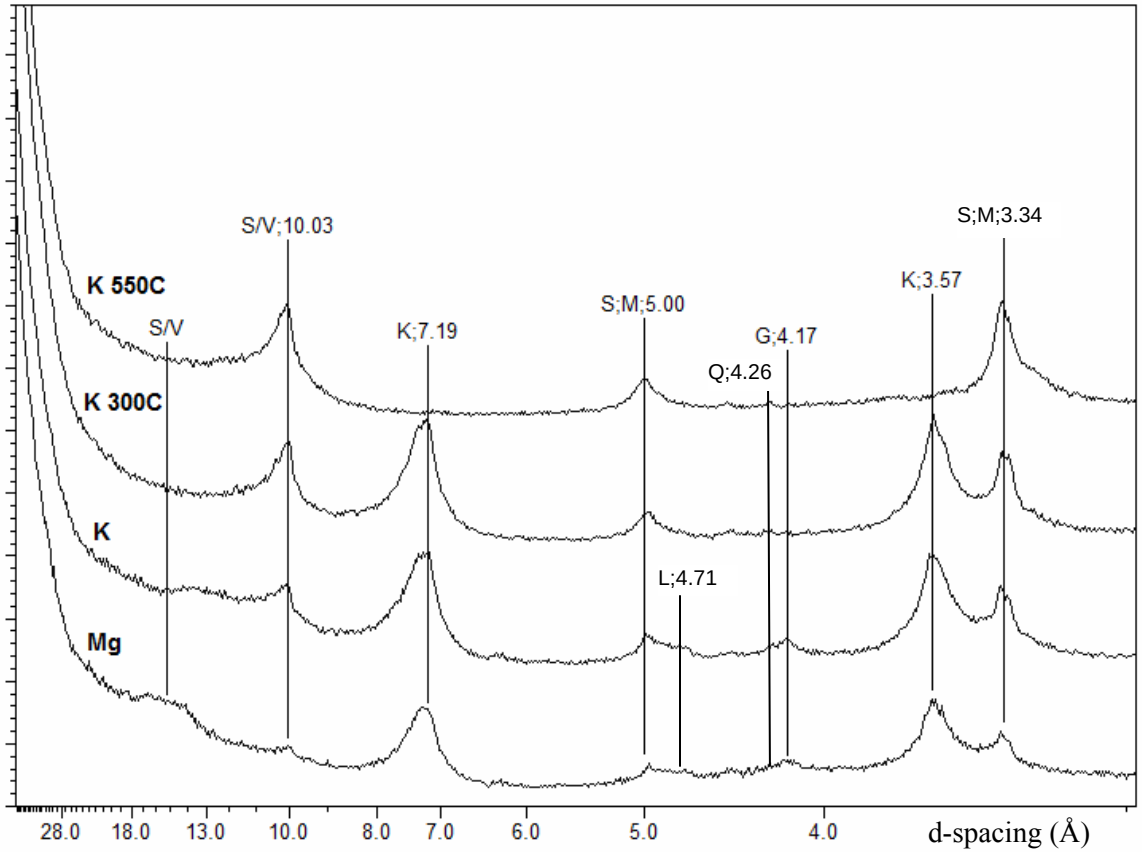

FLI-2 Sand Fractions

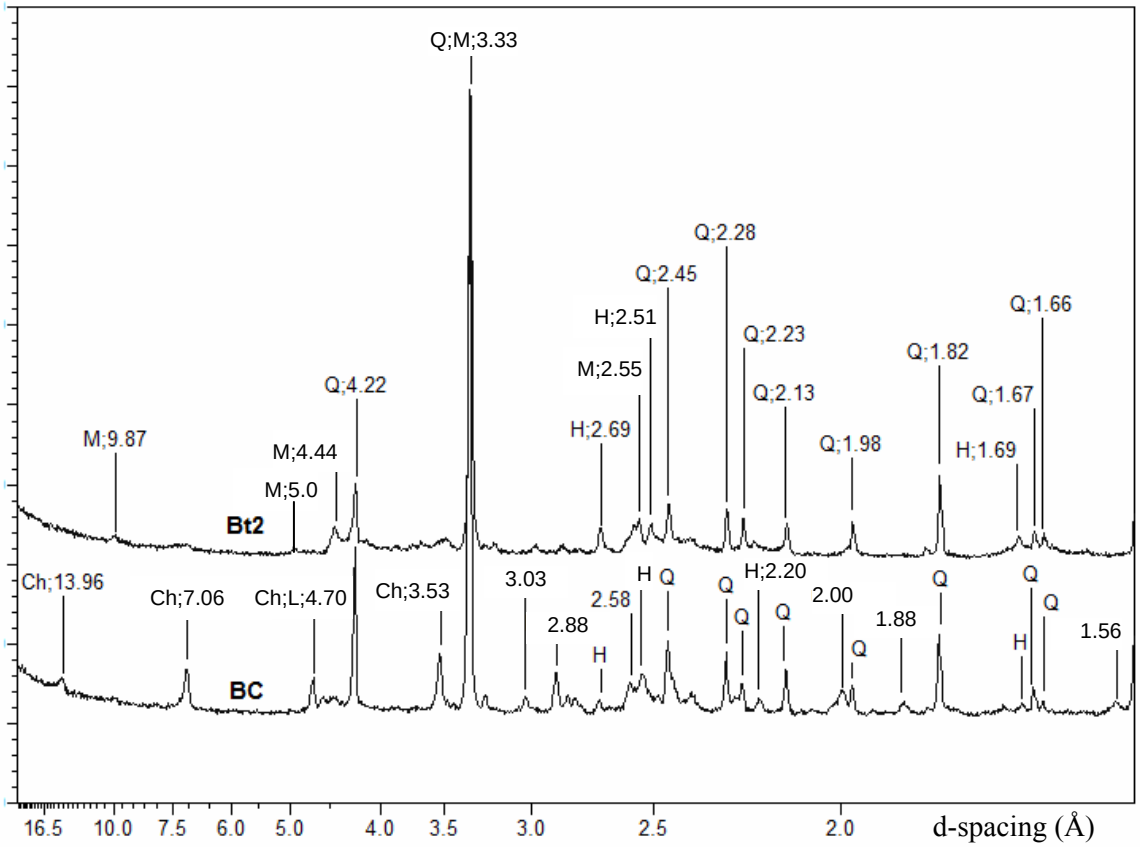

FLI-2 Silt Fractions

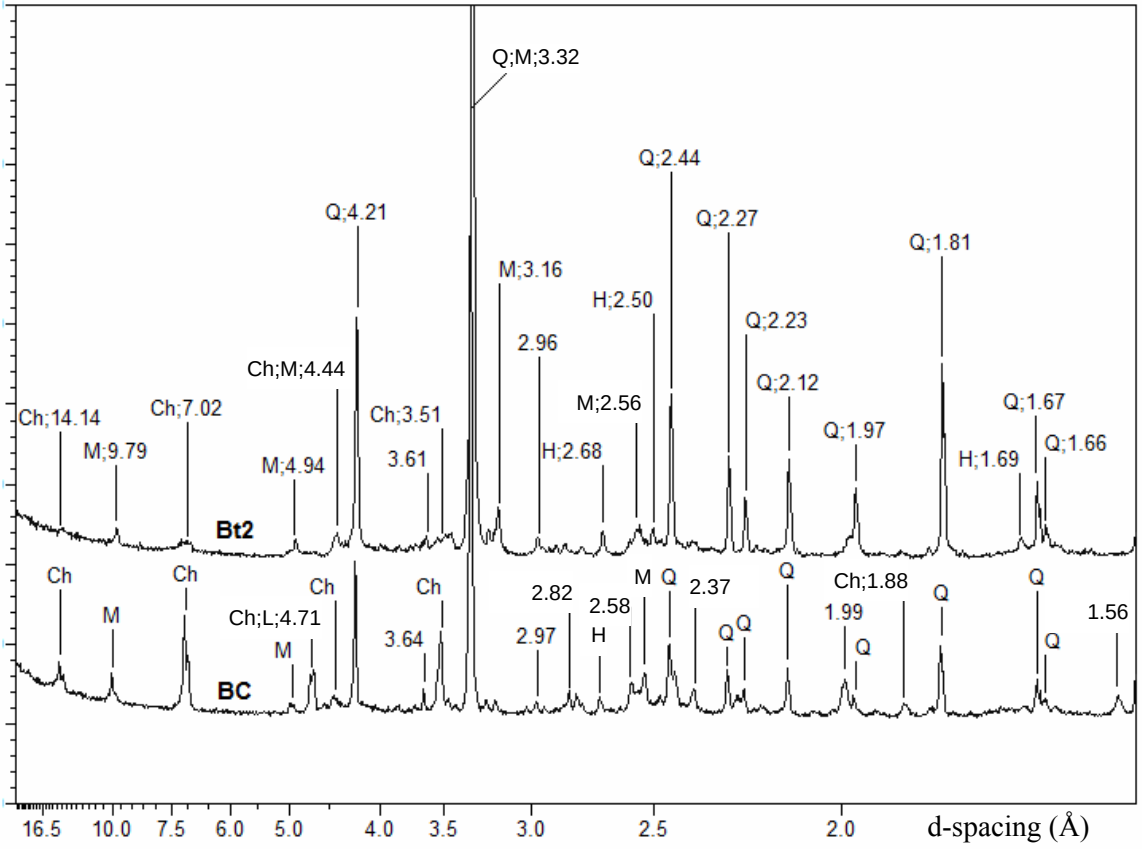

FLI-2 Bt2 Clay Fraction

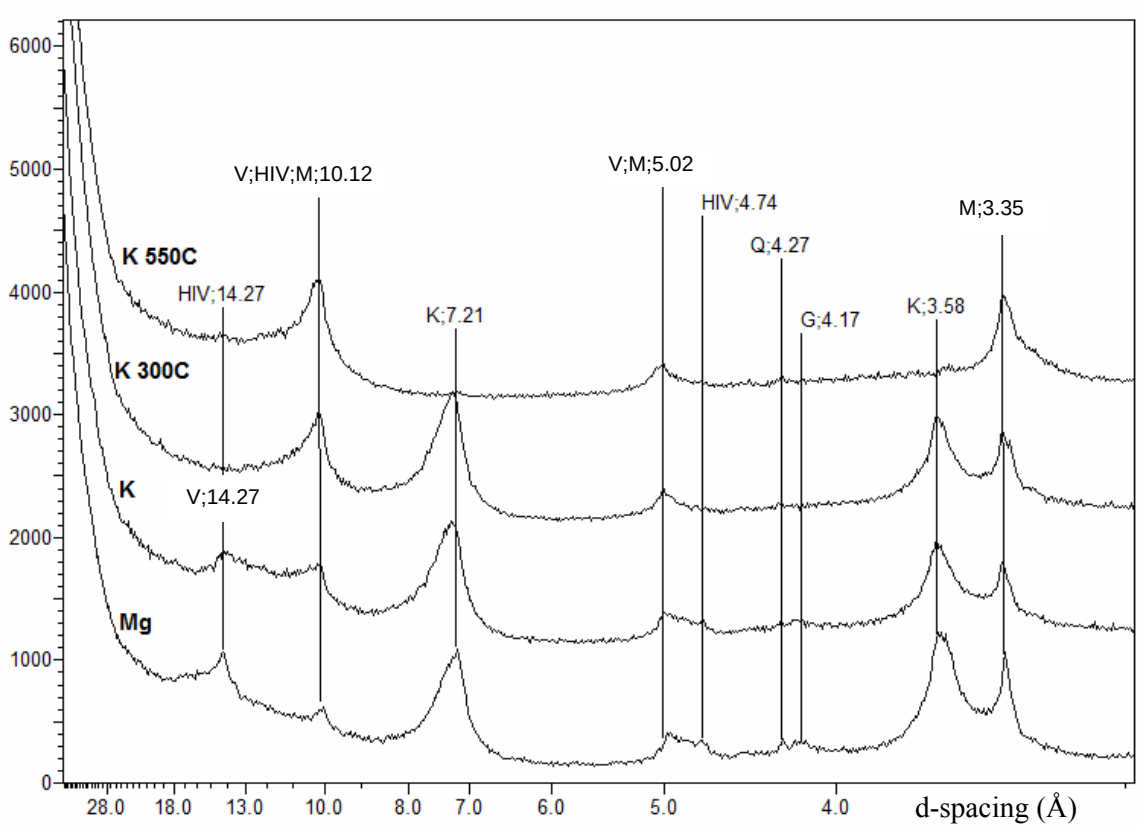

FLI-2 BC Clay Fraction

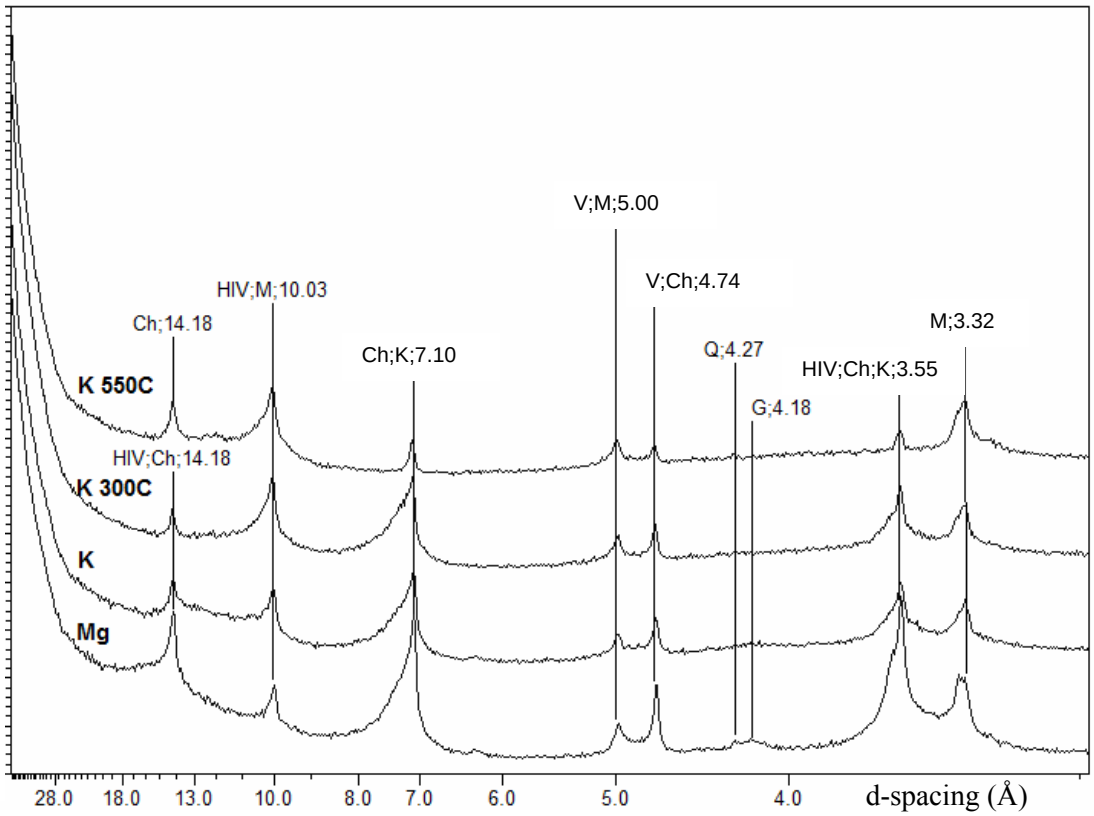

APPENDIX C

Fourier Transform Infrared (FTIR) Spectra

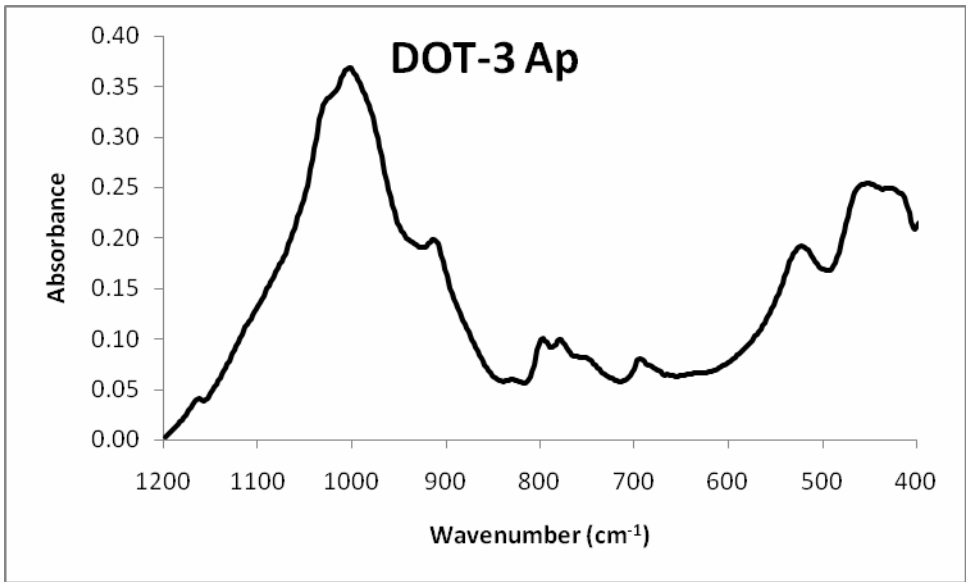

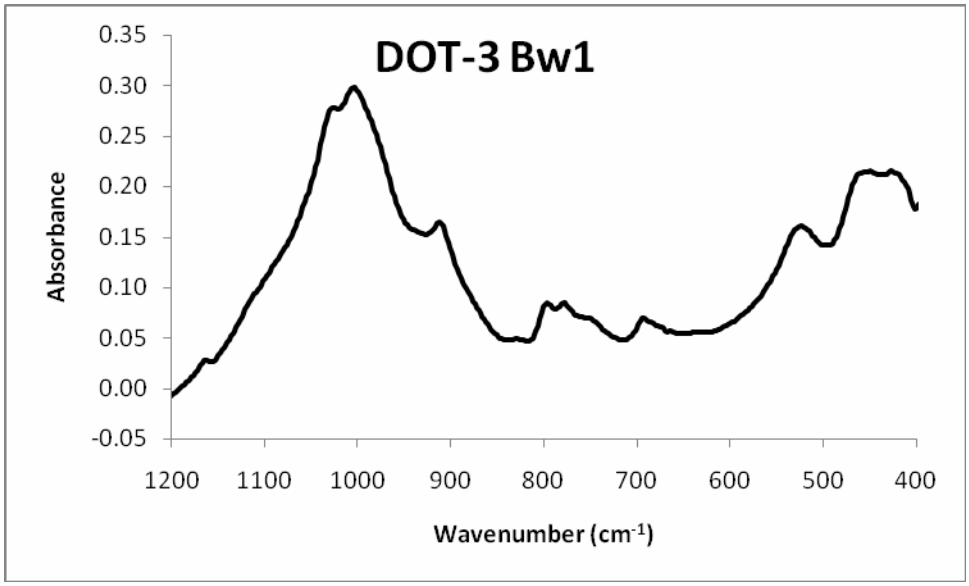

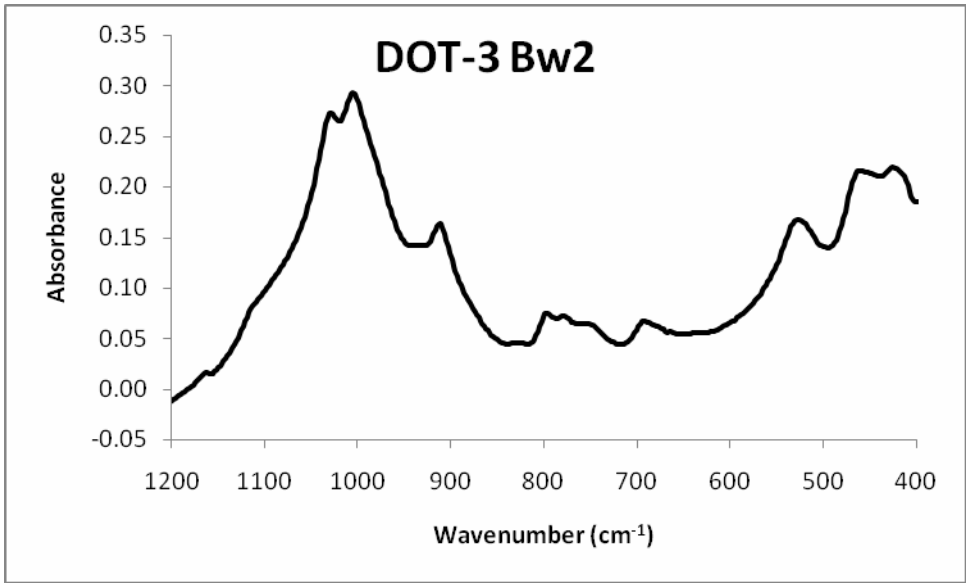
DOT-3 Bw2
Absorbance
0.35
0.30
0.25
0.20
0.15
0.10
0.05
0.00
-0.05
1200
1100
1000
900
800
700
600
500
400
Wavenumber (cm-1)

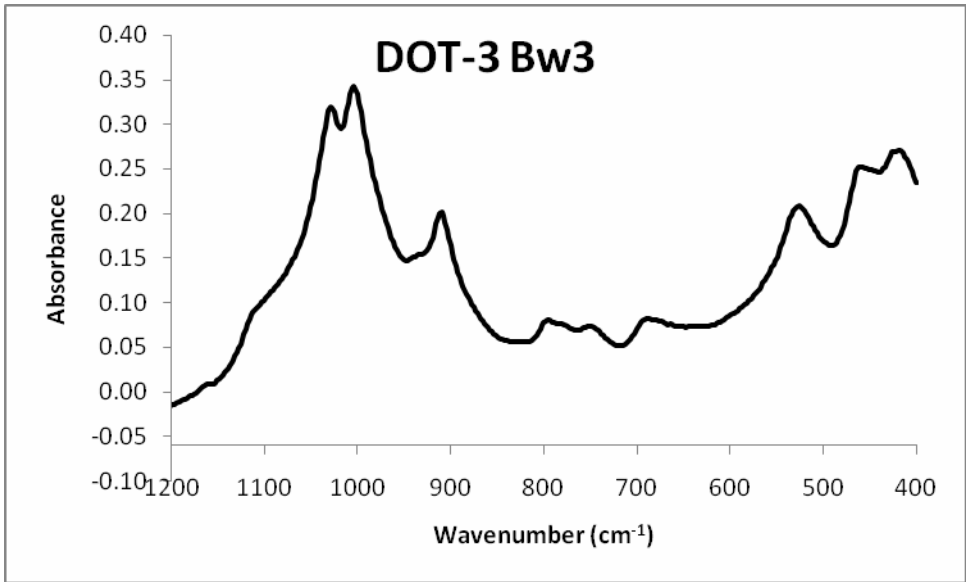
DOT-3 Bw3
Absorbance
0.40
0.35
0.30
0.25
0.20
0.15
0.10
0.05
0.00
-0.05
-0.10
1200
1100
1000
900
800
700
600
500
400
Wavenumber (cm-1)

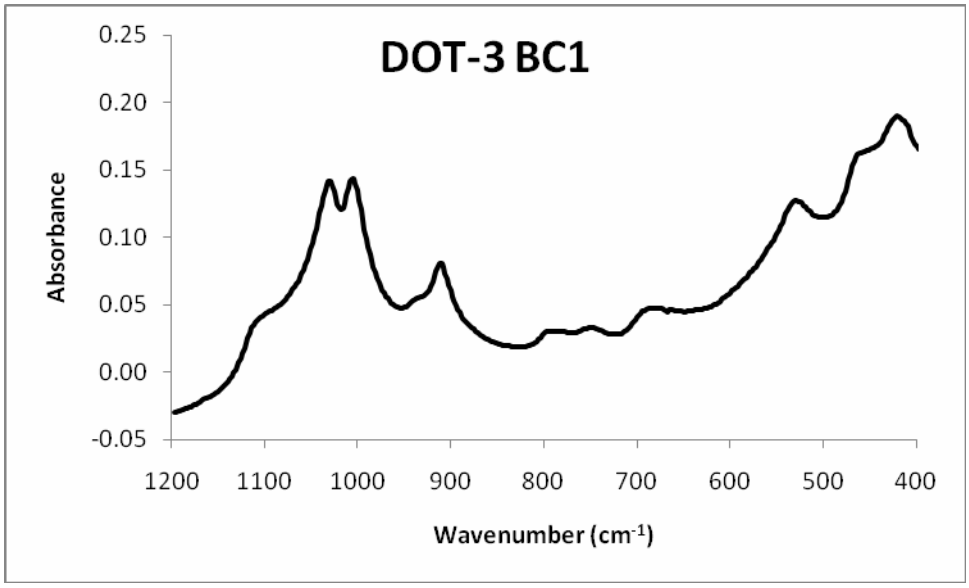
DOT-3 BC1
Absorbance
0.25
0.20
0.15
0.10
0.05
0.00
-0.05
1200
1100
1000
900
800
700
600
500
400
Wavenumber (cm-1)

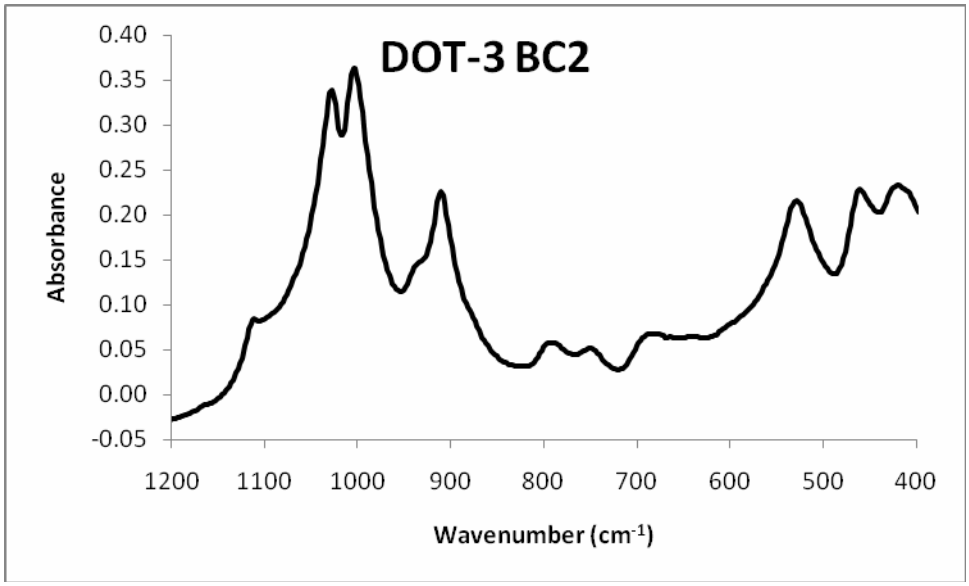
DOT-3 BC2
Absorbance
0.40
0.35
0.30
0.25
0.20
0.15
0.10
0.05
0.00
-0.05
1200
1100
1000
900
800
700
600
500
400
Wavenumber (cm-1)

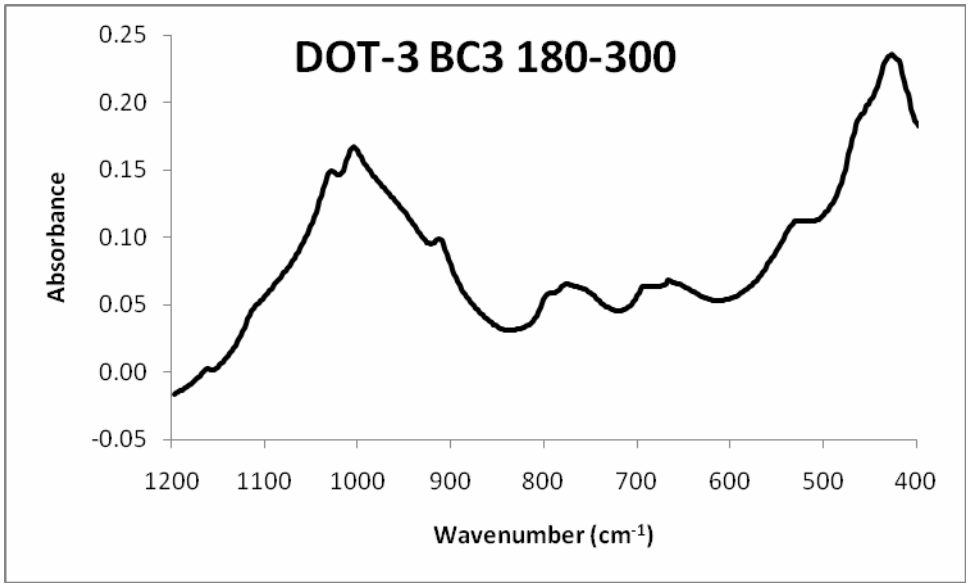
DOT-3 BC3 180-300
Absorbance
0.25
0.20
0.15
0.10
0.05
0.00
-0.05
1200
1100
1000
900
800
700
600
500
400
Wavenumber (cm-1)

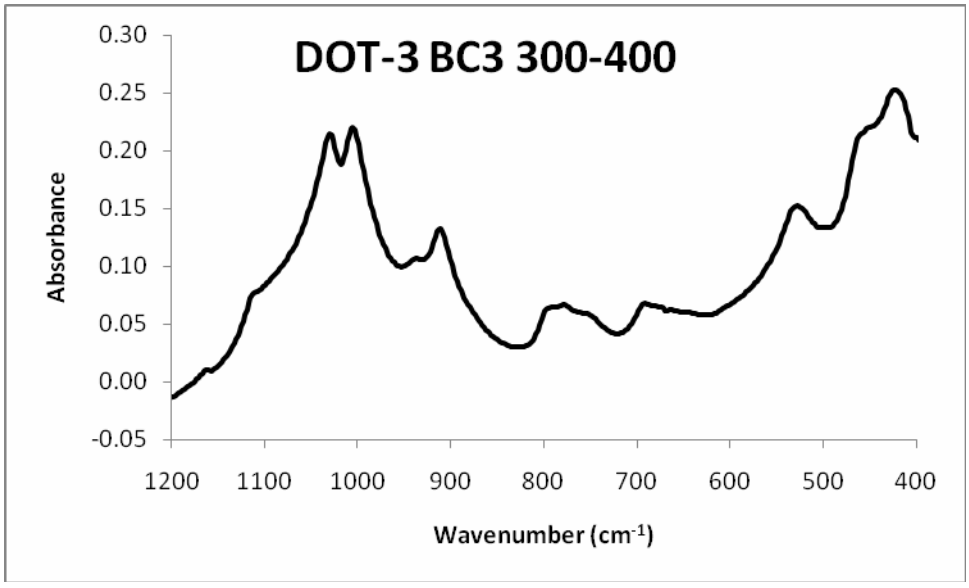
DOT-3 BC3 300-400
Absorbance
0.30
0.25
0.20
0.15
0.10
0.05
0.00
-0.05
1200
1100
1000
900
800
700
600
500
400
Wavenumber (cm-1)

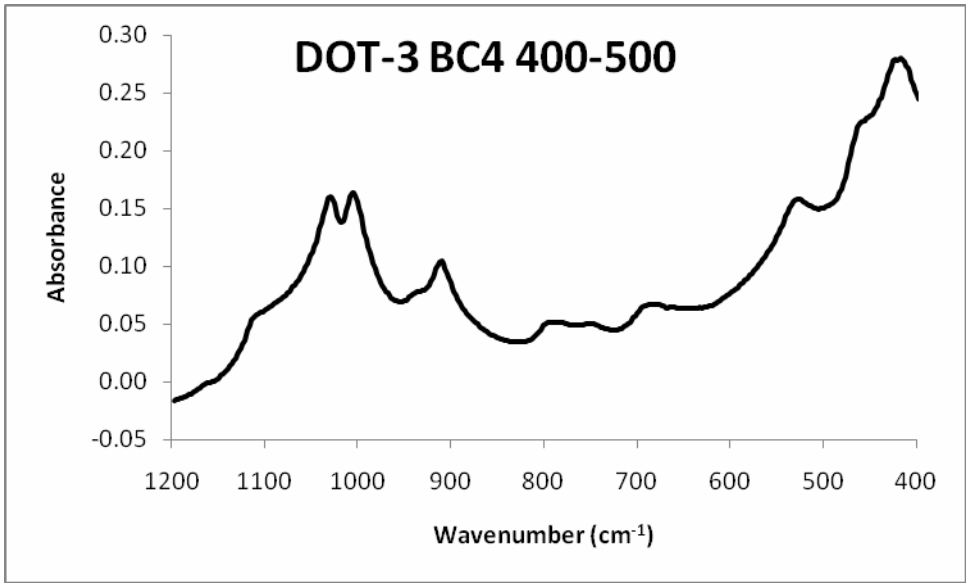
DOT-3 BC4 400-500
Absorbance
0.30
0.25
0.20
0.15
0.10
0.05
0.00
-0.05
1200
1100
1000
900
800
700
600
500
400
Wavenumber (cm-1)

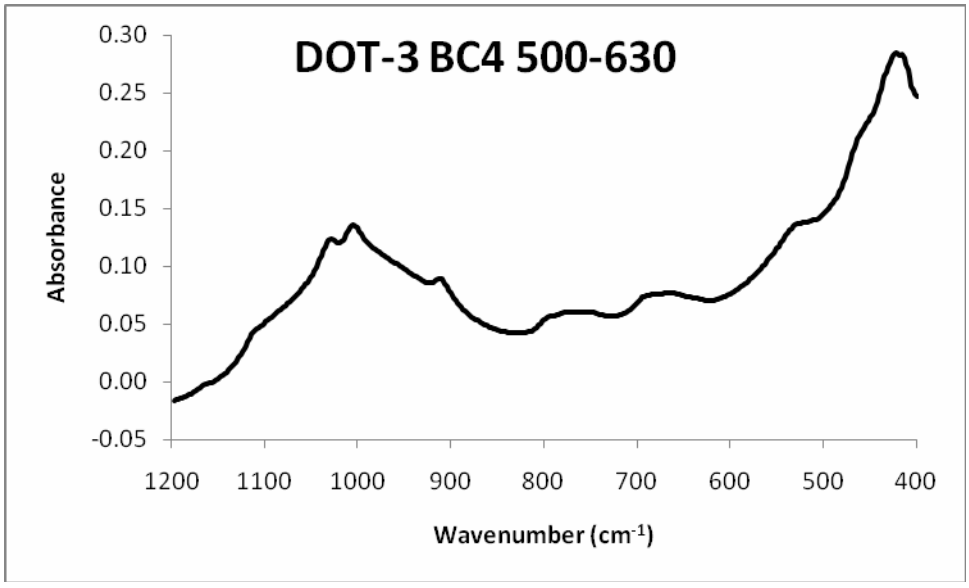
DOT-3 BC4 500-630
Absorbance
0.30
0.25
0.20
0.15
0.10
0.05
0.00
-0.05
1200
1100
1000
900
800
700
600
500
400
Wavenumber (cm-1)

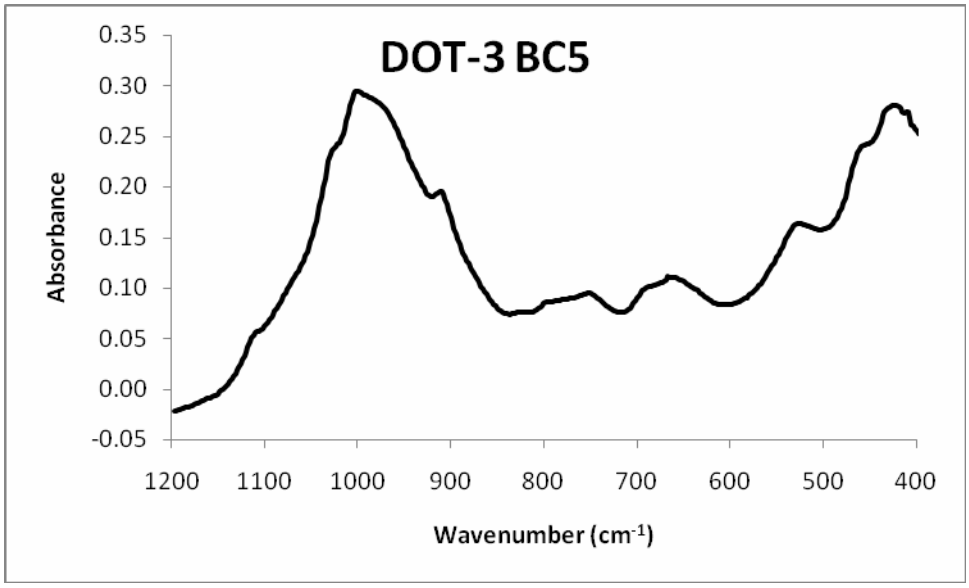
DOT-3 BC5
Absorbance
0.35
0.30
0.25
0.20
0.15
0.10
0.05
0.00
-0.05
1200
1100
1000
900
800
700
600
500
400
Wavenumber (cm-1)

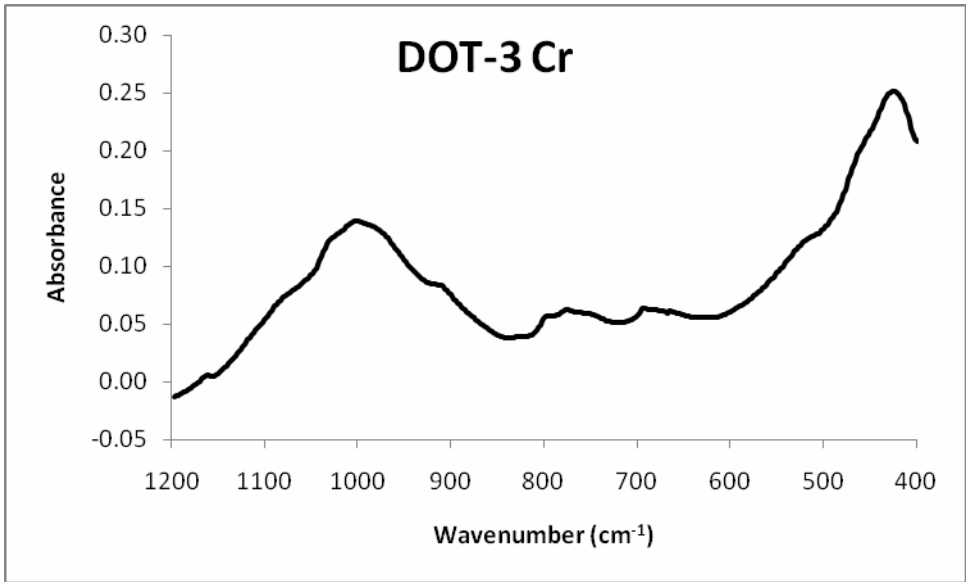
DOT-3 Cr
Absorbance
0.30
0.25
0.20
0.15
0.10
0.05
0.00
-0.05
1200
1100
1000
900
800
700
600
500
400
Wavenumber (cm-1)

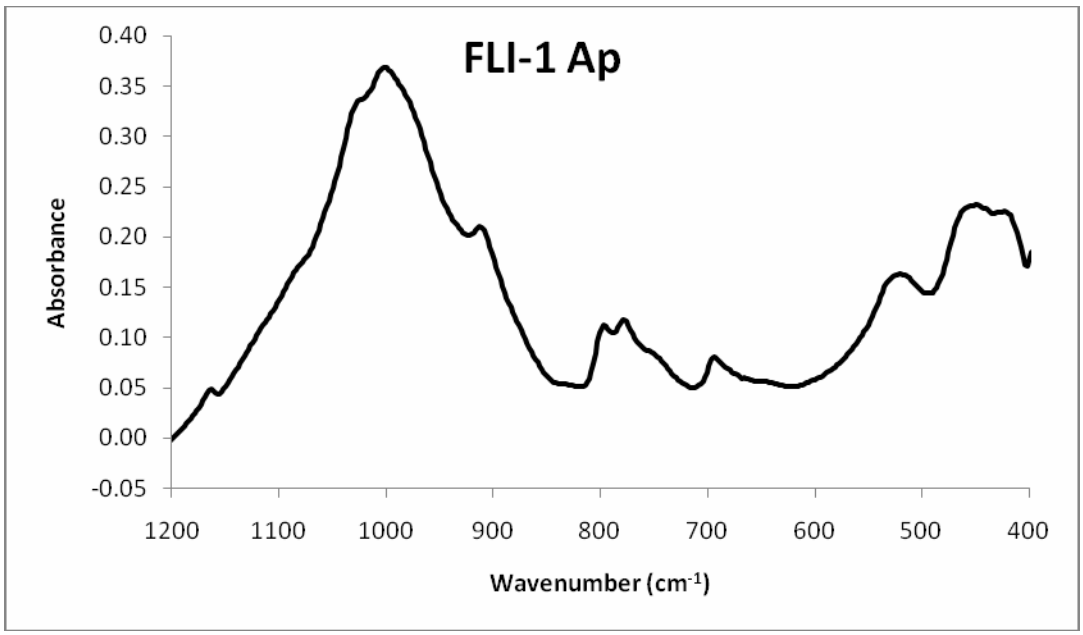
FLI-1 Ap
Absorbance
0.40
0.35
0.30
0.25
0.20
0.15
0.10
0.05
0.00
-0.05
1200
1100
1000
900
800
700
600
500
400
Wavenumber (cm-1)

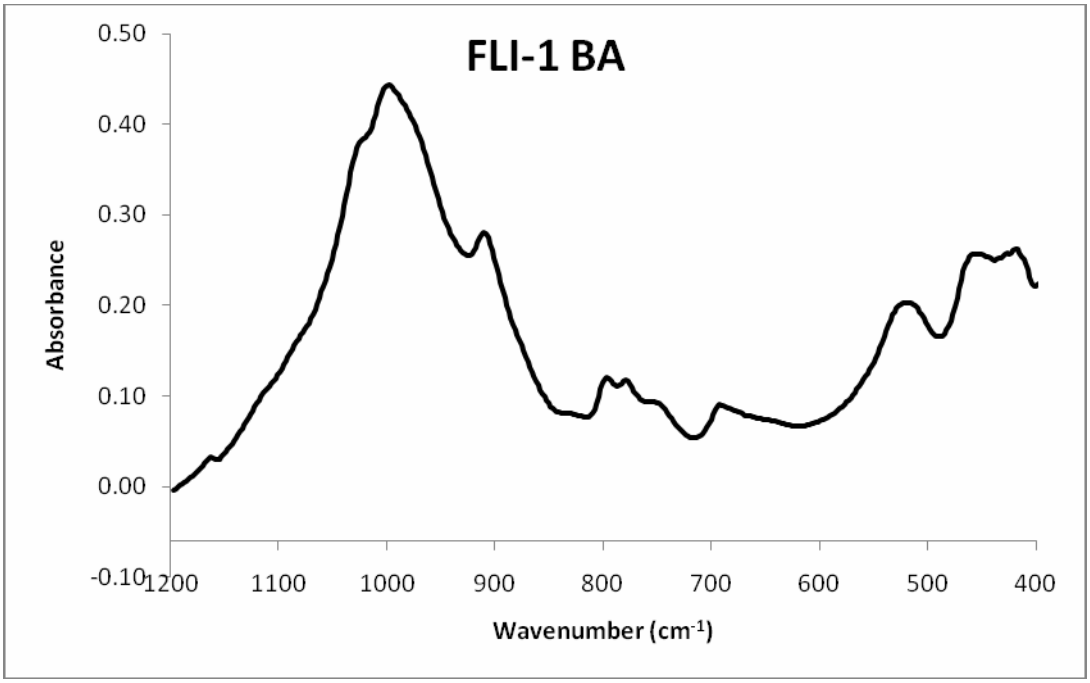
FLI-1 BA
Absorbance
0.50
0.40
0.30
0.20
0.10
0.00
-0.10
1200
1100
1000
900
800
700
600
500
400
Wavenumber (cm-1)

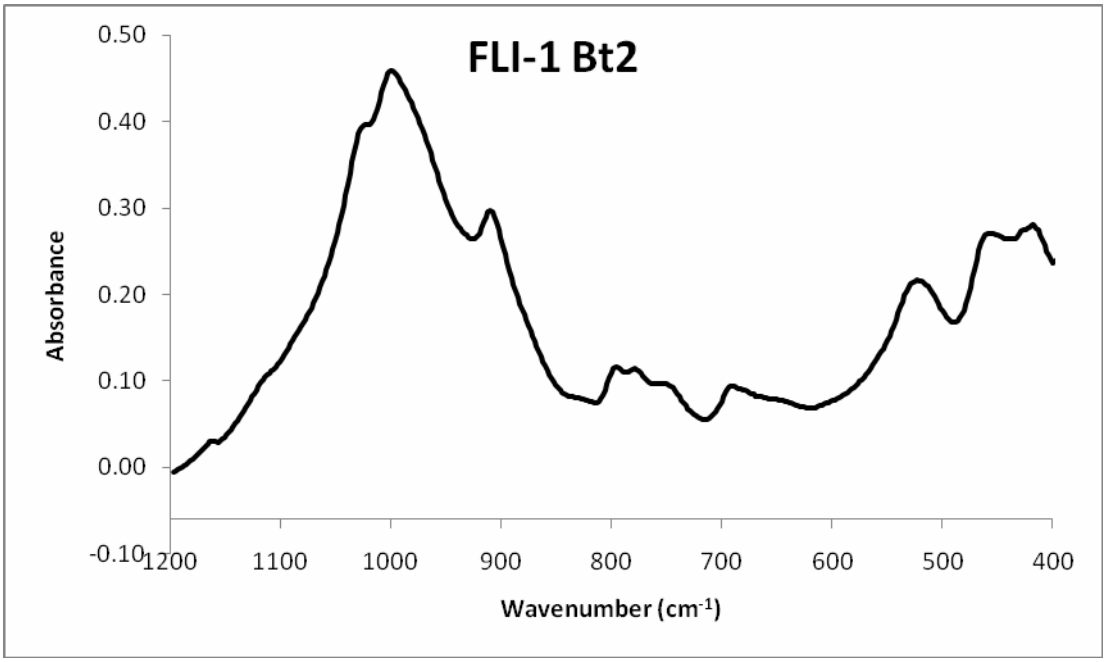
FLI-1 Bt2
Absorbance
0.50
0.40
0.30
0.20
0.10
0.00
-0.10
1200
1100
1000
900
800
700
600
500
400
Wavenumber (cm-1)

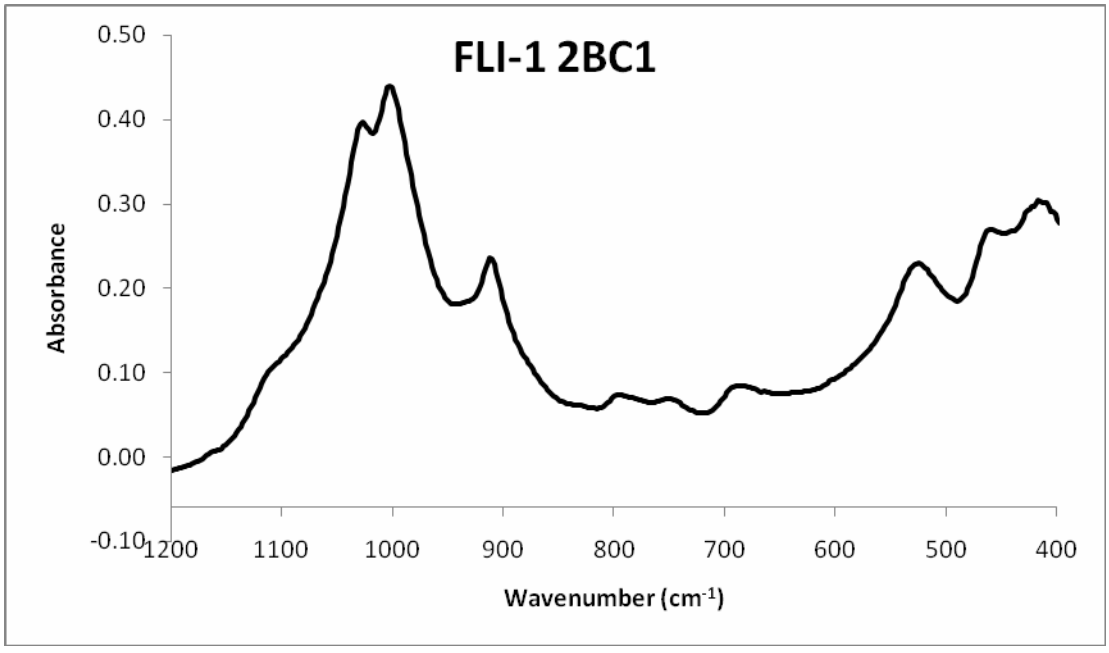
FLI-1 2BC1
Absorbance
0.50
0.40
0.30
0.20
0.10
0.00
-0.10
1200
1100
1000
900
800
700
600
500
400
Wavenumber (cm-1)

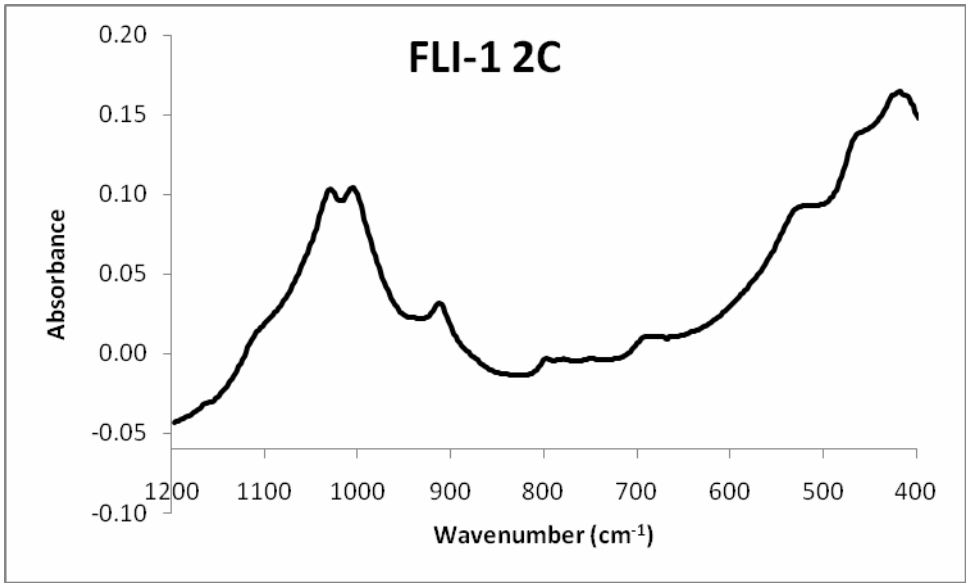
FLI-1 2C
Absorbance
0.20
0.15
0.10
0.05
0.00
-0.05
-0.10
1200
1100
1000
900
800
700
600
500
400
Wavenumber (cm-1)

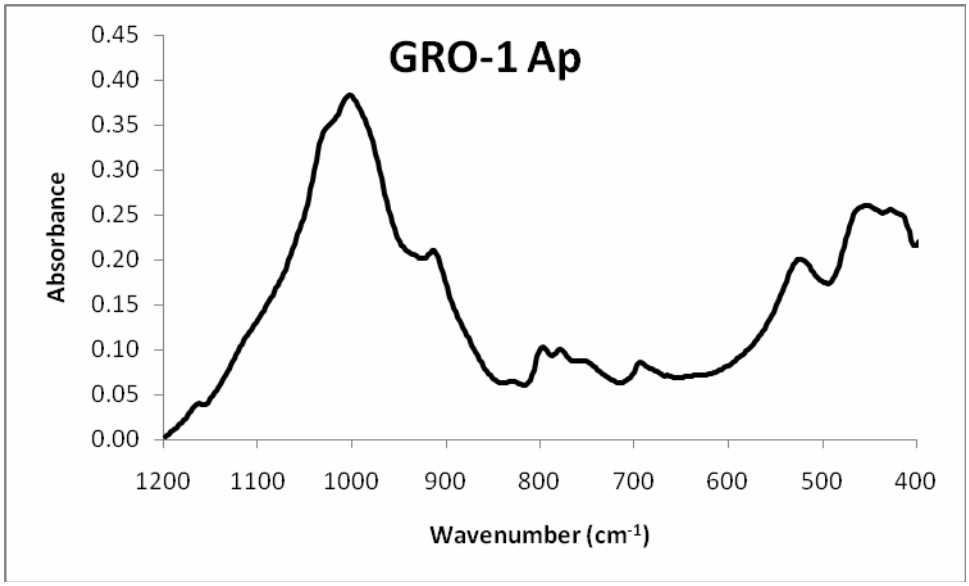
GRO-1 Ap
Absorbance
0.45
0.40
0.35
0.30
0.25
0.20
0.15
0.10
0.05
0.00
1200
1100
1000
900
800
700
600
500
400
Wavenumber (cm-1)

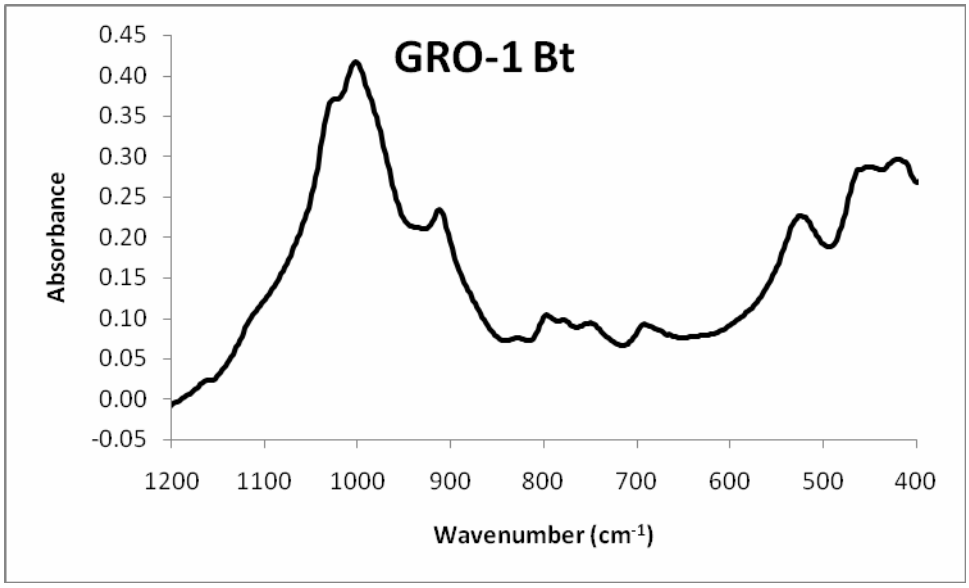
GRO-1 Bt
Absorbance
0.45
0.40
0.35
0.30
0.25
0.20
0.15
0.10
0.05
0.00
-0.05
1200
1100
1000
900
800
700
600
500
400
Wavenumber (cm-1)

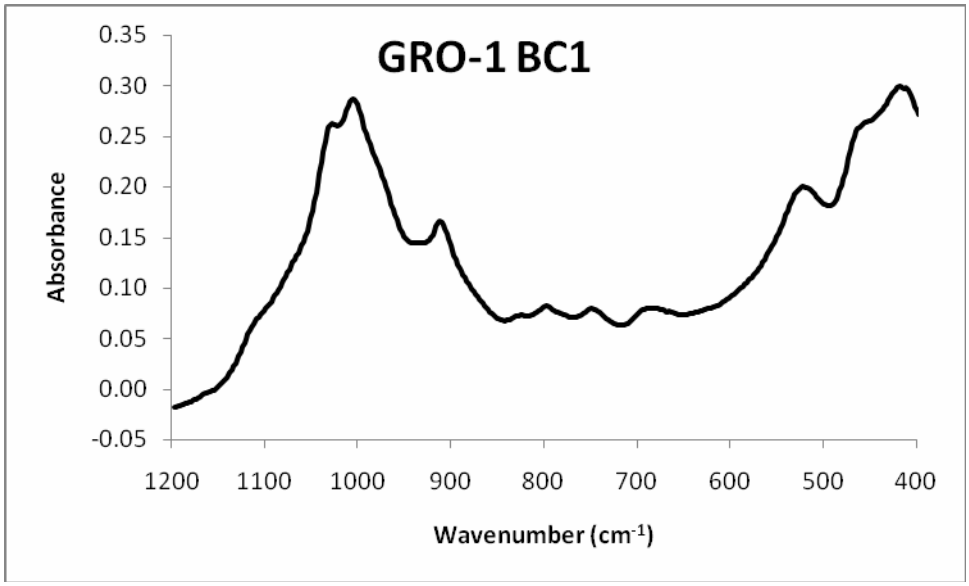
GRO-1 BC1
Absorbance
0.35
0.30
0.25
0.20
0.15
0.10
0.05
0.00
-0.05
1200
1100
1000
900
800
700
600
500
400
Wavenumber (cm-1)

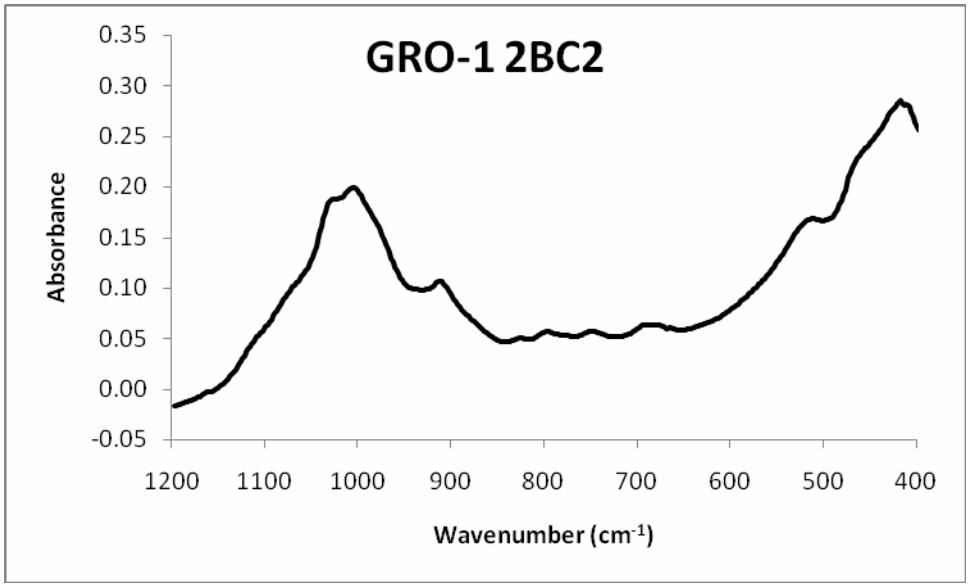
GRO-1 2BC2
Absorbance
0.35
0.30
0.25
0.20
0.15
0.10
0.05
0.00
-0.05
1200
1100
1000
900
800
700
600
500
400
Wavenumber (cm-1)

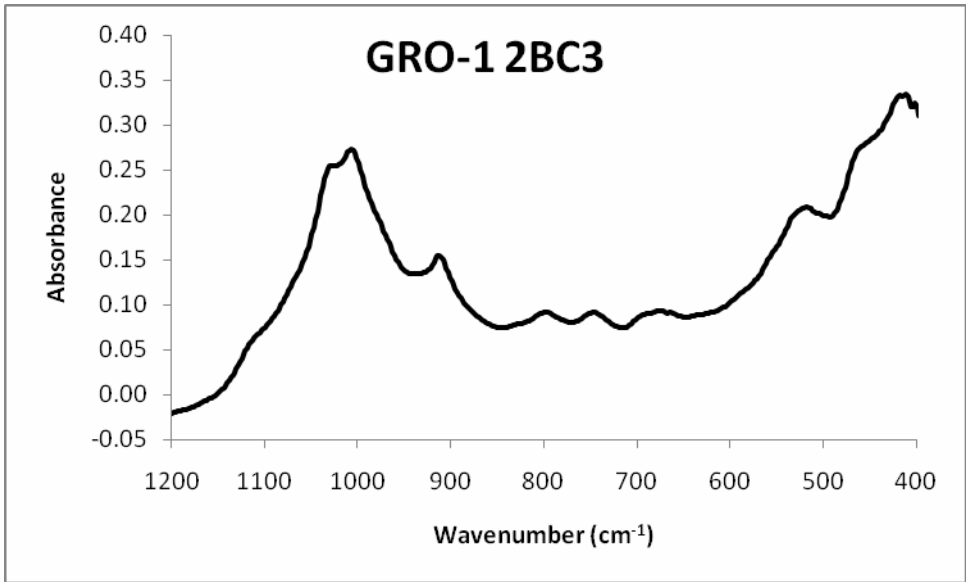
GRO-1 2BC3
Absorbance
0.40
0.35
0.30
0.25
0.20
0.15
0.10
0.05
0.00
-0.05
1200
1100
1000
900
800
700
600
500
400
Wavenumber (cm-1)

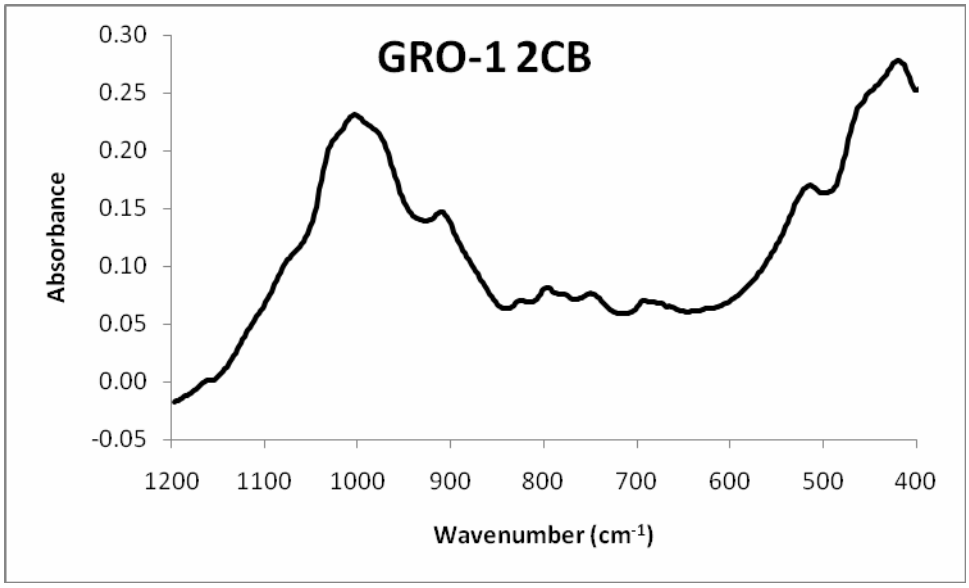
GRO-1 2CB
Absorbance
0.30
0.25
0.20
0.15
0.10
0.05
0.00
-0.05
1200
1100
1000
900
800
700
600
500
400
Wavenumber (cm-1)

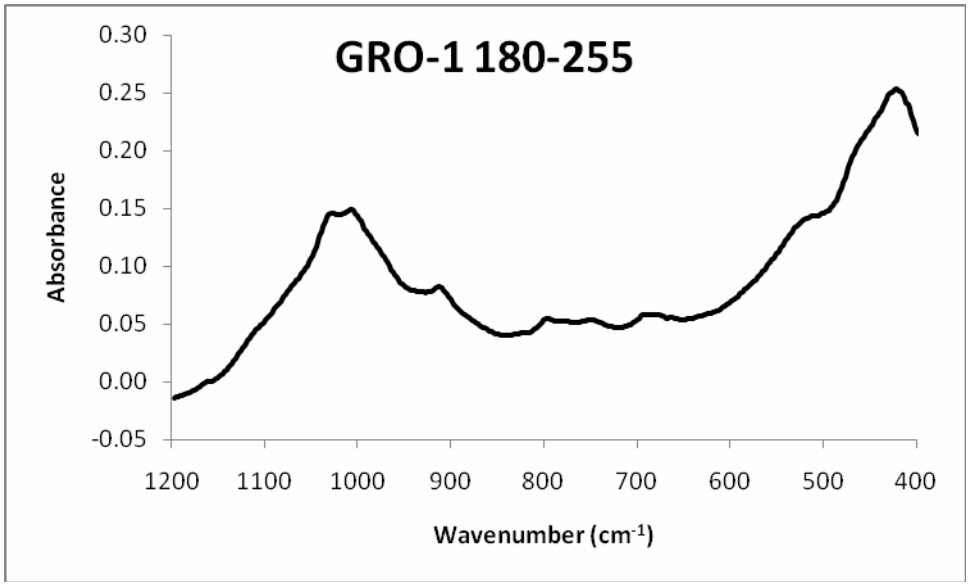
GRO-1 180-255
Absorbance
0.30
0.25
0.20
0.15
0.10
0.05
0.00
-0.05
1200
1100
1000
900
800
700
600
500
400
Wavenumber (cm-1)

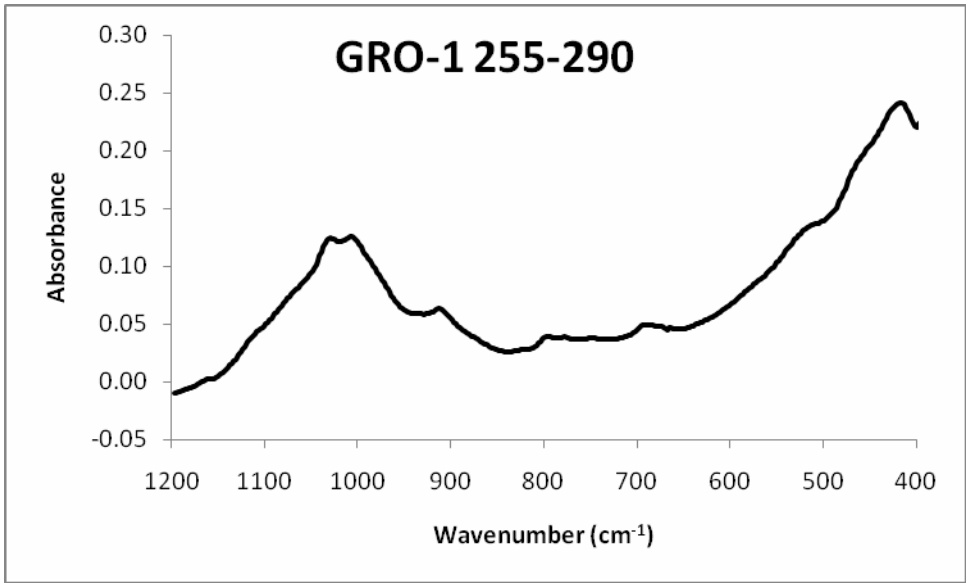
GRO-1 255-290
Absorbance
0.30
0.25
0.20
0.15
0.10
0.05
0.00
-0.05
1200
1100
1000
900
800
700
600
500
400
Wavenumber (cm-1)

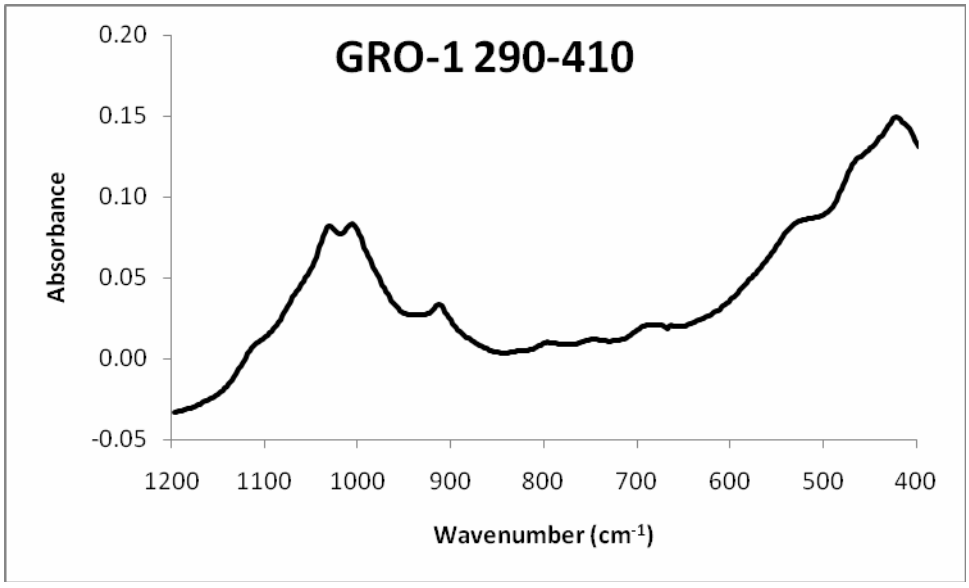
GRO-1 290-410
Absorbance
0.20
0.15
0.10
0.05
0.00
-0.05
1200
1100
1000
900
800
700
600
500
400
Wavenumber (cm-1)

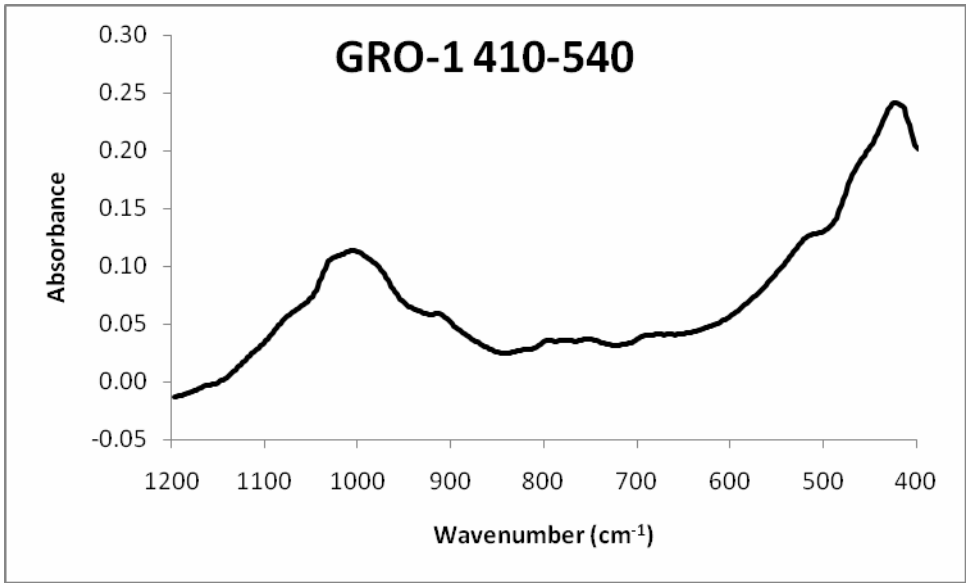
GRO-1 410-540
Absorbance
0.30
0.25
0.20
0.15
0.10
0.05
0.00
-0.05
1200
1100
1000
900
800
700
600
500
400
Wavenumber (cm-1)

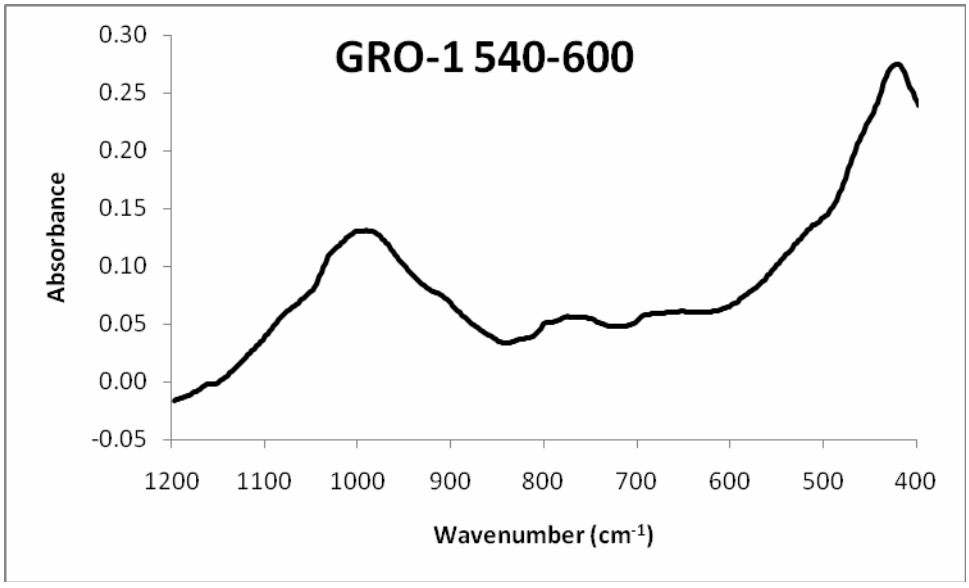
GRO-1 540-600
Absorbance
0.30
0.25
0.20
0.15
0.10
0.05
0.00
-0.05
1200
1100
1000
900
800
700
600
500
400
Wavenumber (cm-1)

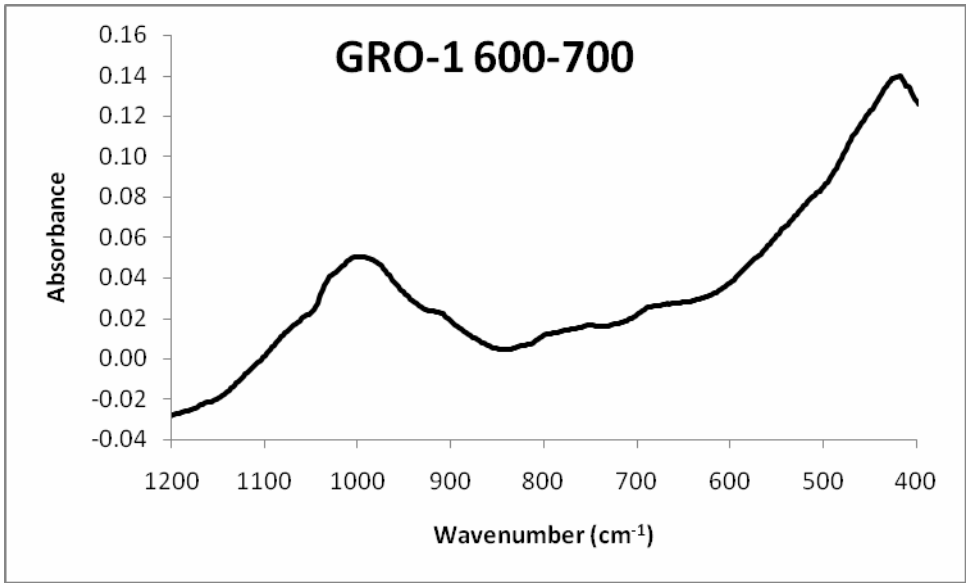
GRO-1 600-700
Absorbance
0.16
0.14
0.12
0.10
0.08
0.06
0.04
0.02
0.00
-0.02
-0.04
1200
1100
1000
900
800
700
600
500
400
Wavenumber (cm-1)

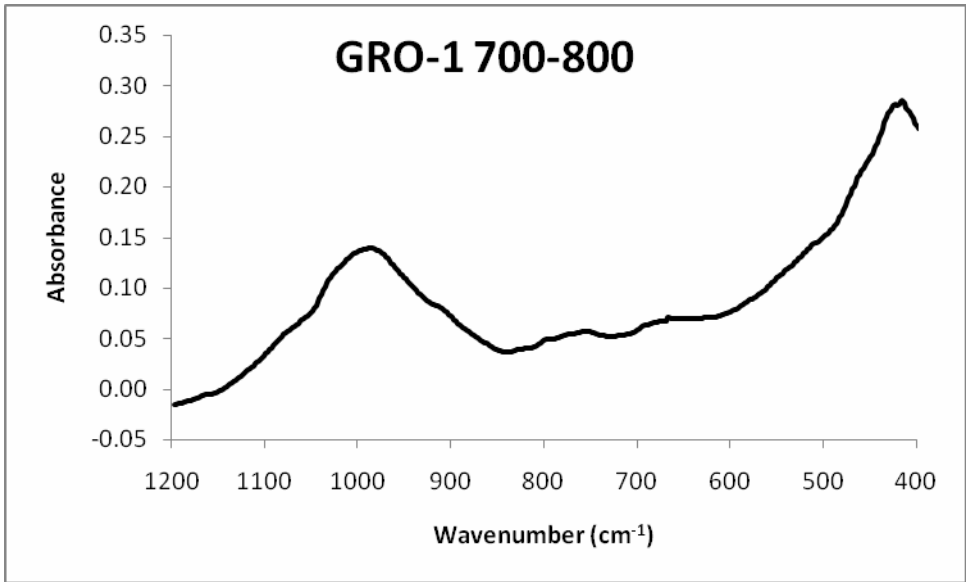
GRO-1 700-800
Absorbance
0.35
0.30
0.25
0.20
0.15
0.10
0.05
0.00
-0.05
1200
1100
1000
900
800
700
600
500
400
Wavenumber (cm-1)

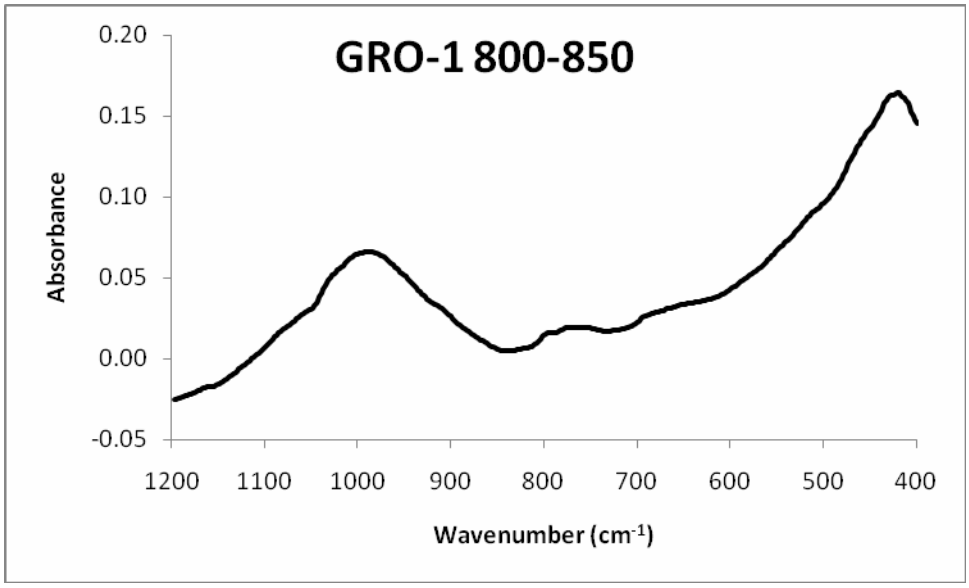
GRO-1 800-850
0.20
0.15
0.10
0.05
0.00
-0.05
Absorbance
1200
1100
1000
900
800
700
600
500
400
Wavenumber (cm-1)

LITERATURE CITED

Bartlett, R.J. 1988. Manganese redox reactions and organic interactions in soils. p. 59-73. *In* R.D. Graham et al. (ed.) Manganese in soils and plants. Kluwer Academic Publ., Dordrecht, the Netherlands.

Bartlett, R.J., and B.R. James. 1988. Mobility and bioavailability of chromium in soils. p. 267-283. *In* J.O. Nriagu (ed.) Advances in environmental science and technology. John Wiley and Sons, New York.

Bartlett, R.J., and B.R. James. 1993. Redox chemistry of soils. p. 151-208. *In* D.L. Sparks (ed.) Advances in agronomy. Academic Press, New York.

Bartlett, R.J., and D.S. Ross. 2005. Chemistry of redox processes in soils. p. 461-487. *In* D.L. Sparks and M.A. Tabatabai (ed.) Chemical processes in soils. SSSA Book Series no. 8. SSSA, Madison, WI.

Blake, G.R., and K.H. Hartge. 1986. Bulk density. p. 363-376. *In* E.A. Klute (ed.) Methods of Soil Analysis, Part 1: Physical and Mineralogical Methods. SSSA Book Series no. 5. SSSA, Madison, WI.

Blake, G.R., and K.H. Hartge. 1986. Particle density. p. 377-382. *In* E.A. Klute (ed.) Methods of Soil Analysis, Part 1: Physical and Mineralogical Methods. SSSA Book Series no. 5. SSSA, Madison, WI.

Bigham, J.M., R.W. Fitzpatrick, and D.G. Schulze. 2002. Iron oxides. p. 323-366. *In* J.B. Dixon and D.G. Schulze (ed.) Soil mineralogy with environmental applications. SSSA Book Series no. 7. SSSA, Madison, WI.

Brady, N.C., and R.R. Weil. 2007. The nature and properties of soils. 14th ed. Prentice Hall, Upper Saddle River, NJ.

Bronger, A., J. Ensling, and E. Kalk. 1984. Mineral weathering, clay mineral formation and rubefication of terrae calcis in Slovakia: a contribution to paleoclimatic evidence of limestone Rotlehm (terra rossa) in Central Europe. Catena 11:115-132.

Bronger, A., and N. Bruhn-Lobin. 1997. Paleopedology of terrae rossae-rhodoxeralfs from Quaternary calcarenites in NW Morocco. Catena 28:279-295.

Cockx, L., M. Van Meirvenne, and B. De Vos. 2007. Using the EM38DD soil sensor to delineate clay lenses in a sandy forest soil. Soil Sci. Soc. Am. J. 71:1314-1322.

Cooperative Extension Service, College of Tropical Agriculture & Human Resources, University of Hawaii at Manoa (CTAHR). 1998. Managing manganese toxicity in former sugarcane soils on Oahu. Soil and Crop Management (SCM-1), June.

Diem, D., and W. Stumm. 1984. Is dissolved Mn^{2+} being oxidized by O_2 in absence of Mn-bacteria or surface catalysts. Geochem. Cosmochim. Acta 48:1571-1573.

Dixon, J.B. 1988. Todorokite, birnessite and lithiophorite as indicator minerals in soils. p. 3–4. *In* M.J. Webb et al. (ed.) International Symposium on Manganese in Soils and Plants: Contributed papers. Adelaide, South Australia. 22–26 Aug. 1988. Manganese Symposium 1988 Inc., Adelaide, Australia.

Dixon, J.B., and H.C. Skinner. 1992. Manganese minerals in surface environments. Catena supplement 21:31.

Dixon, J.B., and G.N. White. 2002. Manganese oxides. p. 367-388. *In* J.B. Dixon and D.G. Schulze (ed.) Soil mineralogy with environmental applications. SSSA Book Series no. 7. SSSA, Madison, WI.

Doolittle, J.A., K.A. Sudduth, N.R. Kitchen, and S.J. Indorante. 1994. Estimating depth to claypans using electromagnetic induction methods. J. Soil and Water Conservation 49:572-575.

Dowding, C.E. and M.V. Fey. 2007. Morphological, chemical, and mineralogical properties of some manganese-rich oxisols derived from dolomite in Mpumalanga province, South Africa. Geoderma 141:23-33.

Drever, J.I. 1973. The preparation of oriented clay mineral specimens for X-ray diffraction analysis by a filter-membrane peel technique. Am. Miner. 58:553-554.

Durn, G., D. Slovenec, and M. Covic. 2001. Distribution of iron and manganese in terra rossa from Istria and its genetic implications. Geologia Croatica 54:27-36.

Edwards, J., Jr. 1986. Geologic map of the Union Bridge Quadrangle [map]. 1:24,000. 7.5-minute series. Maryland Geological Survey, Baltimore, MD.

Elless, M.P. 1992. Morphology, mineralogy, and hydrology of soils in the Triassic Culpeper Basin of Maryland. Ph.D. Dissertation, University of Maryland, College Park.

Eriksson, K.A., T.S. McCarthy, and J.F. Truswell. 1975. Limestone formation and dolomitization in a lower Proterozoic succession from South Africa. J. Sedimentary Petrology 45:604-614.

Foss, J.E., F.P. Miller, and D.S. Fanning. 1969. Soil characterization studies in Maryland: summary of data 1950-1966. University of Maryland Agronomy Dept. in cooperation with Soil Conservation Service, United States Dept. of Agriculture.

Foster, J., D.J. Chittleborough, and K. Barovich. 2004. Genesis of a Terra Rossa soil over marble and the influence of a neighbouring texture contrast soil at Delamere, South Australia. p. 1-8. SuperSoil 2004: 3rd Australian New Zealand Soils Conference, 5-9 December 2004. University of Sydney, Australia. Available online at http://www.regional.org.au/au/asssi/supersoil2004/pdf/1607_fosterj.pdf. Accessed Dec. 1, 2008.

Foster, J. and D. Chittleborough. 2003. Soil development on dolomites of the Cambrian Normanville Group at Delamere, South Australia. p. 131-132. *In* Roach, I.C. ed. Advances in Regolith.

Fujimoto, C. and G.D. Sherman. 1948. Behavior of manganese in the soil and the manganese cycle. Soil Sci. 66:131-145.

Gee, G.W., and J.W. Bauder. 1986. Particle size analysis. p. 383-411. *In* E.A. Klute (ed.) Methods of Soil Analysis, Part 1: Physical and Mineralogical Methods. SSSA Book Series no. 5. SSSA, Madison, WI.

Golden, D.C., J.B. Dixon, and Y. Kanehiro. 1993. The manganese oxide mineral, lithiophorite, in an Oxisol from Hawaii. Aust. J. Soil Res. 31:51-66.

Hawker, L.C., and J.G. Thompson. 1988. Weathering sequence and alteration products in the genesis of the Graskop manganese residua, Republic of South Africa. Clays and Clay Minerals 36:448-454.

Hue, N.V., S. Vega, and J.A. Silva. 1999. Manganese toxicity in a Hawaiian Oxisol affected by soil pH and organic amendments. Soil Sci. Soc. Am. J. 65:153-160.

Inman, D.J., R.S. Freeland, J.T. Ammons, and R.E. Yoder. 2002. Soil investigations using electromagnetic induction and ground-penetrating radar in southwest Tennessee. Soil Sci. Soc. Am. J. 66:206-211.

Jackson, M.L. 1974. Soil chemical analysis – advanced course. Published by the author. University of Wisconsin, Madison, WI.

Kohut and Warren 2002. Chlorites. p. 531-553. *In* J.B. Dixon and D.G. Schulze (ed.) Soil mineralogy with environmental applications. SSSA Book Series no. 7. SSSA, Madison, WI.

Kraft, J.S. 2002. Soil Survey of Frederick County, Maryland. United States Department of Agriculture, Natural Resources Conservation Service.

Krauskopf, K.B. 1972. Geochemistry of micronutrients. p. 7-40. *In* J.J. Mortvedt, P.M. Giordano, and W. Lindsay (ed.) Micronutrients in Agriculture. SSSA, Madison, WI.

Leinigen, W. Graf zu. 1929. Die Roterde (Terra rossa) als Lösungsrest mariner Kalkgesteine. Chem. Erde 4:178-187.

Lund, E.C., C.D. Christy, and P.E. Drummond. 1999. Practical applications of soil electrical conductivity mapping. p. 1-9. *In* Proc. 2nd European Conference on Precision Agriculture, July 1999. Available online at: http://www.veristech.com/pdf_files/europe_1999.pdf. Accessed Dec. 1, 2008.

Maryland Geological Survey. 1967. Generalized geologic map of Maryland [map]. 1:1584000. Available online at: http://www.mgs.md.gov/esic/publications/download/gengeomap.pdf. Accessed Dec. 1, 2008.

Matthews, E.D. 1969. Soil Survey of Carroll County, Maryland. United States Department of Agriculture, Soil Conservation Service.

McBride, R.A., A.M. Gordon, and S.C. Shrive. 1990. Estimating forest soil quality from terrain measurements of apparent electrical conductivity. Soil Sci. Soc. Am. J. 54:290-293.

McDaniel, P.A., and S.W. Buol. 1991. Manganese distributions in acid soils of the North Carolina Piedmont. Soil Sci. Soc. Am. J. 55:152-158.

Mehra, O.P., and M.L. Jackson. 1960. Iron oxide removal from soils and clays by a dithionite-citrate system buffered with sodium bicarbonate. p. 317-327. *In* Ada Swineford (ed.) Clays and Clay Minerals, Proc. 7th Natl. Conf., Washington DC, 1958. Pergamon Press, New York.

Moresi, M., and G. Mongelli. 1988. The relation between the terra rossa and the carbonate-free residue of the underlying limestones and dolostones in Apulia, Italy. Clay Minerals 23:439-446.

Neaman, A., B. Waller, F. Mouélé, F. Trolard, and G. Bourrié. 2004. Improved methods for selective dissolution of manganese oxides from soils and rocks. Eur. J. Soil Sci. 55:47-54.

Nelson, D.W., and L.E. Sommers. 1982. Total carbon, organic carbon, and organic matter. *In* Page et al. (ed.) Methods of soil analysis: Part 2 - chemical and microbiological properties. 2nd ed. ASA and SSSA, Madison, WI.

Olson, C.G., R.V. Ruhe, and M.J. Mausbach. 1980. The terra rossa limestone contact phenomena in karst, southern Indiana. Soil Sci. Soc. Am. J. 44:1075-1079.

Piper, C.S. 1942. Organic matter. p. 213. *In* Soil and plant analysis. Interscience Publishers Inc., New York.

Potter, R.M., and G.R. Rossman. 1979. The tetravalent manganese oxides: identification, hydration, and structural relationships by infrared spectroscopy. Am. Mineralogist 64:1199-1218.

Prothero, D.R., and F. Schwab. 2004. Sedimentary geology: an introduction to sedimentary rocks and stratigraphy. 2nd ed. W.H. Freeman and Co., New York.

Rabenhorst, M.C., and L.P. Wilding. 1984. Rapid method to obtain carbonate-free residues from limestone and petrocalcic materials. Soil Sci. Soc. Am. J. 48:216-219.

Rhoades, J.D., and D.L. Corwin. 1981. Determining soil electrical conductivity-depth relations using an inductive electromagnetic conductivity meter. Soil Sci. Soc. Am. J. 45:255-260.

Robinette, C.E., M.C. Rabenhorst, and L.M. Vasilas. 2004. Identifying problem hydric soils in the Mid-Atlantic region. p. 85-103. *In* L.M. Vasilas and B.L. Vasilas (ed.) A guide to hydric soils in the Mid-Atlantic region, version 1.0. Natural Resources Conservation Service, Morgantown, WV. Avaiable online at: http://www.epa.gov/reg3esd1/wetlands/pdf/hydric_soils_midatlantic_2_2004.pdf. Accessed 22 November 2008.

Ross, D.S., and R.J. Bartlett. 1981. Evidence for nonmicrobial oxidation of manganese in soil. Soil Sci. 132:153-160.

Schoeneberger, P.J., D.A. Wysocki, E.C. Benham, and W.D. Broderson (editors). 2002. Field book for describing and sampling soils, version 2.0. Natural Resources Conservation Service, National Soil Survey Center, Lincoln, NE.

Schwertmann, U., and D. S. Fanning. 1976. Iron-manganese concretions in hydrosequences of soils in loess in Bavaria. Soil Sci. Soc. Am. J. 40:731-738.

Shacklette, H.T., and J.G. Boerngen. 1984. Element concentrations in soils and other surficial materials of the conterminous United States. U.S. Geol. Surv. Prof. Pap. 1270:105.

Shindo, H. 1990. Catalytic synthesis of humic acids from phenolic compounds by Mn(IV) oxide. Soil Sci. Plant Nutr. 36:679-682.

Soil Survey Staff, Natural Resources Conservation Service, United States Department of Agriculture. Soil Survey Geographic (SSURGO) Database. Available online at http://soildatamart.nrcs.usda.gov. Accessed 22 November 2008.

Soil Survey Staff, Natural Resources Conservation Service, United States Department of Agriculture. Official Soil Series Descriptions. Available online at: http://soils.usda.gov/technical/classification/osd/index.html. Accessed 22 November 2008.

Stevenson, F.J., and M.A. Cole. 1999. Cycles of soil: carbon, nitrogen, phosphorus, sulfur, micronutrients, 2nd ed. John Wiley and Sons, New York.

Tebo, B.M, H.A. Johnson, J.K. McCarthy, and A.S. Templeton. 2005. Geomicrobiology of manganese(II) oxidation. Trends in Microbiology 13:421-428.

Thomas, G.W. 1996. Soil pH and soil acidity. p. 475-490. *In* D.L. Sparks (ed.) Methods of Soil Analysis, Part 3: Chemical Methods. SSSA Book Series no. 5. SSSA, Madison, WI.

Tokashiki, Y., J.B. Dixon, and D.C. Golden. 1996. Manganese oxide analysis in soils by combined X-ray diffraction and selective dissolution methods. Soil Sci. Soc. Am. J. 50:1079-1084.

Tokashiki, Y, T. Hentona, M. Shimo, and L. P. Vidhana Arachchi. 2003. Improvement of the successive selective dissolution procedure for the separation of birnessite, lithiophorite, and goethite in soil manganese nodules. Soil Sci. Soc. Am. J. 67:837-843.

United States Dept. of Agriculture, Natural Resources Conservation Service. 1999. Standards and specifications for high intensity soil survey for agriculture in Illinois. http://www.il.nrcs.usda.gov/technical/soils/specs.html. Accessed 22 November 2008.

Uzochukwu, G.A., and J.B. Dixon. 1986. Manganese oxide minerals in two soils of Texas and Alabama. Soil Sci. Soc. Am. J. 50:1358-1363.

Vodyanitskii, Y.N., A.A. Vasil'ev, S.N. Lesovaya, E.F. Sataev, and A.V. Sivtsov. 2003. Formation of manganese oxides in soils. Eurasian Soil Sci. 37:572-584.

Wada, H., A. Seirayosakol, M. Kimura, and Y. Takai.1978. The process of manganese deposition in paddy soils: 1. A hypothesis and its verification. Soil Sci. Plant Nutr. 24:55-62.

Williams, B., and D. Hoey. 1987. The use of electromagnetic induction to detect the spatial variability of the salt and clay content of soils. Aust. J. Soil Res. 25:21-27.

Wolf, K.H., G.V. Chilinger, and F.W. Beales. 1967. Elemental composition of carbonate skeletons, minerals and sediments. pp. 23-150. *In* Chilinger, G.V., H.J. Bissel, and R.W. Fairbridge (ed.) Developments in Sedimentology, vol. 9B, Elsevier, Amsterdam.

Yaalon, D.H. 2007. Soils in the Mediterranean region: what makes them different? Catena 28:157-169.